Doctoraatsproefschrift nr. 1117 aan de faculteit Bio-ingenieurswetenschappen van de KU Leuven

RESPONSE OF APPLE (*MALUS* X *DOMESTICA*) TO *VENTURIA INAEQUALIS*, THE CAUSAL AGENT OF APPLE SCAB: A REAL-TIME PCR AND PROTEOMICS STUDY

Bruno DANIELS

Supervisor:
Prof. W. Keulemans

Co-supervisor:
Dr. M. Davey

Members of the Examination Committee:
Prof. B. Nicolai, chair
Prof. R. Swennen
Prof. B. Cammue
Prof. S. Carpentier
Prof. R. Valcke, Universiteit Hasselt
Prof. D. Job, CNRS / Bayer Cropscience

Dissertation presented in partial fulfillment of the requirements for the degree of Doctor of Bioscience Engineering

July 2013

© 2013 Katholieke Universiteit Leuven, Groep Wetenschap & Technologie, Arenberg Doctoraatsschool, W. de Croylaan 6, 3001 Heverlee, België

Alle rechten voorbehouden. Niets uit deze uitgave mag worden vermenigvuldigd en/of openbaar gemaakt worden door middel van druk, fotokopie, microfilm, elektronisch of op welke andere wijze ook zonder voorafgaandelijke schriftelijke toestemming van de uitgever.

All rights reserved. No part of the publication may be reproduced in any form by print, photoprint, microfilm, electronic or any other means without written permission from the publisher.

Cover image: illustration by Adelaide Tyrol.

ISBN 978-90-8826-309-5
Legal depot D/2013/11.109/36

Dankwoord

Dit is het laatste stukje van mijn 'boekske' dat ik schrijf, maar waarschijnlijk het eerste dat velen zullen lezen. Ik wil hier dan ook alle mensen hartelijk bedanken die – mentaal en/of fysiek – hebben bijgedragen tot het welslagen van mijn doctoraat.

Dit doctoraat was op vele vlakken een leerrijke ervaring. Mijn dank gaat daarom in de eerste plaats uit naar mijn promotor, Prof. Wannes Keulemans, die mij deze kans gegeven heeft. Wannes, bedankt voor de grote wetenschappelijke vrijheid die ik gekregen heb om mijn project uit te voeren. Bedankt ook voor alle steun en vertrouwen 'along the way', voor alle discussies en babbels, maar ook om mij de mogelijkheid te geven leerrijke nationale en internationale congressen en meetings bij te wonen.

Ook het IWT wil ik bedanken voor het vertrouwen in mij als onderzoeker en voor de toegekende doctoraatsbeurs.

Vervolgens zou ik ook mijn co-promotor Mark Davey willen bedanken, oa. voor het vele grondige nalees- en verbeterwerk. Ik heb veel geleerd uit onze samenwerking.

Dank ook aan mijn assessoren Prof. Rony Swennen en Prof. Bruno Cammue voor de tussentijdse suggesties. Many thanks also to the other members of my Examination Committee for reading this manuscript and for your comments and suggestions.

Veel dank gaat ook uit naar mijn collega's in het labo. Iedereen was steeds bereid elkaar te helpen, en ook te steunen in de moeilijkere momenten. Laborantes Yasemin en Katrien hebben mij bovendien veel nuttige informatie en praktische tips bezorgd. Maar ook aan Roos heb ik veel gehad, zowel op wetenschappelijk als niet-wetenschappelijk vlak. En uiteraard mag ik al mijn (ex-)collega's doctoraatsstudenten – en de thesisstudenten – van het labo niet vergeten. Julie zorgden ook voor de nodige momenten van ontspanning, zowel binnen als buiten het labo. Francis, I'll really miss our chats! En Sebastiaan, ik mocht van geluk spreken zo'n goeie thesisstudent als jou te hebben.

Maar ook andere collega's zoals Christine Vos, An Ceustermans, Willem Abts,… wil ik bedanken voor de leuke babbels tussendoor en voor alle aanmoedigingen en geruststellingen in de laatste momenten naar de eindstreep toe. En ook Anke, bedankt voor de leuke tijd en de lekkere pannekoeken ☺

Ook de secretaresses Inge, Griet en An wil ik zeker bedanken voor de hulp allerlei!

Een speciaal woordje van dank gaat naar de collega's van MeBioS en het laboratorium Tropische Plantenteelt, om mij steeds bijzonder gastvrij te ontvangen en wegwijs te maken in het labo. Ook bedankt om samen met ons labo een team te vormen in de facultaire middagsportcompetities ;-).

In het bijzonder wil ik natuurlijk Sebastien Carpentier bedanken, die mij de geheimen van 2D-PAGE heeft helpen doorgronden en mij steeds wist bij te staan met raad en daad. Seb, bedankt voor alle tijd en moeite die je in mijn werk gestoken hebt!

Ook Etienne Waelkens (KUL), Yves Guisez en Karin Schildermans (CeProMa, Universiteit Antwerpen) wil ik bedanken om m.b.v. de krachtige MALDI-TOF/TOF instrumenten de identiteit van interessante eiwitten te onthullen en mij zo te helpen mijn ontdekkingstocht doorheen de appelschurftverdedigings-mechanismen te ondernemen.

Maar daar zou ik al helemaal niet toe gekomen zijn zonder het geschikte startmateriaal: mijn appelboompjes! Poi, bedankt om mij in de serre bij te staan met raad en daad, zodat ik mijn boompjes in de best mogelijke omstandigheden kon opkweken!

Bedankt ook aan Bart Lievens van Scientia Terrae en Jane Debode van het ILVO om mij de geschikte DNA-extractie-protocols aan te leren.

Ook wil ik de studenten bedanken aan wie ik practicum gegeven heb. Jullie werkten niet alleen (bijna) altijd goed mee, maar zorgden ook voor de nodige afwisseling.

Zeker wil ik mijn 'Aarschot-vrienden', 'bio-ingenieur-vrienden', oude en nieuwe badmintonvrienden, Annelies en alle andere vrienden bedanken voor de steun en de momenten van ontspanning. De goeie en leuke babbels, (Alma- en andere) etentjes, 'cafeetjes', gezelschapsspelen, badmintonpartijtjes, mountainbike-tochtjes, weekendjes weg,… gaven mij vaak terug de nodige portie energie om verder te zetten.

En uiteraard mogen hierbij mijn broer Wouter, Loes, oma, en mijn ouders niet vergeten worden. Bedankt voor jullie interesse in mijn doctoraat. En mama en papa, bedankt om altijd achter mij te blijven staan en in mij en mijn doctoraat te blijven geloven. Vooral in de moeilijkere momenten waren jullie een grote steun! En natuurlijk ook bedankt om mijn appelboompjes te helpen oppotten! En papa, zonder jou zou mijn doctoraat statistisch gezien minder waard zijn. Maar ook Anny, Jos (†), schoonbroers Joost en Stijn en 'schoon( )schoonzussen' Olivia en Annick, bedankt voor de interesse en voor de ontspannende momenten!

En tot slot, Dorien, bedankt om steeds een luisterend oor te willen zijn. Bedankt voor de nodige kalmte, voor je relativeringsvermogen en oeverloze geduld. Bedankt om deze onderneming voor mij veel makkelijker te maken! X

En nog één iemand mag ik zeker niet vergeten: Ruben. De bedoeling was dat je zou opdagen als mijn doctoraat afgelopen was, maar je was er iets vroeger, of ik iets later. Hoewel je het aantal werkuren op een dag deed inkorten, heb je in belangrijke mate bijgedragen tot het welslagen van mijn doctoraat. Je deed me alles relativeren en maakte me rustiger. Een glimlach van jou was genoeg om schrijffrustraties te laten wegsmelten als sneeuw voor de zon. Ik zal jou mijn dankbetuiging later zeker eens laten lezen!

Nogmaals aan iedereen én aan iedereen die ik mocht vergeten zijn: BEDANKT!

Bruno

Samenvatting

Appelschurft, veroorzaakt door de ascomyceet *Venturia inaequalis* (Cooke) G. Wint., is wereldwijd de belangrijkste ziekte van de gecultiveerde appel (*Malus* x *domestica*). Ze veroorzaakt aanzienlijke kwaliteit- en opbrengstverliezen van het fruit. De economische verliezen door een slechte controle van appelschurft kunnen oplopen tot 70% van de productiewaarde (Gupta, 1992). De voornaamste strategie in de controle van appelschurft bestaat nog steeds uit frequente behandelingen met fungiciden tijdens het seizoen. Selectiedruk heeft echter geresulteerd in het ontstaan van fungicide-resistente schurftstammen die een bedreiging vormen voor de sector. Daarom zien de meeste Westerse veredelingsprogramma's de selectie van schurftresistente appelcultivars tegenwoordig als een prioriteit. De meeste huidige schurftresistente cultivars zijn voor hun resistentie afhankelijk van één enkel gen, *Rvi6* (*Vf*), dat afkomstig is van de sierappel *Malus floribunda* 821. *Rvi6*-resistentie is echter reeds doorbroken door nieuwe *V. inaequalis* rassen. Dit heeft de interesse gewekt in andere major resistentiegenen, in polygenetisch gecontroleerde resistentie, veroorzaakt door meerdere minor resistentie-genen, en in 'pyramiding' van verschillende resistentiebronnen, om meer duurzame resistentie te bekomen. Er is echter nog steeds een gebrek aan fundamentele kennis van de appel – *V. inaequalis* interactie met betrekking tot de resistentiemechanismen. Zelfs het werkingsmechanisme van *Rvi6*-resistentie is nog steeds grotendeels onbekend. Deze inzichten zijn essentieel voor de ontwikkeling en toepassing van nieuwe merkers in veredelingsprogramma's en dus voor de ontwikkeling van nieuwe resistente cultivars met duurzame resistentie. Dit onderzoek had daarom tot doel een beter inzicht te krijgen in deze resistentie- en verdedigingsmechanismen van appel tegen *V. inaequalis*.

Daartoe werd een high-throughput 'proteomics' technologie toegepast: twee-dimensionele gelelektroforese (2-DE). In eerste instantie moesten een aantal experimentele omstandigheden en procedures op punt gesteld worden. De schurftinfectieprocedure werd geoptimaliseerd en een monogeen *Rvi6*-resistente cultivar ('Topaz'), een polygeen resistente cultivar ('Discovery') en een *V. inaequalis* (ras 1)-gevoelige cultivar ('Golden Delicious') werden geselecteerd voor verder onderzoek. Geschikte 2-DE condities, zoals protocols voor eiwitextractie, eerste- en tweede-dimensiescheiding en eiwitvisualisatie, moesten eveneens geselecteerd worden. De eiwitten werden geëxtraheerd uit de volledige celinhouden van de

appelbladeren en om de resolutie van de eiwitscheiding te optimaliseren, werd geopteerd voor 24 cm IPG strips met pH-bereik 4-7 voor de eerste-dimensiescheiding. Om de eiwitten te visualiseren, werden ze in de meeste experimenten CyDye^{TM} gelabeld alvorens ze via 'difference-in-gel electrophoresis' (DIGE) in de tweede dimensie te scheiden.

Om de plant-schimmel interacties te bestuderen voor resistentieveredelingdoeleinden, is vroege en accurate detectie en kwantificatie van de pathogeen meestal vereist voor een grondige evaluatie van de virulentie van de schimmel en de resistentie van de gastheer. Tot dusver is de evaluatie van schurftresistentie bij appel vooral gebaseerd op artificiële inoculaties en een ziektebeoordeling op basis van chlorose-, necrose- en sporulatiesymptomen van de bladeren (Chevalier *et al*., 1991). Deze methode geeft echter geen accuraat beeld van de infectiegraad en kan geen vroege schimmelontwikkeling in symptoomloze bladeren detecteren. Daarom ontwikkelden we een real-time PCR assay die de 'internal transcribed spacer 2' (ITS2) regio van het 5.8S rRNA-gen van uitsluitend *Venturia* spp. vermenigvuldigt. De resultaten werden vergeleken met de klassieke fenotypische ziektebeoordelingsscores en het assay bleek een snelle, gevoelige en objectieve methode te zijn om schimmelgroei te monitoren en om gastheerresistentie te evalueren.

Vervolgens werden de eiwitprofielen van de *V. inaequalis* geïnoculeerde, mock (water)-geïnoculeerde en controle-bladeren van de *Rvi*6-resistente cultivar 'Topaz' vergeleken. Twee en drie dagen *post* inoculatie (dpi) waren er nog geen verschillen, of waren ze minder uitgesproken of ten hoogste vergelijkbaar met 5 dpi. Op 5 dpi vertoonden de *V. inaequalis* geïnoculeerde bladeren vertoonden een up-regulatie van eiwitten die vooral betrokken zijn in stress-responsen (34 %) en/of in katabolisme (glycolyse en citroenzuur-cyclus; 24 %). Daarentegen waren 60 % van de down-gereguleerde eiwitten betrokken in anabolische processen, nl. in koolstoffixatie (zowel de licht-afhankelijke reacties van de fotosynthese als de licht-onafhankelijke reacties van de Calvincyclus; 40 %) en in gluconeogenese (20 %). Van sommige eiwitten die betrokken zijn in de genoemde pathways detecteerden we verschillende isovormen met differentiële accumulaties. Samenvattend kan gesteld worden dat het energiemetabolisme van de *Rvi*6-resistente 'Topaz'-bladeren gewijzigd werd na infectie. Wanneer de eiwitprofielen van 'Topaz' en de schurftgevoelige cultivar 'Golden Delicious' vergeleken werden, werden dezelfde (categorieën van) eiwitten geïdentificeerd die uitsluitend na infectie differentieel geaccumuleerd waren. De vastgestelde

verdedigingsrespons van ‘Topaz’ bleek minder uitgesproken in ‘Golden Delicious’, wat de verschillen in schurftgevoeligheid tussen beide cultivars zou kunnen verklaren.

Tenslotte werden de responsen na infectie vergeleken van monogeen resistente ‘Topaz’-planten die wel en niet vooraf behandeld waren met fosetyl-Al (Aliette®). Dit preventief, systemisch fungicide veroorzaakte een reductie in ziektesymptomen op de bladeren én in de schimmelgroei zoals gemeten m.b.v. real-time PCR. Het effect van Aliette® was duidelijker waarneembaar m.b.v. de real-time PCR-techniek in vergelijking met de fenotypische ziektebeoordeling. Analyse van de 2-DE eiwitprofielen van de Aliette®-behandelde ‘Topaz’ bladeren toonde aan dat fosetyl-Al de respons van appel op schurftinfectie, die reeds geobserveerd was in de niet-behandelde bladeren, versterkte: dezelfde (categorieën van) eiwitten waren up- en downgereguleerd in de Aliette®-behandelde t.o.v. de niet-behandelde bladeren. Opmerkelijk was dat de geobserveerde Aliette®-geïnduceerde reductie in infectiegraad duidelijk minder uitgesproken was in de schurftgevoelige cultivar ‘Golden Delicious’ (*ca*. 20 % t.o.v. *ca*. 60 % in ‘Topaz’). Dit suggereert dat het voor appeltelers nuttig kan zijn om het gebruik van (monogene) resistentiebronnen en de toepassing van systemische fungiciden zoals Aliette® te combineren.

Samengevat kan gesteld worden dat het gebruik van de 2D-DIGE technologie en het door ons ontwikkelde *Venturia*-specifieke real-time PCR assay enkele interessante inzichten opleverden in de respons van appel na infectie met *V. inaequalis*. Bovendien laten ze ons toe verschillende nieuwe werkhypotheses te formuleren, zoals:

- de infectie-geïnduceerde up-regulatie van eiwitten betrokken in catabolische processen zoals de glycolyse en de citroenzuurcyclus om in een extra energie-voorraad voor de stress-respons te voorzien;
- de infectie-geïnduceerde down-regulatie van eiwitten betrokken in de anabolische koolstoffixatie, d.i. in de fotosynthese en de Calvin cyclus;
- de infectie-geïnduceerde down-regulatie van processen die reactieve zuurstofspecies neutraliseren in een monogeen resistente cultivar vergeleken met een gevoelige cultivar;
- de gelijkenis in de responsen op verschillende soorten stress, zoals abiotische stress (bijvoorbeeld mock-infectie) en biotische stress (bijvoorbeeld schimmelinfectie) en de hypothese dat de aanpassing van de plant aan de verschillende soorten stress

gecontroleerd wordt door gesofisticeerde kwantitatieve effecten eerder dan kwalitatieve;

- de hypothese dat de verschillen in de veranderingen in accumulatie van eiwitten (betrokken in zowel primair metabolisme als verdedigingsrespons) tussen compatibele en incompatibele interacties eerder kwantitatief dan kwalitatief zijn.

Verder onderzoek is nodig om deze hypotheses te valideren en om te bepalen of ingrijpen in de betrokken eiwitten en pathways een strategie zou kunnen zijn om nieuwe resistente cultivars met duurzame resistentie te ontwikkelen.

Summary

Apple scab, caused by the ascomycete *Venturia inaequalis* (Cooke) G. Wint., is the most detrimental disease of cultivated apple (*Malus* x *domestica*) worldwide, causing severe reductions in fruit quality and yield. In case of insufficient control of apple scab, the economic losses can increase up to 70 % of the production value (Gupta, 1992). The main strategy used for scab control is still the frequent application of fungicides throughout the season. However, selection pressure has resulted in the evolution of fungicide-resistant strains of scab that represent a threat to the industry. Therefore, all major Western breeding programs currently view the selection of disease-resistant cultivars as a priority. Most of today's scab-resistant cultivars rely on the introduction of a single gene for scab resistance from the ornamental apple *Malus floribunda* 821, referred to as *Rvi*6 (*Vf*) resistance. However, *Rvi*6 resistance has been overcome by new pathotypes of *V. inaequalis*. This has aroused interest in other major resistance genes, in polygenically controlled resistance, effected by several minor resistance genes, and in 'pyramiding' of different sources of resistance, to confer more durable resistance. However, there is still a lack of fundamental knowledge on the apple – *V. inaequalis* interaction with regard to the resistance mechanism. Even the mechanism of action of *Rvi*6 resistance is still largely unknown. These insights are essential for the development and application of new markers in breeding programs, and thus for the development of new resistant cultivars and for attaining durable resistance. Therefore, the aim of the research presented in this thesis was to gain a better insight in these resistance and defense mechanisms of apple against *V. inaequalis*.

To this end, a high-throughput proteomics technology, two-dimensional gel electrophoresis (2-DE), was applied. First, we needed to fine-tune some experimental conditions and procedures. The scab infection procedure was optimized and a monogenic *Rvi*6/*Vf*-resistant cultivar ('Topaz'), a polygenic resistant cultivar ('Discovery') and a scab race 1 susceptible cultivar ('Golden Delicious') were chosen for further research. The 2-DE conditions, including protein extraction, first and second dimension separation, and protein visualization, also needed optimization. To optimize the resolution of the protein separation, we decided to use 24 cm IPG strips of pH-range 4-7 for the first dimension separation of the proteins extracted from the complete cells of the apple leaves. To visualize the proteins, they were

CyDye™ labeled prior to a two-dimensional difference-in-gel electrophoresis (2D-DIGE) in most experiments.

To study plant-fungus interactions for resistance breeding purposes, early and accurate detection and quantification of the plant pathogen is often required for proper evaluation of fungal virulence and host resistance. So far, the evaluation of scab resistance in apple was mainly based on artificial inoculation and a disease rating that takes into account foliar chlorosis, necrosis and sporulation symptoms (Chevalier *et al*., 1991). However, this method does not provide an accurate measurement of the degree of infection and cannot detect early fungal development in symptomless leaves. Therefore, we developed a real-time PCR assay that amplifies the internal transcribed spacer 2 (ITS2) region of the 5.8S rRNA gene of *Venturia* spp. only. Results were compared with the classical phenotypic disease rating scores and the assay proved to be a fast, sensitive and objective method to monitor fungal growth and to evaluate host resistance.

Further, we compared the proteomes of the *V. inaequalis* inoculated, mock-inoculated and control leaves of the *Rvi*6-resistant cultivar 'Topaz'. At 2 and 3 days *post*-inoculation (dpi), differences appeared not to be present yet, were less distinct, or at most comparable to 5 dpi. At 5dpi the *V. inaequalis* inoculated leaves showed an up-regulation of proteins mainly known to be involved in stress responses (34 %) and/or in catabolism (glycolysis and TCA pathway; 24 %). On the other hand, 60 % of the down-regulated proteins were involved in anabolic processes, i.e. in carbon fixation (both light-dependent reactions of photosynthesis and light-independent reactions of the Calvin cycle; 40 %) and in gluconeogenesis (20 %). Besides, we detected different isoforms of proteins involved in some of these pathways that were differentially accumulated. In summary, the energy metabolism of the *Rvi*6-resistant 'Topaz' leaves was altered upon infection. When comparing the protein profiles of 'Topaz' and the susceptible cultivar 'Golden Delicious', we could identify the same (categories of) proteins that were differentially accumulated exsclusively after infection. The established response of 'Topaz' seemed less explicit in 'Golden Delicious', which could explain the differences in susceptibility of both cultivars.

Finally, the responses upon infection of the monogenic resistant cultivar 'Topaz' with and without preceding treatment with fosetyl-Al (Aliette®) were compared. This preventative, systemic fungicide caused a reduction in foliar disease symptoms and in hyphal growth as

measured by real-time PCR. The effect of Aliette® was more clear using the real-time PCR technique as compared to the phenotypic disease rating score. When we analyzed the 2-DE protein profiles of Aliette®-treated 'Topaz' leaves, we could verify that fosetyl-Al intensifies the apple response upon scab infection that was already observed in the prior experiment (i.e. up- and down-regulation of the same (catgeories of) proteins in the Aliette®-treated leaves compared to the non-treated leaves). Interestingly, the observed Aliette®-induced reduction in degree of infection was notably less distinct in the scab-susceptible cultivar 'Golden Delicious' (~20 % compared to ~60 % in 'Topaz'). This suggests that, for cultivating purposes, it seems useful to combine the use of (monogenic) resistance sources with the application of systemic fungicides such as Aliette®.

In summary, we can state that the use of the 2D-DIGE technology and our developed *Venturia* specific real-time PCR protocol delivered some interesting insights in the response of apple upon *V. inaequalis* infection and allowed us to formulate several new working hypotheses, such as:

- the infection-induced up-regulation of proteins involved in catabolic pathways such as glycolysis and TCA cycle in order to provide an extra energy supply necessary for stress response;
- the infection-induced down-regulation of proteins involved in the anabolic carbon fixation pathways, *i.e.* photosynthesis and Calvin cycle;
- the infection-induced down-regulation of ROS scavenging mechanisms in a monogenic resistant cultivar compared to a susceptible cultivar;
- the similarity in cellular responses to different stresses, including abiotic stresses (such as mock-infection) and biotic stresses (such as fungal infection), and the hypothesis that plant acclimation to different stresses is controlled by sophisticated quantitative rather than qualitative effects;
- the hypothesis that the differences in the changes in accumulation of proteins (involved in primary metabolism as well as defense response) between compatible and incompatible interactions are rather quantitative than qualitative.

Further research is needed to validate these hypotheses and to determine whether interfering with the involved proteins and pathways could represent a strategy for developing new resistant cultivars and for attaining durable resistance.

List of abbreviations

2-DE	two-dimensional gel electrophoresis
2D-DIGE	two-dimensional difference gel electrophoresis
2D-PAGE	two-dimensional polyacrylamide gel electrophoresis
A	Ampere
ABA	abscisic acid
ABC	ATP binding cassette
ACRE gene	Avr9/Cf-9 rapidly elicited gene
AFLP	amplified fragment length polymorphism
Al	aluminium
ANOVA	analysis of variance
APGM	apple phosphoglyceromutase
app.	Approximately
APX	ascorbate peroxidase
AsA	ascorbic acid
ATP	adenosine triphosphate
Avr gene	avirulence gene
BAC	bacterial artificial chromosome
BLAST	basic local alignment search tool
BLASTn	nucleotide BLAST
bp	base pair
BP	band pass
BSA	bovine serum albumin
C	control
C.	*Cladosporium*
CaMV	*Cauliflower mosaic virus*
CBB	Coomassie Brilliant Blue
cDNA	complementary DNA
CeProMa	Centre for Proteome Analysis & Mass Spectrometry
Cf gene	*Cladosporium fulvum* resistance gene
CHAPS	3-[(3-cholamidopropyl)dimethylammonio]-1-propanesulfonate

CHCA	α-Cyano-4-hydroxycinnamic acid
CoA	Coenzyme A
Ct	cycle threshold
cv.	cultivar
DC	compatible with detergents
DHA	dehydroascorbate
DHAR	dehydroascorbate reductase
DIGE	difference gel electrophoresis
DMI	demethylation inhibitor
DNA	deoxyribonucleic acid
dpi	days post-inoculation
dpi	dots per inch
DTT	dithiothreitol
EC	Enzyme Commission
EDS	enhanced disease susceptibility
EDTA	ethylenediaminetetra-acetic acid
ef	elongation factor
ELISA	enzyme-linked immunosorbent assay
EST	expressed sequence tag
EtOH	ethanol
FAD(H_2)	flavin adenine dinucleotide
FBA	fructose-bisphosphate aldolase
FDR	false discovery rate
fig.	figure
fosetyl-Al	fosetyl-aluminium
gDNA	genomic DNA
GFP	green fluorescent protein
GO	Gene Ontology
Gol	'Golden Delicious'
GR	glutathione reductase
Hcr9 genes	homologues of *Cladosporium fulvum* resistance gene *Cf*-9
HcrVf genes	homologues of *Cladosporium fulvum* resistance genes of *Vf* region

HR	hypersensitive response
HSP	heat-shock protein
I	inoculated
ID	identity
IEF	isoelectric focusing
IGG	bovine-γ globuline
IPG	immobilized pH gradient
ITS	internal transcribed spacer
JA	jasmonic acid
kDa	kilodalton
LC	liquid chromatography
LG	linkage group
LMW	low molecular weight
log	logarithm
LRPKm	leucine-rich repeat receptor-like protein kinase
LRR	leucine-rich repeat
M	mock-inoculated
M.	*Malus*
MALDI	matrix assisted laser desorption/ionization
MAT	mating type
MDA	monodehydroascorbate
MDAR	monodehydroascorbate reductase
MOWSE	molecular weight search
mRNA	messenger RNA
MS	mass spectrometry
MS/MS	tandem mass spectrometry
MW	molecular weight
N.	*Nicotiana*
NAD(H)	Nicotinamide adenine dinucleotide
NADP(H)	Nicotinamide adenine dinucleotide phosphate
NCBI	National Center for Biotechnology Information
NDPK	nucleoside diphosphate kinase

No.	number
ON	overnight
PAGE	polyacrylamide gel electrophoresis
PAMP	pathogen-associated molecular pattern
PCD	programmed cell death
PCR	polymerase chain reaction
PDA	potato dextrose agar
PDI	protein disulfide isomerase
PDR	pleiotropic drug resistance
PGK	phosphoglycerate kinase
pI	isoelectric point
PMF	peptide mass fingerprint
PMSF	phenylmethylsulfonyl fluoride
PMT	photo multiplier tube
PR	pathogenesis-related
PTM	post-translational modification
PVPP	polyvinylpolypyrrolidone
QoI	quinone-outside inhibitor
qPCR	quantitative polymerase chain reaction
QTL	quantitative trait locus
R gene	resistance gene
R protein	resistance protein
R^2	coefficient of determination
RC	compatible with reducing agents
rDNA	ribosomal DNA
RH	relative humidity
RNA	ribonucleic acid
ROS	reactive oxygen species
RT	room temperature
RuBisCO	Ribulose-1,5-bisphosphate carboxylase oxygenase
Rvi gene	*Venturia inaequalis* resistance gene
SA	salicylic acid

SAGE	serial analysis of gene expression
SDS	sodium dodecyl sulphate
SOD	superoxide dismutase
spp.	species
SSH	suppression subtractive hybridization
TCA	tricarboxylic acid
TCP	T-complex protein
TH	Towsend-Heuberger
T_m	melting curve temperature
TMV	tobacco mosaic virus
TOF	time of flight
Top	'Topaz'
Tris	tris(hydroxymethyl)-methyl glycine
tRNA	transfer RNA
UniProt	Universal Protein Resource
UniProtKB	UniProt Knowledgebase
USP	universal stress protein
V	Volt
Vh	Volt hours
V. inaequalis	*Venturia inaequalis*
v/v	volume/volume
W	Watt
w/v	weight/volume

Table of contents

Dankwoord ..... **I**

Samenvatting ..... **III**

Summary ..... **VII**

List of abbreviations ..... **XI**

Table of contents ..... **XIII**

1. General introduction **1**

1.1. Rationale 1

1.2. Objectives and outline of the thesis 3

2. Literature review **5**

2.1. Apple scab 5

2.1.1. Life cycle and epidemiology 5

2.1.1.1. Primary phase and primary infection 5

2.1.1.2. Secondary phase and secondary infection 8

2.1.2. Attempts to control apple scab 9

2.1.3. Infection symptoms 10

2.1.3.1. Symptoms on leaves and their evaluation 10

2.1.3.2. Symptoms on fruits 13

2.2. Apple – *Venturia inaequalis* interaction 14

2.2.1. Host resistance 14

2.2.1.1. Gene-for-gene model 14

2.2.1.2. The *Rvi6* locus 16

2.2.1.3. Other resistance loci 21

2.2.1.4. *Venturia inaequalis* 'races' and plant resistance 23

2.2.2. Polygenic resistance 24

2.3. Defense mechanisms 27

2.3.1. The cuticle 27

2.3.2. Reactive oxygen species (ROS) 28

2.3.3. Defense proteins 28

2.3.3.1. R proteins 29

2.3.3.2. Pathogenesis-related (PR) proteins 29

2.3.3.3. ROS detoxification enzymes 31

2.3.3.4. Proteins involved in signal transduction 31

2.3.3.5. Proteins involved in transcription 32

2.3.3.6. Other proteins involved in defense 33

2.3.3.7. The basal metabolism is down-regulated 34

2.3.4. Other molecules involved in defense 34

2.3.4.1. Phytoalexins 34

2.3.4.2. Phytoanticipins 35
2.3.4.3. Hormones involved in signal transduction 35
2.3.4.4. Structural polymers 36
2.3.5. Ontogenic resistance 36
2.4. The use of real-time quantitative polymerase chain reaction (qPCR) for accurate quantification of fungal development in leaves 39
2.5. Proteomics: a tool to investigate plant defense mechanisms 41
2.5.1. Why proteomics among all 'omics' platforms? 41
2.5.2. The art of proteomics 44
2.5.2.1. Gel-based proteomics: two-dimensional gel electrophoresis 44
2.5.2.1.1. Protein extraction 44
2.5.2.1.2. Protein separation 44
2.5.2.1.3. Protein visualization 46
2.5.2.1.4. Mass spectrometry based protein identification 47
2.5.2.2. Gel-free proteomics 49
3. Materials and methods 51
3.1. Plant material 51
3.2. *V. inaequalis* isolates 51
3.3. Inoculation conditions 52
3.4. Visual evaluation of *V. inaequalis* infection 53
3.5. Quantification of *V. inaequalis* growth by real-time PCR 54
3.5.1. Sample preparation and DNA extraction 54
3.5.2. Primer design 54
3.5.3. Real-time PCR amplification and quantification 55
3.6. Statistical analysis 56
3.7. Proteomics 56
3.7.1. Sample preparation and protein extraction 56
3.7.2. Protein quantification 57
3.7.3. CyDye™ labeling for 2D-DIGE 57
3.7.4. Two-dimensional gel electrophoresis (2-DE) 58
3.7.5. Protein visualization, image analysis and quantification 58
3.7.6. Statistical analysis 59
3.7.7. Spot picking and identification 60
4. Symptom evaluation and real-time PCR quantification of *V. inaequalis* infection of apple 63
4.1. Introduction 63
4.2. Choice of three cultivars based on observations of leaf symptoms after inoculation with *V. inaequalis* 64
4.2.1. Experimental setup 64
4.2.2. Results and discussion 64
4.3. Optimization of the scab infection procedure 66

4.3.1. Experimental setup 66
4.3.2. Results and discussion 66
4.4. Visual evaluation of *V. inaequalis* infection 67
4.4.1. Experimental setup 67
4.4.2. Results 68
4.5. Real-time PCR 70
4.5.1. Experimental setup 70
4.5.1.1. Quantification of hyphal growth of *V. inaequalis* 70
4.5.1.2. Sensitivity, specificity, and reproducibility 71
4.5.2. Results 71
4.5.2.1. Validation of the selected *Venturia*-specific primer pair 71
4.5.2.2. Sensitivity, selectivity, and reproducibility of the real-time PCR assay 72
4.5.2.3. Optimization of DNA extracts for real-time PCR quantification of *Venturia* spp. in apple leaves 73
4.5.2.4. Real-time PCR quantification of hyphal growth of *V. inaequalis* 74
4.6. General discussion 77
4.7. Conclusions 81
5. Proteomic analysis of responses of apple to *V. inaequalis* infection 83
5.1. Introduction 83
5.2. Introductory experiments: evaluation of 2-DE protocols 83
5.2.1. Initial 2-DE methods of choice 83
5.2.1.1. Protein extraction and sample preparation 84
5.2.1.2. Protein quantification 84
5.2.1.3. 2-DE 85
5.2.1.4. Protein visualization 85
5.2.2. Results and discussion 86
5.2.2.1. Protein extraction and quantification 86
5.2.2.2. 2-DE and protein visualization 87
5.3. Proteome analysis during infection of a resistant and a susceptible apple cultivar 89
5.3.1. Experimental setup 89
5.3.2. Results and discussion 90
5.3.2.1. Changes in the leaf proteome of the resistant apple cultivar 'Topaz' in response to *V. inaequalis* infection 92
5.3.2.2. Up-regulation of proteins known to be involved in stress responses 100
5.3.2.3. Differential accumulation of proteins involved in the energy and carbohydrate metabolism of 'Topaz' plants 103
5.3.2.4. Six proteins were exclusively up-regulated in the *V. inaequalis* inoculated leaves 107

5.3.3. Comparison of the *Rvi6* scab-resistant cultivar 'Topaz' with the scab race 1 susceptible cv. 'Golden Delicious' 108
5.3.3.1. Higher levels of proteins known to be involved in stress responses 119
5.3.3.2. Down-regulation of ROS scavenging mechanisms 119
5.3.3.3. Differential accumulation of proteins involved in the energy and carbohydrate metabolism 121
5.4. Concluding remarks 121
6. Effect of preventative treatment with fosetyl-Al on responses of apple to V. inaequalis infection 127
6.1. Introduction: Fosetyl-Al (Aliette®), an alternative, systemic fungicide 127
6.2. Experimental setup 130
6.3. Results and discussion 131
6.3.1. Effect of Aliette® on foliar disease symptoms 131
6.3.2. Aliette® reduces hyphal growth of *V. inaequalis* 137
6.3.3. Proteomics analysis of Aliette®-treated 'Topaz' leaves 139
6.3.3.1. Similar alterations in the proteomes of Aliette®-treated and non-treated leaves upon infection 139
6.3.3.2. Aliette® stimulates apple response to scab infection 150
6.4. Concluding remarks 154
7. General conclusions and future perspectives 157

Reference list 167

Appendix I 189

Appendix II 190

Appendix III 191

List of publications 199

Chapter 1

General introduction

1.1. Rationale

Apple scab, caused by the fungus *Venturia inaequalis*, is the most important disease of cultivated apple (*Malus* x *domestica*) worldwide in relation to economic cost of control (Carisse and Bernier, 2002). *V. inaequalis* has a wide geographical range and is found in almost all areas in which apples are grown commercially. However, the disease is more severe in temperate countries with cool, moist climates during early spring (MacHardy, 1996), such as Belgium.

Most major commercial apple cultivars are highly susceptible to this disease (Gessler *et al*., 2006). The fungal infection causes damages to leaves and fruits, which results in severe reductions in fruit quality and yield. In case of insufficient control of apple scab, the economic losses can increase up to 70 % of the production value (Gupta, 1992). On the one hand, yield loss is caused by direct infection of fruits and pedicels. On the other hand, severe leaf damage can lead to a weakened tree with reduced flower bud formation (Verma and Sharma, 1999).

To produce spotless apple fruits and to avoid damage that develops during storage, growers apply fungicide on a regular or weather-determined basis during spring and summer. When interventions start too late, control of apple scab may even require up to 20 fungicide applications in a single growing season (MacHardy, 1996; Holb *et al*., 2003). These intense chemical control programs are costly and pollute the environment. Moreover, selection pressure has resulted in the evolution of fungicide-resistant strains (MacHardy, 1996). Because of all these factors, the growing awareness of the consumers and the implementation of more strict regulations with regard to the use of fungicides, there is clearly a need for a realistic alternative for chemical control.

To limit the need for fungicide applications, scientists acknowledged the importance of breeding for resistance and some apple breeders recognized the potential benefit from

introgressing disease resistance from wild *Malus* species into commercial lines (Hough *et al*., 1953; Dayton and Mowry, 1970; Kellerhals and Furrer, 1994). Currently, all major Western breeding programs view the selection of disease-resistant cultivars as a priority (Gessler and Pertot, 2012).

Backcrossing is used to eliminate unwanted traits from wild *Malus* and select new cultivars that are attractive to both producers and consumers. This process, from the first cross of a commercial cultivar with a wild, disease-resistant *Malus*, is extremely long due to apple's long juvenile phase, the need for more than seven backcrosses and the high heterozygosity of this genus. Therefore, most of today's scab-resistant cultivars rely on the introduction of a single gene for scab resistance from the ornamental apple *Malus floribunda* 821, referred to as *Vf* or *Rvi6*[1]. However, *Rvi6* resistance has been overcome by new pathotypes of *V. inaequalis* (Parisi *et al.*, 1993; Malnoy *et al.*, 2008; Soriano *et al.*, 2009).

This has aroused interest in other major resistance genes, in polygenically controlled resistance, effected by several minor resistance genes, and in 'pyramiding' of different sources of resistance, to confer more durable resistance (Lespinasse *et al*., 2002; Sansavini *et al*., 2002; ; Kellerhals *et al*., 2006). The dependence of scab control on the significant input of agrochemicals is not likely to stop before durable scab resistance is incorporated into new apple cultivars (Bowen *et al*., 2011).

However, there is still a lack of fundamental knowledge on the apple – *V. inaequalis* interaction with regard to the resistance mechanism. Even the mechanism of action of *Rvi6* resistance is still largely unknown. These insights are essential for the development and application of new markers in breeding programs, and thus for the development of new resistant cultivars and for attaining durable resistance (Crosby *et al*., 1992; Gessler and Pertot, 2012).

Since there is a possible discrepancy between the messenger (transcript) and its final effector (mature protein), and since most biological functions in a cell are executed by proteins rather than by messenger RNA (mRNA) (Carpentier *et al*., 2008b), we decided to investigate the apple – *V. inaequalis* interaction in this research project via a proteomics

[1] As the naming of resistances after their origin and the various pathotypes of *V. inaequalis* able to overcome these resistances with numbers may lead to confusions, Bus *et al*. (2009) renamed all resistances and corresponding pathotypes, so that in future the *Vf* resistance will change to *Rvi6*, all pathotypes of *V. inaequalis* unable to infect a *Rvi6*, will be named race *AvrRvi6* and those able to infect a *Rvi6*, *virRvi6*.

approach. Moreover, different post-transcriptional control mechanisms (such as transcript turnover and translational control, e.g. by the action of microRNAs) have an important influence on the phenotype (Mata *et al*., 2005; Valencia-Sanchez *et al*., 2006) and it is more and more demonstrated that these mechanisms play an important role in the regulation of plant defense against pathogens (Voinnet, 2008). With proteomics, we can explore these responses of plants to pathogen attacks at the protein level.

1.2. Objectives and outline of the thesis

The goal of this project was to gain a better insight in the response mechanisms of apple to *V. inaequalis* infection.

The **general objective** was to identify proteins potentially involved in resistance and defense mechanisms. Identification of such proteins could:

- reveal possible targets for use as markers in resistance breeding and contribute to the development of durable resistance;
- deliver new, general insights in plant defense mechanisms, that can create the motivation for similar research in other plant-pathogen interactions and for exploration of the possible use of artificial induction of resistance through elicitors and/or preventative fungicides.

To attain this general objective, we wanted to compare a selection of apple cultivars with different levels of resistance to apple scab (monogenic resistant, polygenic resistant and susceptible cultivars) and relate physiological observations to (changes in) protein profiles.

Since the different visual symptoms upon scab infection and their relation with the protein profiles can be better studied in apple leaves, we decided to investigate the leaves and not the fruits. Although the breeder is mainly concerned about the scab lesions on the fruits, susceptibility of the leaves and the fruits on one tree are related since scab susceptibility is a cultivar specific characteristic. Moreover, because of the long juvenile period of apple trees, it is much more practical to work on the leaves of young, juvenile plants than on the fruits of mature apple trees. Finally, scab resistance breeding is also done based on observations of leaf symptoms upon infection with *V. inaequalis*.

Our **first concrete objective** was the optimization of the conditions for the systematic study of the *V. inaequalis* – *Malus* interaction in these apple cultivars:

- On the basis of observations of external symptoms after scab inoculation, we wanted to choose three appropriate cultivars for further research (one susceptible, one monogenic resistant and one polygenic resistant).
- By means of two-dimensional polyacrylamide gel electrophoresis (2D-PAGE), we wanted to examine which pI protein subsets were interesting for further research, and which staining techniques are the most effective for visualization of the gel separated proteins. After optimization of the 2D-PAGE conditions, we wanted to select the time points after infection that are most relevant for leaf sampling.

The **second objective** was to acquire a detailed image of the evolution of the differences in external leaf symptoms and in infection degree between the monogenic resistant, polygenic resistant and scab susceptible cultivars after inoculation with a characterized *V. inaequalis* race 1.

A **third objective** was to identify the proteins potentially involved in resistance and defense mechanisms of apple against scab (on the level of leaf tissue) by means of 'comparative proteomics'. We did this via:

- a comparison of the constitutive protein profiles of a monogenic resistant and susceptible cultivar
- a comparison of induced protein profiles of compatible (susceptible) and incompatible (monogenic resistant) interactions

After characterization and functional annotation of the identified proteins, we verified the relationships between the protein profiles and the accomplished physiological observations.

The **fourth objective** was to compare the responses of the monogenic resistant cultivar with and without preceding treatment with fosetyl-Al (Aliette®), a systemic fungicide.

Chapter 2

Literature review

2.1. Apple scab

2.1.1. Life cycle and epidemiology

The ascomycete *Venturia inaequalis* Cooke (Wint.) (anamorph: *Fusicladium pomi* (Fr.) Lind or *Spilocaea pomi* (Fr.)) infects members of the subfamily Maloideae, and causes the disease apple scab, the most important disease of apple worldwide. *V. inaequalis* is a hemibiotrophic fungus, which means that it does not only grow on/in living leaves, but also has a necrotrophic phase. The life cycle of *V. inaequalis* can be subdivided into two phases: a sexual or primary phase and an asexual or secondary phase (Fig. 2.1). The primary phase mainly takes place in winter, the secondary in summer (MacHardy, 1996; Verma and Sharma, 1999).

2.1.1.1. Primary phase and primary infection

The fungus overwinters predominantly as pseudothecia (sexual fruiting bodies) that develop in apple leaf litter following a short phase (maximum of four weeks) of saprophytic vegetative growth after leaf abscission (i.e. necrotrophic phase). As most ascomycetes, *V. inaequalis* is anisogamous: the sex organs are differentiated into antheridia in the male and ascogonia in the female haploid parent. Also, it is heterothallic: plasmogamy of the two gametangia can only proceed if the ascogonium and the antheridium originate from parents of opposite mating type, i.e. carry different mating type alleles on the mating type (MAT) locus. The mating type is the result of a complex interaction between the gene products encoded by the different genes situated on this MAT locus (Gisi *et al.*, 2002; Billiard *et al.*, 2011). The ascospores (sexual spores) are produced in the asci, which are in turn carried by the pseudothecium. The optimal temperature for the formation of ascogonia is 8-12°C. The optimal temperature for the maturation of the ascospores is 16-18°C (Verma and Sharma, 1999; Turechek, 2004).

The primary inoculum is released by rainfall in spring during five to nine weeks and mainly consists of ascospores (Verma and Sharma, 1999). These sexual spores have an inner and outer cell wall. The outer cell wall is thin and fragile. The inner cell wall is thick and elastic and protects the ascospores from winter conditions (Jha *et al.,* 2009).

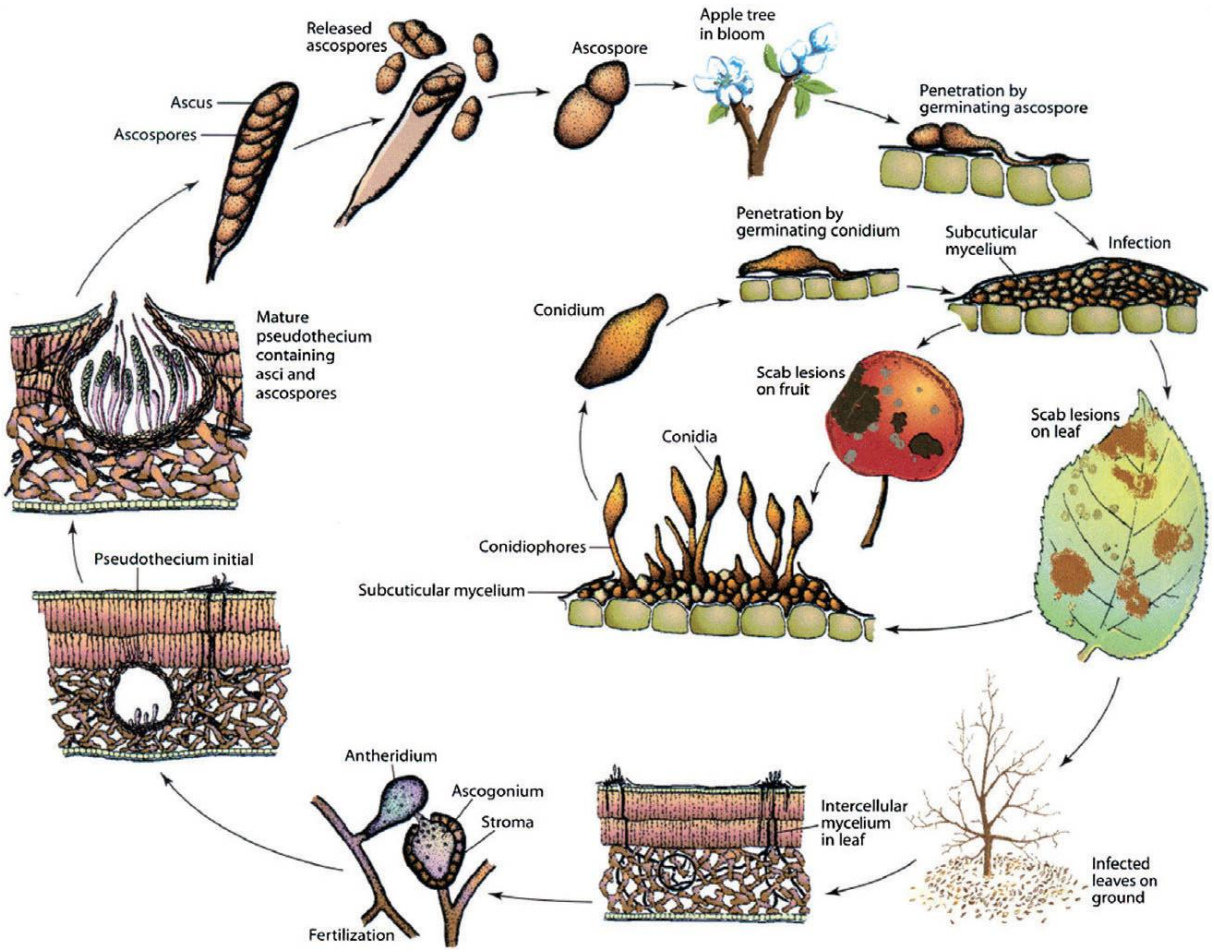

Fig. 2.1. The life cycle of *Venturia inaequalis*. (This diagram was published in Agrios, *Plant Pathology*, p. 506. Copyright Elsevier 2005.)

The asci also have a double cell wall. The release of ascospores can only take place if the inner and outer cell wall of the asci break. During rainfall, a thin waterfilm is formed around the pseudothecia as a result of which the asci adsorb water and expand. Because of the building pressure first the outer cell wall breaks and, in course of time, also the inner. The release of ascospores is favored by sunlight and mainly takes place during the day (Rossi *et al.*, 2001). The spores are spread by the wind up to 200 m from the source (Turechek, 2004).

The primary inoculum lands on the plant (inoculation) after which an infection can take place when conditions are favorable. Free moisture on the leaf surface is absolutely necessary for spore germination. Once initiated, the germination will continue as long as the relative humidity (RH) stays above 95% (Turechek, 2004). Spore germination does not guarantee infection, i.e. invasion and growth of the pathogen. The further development of the fungus is dependent on the temperature, the duration of leaf wetness and the susceptibility of the plant itself and of the inoculated plant organ (leaves vs. sepals and petals, age of the leaf,…). Meteorological criteria defining the duration of (leaf) wetness required for infection at different temperatures were first proposed by Mills and LaPlante (1954), and are known as Mills' periods (Fig. 2.2). These criteria have become a standard tool, in conjunction with electronic weather monitoring, for identifying when conditions suitable for infection occur, so that fungicide applications can be targeted effectively. Infection risk is greatest early in the growing season when leaves and fruit are young and at their most susceptible developmental stage (Xu and Robinson, 2005).

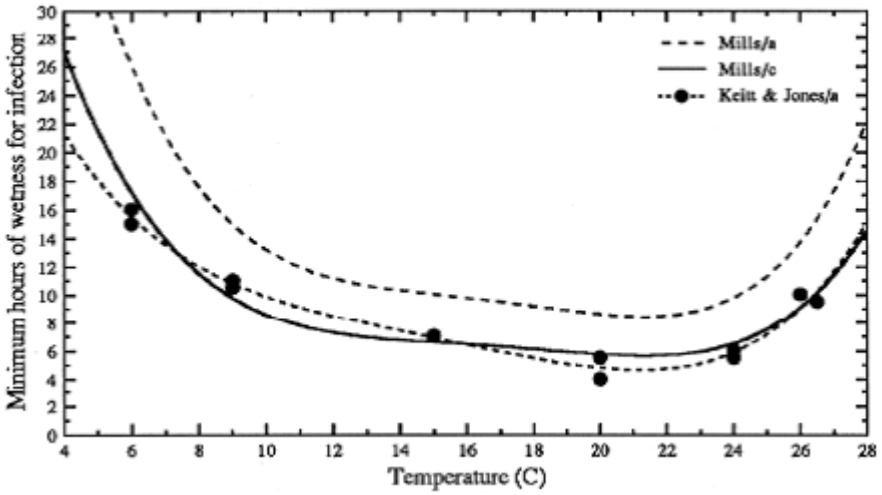

Fig. 2.2. Mills' infection curve depicts the duration of (leaf) wetness that is required at different temperatures for infection by ascospores in field conditions (Mills/a), in a controlled environment (Keitt & Jones/a), and for infection by conidia in field conditions (Mills/c) (MacHardy, 1996).

The germ tubes arising from ascospores penetrate through the cuticle (not through stomata) via an appressorium and differentiate to form subcuticular runner hyphae. At regular intervals, from these subcuticular hyphae, multilayered, pseudoparenchymatous structures, termed stromata, develop. Stromata are made up of laterally dividing cells and are

presumed to obtain nutrients from the subcuticular space. No host (epidermal) cell penetration occurs (Jha *et al.*, 2009; Bowen *et al*., 2011).

2.1.1.2. Secondary phase and secondary infection

Conidiophores are formed following enlargement of the uppermost cells of the stroma, damage and break through the cuticle, and cause the characteristic leaf and fruit lesions that give the disease the name of scab. These macroscopic symptoms become clearly visible at eight to seventeen days after infection. At the top of the conidiophores conidia (or conidiospores) are produced. These spores, produced asexually, are disseminated by rain (and wind) from lesions and allow secondary infection to occur within the orchard throughout the fruit development period. Conidia are less widely spread than ascospores (less than 100 m from the source) and infect mostly the originating plant (Turechek, 2004).

Upon contact with the cuticle, the germ tube of the conidiospore gets differentiated into an appressorium. As the appressorium matures, it becomes firmly attached to the plant surface and a dense layer of melanin is laid down in the appressorium wall, except across a pore at the plant interface. Turgor pressure increases inside the appressorium and a penetration hyphae emerges at the pore, which is driven through the plant cuticle. The important factors for infection are similar to those of the ascospores (Jha *et al.*, 2009).

Many asexual cycles can take place during one growing season. The number is dependent on the host and on the weather conditions during the growing season. The degree of infection will be greater during short wet periods as a result of the rapid production of conidiospores. Indeed, these asexual spores are largely responsible for the scab epidemic if measures are not taken in time in the beginning of the growing season when the ascospores are produced (MacHardy, 2001).

Some overwintering may also occur as conidial pustules in the inner bud tissues without the involvement of the teleomorph (sexual stage), arising from a high level of scab the previous autumn. However, conidia are unlikely to overwinter on the surface of shoots or outer bud tissues, where they are exposed to fluctuating environmental conditions, and, consequently, are unlikely to play a role in initiating an early epidemic of apple scab in the spring (Becker *et al*., 1992; Holb *et al*., 2004).

2.1.2. Attempts to control apple scab

Although our understanding of the life cycle and epidemiology of apple scab has reduced fungicide usage, management of the disease still relies heavily upon chemical control (Bowen *et al*., 2011). During the past five decades, the release of fungicides with new modes of action has occurred concomitant with the development of resistance in older fungicide classes. Dodine was first released in 1959 to control scab, and 10 years later resistance was first recorded (Szkolnik and Gilpatrick, 1969). Since then, apple growers relied on the benzimidazole class of fungicides, such as benomyl, until resistance developed in the 1970s (Jones and Walker, 1976). Today, growers rely on protectant fungicides like captan and dithianon and on the QoIs (quinone-outside inhibitors or strobilurines) completed by a curative control mainly coming from two classes of curative fungicides, the demethylation inhibitors (DMIs), such as myclobutanil (Kuck *et al*., 1995) and difeniconazole, and the anilinopyrimidines like pyrimethanyl and cyprodinil (Piet Creemers, PCFruit - personal communication). However, resistance of *V. inaequalis* to DMI fungicides was documented in practice (Braun and McRae, 1992; Braun, 1994). Although cross-resistance to this and former fungicide classes is not observed, it has been noted that resistance to either benomyl or DMI occurs at a higher frequency in *V. inaequalis* isolates already resistant to dodine compared with sensitive isolates (Köller and Wilcox, 2001). QoI fungicides have been used in Europe for the management of apple scab in commercial orchards since 1996 (Bartlett *et al*., 2002). However, a study in 2004 by Köller *et al*. showed that some *V. inaequalis* isolates had decreased sensitivity to this class of fungicides after only 2 years of use. Also towards anilinopyrimidines resistance of *V. inaequalis* has been reported (Küng *et al*., 1999). Remarkably, no curative fungicides with new modes of action have been developed recently (Chapman *et al*., 2011). Strategies to delay the development of resistance to the different classes of fungicides under field conditions rely on restricting the number of applications per season of fungicides in each class and mixing or alternating fungicides of different classes (Bowen *et al*., 2011). Models for scab management like RIMpro contribute to optimize the spray schedule (Hindorf *et al*., 2000). Nevertheless, new strategies for development of a durable control of apple scab are clearly necessary. The use of compounds or fungicides, acting via elicitation or priming for plant defense enhancement, and the development of new, durable scab-resistant apple cultivars will most likely gain importance in future apple scab management strategies.

2.1.3. Infection symptoms

Although some symptoms of infection by *V. inaequalis* in apple are visible on sepals and petals, young shoots and bud scales, the symptoms are most obvious on leaves and fruits (Turechek, 2004).

2.1.3.1. Symptoms on leaves and their evaluation

Classification

After an incubation period of at least one week, symptoms of scab infection start to appear on the apple leaves. Different apple cultivars have different levels of scab resistance and therefore show very different, specific leaf symptoms that can be attributed to different responses. A well defined classification system of these symptoms is required (Gessler *et al.*, 2006).

A first classification attempt was undertaken by Hough *et al*. (1953). They defined five classes of symptoms using macroscopic criteria. Subsequently, several improvements were made. The updated classification system of Chevalier *et al*. (1991) is widely used today. The symptoms are classified into six classes based on micro- and macroscopically visible reactions in a cross of a commercial cultivar and a *Rvi6*-resistant plant: classes 0, 1, 2, 3a, 3b and 4 (Fig. 2.3). Plants with symptoms of classes 1, 2 and 3a are considered to be resistant to scab. Plants of classes 3b and 4 are considered to be susceptible (Chevalier *et al.*, 1991).

Class 0 comprises plant-pathogen interactions that do not involve any (microscopically visible) symptoms. Class 1 is characterized by the so-called pin-point pits on the leaf surface. These are small (diameter of less than 1 mm), dark depressions in the leaf surface that are the result of a hypersensitive response (HR) of the host to the pathogen attack (Chevalier *et al.*, 1991). At the epicenter of the response zone, the epidermal cells collapse, creating the small pit. The response goes beyond the initially affected cell into the pallisade parenchyma and neighboring epidermal cells, often affecting a large number of cells, presumably involving cell-to-cell signaling (Bus *et al.*, 2005a). Class 2 comprises apple – *V. inaequalis* interactions that result in chlorosis only; classes 3a and 3b comprise those interactions that are characterized by both chlorosis and necrosis. Chlorosis and necrosis can appear joint or separately. The difference between classes 3a and 3b is determined by the intensity of sporulation. In class 3a only a minimal degree of sporulation (<1% of leaf surface) is

observed; in class 3b the sporulation is rather significant (1-50% of leaf surface). Class 4 comprises interactions that are characterized by severe sporulation (>50%) of the leaves without (significant) chlorotic or necrotic lesions (Chevalier *et al.*, 1991).

According to the site of infection, the symptoms develop at the abaxial (lower) or adaxial (upper) surface of the immature leaf. As an end result of scab infection, young leaves can curl, dry out, and drop off early (Turechek, 2004).

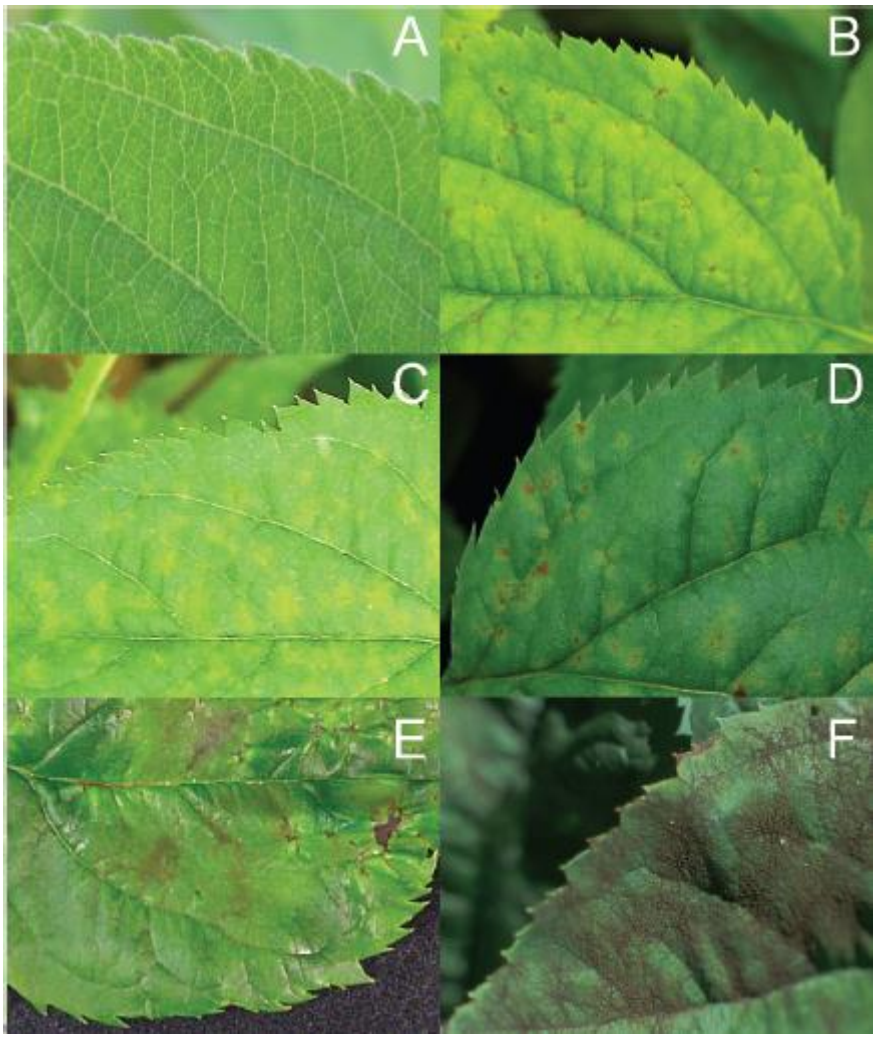

Fig. 2.3. Pictures of the six scab reaction classes of Chevalier *et al.* (1991) about 21 days after *V. inaequalis* inoculation: A. class 0 or no symptoms; **B.** class 1 or 'pin-point pits' (e.g. *Rvi5/Vm* and *Rvi4/Vh4*); **C.** class 2 or chlorosis only; **D.** class 3a or chlorosis and necrosis; **E.** class 3b or chlorosis, necrosis and significant sporulation; **F.** class 4 or complete susceptibility with only sporulation (Gessler *et al*., 2006).

Characteristic leaf symptoms

There are different major resistance genes (see 2.2.1.3) and the presence of each gene can give rise to specific symptoms after infection. For example, the presence of the *Vh2/Rvi2* gene or the *Vh8/Rvi8* gene induces stellate necrosis four to six days after inoculation (Fig. 2.4). Because the resistance response takes off rather late, limited subcuticular growth is possible. Very fine mycelial structures grow from the infection site and cause the typical stellate necrotic lesions. This symptom is classified into Chevalier class 3a (Bus *et al*., 2005a; 2005b).

Fig. 2.4. Stellate necrosis (about 21 days) after *V. inaequalis* inoculation (e.g. *Vh2/Rvi2* and *Vh8/Rvi8*) (Gessler *et al*., 2006).

When a HR is involved, the response is often induced immediately after the cuticle is penetrated. For example, in the case of the *Vm*/*Rvi5* gene (see 2.2.1.3) , the pin-point pits are visible 2–3 days after infection. However, when other *R* genes are involved, e.g. *Rvi15*, it may take 10–11 days for the reaction to be obvious (Galli *et al*., 2010).

Symptom development is also dependent on the genetic background of such major resistance genes. Plants that carry the *Rvi6* region can belong to different classes (0, 2, 3a, 3b and sometimes even 4). Indeed, different *Rvi6*/*Vf*-resistant cultivars show different responses with accompanying symptoms going from barely visible chlorosis to clear necrotic and sporulating lesions (Gianfranceschi *et al.*, 1996). The phenotype is dependent on the genetic background of these *Rvi6*/*Vf*-resistant cultivars. Other major resistance genes can be present, but also 'modifier genes', present in any *Malus* cultivar, whether resistant or susceptible to scab, influence the resulting resistance. *Rvi6* modifiers have an identifiable

effect on pathogenesis only in combination with the major *Rvi6* gene (Gessler *et al.*, 2006). Support for this theory has come from QTL analysis (Seglias, 1997). The study reported the identification of different loci that 'modified' the expression of scab resistance and were effective only in the presence of the *Rvi6* gene (modifier by definition).

The phenotype is not only dependent on the genotype of the cultivar, but also on the genotype of the pathogen. The different genotypes of *V. inaequalis* are subdivided into races (see 2.2.1.4). The environmental conditions influence the symptom development as well. Usually, plants in the field are more susceptible to scab than in greenhouse conditions (Gessler *et al.*, 2006).

2.1.3.2. Symptoms on fruits

Apple scab can cause lesions on fruits as well. These lesions can appear everywhere on the fruit surface, but focus mainly around the calyx. Older lesions turn dark brown, become corky and impede further growth of the fruit in that area. Eventually, they cause necrosis of the epidermis cells and the fruit will show cracks (Fig. 2.5). In this way, the fruit is more susceptible to infections by secondary pathogens (Turechek, 2004; Jha *et al.*, 2009).

Scab susceptibility is a cultivar specific characteristic. Susceptibility of the leaves and the fruits of one tree are therefore related. Just like leaves, fruits become less susceptible with maturity.

Fig. 2.5. Typical scab symptoms on apple fruit caused by *Venturia inaequalis*.

2.2. Apple – *Venturia inaequalis* interaction

Venturia inaequalis mainly infects plants of the genus *Malus*. This includes both cultivated apples (*Malus* x *domestica*) and ornamental apple species (Jha *et al*., 2009). Although most commercial apple cultivars are susceptible to the fungus, resistant cultivars with specific resistance mechanisms exist. At the basis of the different resistance mechanisms lie one or more resistance genes, that are used in breeding programs. The one that is most frequently used, is the well-known *Rvi6*/*Vf* 'gene'. However, the occurrence of new races of *V. inaequalis*, such as race 6 and race 7, that have overcome the *Rvi6* resistance mechanism, explains the necessity to constantly search for new and more durable resistance mechanisms (Soriano *et al*., 2009).

Plant disease resistance mechanisms, and more specifically apple scab resistance mechanisms, can be subdivided into two main groups: host resistance and polygenic resistance.

2.2.1. Host resistance

As from the first physical contact between host and pathogen, a specific interaction can arise. A mechanism that often appears in resistance against hemibiotrophic fungi, and also forms the genetic basis for host resistance of *Malus* against *V. inaequalis*, is the 'gene-for-gene' model (Flor, 1971).

2.2.1.1. Gene-for-gene model

The gene-for-gene model is based on a molecular mechanism by which the product of an avirulence gene (*Avr*) of the pathogen (e.g. an effector) is recognized by the product of a dominant resistance gene (*R*) of the host. The R gene product often is a receptor, therefore the recognition is based on a receptor-ligand model (Flor, 1955; 1971). Most characterized effectors from filamentous fungi, such as *V. inaequalis*, have common features, i.e. they encode small (<400 amino acids in length), cysteine-rich proteins with a putative signal peptide (de Wit *et al*., 2009). The interaction between the Avr molecule and the R protein induces the defense response. This is called an incompatible interaction: the pathogens growth is stopped and no sporulation takes place. When the pathogen is not specifically

recognized by the plant, but is able to grow in the plant and to sporulate, the interaction is named compatible (Fig. 2.6).

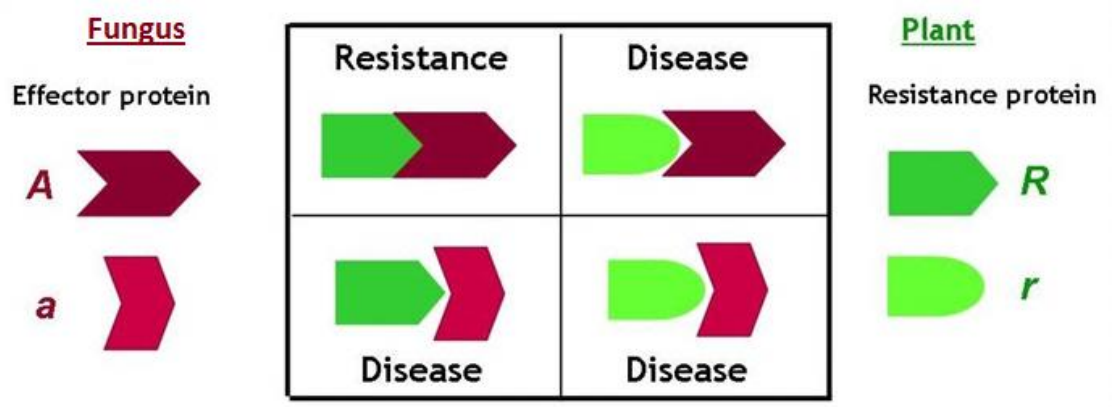

Fig. 2.6. The gene-for-gene model is based on a molecular mechanism by which the product of an avirulence gene (*Avr*) of the pathogen (e.g. an effector) is recognized by the product of a dominant resistance gene (*R*) of the host. Upon recognition, a defense response is induced and there is no disease development. The plant is resistant to the fungus. This is called an incompatible interaction. In the opposite case, disease development is not stopped. This is called a compatible interaction.

The *Malus* – *V. inaequalis* interaction was one of the first reported gene-for-gene interactions. However, such simple interactions based on only two genes occur rather rarely (Bus *et al.*, 2005a). More recently, the 'guard hypothesis' was postulated (Fig. 2.7). The idea is that the pathogen effectors are not directly recognized, but the modification of the host target protein is recognized by the R protein. The R protein thus 'guards' the target of the Avr protein. The advantage of this strategy is that possible changes in the Avr protein do not hamper the recognition by the 'guard' R protein without influencing the virulence action. This guard system was mainly investigated in bacterial attacks, but also appears in fungal interactions of plants (DeYoung and Innes, 2006).

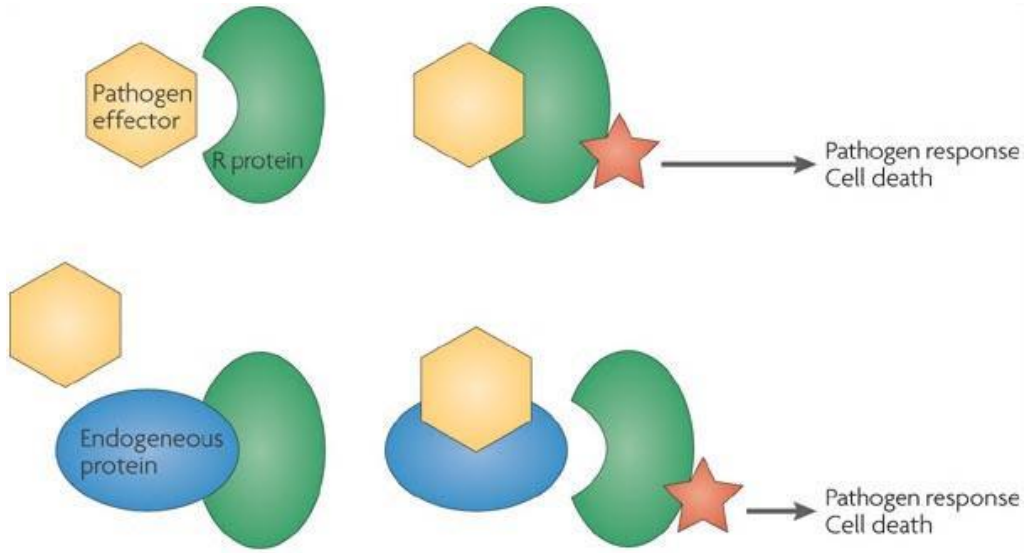

Fig. 2.7. Two major recognition pathways through which plant *R* genes can mediate recognition of pathogen virulence factors. At the top: the **classical gene-for-gene interaction** by which an R protein is activated (indicated by a star) upon direct recognition of pathogen effector molecules. This leads to activation by the plant of pathogen-response signalling cascades, which often culminates in programmed cell death. **At the bottom**: an alternative, indirect strategy, commonly referred to as the **guard hypothesis** by which the plant R proteins associate with and 'guard' host proteins that are common targets of pathogen attack. When pathogen effectors interact with the target host protein and modify it, the associated R protein recognizes the change, is activated and, consequently, triggers the plant's pathogen-response (Bomblies and Weigel, 2007).

2.2.1.2. The *Rvi6* locus

The *Rvi6*/*Vf* resistance locus originates from the ornamental apple *Malus floribunda* 821 (Crandall, 1926). Of all resistance mechanisms the *Rvi6* mechanism was the most widely studied and applied in resistance breeding, and during more than fifty years, it was considered to be a durable resistance mechanism. However, due to intensive use in the breeding of commercial apple cultivars, this source of resistance has been overcome by different pathotypes of *V. inaequalis* (races 6 and 7; Parisi *et al.*, 1993; Bénaouf and Parisi, 2000).

Crossbreeding experiments showed that *Rvi6* resistance is inherited as a monogenic trait. Therefore, this kind of host resistance is often called monogenic resistance. It inherits like a single dominant gene; crosses between a heterozygous *Rvi6* plant and a susceptible cultivar results in a 1:1 ratio of resistant/susceptible progeny. Also, because its effect is consistent

over many generations, i.e. no genetic erosion as would be expected from a complex of many additive genes (QTLs; see 2.2.2) on the same chromosome, the *Rvi6* resistance is indeed qualitative (yes/no) and governed by a single gene (allele) in a gene-for-gene reaction (see 2.2.1.1 above). The fact that the *Rvi6* resistance can be broken by a specific *V. inaequalis* race with a specific genotype, such as race 6, illustrates the qualitative aspect of this resistance as well (Gessler *et al.*, 2006).

However, the *Rvi6* resistance also has some attributes of a quantitative resistance (more/less) and is not strictly dominant. Homozygous *Rvi6* individuals appear to express a stronger resistance than the heterozygous in populations derived from a cross of two heterozygous *Rvi6* parents (Gessler *et al*., 1997; Tartarini *et al*., 2000). Moreover, the *Rvi6* resistance reaction depends on the genetic background in which it is embedded. Next to the effect of the *Rvi6* modifier genes discussed earlier (see Section 2.1.3.1), the existence of a second dominant gene in the original *M. floribunda* 821 tree was demonstrated. This gene, which is linked to *Rvi6*/*Vf*, was originally named *Vfh* because it seemed to induce a hypersensitive reaction. The descendents of *M. floribunda* 821 who carry this *Rvi7*/*Vfh* resistance next to the *Rvi6* resistance showed a residual resistance when the *Rvi6* resistance was broken (Bénaouf and Parisi, 2000).

Identification and characterization of the Rvi6 genes

The apple genome counts 17 linkage groups (LGs) or chromosome pairs (Calenge et al., 2004). The *Rvi6* region is located on linkage group (LG) 1 (Bus *et al.*, 2005a). In efforts to identify the gene(s) responsible for *Rvi6*, Bacterial Artificial Chromosome (BAC) clone contigs in the *Rvi6* region were obtained (Patocchi *et al*., 1999; Xu *et al*., 2001). In 2001 firstly Vinatzer *et al*. reported the identification of a cluster of four receptor-like genes with homology to the family of tomato genes associated with resistance to *Cladosporium fulvum*. They named these four genes *HcrVf1, HcrVf2, HcrVf3 and HcrVf4* (homologous to *Cladosporium fulvum* resistance genes). The same genes have also been identified independently by Xu and Korban (2002), who named them *Vfa1* through *Vfa4*.

It is hypothesized that in the course of evolution two duplication events of the *Rvi6/Vf* gene have occurred, as a result of which the four *HcrVf* genes would be paralogous. Indeed, *HcrVf*1 and *HcrVf*2 are almost identical. However, a certain number of nucleotide

substitutions have taken place and their promoter is different. The sequences of *HcrVf*3 and *HcrVf*4 would be nearly identical as well. The pairwise resemblance could have influenced the co-evolution with the *Avr* gene of *V. inaequalis*. Whether these apple genes recognize the same effector, is not known (Gessler *et al.*, 2006; Malnoy *et al.*, 2008).

Three of the four *HcrVf* genes always co-segregate with *Rvi6* resistance. The transcription of *HcrVf*1, *HcrVf*2 and *HcrVf*4 is complete, while the *HcrVf3* is not functional being its sequence truncated (Belfanti *et al.*, 2004). Thus, *HcrVf*3 is a pseudogene. Differential expression profiles were observed among the three other paralogues during leaf development. *HcrVf1* and *HcrVf2* are highly expressed in immature leaves, but negligibly in mature leaves and, conversely, the expression of *HcrVf4* is higher in mature than in immature leaves (see 2.3.5; Xu and Korban, 2002).

Using Agrobacterium-based transformation techniques, *HcrVf2* was introduced into the scab-susceptible cultivar (cv.) 'Gala' under the control of the strong constitutive *Cauliflower mosaic virus* (CaMV) 35S promoter (Sansavini *et al*., 2003). Under greenhouse conditions, no scab symptoms were present on these regenerated transgenic plants inoculated with *V. inaequalis* (Belfanti *et al*., 2004). The *HcrVf2* gene regulatory sequences were identified (Silfverberg-Dilworth *et al*., 2005) and used in transformation experiments involving 'Gala' and 'Elstar' (Szankowski *et al*., 2009; Joshi, 2010). In most cases, the transformants were resistant to scab and the quantitative expression of the target gene was clearly more similar to the expression observed in classical *Rvi6*-resistant cultivars ('Florina', 'Santana') than that observed in plants transformed using the 35S promoter.

Similar transformation experiments were performed by Malnoy *et al*. (2008) using *HcrVf1*, *HcrVf2* and *HcrVf4*. Only *HcrVf1* and *HcrVf2* incited resistance against scab once inserted into the susceptible cultivars 'Galaxy' and 'McIntosh'. The role of *HcrVf1* in resistance is however questionable, as Joshi *et al*. (2011), in a very detailed analysis, were not able to identify any change in susceptibility, even in transformants expressing the gene at levels several hundred-fold higher than the *Rvi6* control ('Santana').

In summary, it is clear that of the four originally identified *HcrVf* genes, *HcrVf3* is not functional, *HcrVf1* and 4 do not seem to play a role in scab resistance while in all published reports *HcrVf2* has been shown to provide a variable degree of resistance, and this resistance is generally similar to the resistance symptom spectrum found in a set of *Rvi6*

progeny (ranging from no symptoms to necrosis and slight sporulation). *HcrVf2* is also expressed constitutively in transgenic plants under the control of its own promoter and terminator sequences, similarly to the classical bred *Rvi6* cultivars. *HcrVf2*-transformed plants recognize all scab genotypes, except pathotypes 7 (Silfverberg *et al*., 2005) and 6 (Joshi, 2010). Strains of these two pathotypes[2] sporulate on the *HcrVf2* transformants just as they do on the original 'Gala' (Silfverberg *et al*., 2005). Gessler and Pertot (2012) therefore conclude that *HcrVf2* functions in the transformants just as it does in the classically bred *Rvi6* cultivars and that the defense cascade induced by the mechanism of *Rvi6* resistance present in the *Rvi6* cultivars is also present, intact and functional in the susceptible cultivars. For the time being, the mechanism of *Rvi6* resistance is still not understood, as no element of the defense pathway has yet been identified nor have we any explanation of the genes that modify *Rvi6* resistance (Gessler and Pertot, 2012).

Recognition of the pathogen by Rvi6

Although *R* genes have been cloned, many questions still remain as to how they operate. The *HcrVf2* gene, and its paralogues at the *Rvi6/Vf* locus, is most closely related to the *Cf* genes of tomato for resistance to *Cladosporium fulvum*, particularly those belonging to the *Hcr9* (homologues of *C. fulvum* resistance gene *Cf*-9) gene family: *Cf-4*, *Cf-4E*, *Cf-9B* and*Cf-9* (Kruijt *et al*., 2005). The proteins predicted to be encoded by *HcrVf* and the *Hcr9* gene family show the same overall structure with similar functional domains (Fig. 2.8). The predicted protein includes a signal peptide that eventually is cut off (domain A), the cysteine-rich NH_2 terminus of the mature protein (B), a leucine-rich repeat (LRR) region (C), a domain with an unknown function (D), an acidic domain (E) and a hydrophobic transmembrane domain (F) with a basic C-terminus (G) (Vinatzer *et al*., 2001).

The structural similarities between apple and tomato for the *HcrVf* and *Cf-9* genes suggest the presence of similar resistance mechanisms between the two systems. LRR domains, such as domain C, are typical for recognition proteins of a gene-for-gene interaction (Broggini *et al.*, 2009). In the consensus sequence of the LRR, a significant number of glycines are present, suggesting an extracellular location. Although it is well-known that many fungal toxins can be taken up by the plant cell, this implies an extracellular recognition of the

[2] Using the new nomenclature (Bus *et al*., 2009) we would refer to the two pathotypes as races virRvi6 and virRvi7

pathogen, analogous to the Cf resistance proteins (Bowen *et al.*, 2009). The acidic domain E and the basic domain G are consistent with the predicted orientation and anchoring of the protein in the membrane (Gessler *et al.*, 2006; Belfanti *et al.*, 2004).

However, inferences as to whether the *HcrVf* gene products operate by a direct interaction with their cognate Avr effector or are a component of a guard system are harder to draw, as members of the *Hcr9* gene family may operate by either method (Chakrabarti *et al*., 2009; Wulff *et al*., 2009). Also the mechanism by which association with either a modified host protein or a *V. inaequalis* protein would lead to possible conformational changes of the HcrVf protein and to activation of 'downstream' signaling leading to pathogen resistance, is yet unknown (Gessler and Pertot, 2012).

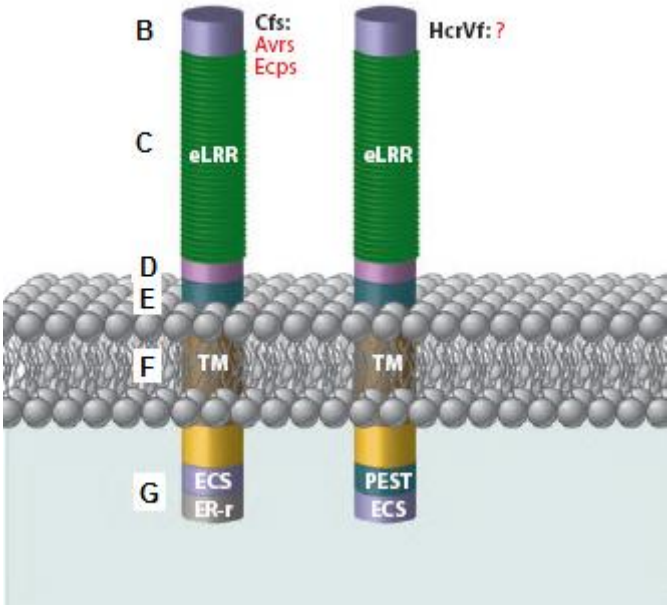

Fig. 2.8. Structure of the homologous tomato Cf and apple HcrVf resistance proteins. Tomato Cfs directly or indirectly recognize *Cladosporium fulvum* avirulence (Avrs) and extracellular (Ecps) proteins, respectively; apple HcrVfs cognate effectors are not known yet. The mature proteins include a cysteine-rich NH_2 terminus (B), a leucine-rich repeat (LRR) region (C), a domain with an unknown function (D), an acidic domain (E) and a hydrophobic transmembrane domain (F) with a basic C-terminus (G). Additional abbreviations: ECS, endocytosis signature (YXX: Tyr-X-X); eLRR, extracellular leucine-rich repeat proteins; ER-r, endoplasmic reticulum retrieval signature (KKRY: Lys-Lys-Arg-Tyr); PEST, Pro–Glu–Ser–Thr signature; TM, transmembrane. Figure is not drawn to scale (adapted from Stergiopoulos and de Wit, 2009).

2.2.1.3. Other resistance loci

Until recently the *Rvi6* locus, originating from *Malus floribunda* 821, was the only scab resistance locus of which the genomic sequences of its genes (*HcrVf1*, *HcrVf2*, *HcrVf3* and *HcrVf4*) were published (Genbank accession numbers AJ297739, AJ297740, AJ297741 and EU794466, respectively). However, Dunemann *et al*. (2012) recently cloned *HcrVf*-like genes from related *Malus* species. Indeed, apart from the *Rvi6* locus, there are quite a lot of other major scab resistance loci known in apple. To date, 17 *R–Avr* gene pairings have been defined (Table 2.1). Throughout history, a lot of changes of names have occurred, because of which it has not always been clear which resistance locus was meant. In 2009, Bus *et al*. have tried to make the nomenclature and the classification more unambiguous and in accordance with other plant-pathogen interactions (Table 2.1).

With the definition of a resistance gene/locus, it is important to clearly describe the macroscopic symptoms, something that has not always been done in the past (Bowen *et al*., 2011). Based on foliar resistance reactions, apple *R* genes can be grouped into three predominant resistance classes exhibiting distinctive resistance responses: the classical hypersensitive response (HR) in which fungal growth is normally terminated very rapidly on penetration inducing pin-point pits (Chevalier class 1; see 2.1.3.1); responses involving limited subcuticular growth inducing stellate necrosis (class 3a); and chlorosis (class 2), sometimes accompanied by necrosis and/or limited sporulation (class 3a; Bowen *et al*., 2011).

Vm/Rvi5, discovered in the wild apple species *Malus micromalus*, and *Vh4/Rvi4* were localized on LG17 (Patocchi *et al.*, 2005) and LG2 (Bus *et al.*, 2005a) respectively, and induce the hypersensitive response (see 2.1.3.1; class 1) upon germination, resulting in pin-point pits 2-3 days after infection. The *Vr2/Rvi15* gene (LG2) also induces HR, though it may take 10–11 days for the reaction to be macroscopically visible (Patocchi *et al.*, 2004; Galli *et al*., 2010). *Va* resistance is a collective term for all resistance mechanisms put into effect by genes originating from the Russian cv ‘Antonovka’. Different progenies of ‘Antonovka’ carry different resistance genes. One particular *Va/Rvi10* gene is considered to be the ‘true’ *Va* gene (Table 2.1; Gessler *et al.*, 2006). This gene is located on LG1 and also causes a pin-point type of reaction (Bus *et al.*, 2005a).

Table 2.1. Nomenclature of the differential host–pathogen interactions of *Malus* and *Venturia inaequalis*, according to the old en new (Bus *et al*., 2009) nomenclature. Every host that is representative of a certain *Rvi* resistance locus, is allocated a number. For example, Golden Delicious is h(1). The *V. inaequalis* races are defined by the avirulence genes they are lacking, hence resulting in susceptibility on the complementary host (Bus *et al*., 2011). Research is in progress to identify F1 progeny in current differential hosts.

Malus						*Venturia inaequalis*		
Differential host		Phenotype	Resistance locus			Avirulence locus		Race
Number	Accession		Historical	LG[a]	New	New	Old	
h(0)	Royal Gala	susceptibility			–	–		(0)
h(1)	Golden Delicious	necrosis	*Vg*	12	*Rvi1*	*AvrRvi1*		(1)
h(2)	TSR34T15	stellate necrosis	*Vb2*	02	*Rvi2*	*AvrRvi2*	*p-9*	(2)
h(3)	Geneva[b]	stellate necrosis	*Vb3*	04	*Rvi3*	*AvrRvi3*[d]	*p-10*	(3)
h(4)	TSR33T239	hypersensitive response	*Vb4 = Vx = Vr1*	02	*Rvi4*	*AvrRvi4*[d]		(4)
h(5)	9-AR2T196	hypersensitive response	*Vm*	17	*Rvi5*	*AvrRvi5*		(5)
h(6)	Priscilla	chlorosis	*Vf*	01	*Rvi6*	*AvrRvi6*		(6)
h(7)	*Malus* x *floribunda* 821[b]	hypersensitive response	*Vfb*	08	*Rvi7*	*AvrRvi7*		(7)
h(8)	B45	stellate necrosis	*Vb8*	02	*Rvi8*	*AvrRvi8*		(8)
h(9)	K2	stellate necrosis	*Vdg*	02	*Rvi9*	*AvrRvi9*	*p-8*	(9)
h(10)	A723–6[b]	hypersensitive response	*Va*	01[c]	*Rvi10*	*AvrRvi10*[d]		(10)
h(11)	A722–7	stellate necrosis/chlorosis	*Vbj*	02	*Rvi11*	*AvrRvi11*[d]		(11)
h(12)	Hansen's baccata #2[b]	chlorosis	*Vb*	12	*Rvi12*	*AvrRvi12*[d]		(12)
h(13)	Durello di Forlì	stellate necrosis	*Vd*	10	*Rvi13*	*AvrRvi13*[d]		(13)
h(14)	Dülmener Rosenapfel[b]	chlorosis	*Vdr1*	06	*Rvi14*	*AvrRvi14*[d]		(14)
h(15)	GMAL2473	hypersensitive response	*Vr2*	02	*Rvi15*	*AvrRvi15*[d]		(15)
h(16)	MIS op 93.051 G07–098[b]	hypersensitive response	*Vmis*	03	*Rvi16*	*AvrRvi16*[d]		(16)
h(17)	Antonovka APF22[b]	chlorosis	*Va1*	01	*Rvi17*	*AvrRvi17*[d]		(17)

[a] LG = linkage group of apple

[b] Temporary differential host until the host has been confirmed as being monogenic, or a monogenic progeny from this polygenic host has been selected.

[c] Provisional placement based on the assumption that the resistance in sources PI 172623 and PI 172633 are identical.

[d] Gene-for-gene relationship not confirmed to date.

Apple cultivars containing *Vh2/Rvi2* or *Vh8/Rvi8* (both LG2) display stellate necrosis upon infection (see 2.1.3.1; Bus *et al.*, 2005a and 2005b). The *Vh8/Rvi8* gene of *M. sieversii* was described together with the according avirulence gene *AvrVh8* of *V. inaequalis* (race 8) by Bus *et al.* (2005b). *Rvi8* appeared to be linked to and possibly allelic to the *Rvi2* gene. *Vr* was first described by Aldwinckle (1976). However, it would concern *Vh2/Rvi2*, which is located at the end of LG2, and, accordingly, it also induces stellate necrosis (Bus *et al*., 2005a).

Other apple *R* genes exhibit resistance responses that lead to chlorosis, sometimes accompanied by necrosis and/or limited sporulation (class 3a), hence providing only partial resistance. The *Vb*/*Rvi*12 gene, originating from 'Hansen's baccata #2' was first located on LG1. However, *Rvi12* appeared not to be linked to the *Rvi6* locus (Hemmat *et al.*, 2003) and was finally located on LG12 (Erdin *et al.*, 2006). The *Rvi*12 resistance reaction is characterized by chlorotic lesions. *Vbj*/*Rvi*11 is a dominant gene originating from *M. baccata* 'Jackii' and is situated on LG2. The resistance response is accompanied with chlorotic and necrotic lesions and sometimes slight sporulation. These symptoms are similar to those caused by *Rvi6* resistance (Gygax *et al.*, 2004). *Vg*/*Rvi*1 originates from Golden Delicious. The gene was located on LG12 and induces typical necrotic lesions (Calenge *et al.*, 2004).

These differences in phenotypic expression of resistance (HR, stellate necrosis and chlorosis) may reflect differences in the defense signaling cascades and resistance reactions induced as a consequence of the different *R* gene-mediated recognition events. In addition, they may also reflect the virulence role of their cognate fungal effectors, perhaps involving suppression of components of the resistance reaction, or differences in the temporal expression of these effectors (Bowen *et al*., 2011).

2.2.1.4. *Venturia inaequalis* 'races' and plant resistance

Venturia inaequalis is genetically not uniform. In 1899 already, Aderhold decided to subdivide the fungus into different 'races'. The differentiation between the different entities is based on the ability to sporulate on different (initially resistant) apple cultivars (MacHardy, 1996). In order to determine to which race an entity of the fungus belongs, the major resistance genes that no longer show resistance to this entity are considered. Indeed, an apple cultivar is resistant to only a limited number of *V. inaequalis* races, and, vice versa, a certain fungal entity is only able to infect a limited number of cultivars. This way, throughout the years, different races have been described. According to the new classification system of Bus *et al*. (2009), up till now 17 *V. inaequalis* races have been defined (Table 2.1; Bus *et al*., 2011). In the future, the notion 'race' will most probably be genotypically characterized in order to obtain a definite, clear-cut classification system.

V. inaequalis can be modified during the sexual reproduction cycle. Moreover, because of the repetitive asexual reproduction cycles throughout the season, it can constantly be

modified by mutations. The fungal genetic material is so-called hypervariable (Jha *et al.*, 2009). The occurrence of new, virulent races of the pathogen, such as races 6 and 7 in Europe, explains the necessity to constantly search for new and more durable resistance mechanisms. The combination of two or more resistance genes in the same genetic background is a possibility and is called 'pyramiding'. Besides the combination of major resistance genes, 'polygenic resistance' (see next section 2.2.2) is of crucial importance in pyramiding (Malnoy *et al.*, 2008; Soriano *et al*., 2009). Many resistance genes tend to group together in gene clusters, for example in a cluster located on LG2 (Bus *et al.*, 2005a). The favorable alleles of these resistance loci often occur in different genetic backgrounds and are difficult to combine through traditional breeding methods. More directed methods that make use of genetic markers, linked to resistance loci, are necessary (see also Fig. 2.9 p.26; Gygax *et al.*, 2004).

2.2.2. Polygenic resistance

Besides the apple cultivars that depend on a certain major resistance gene, cultivars exist that show scab resistance without the presence of such a *R* gene. The resistance of cv. 'Discovery' for example is not induced by a specific recognition gene, but is realized by different genes and thus is inherited polygenically, hence the name polygenic resistance. Because of the complexity of the resistance mechanism and the (possible) interaction between the different genes involved, relatively little research has been done regarding polygenic resistance in apple, especially compared to monogenic resistance.

Polygenic defense mechanisms are constitutively present in the host, regardless the presence of the pathogen, and/or are induced by the penetration of a pathogen. Examples of constitutive defense mechanisms are structural barriers or certain toxic substances (phytoanticipins; see 2.3.4.2). Induced defense mechanisms can be considered to be part of a general stress response. They are induced a few minutes after pathogen attack by the presence of 'pathogen-associated molecular patterns' (PAMPs). Examples of PAMPs are chitin fragments and glucans from the fungal cell wall and extracellular glycoproteins and peptides. Examples of induced defense mechanisms are membrane depolarization, an increase in cytosolic Ca^{2+} concentration, protein modifications and the synthesis of 'pathogenesis-related' (PR) proteins (see 2.3.3.2; Jha *et al*., 2009).

It is important to notice that the constitutive defense mechanisms can change during ontogenesis of the host (or the leaf; see 2.3.5). Moreover, certain PR proteins can accumulate constitutively in one cultivar and in an induced manner in another (Paris *et al.*, 2009).

A number of scab resistance quantitative trait loci (QTLs) have been identified to date in both greenhouse (Calenge *et al*., 2004) and field (Liebhard *et al*., 2003) experiments. A quantitative trait locus is a part of a chromosome that is strongly linked to a certain phenotypical property. QTL analysis is used to localize regions of the genome that contain genes that are altogether involved in a certain quantitative trait. Some of the scab resistance QTLs map to the same regions in which major scab *R* genes have been located, e.g. on linkage groups 1 and 2 (Fig. 2.9; Calenge *et al*., 2004; Dunemann and Egerer, 2010; Durel *et al*., 2003 and 2004; Soriano *et al*., 2009). About half of the LGs of *Malus* contains such *R* gene associated QTLs (Bus *et al.*, 2005a). Other QTLs, such as those on LG11 and LG17, are not associated with major genes, with LG17 being a particular 'hot-spot' for broad-spectrum scab resistance QTLs (Fig. 2.9). QTLs generally confer low levels of partial resistance to a broad spectrum of the pathogen population. In apple, it is increasingly becoming evident, however, that some QTLs are only active against a narrow spectrum of the *V. inaequalis* population. For example, Calenge *et al*. (2004) detected three QTLs with only a single *V. inaequalis* isolate of the eight that were tested and, although some of the other QTLs had a broad spectrum, it was never complete; none of the 24 QTLs were identified with all isolates tested. An isolate-specific QTL was also identified by Durel *et al*. (2003) in close proximity to the *Rvi6* gene. The individual effects of QTLs are variable, ranging from marked to weak (Calenge *et al*., 2004). However, when combined, complementation results in an overall strong resistance. A good example of this is the cultivar 'Antonovka', in which quantitative resistance is the result of a combination of narrow-spectrum genes that together provide a strong and seemingly durable resistance to the pathogen population at large (Gessler *et al*., 2006).

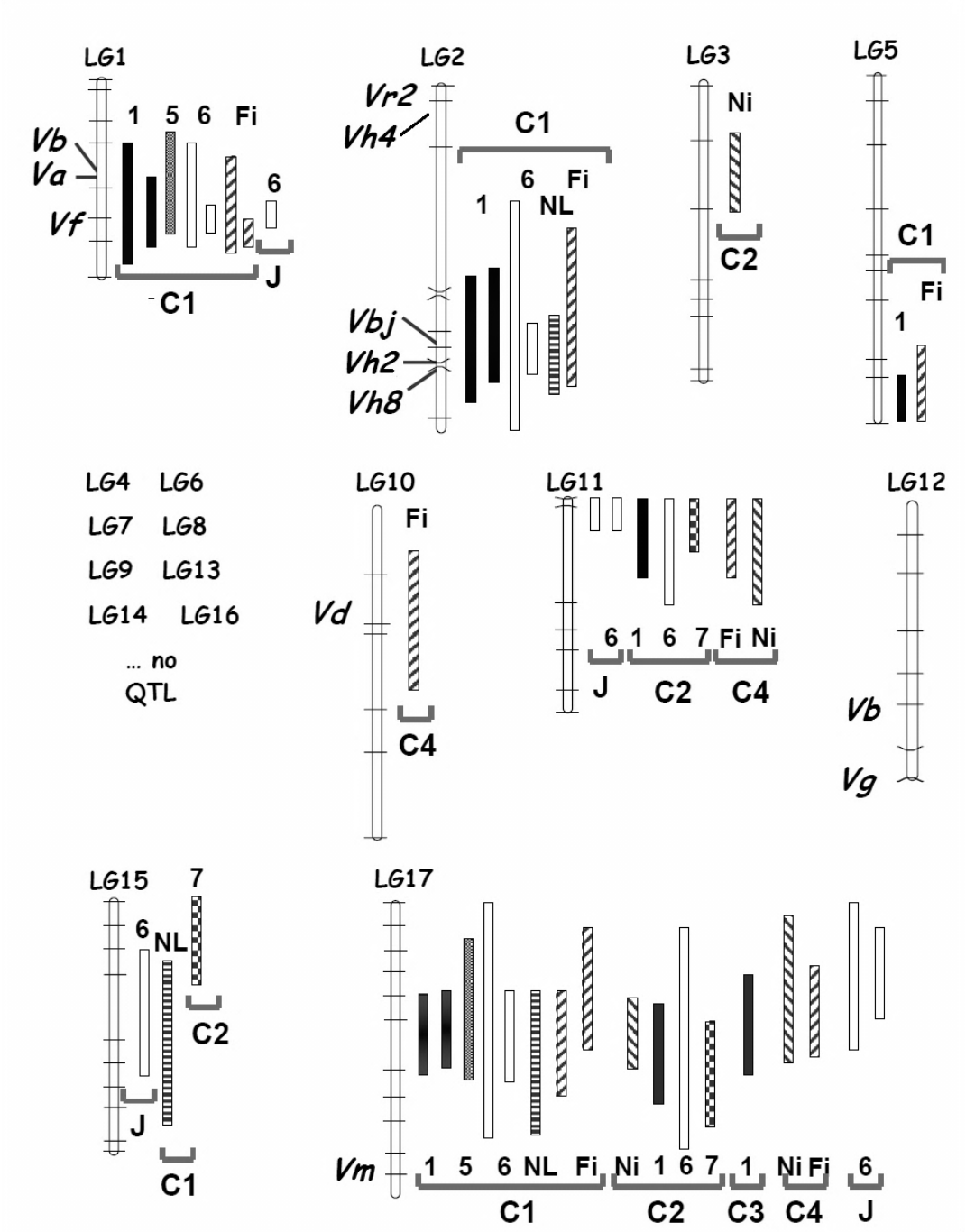

Fig. 2.9. Genomic organization of scab resistance factors in apple. Only those linkage groups (LGs) containing resistance factors are depicted. Vertical bars represent the confidence intervals of the position of the QTLs (2-LOD interval support). Isolates tested: race 1 (black), race 5 (grey), race 6 (white), race 7 (draughtboard), Dutch isolate (NL, horizontal stripe), field isolate (Fi, ascending line), natural inoculation (Ni, descending line). Each bar presents the result of a single isolate. Since in some cases more than one isolate of a race was tested, various bars can be present for a single race. Symbols C1 to C4 and J represent the five F1 progenies studies. The five progenies were derived from crosses between three partial resistant cultivars or hybrids ('Discovery', TN10-8, and 'Durello di Forli'), one moderately susceptible cultivar ('Fiesta'), and one cultivar carrying the *Vf* and *Vg* major resistance genes ('Prima'). Forty common microsatellite markers well-distributed over the genome (horizontal lines) were selected to allow alignment of the constructed genetic maps for the five progenies (adapted from Durel *et al.*, 2004).

2.3. Defense mechanisms

The most important factors for survival of the fungus in the host are the climate and nutritional conditions in the period of time between spore germination and development of the primary hyphae, since the reserves in the spore run out early upon growth through and underneath the cuticle. Next to this, the fungus needs to resist the barriers, both mechanical and chemical, of the host against the pathogen (MacHardy, 1996; Jha *et al.*, 2009).

In the study of the defense mechanisms of apple against scab, it is important to emphasize the importance of *in vivo* studies. Not seldom, defense mechanisms observed *in vitro* could not be confirmed *in vivo*. For example, in contrast with observation *in vitro*, the role of exudates is rather limited *in vivo* (MacHardy, 1996).

2.3.1. The cuticle

In order to survive, the fungal spores must first be able to germinate and grow. For this purpose, *V. inaequalis* demands a certain amount of free water on the leaf surface. Next to the duration of leaf wetness (see Section 2.1.1.1), the hydrophilic properties of the leaf surface, hence the composition of the cuticle, are important in this matter. The cuticle is a rather thin membrane consisting of cutin, polysaccharides and associated solvent-soluble lipids, called cuticular waxes. Cutin consists of a three-dimensional polymer of mostly C16 and C18 hydroxy fatty acids cross-linked by ester bonds (Beisson *et al*., 2012). The cuticular waxes are a complex mixture of very long chain lipids deriving from fatty acids, predominantly of chain lengths from 26 to 34 carbons. Arabidopsis mutants showed that proper expression of genes of the *cer2*-like family (i.e., *cer2* and *cer26*) is very important for the very long chain fatty acid elongation process of these cuticular wax precursors (Pascal *et al*., 2013). The physical and chemical properties of these waxes determine vital functions for plants (Dominguez *et al*., 2011). Indeed, besides playing a major role in limiting uncontrolled water loss, cuticular waxes are important in plant defense against bacterial and fungal pathogens (Raffaele *et al*., 2009).

Next to the composition of the cuticle, also its thickness and robustness determine the rapidity with which the fungus is able to penetrate. The accumulation of cutinase inhibitors in the cuticle and the general structure of the cuticle can attribute to its robustness.

Importantly, the properties of the cuticle and the hydrophilicity of the leaf change during development. This would play a role in ontogenic resistance (see 2.3.5; Köller *et al*., 1991; Jha *et al.*, 2009).

2.3.2. Reactive oxygen species (ROS)

Certain apple cultivars react immediately to the fungal attack by the production of reactive oxygen species (ROS), such as hydrogen peroxide (H_2O_2) and superoxide (O_2^-). This is called 'oxidative burst'. These molecules can be converted to even more reactive ones such as the free oxygen radicals $HO_2^{\cdot}$ and $OH^{\cdot}$. ROS play a role in the hypersensitive response and thus are associated with pin-point symptoms (see 2.1.3.1). This oxidative burst typically occurs in cultivars with certain major *R* genes (see 2.2.1.3), but can also be associated with the recognition of PAMPs. After the pathogen attack, certain proteins accumulate that protect the plant from ROS (see 2.3.3.3). ROS can also function as signal molecules for further defense mechanisms (Lamb and Dixon, 1997; Torres *et al.*, 2006).

2.3.3. Defense proteins

Little research has been done on the proteins important in apple scab defense and on the interaction of these proteins with each other and with other molecules. The knowledge of defense mechanisms of model crops (such as *Arabidopsis*, rice, wheat and tobacco) against their respective pathogens can be used as a basis for the research on apple scab defense (Kim and Kang, 2008).

As mentioned before, the up- and down-regulation of the accumulation of certain proteins is induced during defense response. This induced response is triggered by the specific recognition of the pathogen or as part of a more general stress response (as described above). Other defense proteins are constitutively present. Certain proteins are constitutively present in high concentrations in one cultivar, but attain these concentrations in other cultivars only after infection (Gau *et al*., 2004). The accumulation of defense proteins demands energy of the plant and can be considered to be a disadvantage in absence of the pathogen.

2.3.3.1. R proteins

The induced defense mechanisms are difficult to study, since they are part of a complex combined action of different factors. The host response to a pathogen attack is induced when a signal is recognized that indicates the presence of the pathogen. In the case of the specific recognition of the pathogen (i.e. host resistance), the different apple scab resistance genes (*R* genes) discussed earlier (see 2.2.1), such as the *HcrVf2* gene, code for the recognition proteins. The recognition of a yet unknown avirVf product of the pathogen by the HcrVf2 protein induces a defense cascade of different molecules that is still largely unknown. The difference between a *Rvi6* scab-resistant individual and a susceptible is the lack of the *HcrVf2* gene or rather the correct allele and its product, the recognition protein (Gessler and Pertot, 2012).

Most *R* genes are constitutively present, but certain *R* genes accumulate more after infection, e.g. a gene of apple that is very similar to the *Xa*21 resistance gene of rice (*Oryza sativa*). It is translated into a cytoplasmic protein that possibly interacts with the HcrVf2 receptor and would be used for signal transduction to the nucleus (Paris *et al*., 2009).

2.3.3.2. Pathogenesis-related (PR) proteins

Pathogenesis-related proteins or PR proteins accumulate (more) in the plant as a result of biotic or abiotic stress. They play an important role in the defense against pathogens and the adaptation to stress conditions (Edreva, 2005; van Loon *et al.*, 2006). Also in apple scab defense, the role of a number of PR proteins has been demonstrated. A lot of the PR proteins that are induced in certain, susceptible apple cultivars, are constitutively present in other, resistant cultivars (Gau *et al.*, 2004; Degenhardt *et al.*, 2005; Paris *et al.*, 2009).

Gau *et al*. (2004) compared the apoplastic protein accumulation of the *Rvi6*-resistant cv. ‘Remo’ and the susceptible cv. ‘Elstar’. The apoplast is formed by the continuum of cell walls of adjacent cells as well as the extracellular matrix. It is important for all the plant's interaction with its environment. By means of two-dimensional gel electrophoresis (2-DE) and mass spectrometry (see Section 2.5.2.1), differences in concentration of a number of PR proteins between both cultivars were detected. In the susceptible ‘Elstar’ the number of detectable apoplastic proteins more than doubled after infection. Most of the extra proteins detected had an isoelectric point (pI; see Section 2.5.2.1) between 4 and 5 (Gau *et al.*, 2004).

The concentrations of the respective PR-2, PR-3 and PR-8 proteins *β*-1,3-glucanase (36-40 kDa), chitinase (27-28 kDa) and endochitinase type III (27-28 kDa) are higher prior to infection in cv. 'Remo' than in 'Elstar'. After infection by *V. inaequalis*, the concentrations in 'Elstar' become similar to those in 'Remo'. This suggests a constitutive accumulation of these proteins only in the resistant cultivar. *β*-1,3-glucanase, chitinase and endochitinase are able to hydrolyze the fungal cell wall. The chito-oligosaccharides that are formed as a result of the endochitinase activity, would induce defense mechanisms through a yet uncharacterized pathway (Ramonell *et al.*, 2002; Paris *et al.*, 2009). These proteins were also detected in tobacco plants infected by the tobacco mosaic virus (TMV; Sindelarova and Sindelar, 2001; Gau *et al.*, 2004; Degenhardt *et al.*, 2005).

A thaumatin-like protein (PR-5) is constitutively present in higher concentrations in the apoplast of the resistant cv. Remo. In the susceptible 'Elstar', the accumulation increases upon infection. Thaumatin (21 kDa) is a sweet-tasting protein and considered a prototype for a pathogenesis-related protein (Gau *et al.*, 2004).

Gau *et al*. (2004) also detected osmotin-like proteins and a PR-1 protein (15-16 kDa). These are constitutively present in the resistant 'Remo' but not in 'Elstar'.

The 'Elstar' concentration of a non-specific lipid transfer protein (9 kDa; PR-14) declined to a non-detectable level within the first week after infection by *V. inaequalis* (Gau *et al.*, 2004). A possible explanation is that this protein would play a role in the recognition of the pathogen and the onset of the defense response. It would interact with pathogen's effectors and induce a non-specific, systemic resistance (Blein *et al.*, 2002). Consequently, the expression will decrease when its job is done. The lipid transfer protein also transfers phospholipids through membranes and would play a role in the formation of the cuticle and the epicuticular wax (Diaz-Perales *et al.*, 2002). The reduced accumulation of the *Mal d 3* gene that codes for this lipid transfer protein, was confirmed by Paris *et al.* (2009).

The accumulation of a number of Mal d 1 proteins of the ribonuclease type (PR-10) is increased after infection in a *HcrVf2* transformed 'Gala' (Paris *et al.*, 2009). Besides, the expression of genes that code for defensin-like proteins (PR-12) is also increased after infection. Plant defensins would exert their antifungal activity by altering fungal membrane permeability and by inhibiting fungal macromolecule biosynthesis (Thevissen *et al.*, 1999).

Other proteins involved in defense response are the cysteine proteases. For example, a protein very similar to cathepsin B of *Nicotiana banthamiana* (that is related to tobacco or *N. tabacum*) is upregulated in 'Elstar' after infection. The protease plays an important role in defense by means of induction of apoptosis. In *N. banthamiana* it is involved in the 'non-host' hypersensitive response (Gau *et al.*, 2004; Paris *et al.*, 2009).

The accumulation of a lipoxygenase and a fatty acid hydroperoxide lyase is increased as well in the susceptible cv. 'Elstar' after inoculation, and constitutively in the resistant cv. 'Remo'. These proteins are involved in the metabolism of oxylipins that are involved in the regulation of defense-related genes (Gau *et al.*, 2004; Paris *et al.*, 2009).

2.3.3.3. ROS detoxification enzymes

Reactive oxygen species (ROS) do not only damage the pathogen, but also the plant cells. To counteract this, certain apple cultivars produce protective proteins. For example, in the *HcrVf2* transformed 'Gala', after infection, increased expressions of catalase, ascorbate peroxidase, polyphenol oxidase, glutathione S-transferase and reductase were found. These enzymes are probably involved in the onset of oxidative burst and in the detoxification of ROS (Paris *et al.*, 2009). The increased accumulation of such enzymes was also demonstrated in other plant-pathogen interactions. In TMV-infected tobacco plants, elevated concentrations of peroxidases, polyphenol oxidase, phosphomono-esterase and phosphodi-esterase were found (Sindelarova and Sindelar, 2001).

2.3.3.4. Proteins involved in signal transduction

The expression of certain genes involved in signal transduction is altered after infection. Indeed, once plant receptors recognize a pathogen, a cascade of signal transduction initiates that leads to a spatially and temporally regulated expression of defense reactions. Different types of activators, kinases, phosphatases and 'G-proteins' (i.e. guanine nucleotide-binding proteins that transmit chemical signals originating from outside a cell into the inside of the cell) were found to be differentially accumulated in plants carrying the *Rvi6* gene after pathogen challenge (Paris *et al*., 2009).

Cova *et al*. (2010) described four putative leucine-rich repeat (LRR) receptor-like protein kinases (LRPKm) in 'Golden Delicious', 'Gala' and 'Florina'. Two appear to be transiently up-

regulated 24 h after *V. inaequalis* inoculation in 'Florina' and in the transgenic *Rvi6* 'Gala', but not in the untransformed, susceptible 'Gala' or 'Golden Delicious'. At the cytological level, the LRPKm proteins were localized in the plasma membranes of epidermal cells in resistant genotypes following pathogen challenge. These genes have been mapped on LG 5 and 10 and are not associated with *Rvi6*, which maps on LG 1. It can be speculated that the two LRPKinases may play roles in the signal transduction pathways after pathogen recognition by the HcrVf2 protein (Cova *et al*., 2010).

Paris *et al*. (2009) also detected a sequence similar to the *ACRE* (Avr9/Cf-9 rapidly elicited) genes. It is known that many *ACRE* genes encode for signalling components in the initial development of the defense response. A curculin-like mannose-binding lectin sequence was also found to be up-regulated after infection by *V. inaequalis*. Some lectins have a proven role in plant defense against fungal pathogens, and others have been found to be induced by wounding (Paris *et al.*, 2009).

2.3.3.5. Proteins involved in transcription

Transcriptional re-programming is a key step in a plant's response to pathogen recognition. Different plant-specific transcription factors belonging to different families (like WRKY, AP2, MYB, NAM) are known to be involved in the regulation of genes modulated by pathogen attacks, elicitors and wounding. For example, WRKY factors specifically bind to pathogen response elements, called W boxes (TTGACC/T), in the promoter sequences of defense associated genes (Zhang and Wang, 2005; Paris *et al.*, 2009).

Malnoy *et al*. (2008) postulate that up to 779 bp before the start of the open reading frame of the *Rvi6* locus, there are putative binding sites for activators. The susceptible cultivars 'McIntosh' and 'Galaxy' were transformed with *HcrVf*1, *HcrVf*2 and *HcrVf*4, each with their own promoter. Although the HcrVf2 protein is constitutively present, the expression of the gene can be increased by upregulating transcription factors. The lowered resistance of classically cultivated *Rvi6* resistant apple trees could be due to extra binding sites for repressors in the promoter region (Belfanti *et al.*, 2004; Malnoy *et al.*, 2008; Szankowski *et al.*, 2009).

2.3.3.6. Other proteins involved in defense

There are some more proteins involved in defense mechanisms that do not belong to one of the above mentioned categories.

For example, proteins involved in moving, modifying, storing and degrading proteins are important in stressed apple trees. Mainly the ubiquitin-mediated proteolysis plays a major role (Paris *et al.*, 2009).

In the cv. 'Holsteiner Cox', the elevated levels of certain proteins involved in the nucleic acid metabolism after infection by the non-pathogenic bacterium *Pseudomonas fluorescens* Bk3 implies a drastic change in the translation apparatus. The increased accumulation of an enolase and a NADP-dependent isocitrate dehydrogenase implies a change in the carbon metabolism, and an upregulated O-methyltransferase plays a role in cell wall fortification (Kürkcüoglu *et al*., 2006). In general, enzymes such as pectinases, cellulases, xylanases and polygalacturonases are involved in cell wall synthesis/degradation and composition. Cell wall metabolism plays an important role in the establishment of the resistance reaction (Hückelhoven, 2007).

Elevated levels of a protein similar to patellin 1 were detected in a HcrVf2 modified cv. 'Gala'. Patellin 1 is thought to participate in vesicle-trafficking events. The polarized movement of vesicles to the fungal entry site plays a crucial role in plant defense (Paris *et al.*, 2009). In fact, polarized secretion events give rise to pathogen-induced local cell wall depositions (papillae) by the plant cell directly beneath the penetration hyphae of the fungus. Intriguingly, something similar may happen in the *Malus* - *Venturia* interaction beneath the site of fungal cuticle penetration. These papillae can be formed relatively fast after infection (Hückelhoven, 2007).

Two pleiotropic drug resistance-ATP binding cassette (PDR-ABC) transporters were also identified, and members of this family have proved to be induced by pathogens (Crouzet *et al*., 2006). The expression level of aquaporins would change as well during plant-pathogen interaction. However, the actual role of water transport during plant defense response has yet to be determined (Paris *et al.*, 2009).

2.3.3.7. The basal metabolism is down-regulated

After infection, there is often a down-regulation of the expression of genes involved in primary metabolism, basic signal transduction, basic intracellular traffic, protein destination and storage. Metabolites are rather used in plant defense than in basal metabolism. For example, the down-regulation of the expression of genes involved in chlorophyll synthesis is known in other plant-pathogen interactions. This repression of chlorophyll synthesis could explain the appearance of chlorotic lesions in certain scab resistant apple cultivars (see 2.1.3.1; Paris *et al.*, 2009). However, in order to maintain homeostasis, the catabolic, energy-supplying glycolysis pathway is often up-regulated when a plant is submitted to a stress (Plaxton, 1996). Indeed, the resistance mechanisms that need to be activated in order to respond to stress also require an energy supply (Umeda *et al*., 1994; Block *et al*., 2005).

2.3.4. Other molecules involved in defense

2.3.4.1. Phytoalexins

Phytoalexins are low molecular weight (LMW) molecules that are synthesized *de novo* quite rapidly upon pathogen attack. In spite of the large amount of knowledge on the properties and action of these molecules, there is only little prove on their role in plant defense (Mysore and Ryu, 2004). The role of LMW metabolites is controversial (MacHardy, 1996; Hrazdina *et al.*, 1997).

Phenolic compounds would play a role in the defense of apple against *V. inaequalis*. For instance, the elimination of phenylalanine-ammonia-lyase (PAL), a very important enzyme in the phenol synthesis signal transduction pathway, turns the resistant cv. 'Sir Prize' susceptible (Mayr *et al.*, 1997). PAL catalyzes the first step in the phenyl propanoid pathway and is therefore involved in the biosynthesis of phenolic compounds such as flavonoids, phenylpropanoids and lignin in plants The activity of PAL is known to be induced dramatically in response to various stimuli, including pathogenic attack (MacDonald *et al*., 2007). The main phenolic compounds are present in both susceptible and resistant cultivars. However, the absolute amounts and relative proportions of these compounds differ. *Rvi6* cultivars generally have higher total phenol contents, as well as greater amounts of particular phenolic molecules, as compared with susceptible cultivars, even as these levels vary over the course of the season (Petkovsek *et al*., 2009) and are influenced by cultural

practices (Petkovsek *et al*., 2010). An example of a phenolic compound that is present in higher amounts in older leaves and in resistant apple cultivars is chlorogenic acid (Petkovsek *et al*., 2009). Not only the phenols themselves, but also their degradation products would contribute to resistance development. Phlorizin for example is the most prominent phenolic glycoside in apple and has an inhibitory action on *V. inaequalis* (Gosch *et al.*, 2009). It is mainly present in the cuticle and thus would influence the most critical moment in the survival of the fungus after inoculation: the germination and penetration in the subcuticular space. *V. inaequalis* converts phlorizin to phloretin. This compound has an antifungal action as well (MacHardy, 1996). Gessler *et al.* (2006) conclude from the different studies that it is not the constitutive presence of phenols that causes resistance, but rather a local accumulation and transformation activated by an elicitor.

Infection of apple by *V. inaequalis* also leads to an accumulation of flavanols in the region adjacent to the scab lesions (Treutter, 1998). Malusfuran and derivatives of dibenzofuran are produced upon fungal attack and suppress the germination and growth of *V. inaequalis* (Jha *et al.*, 2009).

2.3.4.2. Phytoanticipins

Plants also produce secondary metabolites with antifungal action that are already present prior to pathogen attack (Mysore and Ryu, 2004). An example of these so-called phytoanticipins is the saponin class of secondary metabolites, that is found in various plant species, including apple (MacHardy, 1996).

2.3.4.3. Hormones involved in signal transduction

Different studies confirm the role of plant hormones as signal molecules in pathogen defense. Examples are ethylene, salicylic acid (SA), jasmonic acid (JA) and abscisic acid (ABA), that can play a role in local and/or systemic defense responses (Robert-Seilaniantz *et al*., 2011).

For instance, in apple, a putative AP2 domain-containing protein, an AP2 transcription factor/ethylene-response element and an EIN3-like protein (EIL2) have been detected in elevated concentrations after infection by *V. inaequalis* (Paris *et al*., 2009). This suggests a possible involvement of ethylene in the establishment of the scab resistance response in

apple. Accordingly, in tobacco, the silencing of the EIL2 transcription factor gene, important in ethylene synthesis, compromised the resistance against blue mold (Borras-Hidalgo *et al*., 2006).

Salicylic acid acts as a signal molecule in systemic acquired resistance, as well as in the localized hypersensitive resistance to avirulent pathogens (Mauch-Mani and Slusarenko, 1996). In leaves of the *Rvi6*-resistant apple cv. 'Florina', transcription of a leucine-rich repeat receptor-like protein kinase (LRPKm1) gene is induced by both *V. inaequalis* infection and salicylic acid treatment. On the other hand, induction of *LRPKm1* was weaker in the inoculated leaves of the susceptible cv. 'Golden Delicious' (Komjanc *et al*., 1999). LRPKm1 is likely to participate in defense-related signalling. In apple, like in other plants, LRR proteins play important roles in recognition in host-pathogen interactions (see Section 2.2.1.2). The activation of genes functioning in perception/transduction, like *LRPKm1*, may provide an explanation to the ability of salicylic acid to induce defense responses.

Although JA and ABA are well-characterized signaling molecules in plant defense responses, their role in apple scab defense has not been studied yet.

2.3.4.4. Structural polymers

In certain plant – pathogen interactions, elicitors could induce the accumulation of structural polymers, such as callose, lignin and suberin. However, in the apple – *V. inaequalis* interaction this could not be verified so far (Colditz *et al.*, 2007).

2.3.5. Ontogenic resistance

Sometimes, *V. inaequalis* lesions on apple leaves appear to reach a maximum radius of 1 cm from the point of infection, then ceasing to expand (MacHardy, 1996). This phenomenon has been attributed to ontogenic resistance that develops as leaves and fruits mature, and is complete by the time leaves are fully expanded and fruits are ripe. Leaf infections become established only on unfolding leaves, with ontogenic resistance developing faster on the adaxial than on the abaxial sides of the leaves during their expansion phase. Ontogenic resistance develops within all apple cultivars, regardless the susceptibility of their younger leaves. However, the leaf age at which this resistance occurs, depends on the cultivar and on environmental conditions. Ontogenic resistance is slower to develop under greenhouse

conditions than in the field, presumably reflecting differential plant tissue maturity rates under different environmental conditions (MacHardy, 1996).

The rates of conidial germination and appressorial differentiation of *V. inaequalis* are not affected by leaf age, but stroma formation and sporulation are reduced in both rate and amount with increasing age of host tissue (Li and Xu, 2002).

The basis of ontogenic resistance is unknown, but the resistance is probably due to a combination of different defense mechanisms. First of all, the constitutive (defense) properties of the leaf can change during ontogenesis (see 2.3.1). Besides, it is known that in certain apple cultivars some defense related proteins are constitutively present in higher concentrations in older leaves than in young leaves. This is the case for Mal d 1, *β*-1,3-glucanase, chitinase and endochitinase type III (van Loon *et al.*, 2006; Paris *et al.*, 2009). Accordingly, in tobacco plants *β*-1,3-glucanase, chitinase en endochitinase are not detectable in young leaves, but do accumulate in older leaves (van Loon *et al.*, 2006).

Insights into the *C. fulvum*–tomato interaction may shed light on the nature of ontogenic resistance in *Malus*. *Cf-9B* confers resistance to mature plants of tomato against *C. fulvum*, but not to seedlings, although it is expressed in young plants (Panter *et al*., 2002). This suggests that the cognate effector of Cf-9B, Avr9B, may target a protein that is guarded by Cf-9B, the accumulation of which is only up-regulated in mature plants (Wulff *et al*., 2009). A similar system could be operating to confer, or contribute to, ontogenic resistance in *Malus*. *HcrVf4* at the *Rvi6* locus is highly expressed in mature leaves, although it is still expressed in immature leaves (Xu and Korban, 2002). Such a gene could be guarding a host target that accumulates at increasing levels throughout maturation, a target for an effector from *V. inaequalis*. However, this would not explain the development of ontogenic resistance in otherwise susceptible cultivars that do not carry such *R* gene.

It has been shown that ontogenic resistance becomes inactive again late in the growing season when leaves start to senesce and dormant lesions renew their development, even on the oldest leaves. This senescence may compromise the ability of the plant to induce a resistance response or may be attended by decreasing activity and amounts of normally constitutively present defense mechanisms and molecules. This phenomenon can be important for the building-up of the primary inoculum of the next growing season (Kollar, 2005).

Ontogenic resistance is observable in all apple cultivars and appears never to have been overcome by the pathogen. If the pathogen can build sufficient biomass to enable successful sexual crossing during winter, despite ontogenic resistance operating, it has no selective drivers to overcome this resistance (MacHardy *et al*., 2001).

2.4. The use of real-time quantitative polymerase chain reaction (qPCR) for accurate quantification of fungal development in leaves

To study plant-fungus interactions for resistance breeding purposes, early and accurate detection and quantification of the plant pathogen is often required for proper evaluation of fungal pathogenicity and host resistance. Currently, the evaluation of *V. inaequalis* in apple is mainly based on artificial inoculation and a disease rating that takes into account foliar chlorosis, necrosis and sporulation symptoms (Chevalier *et al*., 1991; see Section 2.1.3.1 p.10-13). However, this scoring technique has disadvantages. Firstly, several studies in other plant-pathogen interactions have shown that the extent of disease symptoms might be different from the extent of pathogen colonization (Bent *et al*., 1992; Hoffman *et al*., 1999; Thomma *et al*., 1999), meaning that visual evaluation does not always give a reliable insight into the real host-pathogen interaction. Secondly, given the incubation period of *V. inaequalis* of at least one week, symptom-based evaluation gives no idea of early fungal development, while quantification of the pathogen in this symptomless phase is crucial for early assessment of host resistance. Thirdly, the use of an integer scale for rating resistance phenotypes limits the ability of the breeder to discriminate between the plants displaying the highest resistance (Vandemark *et al*., 2002).

To overcome these limitations, techniques are required that can directly measure fungal growth even in the absence of disease symptoms. Such techniques include measurement of fungal-specific constituents such as ergosterol or chitin, immunological-based methods such as ELISA, and the monitoring of fluorescence after inoculations with fungi transformed with a chimeric construct containing the bacterial *uidA* or the green fluorescent protein (GFP) reporter gene. More recently, sequence-based techniques such as RNA hybridization (Mahe *et al*., 1992) and (semi-) quantitative PCR (Hu *et al*., 1993; Lamar *et al*., 1995) have been used to quantify pathogen levels during plant infection. However, there are several disadvantages associated with these techniques (Qi and Yang, 2002; Brouwer *et al*., 2003).

The development of real-time PCR has been an important step forward for accurate pathogen quantification (Heid *et al*., 1996). Real-time PCR differs from classical end-point PCR by the monitoring of the accumulation of the amplicon at each PCR cycle, based on the emission of fluorescence. Quantification of DNA is based on the cycle threshold (Ct) value

measured at the early exponential stage of the amplification process (Mackay *et al*., 2002). Real-time PCR allows accurate template DNA quantification, and due to its high sensitivity (detection in the fg DNA range), the technique is well-suited to study pathogen growth during the initial symptomless phase of infection.

Various types of detection chemistries can be used for monitoring real-time PCR products. They can be divided into either amplicon specific detection methods (Tyagi and Kramer, 1996; Whitcombe *et al*., 1999) or amplicon non-specific methods (Morrison *et al*., 1998). Though the advantage of amplicon specific detection methods (e.g. the TaqMan technology) is the high specificity of the fluorescent signal that is generated, the disadvantage of these specific chemistries is that detection of different amplicons requires different probes. This disadvantage does not apply to amplicon non-specific detection chemistries that are based on fluorophores that associate with double-stranded DNA, such as SYBR Green I. Such fluorophores can also associate with primer-dimers and non-specific amplification products, which can seriously disturb interpretation of the results. However, by including the melting curve temperature analysis (T_m) of the amplicons at the end of the PCR, the accuracy of the amplification PCR can be evaluated (Ririe *et al*., 1997; Schena *et al*., 2004).

The SYBR Green I real-time PCR technique has been increasingly used for detection and quantification of plant pathogenic fungi, including ascomycetes (Schena *et al*., 2004; Lievens *et al*., 2006; Stephens *et al*., 2008; Korsman *et al*., 2012). Most of these protocols use primer sequences that amplify fragments of the internal transcribed spacer regions of the ribosomal RNA genes (rDNA-ITS) of the pathogen. These regions are popular because they have little intraspecific DNA sequence variability but usually sufficient interspecific variability to design species-specific primers (White *et al*., 1990; Lee and Taylor, 1992). Additionally, the fact that rDNA-ITS is present in multiple copies in the genome increases the sensitivity of the protocol (White *et al*., 1990; Borneman and Hartin, 2000). Furthermore, the rDNA-ITS sequences are the most widely available sequences among different organisms in public databases such as GenBank (Benson *et al*., 2004), allowing design of specific primers without the need to determine the nucleotide sequence of the DNA area of interest. Indeed, also the 5.8S rDNA and surrounding ITS1 and ITS2 sequences of different *Venturia* species, including *V. inaequalis*, have already been analyzed (Schnabel *et al*., 1999).

2.5. Proteomics: a tool to investigate plant defense mechanisms

2.5.1. Why proteomics among all 'omics' platforms?

In order to understand how plant cells function, it is necessary to elucidate the different levels of control of cellular processes: the genome, the transcriptome (RNA), the proteome (proteins and peptides) and the metabolome (primary and secondary metabolites).

'Genomics' is the large-scale study of the genome of an organism. The genome holds the basic information which is the same in each cell. This information is independent of time and environmental conditions (Jacobs *et al*., 2000). From a given DNA sequence, a potential function can be assigned, but this potential is not necessarily converted into an actual metabolic role (Cordwell, 1999). Thus, the information available in the DNA is not enough to predict if genes will be expressed and when they will do so, in what amounts the products will be present and how these products might be activated (Jacobs *et al*., 2000). Indeed, other 'omics' approaches such as 'transcriptomics', 'proteomics', and 'metabolomics' are necessary to deal with these dynamic aspects of genome information (Fridman and Pichersky, 2005).

'Transcriptomics' is the study of the whole set of messenger RNA (mRNA) molecules or transcripts produced in a cell and provides a comprehensive view of all active genes at a certain time and condition. mRNA based approaches are high-throughput and highly automated for screening thousands of genes in a massively paralleled manner. However, a transcript is only an intermediate, and there will be a discrepancy between the transcript and the protein encoded (Carpentier *et al*., 2008b). Changes in mRNA transcript levels do not automatically imply corresponding changes in protein amount or activity, and in response to stress, changes occur at the protein level (e.g. post-translational modifications) with no apparent changes in mRNA abundance (Jacobs *et al*., 2000). Moreover, the success of transcriptome studies depends greatly on the genomic progress. Successful approaches like cDNA microarrays, cDNA amplified fragment length polymorphism (AFLP) and serial analysis of gene expression (SAGE) are in practice restricted to model organisms (organisms with elaborate genomic DNA or cDNA/EST sequences available) (Kussmann *et al*., 2006; Carpentier *et al*., 2008a). The genomic sequence of *M. domestica* has only recently become available (Velasco *et al.,* 2010). Therefore, the few transcriptomic studies of the apple-

V. inaequalis interaction (Degenhardt *et al*., 2005; Paris *et al*., 2009) done so far had to make use of the more limited PCR-based suppression subtractive hybridization (SSH) method (Diatchenko *et al*., 1999).

'Proteomics' is the large-scale study of the whole set of proteins present in a cell, tissue or organism at a specific time point under specific conditions (Liska and Shevchenko, 2003). Contrary to genomics and transcriptomics, proteomics had the reputation of being slow and cumbersome. Indeed, because of the 20 amino acid building stones that are chemically much more diverse than the only 4 nucleotides, protein technology is inherently more complex than nucleic acid-based approaches (Carpentier *et al*., 2008a). Subsequently, only a (subcellular/pI/molecular weight) fraction of the total proteome can be analyzed at once. The complexity even expands because of post-translational modifications (PTM). *In vivo* PTMs are covalent processing events that change the properties of a protein by proteolytic cleavage or by addition of a modifying group to one or more amino acids. PTMs can determine a protein's activity state, localization, turnover and interaction with other proteins (Mann and Jensen, 2003). However, improvements of protocols and techniques and the genomic and computational advances that link the genome to the proteome made high-throughput large scale analysis of proteins feasible. Recently, the so-called shotgun proteomics technique (using a combination of high-performance liquid chromatography and mass spectrometry) enabled the identification of even more than 10 000 proteins of *Populus*, mapping to *circa* 25% of the predicted proteome space (Abraham *et al*., 2013). Although, since the beginning of the 21st century, proteomics has become an important research tool, also in the study of plant pathogenic fungi (Gonzalez-Fernandez and Jorrin-Novo, 2012), so far only one proteomics study was done that studies an aspect of the apple-*V. inaequalis* interaction. Gau *et al*. (2004) compared the apoplastic proteome of the scab resistant cv. 'Remo' and the susceptible cv. 'Elstar' and found that several PR proteins are constitutively present in the former but not in the latter (see Section 2.3.3.2).

'Metabolomics' is the most recently introduced '-omics' to support functional genomics. The metabolome is the complete set of metabolites present in a cell, tissue or organism at a specific time point under specific conditions (Hollywood *et al*., 2006). A large portion of the genes in a plant genome encodes enzymes (parts of the proteome) that determine the production and concentrations of the primary and secondary (specialized) metabolites

(Fridman and Pichersky, 2005). Considering that changes in the levels of individual proteins do not necessarily reflect the changes at the level of metabolite concentrations, metabolomics takes the 'omics' approach one step further. However, the metabolites within the cell have no shared chemical features on which a general isolation, separation or identification method can be developed. Metabolic profiling techniques allow for the extraction and separation of only a small subset of metabolites and only a fraction of them have been identified (Hollywood *et al*., 2006).

Finally, we should note that inheritance of biological information to future generations does not only depend on the replication of DNA and the Mendelian principle of distribution of genes. In addition, external and environmental factors can influence traits that can be propagated to offspring, but the molecular details of this are only beginning to be understood. The discoveries of DNA methylation and post-translational modifications on chromatin and histones provided entry points for regulating gene expression, an area now defined as 'epigenetics' and 'epigenomics' (Kessler, 2010). Also microRNAs (miRNAs), non-coding RNAs that range in size from 17 to 25 nucleotides, are known to regulate a large variety of biological functions. MicroRNAs control gene expression generally by affecting mRNA degradation and translation, as well as chromatin structure, thereby having impacts on transcription rates (Valencia-Sanchez *et al*., 2006). Thus, the result of their action will generally be reflected in the proteome. Modern quantitative proteomics can also accurately monitor whole proteome changes in response to epigenetic perturbation of the gene expression machinery (Eberl *et al*., 2011).

Because of the above mentioned shortcomings of transcriptomics and metabolomics, the lack of the genomic sequence of *M. domestica* at the time this research was initiated, and the expertise of our lab and our department in performing proteomics studies (Vanhoucke, 2006; Carpentier *et al*., 2008b), we decided to apply proteomics as a tool to study the defense mechanisms of apple against *V. inaequalis*. In the end, the results from different 'omics' approaches (transcriptomics, proteomics and metabolomics) should be integrated into a single systems biology approach, in order to understand the complexity of the defense mechanisms of apple against its most important pathogen.

2.5.2. The art of proteomics

Proteomics encompasses different steps that rely on various technologies. A typical proteomics workflow consists of: (i) protein extraction (ii) separation and quantification and (iii) mass spectrometry based identification.

There are two main approaches to address proteome analysis: a gel-based approach and a gel-free approach.

2.5.2.1. Gel-based proteomics: two-dimensional gel electrophoresis

In a gel-based approach, proteins are first separated by means of two-dimensional gel electrophoresis (2-DE) and then digested for further mass spectrometry identification. 2-DE is a complete methodology for separation of complex protein mixtures providing a qualitative and quantitative high resolution image of intact proteins.

2.5.2.1.1. Protein extraction

In protein extraction, the goal is to limit protein loss while minimizing the amount of other, interfering compounds in the extract. The watery content of the plant vacuole results in very low protein yields compared to bacteria or animal tissues. Several methods have been reported for protein extraction from plant materials that are able to cope with the presence of interfering compounds such as phenolic compounds, carbohydrates, proteolytic and oxidative enzymes, pigments, etc. A detailed list of protein extraction protocols for a series of species (banana, pear, apple, potato, maize, etc.) has been given by Carpentier *et al*. (2008b).

2.5.2.1.2. Protein separation

The 2-DE protocol separates individual denatured proteins in a complex protein mixture according to two independent properties: isoelectric point (pI) and molecular weight (MW) (Fig. 2.10). This technique was introduced in the 1970's by O'Farrell *et al*. (1975). Briefly, isoelectric focusing (IEF) separates the proteins by their differences in electric charge taking advantage of the amphoteric character of proteins (the fact that proteins change charge depending on the pH of the environment). The intrinsic charge of a protein is the sum of charges of all the amino acid groups. To accomplish the separation, an electric field is

applied onto the proteins that are forced to move through an IPG strip (acrylamide gel matrix copolymerized with a pH gradient; commercially available). When a protein is in a pH region different from its pI, it will be charged and it will migrate. When proteins reach their isoelectric point (pI; pH at which the protein carries no net charge), they stop migrating and are said to be `focused' (Fig. 2.10, steps 1-3; Righetti *et al.*, 2008; Görg *et al.*, 2009).

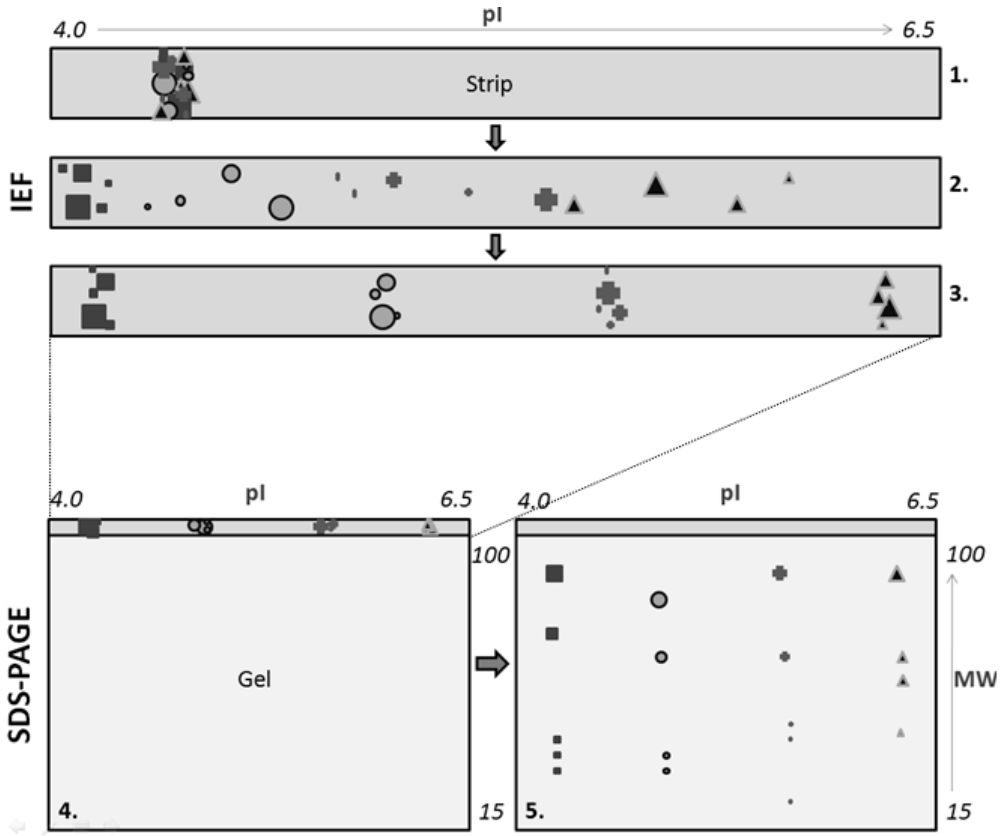

Fig. 2.10. Schematic representation of the separation of proteins in the first dimension by isoelectric focusing (IEF) and in the second dimension by SDS polyacrylamide gel electrophoresis (SDS-PAGE). The proteins are first applied to a medium with an immobilized pH gradient (IPG), *in casu* an IPG strip pH 4-7, via cup loading (step 1). Subsequently, an electric field is applied and the proteins migrate (step 2) until they are 'focused' at the site where the pH of the strip is equal to their intrinsic isoelectric point (pI; step 3). After an equilibration step, when the proteins acquire a constant mass/charge ratio, the IPG strip is applied to a polyacrylamide gel (step 4). During SDS-PAGE, the electrophoretic mobility of proteins is solely dependent on molecular weight (MW; step 5). The resulting two-dimensional map reveals proteins separated on the horizontal axis based on pI and on the vertical axis based on MW.

After completion of the IEF, the IPG strip with the separated proteins is used as starting point for the second dimension separation using SDS-PAGE. SDS polyacrylamide gel

electrophoresis (SDS-PAGE) separates proteins based on molecular weight (MW). Before this second dimension can be carried out, proteins on the IPG strip need to be equilibrated in an excess of the anionic surfactant sodium dodecyl sulphate (SDS) to eliminate the intrinsic charges of the proteins and to become a constant mass/charge ratio. Due to this, the secondary and tertiary structure of proteins are eliminated and after reduction of the disulfide bridges between cysteines, the electrophoretic mobility of proteins is solely dependent on molecular weight. The acrylamide separating gel is composed of different particle sizes; thus, smaller molecules will move faster compared to large molecules which will be slowed down (Fig. 2.10, steps 4-5). With IEF and SDS-PAGE combined, protein separations are possible with an accuracy of 0.02 pH and 3-5 kDa (Righetti *et al.*, 2008).

2.5.2.1.3. Protein visualization

The most commonly used visualization methods for quantitative analysis of gel separated proteins use colloidal Coomassie Brilliant Blue (CBB), silver staining, radiolabeling and fluorescent staining (Miller *et al*., 2006). However, these stains present certain limitations in terms of detection limit (e.g. CBB staining), dynamic range and compatibility with mass spectrometry (e.g. silver staining). Moreover, one of the major limitations of comparative 2-DE using one of these 'post-staining' techniques is the high gel-to-gel variation. This experimental variation can mask small biological differences in accumulation that could be biologically relevant. To overcome this issue, the 'pre-staining' two-dimensional difference-in-gel electrophoresis (2D-DIGE) technology was developed (Alban *et al*., 2003). In 2D-DIGE three samples are labeled prior to the electrophoretic separation with spectrally resolvable cyanine dyes (Cy2, Cy3 and Cy5). Subsequently, the samples are mixed prior to IEF and resolved on the same 2-DE gel. The primary advantage of multiplexing samples is that an internal standard, that consists of equal amounts of protein of each sample under investigation, can be included as one of the three samples to normalize protein abundance across multiple gels. This way, gel-to-gel variation can be traced and compensated for. Moreover, the identical spot pattern of the internal standard in each gel improves the confidence of inter-gel spot matching and quantification of differences in protein abundance. Consequently, 2D-DIGE reduces the number of gels needed in an experiment. Furthermore, this post-staining technique has a very broad linear dynamic range (10^4 to 10^5) and is very sensitive with a limit of protein detection in the lower nanogram range. However,

to achieve these broad dynamic range and good sensitivity, the use of the cyanine fluorescent dyes should be combined with a specialized image scanner, such as the Typhoon™ Variable Mode Imager (GE Healthcare) (Tonge *et al.*, 2001; Alban *et al.*, 2003; Marouga *et al.*, 2005). An experimental flowchart of 2D-DIGE is given in figure 2.11.

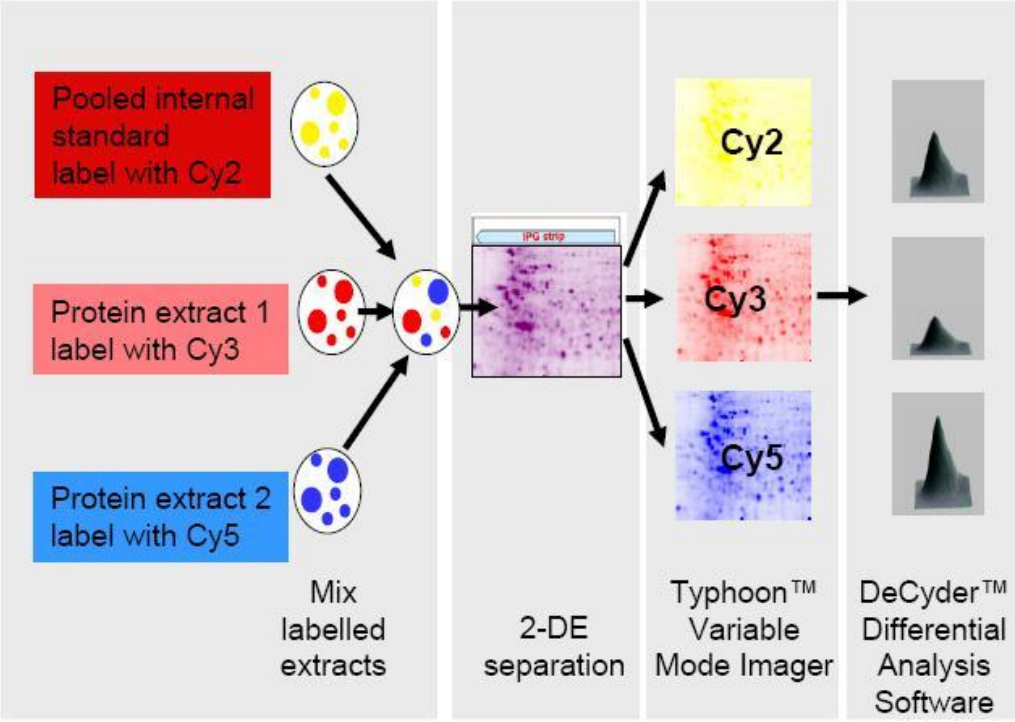

Fig. 2.11. Workflow of 2D-DIGE experiments (GE Healthcare). Two protein test samples and one internal standard sample are labeled with Cy3, Cy5 and Cy2 respectively prior to their separation. The samples are mixed and separated on one gel in two dimensions (multiplexing). Scanning of the gel at three different wavelengths results in three images, corresponding to the three dyes. These images are further used for analysis of differences in protein abundance.

2.5.2.1.4. Mass spectrometry based protein identification

After separation of the proteins and detection and quantification of the differentially accumulated spots, it is key to determine the identity of the corresponding protein. Mass spectrometry (MS), e.g. matrix assisted laser desorption/ionization – time of flight (MALDI-TOF), is the technology most widely used for this purpose. After the unknown proteins of interest are cut out of the gels, they need to be digested into smaller peptides by using a

specific protease, e.g. trypsin, before being introduced in a mass spectrometer. A mass spectrometer consists of an ion source (e.g. MALDI) to produce ions from the sample, one or more mass analyzers (e.g. TOF) to separate the ions based on their mass/charge (m/z) ratios, a detector to register the number of ions coming from the last analyzer, and a computer to process the data and produce the mass spectra. (Steen and Mann, 2004; Lane, 2005).

The introduction of the matrix assisted laser desorption/ionization (MALDI) technique for mass spectrometry analysis of proteins (Karas and Hillenkamp, 1988) has enabled the high-throughput identification of proteins. By using these soft ionization technique, there is minimal fragmentation and mostly entire ions are formed. A schematic representation of the MALDI process is given in figure 2.12.

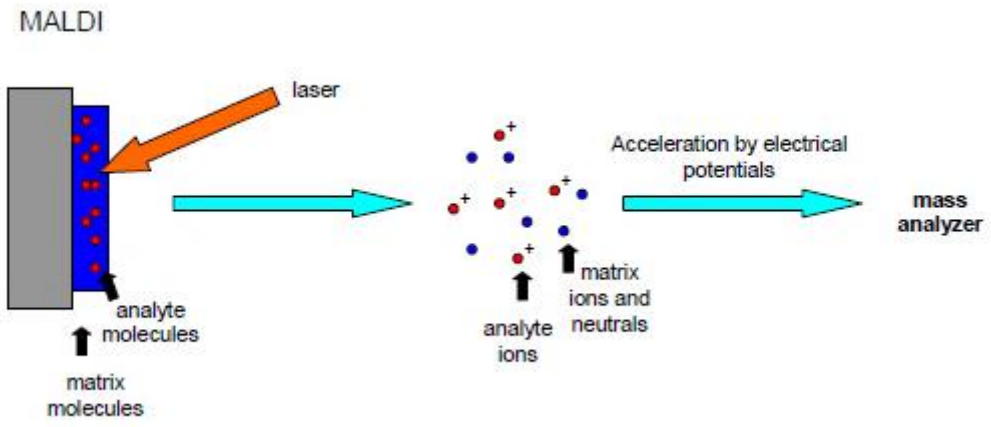

Figure 2.12: **Matrix assisted laser desorption/ionization (MALDI).** In MALDI, the analyte is mixed with a large excess of matrix. Both the analyte and the matrix are irradiated with a laser beam enabling the excess matrix molecules to sublime and transfer the embedded non-volatile analyte molecules into the gas phase. Mostly single protonated ions are formed and accelerated by electric potentials into a mass analyzer (Steen and Mann, 2004).

The formed ions are then separated according to their mass to charge ratio (m/z) in a mass analyzer. A time of flight (TOF) analyzer uses an electric field to accelerate the ions at the same potential. Then, the time needed to reach the detector ('time of flight') is measured. For particles with the same charge, the velocities are solely dependent on their masses (Steen and Mann, 2004).

In this way, in classical MALDI-TOF, a peptide mass fingerprint (PMF) of each spot is taken. Subsequently, the experimentally obtained mass fingerprint is compared to a database containing theoretical mass finger prints (as a result of *in silico* trypsinization) of the known/predicted proteins of the organism of interest. To get a significant hit, only a subset of all peptides from the protein digest need to match. One of the pitfalls of PMF is the reduced power to identify proteins from non-model organisms (with a poorly characterized genome; Mathesius *et al*. 2002).

In MS/MS ('tandem MS'), e.g. MALDI-TOF/TOF, a particular ion (peptide) is isolated, energy is provided by collision with an inert gas (e.g. nitrogen molecules or argon or helium atoms) and as a consequence this energy causes the peptide to fragment typically down to the peptide bond. In this way, a mass spectrum of the resulting fragments is generated (Steen and Mann, 2004). Reconstruction of an unknown peptide from MS/MS data through peptide sequencing is possible (referred as *de novo* peptide sequencing). Proteins generally are made up of 20 different types of amino acids which most of them have different masses. Thus, different peptides will produce different spectra being possible to use the spectrum of a peptide to determine its sequence. In most of the cases, this is carried out by searching uninterpreted data using an algorithm such as MASCOT (Hurkman and Tanaka, 2007; Carpentier *et al*., 2008b).

2.5.2.2. Gel-free proteomics

Gel-based proteomics is a powerful proteomics option for non-model organisms (e.g. apple), being also one of the few general methods able to study protein isoforms and post-translational modifications (Carpentier *et al*., 2008b). However, some of the limitations of this approach are the bias towards high abundant proteins and against membrane proteins (Thelen, 2007). Moreover, 2-DE is very labour-intensive and difficult to automate.

Since total automation is the ultimate objective for a high throughput method, gel-free approaches were developed. In a gel-free approach, intact proteins are digested with a proteolytic enzyme (e.g. trypsin) prior to separation. Tryptic peptide mixtures are more homogeneous than protein extracts, which facilitates automated separation based on hydrophobicity via reverse-phase chromatography. Subsequently, the eluted peptides are sent to a tandem mass spectrometer. All the tandem mass spectra gathered are then used to

search protein databases and reconstruct the original proteins (Roe and Griffin, 2006). However, since the connectivity between peptides derived from the same protein is lost after digestion and separation, protein identification is complicated. Consequently, this concept is only successful when identifying proteins in simple mixtures. Moreover, gel-free approaches have the disadvantage that qualitative and quantitative information on protein isoforms and differential post-translational modifications are lost (Carpentier *et al*., 2008b).

In general, no 'ideal' technique has yet been developed for the analysis of the total leaf proteome. The proteome of a cell or tissue at a specific time point is extremely complex and diverse. Because of the differences in the way proteins are extracted, separated and detected, gel-based and gel-free approaches each analyze a specific subset of proteins, and thus are complementary to each other (Carpentier *et al*., 2008b). Because of the expertise of our lab and our department in performing gel-based proteomics studies (Vanhoucke, 2006; Carpentier *et al*., 2005), and because of the above mentioned disadvantages of gel-free proteomics, e.g., regarding identification of protein isoforms, 2-DE and 2D-DIGE were chosen (in combination with MALDI-TOF/TOF) to investigate changes in the proteome of apple leaves in relation to scab defense mechanisms. However, one should bear in mind that, although 2-DE allows investigating many proteins at a time, for an integrated analysis of the 'complete' proteome, different approaches should be combined.

Chapter 3

Materials and methods

3.1. Plant material

The plant material consisted of young, grafted apple trees. Budwood of all cultivars used was received from Fruitteeltcentrum, KU Leuven (Rillaar, Belgium) and grafted onto certified virus free M9 rootstocks (NV Johan Nicolaï, Sint-Truiden, Belgium). The apple plants were potted in containers of 2.5 L in 'Combitree B MG' potting soil (De Ceuster Meststoffen, Grobbendonk, Belgium), mixed with 3 g/L of the fertilizer 'Osmocote 6 maanden' and 0.75 g/L 'Trianum-G' (Koppert Biological Systems, Berkel en Rodenrijs, the Netherlands). Trianum-G contains spores of the fungus *Trichoderma harzianum* strain T-22 and is directed against soil borne pathogens. Plants were grown in a greenhouse with controlled atmosphere at 16-20/10-14°C day/night temperature and 70% relative humidity (RH) under daylight with additional illumination (25 W/m²) from high-pressure sodium lamps ('400-W SON-T-AGRO', Philips) if daylight intensity is below 100 W/m² to guarantee a 16 h photoperiod.

3.2. *V. inaequalis* isolates

All inoculation experiments were carried out with *V. inaequalis* strain 104, the reference strain of race 1 of *V. inaequalis*, which has broken only one major source of apple resistance, the *Rvi1* (*Vg*) resistance of 'Golden Delicious' (Parisi and Lespinasse, 1996; Bus *et al*., 2009). The isolate was originally obtained from an infected 'Golden Delicious' tree grown under field conditions in Saint-Lézin (France; Bénaouf and Parisi, 1998). Following artificial greenhouse infection of 'Golden Delicious' trees with race 1 *V. inaequalis*, leaves with abundant sporulation were collected, dried at room temperature (RT), and frozen at -20°C. A conidial suspension in demineralized water was obtained from these leaves, adjusted to 2×10^5 conidia ml^{-1}, and used fresh to inoculate grafted 'Golden Delicious' plants. This was repeated until sufficient inoculum was obtained.

To develop the real-time PCR standard curve (see Section 3.5.3), the race 1 isolate was cultivated *in vitro* at RT on potato dextrose agar (PDA) containing 300 µg ml^{-1} streptomycin and 100 µg ml^{-1} tetracycline. To assess the reproducibility of the real-time PCR assay, two more *V. inaequalis* race 1 isolates (301 and EU-B05; Bénaouf and Parisi, 2000; Bus *et al*., 2005a) were received from Valérie Caffier from the French National Institute for Agricultural Research (INRA, Angers, France), and maintained under the same conditions as described for strain 104.

3.3. Inoculation conditions

Only actively growing young apple plants (first growing season) with 8-12 healthy, fully expanded leaves were chosen for inoculation. The youngest fully expanded leaf on each plant was labeled F1, the second and third youngest leaves below F1 were labeled F2 and F3 respectively, and the later expanding younger leaf above F1 was labeled F0. Scab inoculation was performed according to a standardized method. Either demineralized water (mock control) or an aqueous *V. inaequalis* conidial suspension (2×10^5 spores ml^{-1}) was applied as a spray to runoff. To encourage spore germination, the inoculated plants were then incubated for 48 h in the dark at 18-20 °C and 95-100 % RH (constant leaf wetness), after which they were returned to the normal growth conditions of the controlled greenhouse environment as described in Section 3.1 (Fig. 3.1).

Fig. 3.1. Actively growing young apple plants prior to scab inoculation.

3.4. Visual evaluation of *V. inaequalis* infection

Visual assessment of apple scab symptoms was performed by assigning symptoms on leaves F0, F1 and F2 (which are the most susceptible to scab) at different time-points after inoculation to one of the six so-called 'Chevalier classes' (Table 3.1; Chevalier *et al*., 1991).

Table 3.1. The six scab reaction classes of Chevalier *et al.* (1991).

Class 0	no disease symptoms
Class 1	pin-points
Class 2	chlorotic lesions
Class 3a	chlorotic and necrotic lesions, sometimes with light (0-1%) sporulation
Class 3b	chlorotic and necrotic lesions with obvious sporulation (1-50%)
Class 4	severe sporulation (>50%) without necrotic or chlorotic lesions

The Chevalier classes 0 to 3a are considered to be typical symptomatic classes of scab resistant cultivars, while classes 3b and 4 represent scab susceptibility. Additionally, sporulation as a percentage of leaf surface (classes 0-7: respectively 0, 0-1, 2-5, 6-10, 11-25, 26-50, 51-75, >75%) and chlorosis as a percentage of leaf surface (classes 0-4: respectively 0, 1-25, 26-50, 51-75, >75%) were recorded visually for all three leaves, as according to Croxall *et al*. (1952), and as modified by Parisi *et al*. (1993). Pictures were taken of all observed leaves at all evaluated time-points and reassessment of the visual symptoms was performed (in different orders) in order to improve the objectivity of the evaluations. For all three classifications, the formula of Towsend-Heuberger (Fig. 3.2; Towsend and Heuberger, 1943) was calculated for each plant at each time-point. The resulting TH-values between 0 and 100% represent the degree of infection (according to Chevalier) and the degrees of sporulation and chlorosis respectively.

$$TH_I = \frac{\sum (n_i \cdot i)}{N \cdot I} \cdot 100\% \qquad with \qquad \begin{aligned} n_i &= number\ of\ leaves\ (of\ 3)\ in\ class\ i \\ i &= class\ (0\text{-}I) \\ N &= total\ number\ of\ leaves\ (here\ always\ 3) \\ I{+}1 &= total\ number\ of\ classes \end{aligned}$$

Fig. 3.2. The formula of Towsend-Heuberger (Towsend and Heuberger, 1943), used to calculate the average degree of infection (according to the classification of Chevalier), chlorosis and sporulation for every *V. inaequalis* inoculated apple plant.

3.5. Quantification of *V. inaequalis* growth by real-time PCR

3.5.1. Sample preparation and DNA extraction

For real-time PCR, leaves F1 and F2 were harvested, weighed, lyophilized (Freezone 4.5, Labconco), weighed again and stored separately at RT in sealed bags in the presence of dry silica gel. Non-inoculated control leaves were also collected. Total genomic DNA (gDNA) from both control and inoculated apple leaves was extracted from 40 mg lyophilized leaf tissue using the DNeasy Plant Mini Kit (Qiagen) according to manufacturer's instructions. Before suspension in lysis buffer, cells were mechanically disrupted using ceramic beads by reciprocal shaking of the samples for 30 s (FastPrep, Thermo Savant; speed 6).

To establish a standard curve for the real-time PCR analysis, pure *V. inaequalis* gDNA was isolated from patches of mycelium (approximately 5 mm^2), that were cut from the margins of colonies on PDA and transferred to liquid potato dextrose broth medium containing 300 µg ml^{-1} streptomycin and 100 µg ml^{-1} tetracycline. Fungal mycelium was grown at RT, isolated, washed twice with sterilized water, blotted dry, weighed, freeze dried, weighed again, and stored sealed in the presence of dry silica gel at RT. The mycelium samples were mechanically disrupted in a FastPrep system as described above, after which gDNA was extracted from 20 mg (dry weight) starting material using the DNeasy Plant Mini Kit. DNA was eluted in 100 µl of the kits elution buffer, and DNA concentrations were quantified using agarose gel electrophoresis and the AlphaImager Gel Imaging System (Alpha Innotech).

3.5.2. Primer design

Publically available rDNA ITS1-5.8S-ITS2 nucleotide sequences of different *V. inaequalis* isolates and other *Venturia* species were downloaded from NCBI and aligned using ClustalW2 (http://www.ebi.ac.uk/Tools/msa/clustalw2). Primer pairs were designed using the Primer3 software (http://biotools.umassmed.edu/bioapps/primer3_www.cgi) and through manual inspection of the multiple alignment. Primer picking conditions were set as follows: G/C content between 40 and 60%, maximum (self) complementarity of 3, maximum 3' (self) complementarity of 0 (no primer-dimer formation), melting temperature of 60°C (± 1°C), primer size of 20 bases (± 2) and PCR product size between 75 and 125 bases. Candidate primer pairs were also checked for lack of significant homology with other DNA

sequences of flowering plants or fungi using the online basic local alignment search tool (BLAST) (http://blast.ncbi.nlm.nih.gov).

A total of three *Venturia*-specific candidate primer pairs were tested by PCR on 10 ng DNA of infected apple leaves and on a dilution series of *V. inaequalis* DNA, to check for specificity and optimal annealing temperature. Reactions containing 10 ng DNA isolated from non-inoculated 'Golden Delicious', 'Topaz', and 'Discovery' were also included to confirm that the primer pairs selectively amplified gDNA from the pathogen and not from the plant. The primer combination that was selected was V-5.8S-F/R, which amplifies a 123-bp fragment (Table 3.1).

To determine the impact of the presence of *Malus* DNA in the PCR mixture and to quantify the *Venturia* DNA in an inoculated leaf sample of 10 ng apple DNA , we also carried out a *Malus*-specific quantitative PCR, using the eIF-4A primer pair for the *Malus* x *domestica* translation initiation factor *eIF-4A*, a reference 'housekeeping' gene (Genbank ID: AY347787; Table 3.1; Zubini *et al*., 2007).

Table 3.1 Real-time PCR primers used in this study

Primer code[a]	Organism	Sequence (5'→3')	Position (bp)	Amplicon size (bp)	T_{ann}[b]	T_m[c]
V-5.8S-F	*Venturia* spp.	GCGAAATGCGATAAGTAATGTG	340-361[d]	123	58.5	84.0
V-5.8S-R	*Venturia* spp.	GGCTCCAGGGTAGAAATGG	444-462[d]	…	…	…
eIF-4A-F[e]	*Malus* x *domestica*	ATCAGGCTCATCCCGTGT	3-20[f]	119	58.5	82.4
eIF-4A-R[e]	*Malus* x *domestica*	AGCAACACCCTTCCTTCC	104-121[f]	…	…	…

[a] F: forward primer; R: reverse primer.

[b] Annealing temperature (°C).

[c] Melting temperature (°C) at which a specific dissociation peak of increased fluorescence is generated in the melting curve analysis.

[d] Base pair position in sequence of *Venturia inaequalis* 5.8S ribosomal RNA gene and internal transcribed spacer 2 (GenBank Accession No. EU035437).

[e] Zubini *et al*., 2007.

[f] Base pair position in sequence of *Malus* x *domestica* translation initiation factor *eIF-4A* (GenBank Accession No. AY347787).

3.5.3. Real-time PCR amplification and quantification

Real-time PCR was performed in 15-µl reactions using a Rotor-Gene Q instrument (Qiagen). Each reaction contained 2 µl DNA template, 1 µl of each primer (3.75 µM), 7.5 µl ABsolute™ QPCR SYBR® Green Mix (Thermo Fisher Scientific), and 3.5 µl Milli-Q water (Millipore Corporation). DNA extracts were adjusted to 5 ng μl^{-1}. The thermocycling profile for both

Malus- and *Venturia*-specific PCR reactions consisted of 15 min at 95°C and 40 cycles of 20 s at 95°C, 20 s at 58.5°C, and 20 s at 72°C. Signal threshold levels were set automatically by the instrument software. Quantification of *Venturia* DNA was calculated based on the standard curve technique, using a dilution series (10^2, 10^3, 10^4, 10^5, 10^6, and 5×10^6 fg) of gDNA from a *V. inaequalis* race 1 isolate (see sections 3.2 and 3.5.1). For the exact quantification of *Malus* x *domestica* DNA, a dilution series (2, 10, and 20 ng) of gDNA prepared from non-inoculated 'Golden Delicious' leaves was used. Each analysis included a no-template control reaction, in which the DNA was substituted by Milli-Q water. To evaluate amplification specificity, melting curve analysis was performed at the end of each PCR run according to the manufacturer's recommendations. All analyses were carried out in duplicate.

3.6. Statistical analysis

Statistical analyses were performed using the Epi Info™ statistical package, version 6.0. To determine whether differences in the amount of detected *Venturia* DNA were statistically significant ($p < 0.05$), data from the amplification of DNA samples were subjected to a Wilcoxon Mann-Whitney U test. The Wilcoxon Mann-Whitney U test was also used to determine significant differences between TH-values of visual symptoms of different cultivars. For the 'Golden Delicious' leaf samples, the Spearman rank correlation (Ostle, 1954) between the means of pathogen DNA content and degree of sporulation was calculated.

3.7. Proteomics

3.7.1. Sample preparation and protein extraction

Apple leaves F1 and F2 (see Section 3.3) were harvested, pooled and stored at -80°C. For each condition/cultivar three biological replicates (*i.e*. three plants) were used. Protein extraction and sample preparation were performed according to a variant of the extensively applied phenol extraction protocol with accompanying methanol/ammonium acetate precipitation that was optimized for small amounts of recalcitrant plant tissues (Saravanan and Rose, 2004; Carpentier *et al*., 2005). Here, leaf material was ground in a precooled mortar in the presence of liquid nitrogen and 50–150 mg of the homogenate resuspended in 500 µL of ice-cold extraction buffer (50 mM Tris-HCl pH 8.3, 5 mM EDTA, 100 mM KCl, 1 %

w/v DTT, 30 % w/v sucrose, complete protease inhibitor cocktail (Roche Applied Science)) and vortexed for 30 s. Five hundred µL of ice-cold Tris buffered phenol (pH 8.0) was added and the sample was vortexed for 10 min at 4°C. After centrifugation (3 min, 6000 *g*, 4°C) the phenolic phase was collected, reextracted with 500 µL of extraction buffer and vortexed for 30 s. After centrifugation (3 min, 6000 *g*, 4°C) the phenolic phase was collected and precipitated overnight at -20°C with five volumes 100 mM ammonium acetate in methanol. After precipitation, the sample was centrifuged at 20,000 *g* for 60 min at 4°C, the supernatant was removed and the pellet was rinsed twice in ice-cold acetone/0.2% DTT. Between the two rinsing steps, the sample was incubated for 60 min at -20°C. The pellet was air-dried, resuspended in 100 µL lysis buffer (7 M urea, 2 M thiourea, 4 % CHAPS, 1 % IPG-buffer pH 4-7 (GE Healthcare, Upsula, Sweden), 1 % DTT) and vortexed briefly at room temperature until it dissolved. In case of 2D-DIGE, the protein pellets were resuspended in 100 µl DIGE buffer (7 M urea, 2 M thiourea, 4 % CHAPS, 30 mM Tris). By including Tris in the buffer, the pH of the samples was adjusted to pH 8.3-8.5 as required for CyDye™ labeling.

3.7.2. Protein quantification

The protein concentration was determined using the 2-D Quant kit from GE Healthcare. A dilution series (10, 20, 30, 40, and 50 µg) of bovine serum albumin (BSA) was used as a standard curve.

3.7.3. CyDye™ labeling for 2D-DIGE

In the case of the 2D-DIGE experiments, proteins were labeled prior to two-dimensional protein separation using the fluorescent Cy2, Cy3 and Cy5 minimal labeling dyes of GE Healthcare following the manufacturer's guidelines. Here, 50 µg of each protein lysate was labeled with 400 pmol of amine reactive Cyanine dye dissolved in fresh, anhydrous dimethyl formamide. Three biological replicates per condition were independently and randomly labeled with either Cy3 or Cy5. Cy2 was used to label the internal standard composed of equal amounts of all samples to be analyzed. The labeling reaction was incubated in the dark for 30 min and quenched with 10 nmol lysine. An equal volume of 2x sample buffer (7 M urea, 2 M thiourea, 4 % CHAPS, 2 % DTT, 2 % IPG-buffer pH 4-7) was added to each of the labeled samples.

3.7.4. Two-dimensional gel electrophoresis (2-DE)

The sample was diluted with a rehydration buffer (6 M urea, 2 M thiourea, 0.5 % CHAPS, 10 % glycerol, 0.002 % bromophenol blue, 0.5 % IPG-buffer pH 4-7, 0.28 % DTT) to 150 µg (2D-DIGE) or 400 µg protein (CBB staining) per 150 µl, and was applied to an IPG strip via anodic cup loading. We did not use (active or passive) in-gel rehydration, the most common application method, because of possible problems of horizontal streaking caused by abundant, basic and hydrophobic proteins (Rabilloud *et al*., 1994; Görg *et al*., 2009). We applied cup loading at the anodal side to reduce streaking caused by migration of acidic proteins (Hoving *et al*., 2002). In the case of 2D-DIGE the protein sample consisted of two biological samples, that were labeled with Cy3 and Cy5 respectively, and the internal standard labeled with Cy2. Twenty four cm, linear IPG strips, pH 4-7 (GE Healthcare) were rehydrated for at least 8 h in 450 µL rehydration buffer. Proteins were then isoelectrically focused (IEF) in an IPGphor II system (GE Healthcare) at 20 °C with current limit 50 µA/strip, using the following program: 3 h at 300 V, 6 h at 1000 V, 3 h at 1000-8000 V (linear gradient), and 24,000 Vh (2D-DIGE) or 40,000 Vh (CBB staining) at 8000 V. This program is designed to minimize aggregation and precipitation of proteins during the entry of liquid sample from the cup into the gel matrix, to neutralize interfering ions and proteins outside of the pH range and to focus the proteins under optimal conditions. Prior to second dimension analysis, the individual strips were equilibrated for 15 min in 10 ml equilibration solution (6 M urea, 30 % glycerol, 2 % SDS, 0.002 % bromophenol blue, 50 mM Tris pH 8.8) containing 1 % w/v DTT and subsequently for 15 min in 10 ml equilibration buffer containing 4.5 % w/v iodoacetamide. The separation in the second dimension was carried out on an Ettan DALT*six* instrument (GE Healthcare) with lab cast, 1.5 mm (CBB staining) or 1.0 mm (2D-DIGE) SDS polyacrylamide gels (12.5 % T): 45 min at 12 W (2 W/gel), 5 h at 100 W (CBB staining) or only one step of 13 h at 12 W (2D-DIGE).

3.7.5. Protein visualization, image analysis and quantification

Gels in which protein extracts had not been CyDye^{TM} labeled prior to 2-DE, were visualized by colloidal Coomassie Brilliant Blue (CBB) G-250 staining (Neuhoff *et al*., 1988). Here, the gels were first fixed for 1 h in a fixing solution (1 % o-phosphoric acid, 20 % methanol) and then stained overnight in a staining solution (20 % methanol, 0.1 % w/v CBB G-250, 2 % o-

phosphoric acid, and 8 % w/v $(NH_4)_2SO_4$). Gels were neutralized (0.1 M Tris-base titrated to pH 6.5 with o-phosphoric acid) for 2 min and washed in 25% methanol for 1 min. Stained gels were scanned at a resolution of 150 dots per inch (dpi) using the ImageScanner I (GE Healthcare) and calibrated with Labscan 5 software (GE Healthcare). Image analysis was performed with the Image Master 2-D platinum software 6.0 (GE Healthcare). Spot detection was realized without spot editing. The spots were quantified using the % volume criterion.

CyDye™ labeled gels were scanned with a Typhoon 9400 laser scanner (GE Healthcare). Cy2 images were scanned using a 488 nm laser and a 520 nm band pass (BP) emission filter. Cy3 images were scanned using a 532 nm laser and a 580 nm BP emission filter. Cy5 images were scanned using a 633 nm laser and a 670 nm BP emission filter. Gels were scanned at a 100 µm resolution. The PMT (photo multiplier tube) was set to ensure maximum pixel intensity between 75,000 and 95,000 pixels. The gel images were cropped using ImageQuant (GE Healthcare) and further analyzed with the DeCyder 6.5 software (GE Healthcare).

3.7.6. Statistical analysis

For the CBB stained gels, statistical analyses were performed with the Image Master 2-D platinum software (GE Healthcare). Since the assumption of normality underlying a classical analysis of variance (ANOVA) was not fulfilled, the Kolmogorov-Smirnov statistical test was applied to the matched spots to test the significance of the difference between spot abundances of samples due to different treatments. This is a nonparametric two-sample test (an alternative for the T-test) that has a high power-efficiency for small samples (Siegel and Castellan, 1988). Five or six replicate CBB stained gels were run for every sample category. Proteins with a *p* value below 0.05 were considered to be significantly different.

In 2D-DIGE, statistical analyses were performed with the DeCyder 6.5 software (GE Healthcare) and were based on the log standardized protein abundances. The log standardized abundance is the Cy3 or Cy5 sample spot volume divided by the Cy2 standard sample spot volume after ratiometric normalization. Using the DIGE approach, Karp and Lilley gathered strong arguments to assume that the restrictive assumptions of parametric statistics are met after logarithmic transformation of the standardized abundance has been performed (Karp and Lilley, 2005). Therefore, a one-way ANOVA was carried out in order to assess for absolute protein changes among the different treatments. In this procedure, the

p-values were corrected for a false discovery rate (FDR) according to the procedure of Benjamini and Hochberg (2000). Consequently, both a *p*-value and a *q*-value were calculated for each spot. The *q*-value is a measure of significance in terms of FDR. The FDR estimates how many from the spots declared to be significant, are expected not to be significant at all. Matching spots with a *q*-value < 0.05 were considered to be differentially accumulated.

Differentially accumulated spots were manually checked as being proper spots before submitting them for protein identification.

3.7.7. Spot picking and identification

In order to be identified, spots of interest were manually matched to the protein pattern in a set of preparative, CBB stained gels and included in a pick list. The spots were manually excised with a 1.5 mm diameter pipette tip. Mass spectrometry analysis was performed by Karin Schildermans and Prof. Dr. Yves Guisez from CeProMa, the Centre for Proteome Analysis & Mass Spectrometry of the University of Antwerp.

First, gel plugs were dehydrated with 95 % v/v acetonitrile for 3 x 5 min. After reswelling in 6,66 mM DTT for 45 min at 56 °C to reduce disulfide bonds, the plugs were washed twice in 95 % v/v acetonitrile for 2 x 5 min. The alkylating reagent iodoacetamide (55 mM) was added for 30 min at RT (in the dark) and the plugs then washed again twice in 95 % v/v acetonitrile for 2 x 5 min and incubated ON at 4 °C to dehydrate. The gel particles were then rehydrated with 20 µl of a trypsin digest buffer containing 50 mM NH_4HCO_3, 10 % v/v acetonitrile and 0.02 g/l trypsin (proteomics grade, Sigma). After 30 min of incubation at 4 °C, 10 µl of a buffer containing 50 mM NH_4HCO_3 and 10 % acetonitrile was added and the samples were incubated for 3.5 h at 37 °C for protein digestion. Before application onto the MALDI-target, tryptic peptide mixtures were desalted with a nano column solid phase extraction procedure using Perfectpure C_{18}-columns (Eppendorf, Hamburg, Germany). The desalted peptides were eluted directly onto the MALDI-target with 1.2 µl of a saturated solution of α-Cyano-4-hydroxycinnamic acid (CHCA; Sigma) in 50 % v/v acetonitrile, containing traces (25 fmol/µl each) of Glu-fibrinopeptide b (GluFib) and bradykinin. The spotted peptide mixture of each protein was analyzed by MALDI-TOF/TOF on a 4800 Proteomics Analyzer (Applied Biosystems, Foster City, USA). MS/MS spectra of each sample were submitted for identification using the Mascot interface (Mascot 1.9, Matrix Science, London, UK) as a

database search engine. Searches were performed against the *Malus* x *domestica* genome (v1.0, Genome Database for *Rosaceae*; 63,541 sequences), that was recently sequenced by Velasco *et al.* (2010), using a fixed modification of carbamidomethyl (C) and a variable modification of oxidation (M). The query parameters allowed for one single miscleavage, a peptide mass tolerance of ± 40 ppm and a fragment mass tolerance of ± 0.2 Da. Queries returning a protein identification with a MOWSE treshold score above 61 ($p < 0.05$) were regarded as valid protein IDs (Perkins *et al*., 1999). An overview of all the protein identifications can be found in Appendix III.

Chapter 4

Symptom evaluation and real-time PCR quantification of *V. inaequalis* infection of apple

This chapter is based on the manuscript:

Real-time PCR as a promising tool to monitor growth of *Venturia* spp. in scab-susceptible and -resistant apple leaves

Bruno Daniëls, Anke De Landtsheer, Rozemarijn Dreesen, Mark W. Davey, and Johan Keulemans

European Journal of Plant Pathology, 2012, 134: 821‑833

DOI: 10.1007/s10658-012-0058-6

4.1 Introduction

The objective of this thesis was to gain a better insight in the response of apple to *V. inaequalis* infection. For that purpose, we first wanted to choose, through observation of leaf symptoms after scab inoculation, three apple cultivars that would be used for further research: a cultivar that is susceptible to race 1 of *V. inaequalis*, a monogenic resistant cv. and a polygenic resistant one. Some optimization of the scab inoculation procedure appeared to be necessary. Then, we could carry out our main greenhouse experiment. In a first part of our systematic study of the apple – *V. inaequalis* interaction we wanted to properly evaluate fungal pathogenicity and virulence and host resistance and tolerance after inoculation with a characterized *V. inaequalis* race 1 isolate (see Section 3.2). For that purpose, we needed to acquire a detailed image of the evolution of the differences in

external leaf symptoms and in infection degree between the monogenic resistant, polygenic resistant and scab susceptible cultivar. The time course study of the differences in leaf symptoms was based on a disease rating that takes into account foliar chlorosis, necrosis and sporulation symptoms (Chevalier *et al*., 1991; see Section 3.4). However, given the disadvantages of this classical scoring technique for determining the degree of infection (see Section 2.4), we additionally developed a SYBR Green I real-time PCR assay of the *V. inaequalis* 5.8S-ITS2 rDNA region (see Section 3.5) to provide a fast, sensitive and reliable quantification of *V. inaequalis* mycelial growth in apple leaves. To our knowledge, this is the first description of the molecular quantification of *V. inaequalis* directly from apple leaves.

4.2. Choice of three cultivars based on observations of leaf symptoms after inoculation with *V. inaequalis*

4.2.1. Experimental setup

217 young, grafted trees of eight apple cultivars with differences in susceptibility to scab were available (Table 4.1). The cv. 'Golden Delicious' carries the *Rvi1/Vg* resistance gene (Bénaouf and Parisi, 2000), but is consequently susceptible to race 1 of *V. inaequalis*, which carries the *virRvi1* virulence locus (Bus *et al*., 2009; see Table 2.1 in Section 2.2.1.3). The 217 apple plants were randomly divided over a greenhouse compartment. Irrigation, temperature and relative humidity were automatically controlled (see Section 3.1). Actively growing plants with 8-12 fully expanded leaves were inoculated with *V. inaequalis* race 1 strain 104.

4.2.2. Results and discussion

Because of problems in the automatic water supply, the vegetative growth of the apple plants was disturbed. After two months (on 21/11/2007), 47 % of the plants was still not suitable for inoculation because of a lack of shoot development, an insufficient size of the shoots, or a growth stop of sprouted shoots (Fig. 4.1a). The remaining 116 plants were inoculated, but 70 % of the inoculated apple plants developed 'burned' leaves with severe necrotic lesions (Table 4.1 and Fig. 4.1b). The cause was probably a suboptimal vegetative growth, that was however not clearly visible on the inoculated plants at the time of inoculation.

Table 4.1. Apple plants available and eventually used for scab inoculation

Cultivar	Resistance[a]	Nr. of plants	Inoculated	'Burned'[b]
Braeburn	-	29	22	20 (91%)
Golden Delicious	*Rvi1* (*Vg*)	30	22	20 (91%)
Liberty	*Rvi6* (*Vf*)	29	6	3 (50%)
Topaz	*Rvi6* (*Vf*)	29	19	7 (37%)
Murray	*Rvi5* (*Vm*)	27	9	4 (44%)
Angold	*Rvi10* (*Va*)	21	8	5 (63%)
Discovery	polygenic	23	13	11 (85%)
Alkmene	polygenic	29	17	11 (65%)

[a] Monogenic resistance sources are depicted according to their new name (Bus *et al*., 2009), followed by their old name between parenthesis

[b] 'Burned' leaves showed severe necrotic lesions after the period of 48 h following inoculation

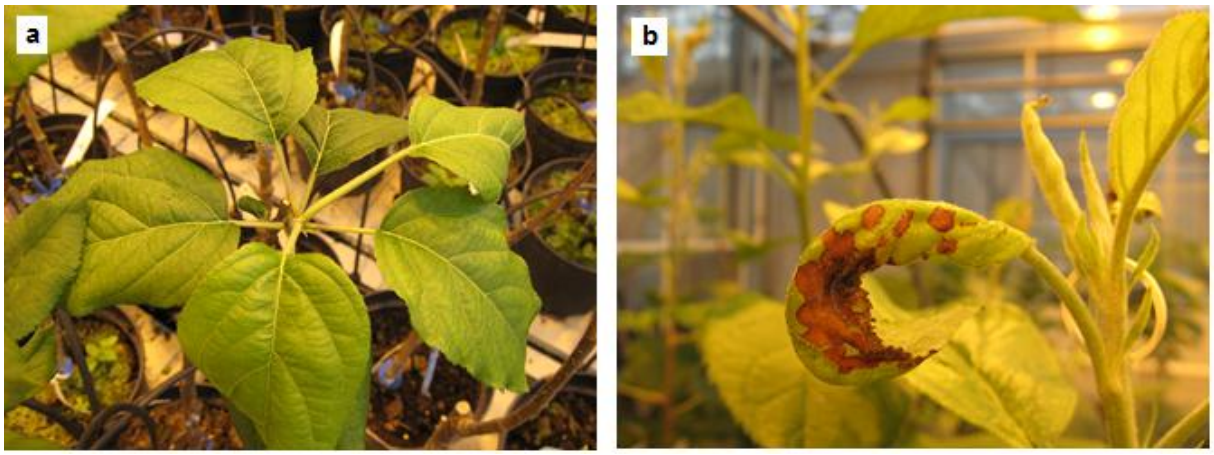

Fig. 4.1. Problems with disturbed vegetative growth, e.g. growth stop of sprouted shoots **(a)**, and development of 'burned' leaves upon scab infection **(b)** make the choice of three suitable cultivars more difficult.

The presence of the necrotic lesions rendered the observation of leaf symptoms after scab inoculation to be unreliable. Of the different apple cultivars not enough inoculated plants with clear scab infection symptoms remained in order to choose three cultivars that are suitable for subsequent research, based on the current infection results. Nevertheless, in order to be able to start off with the actual infection experiments and sampling for real-time PCR and proteomics the following spring, the choice of a monogenic and polygenic resistant and a susceptible cultivar was made at this stage. Hereby, the following considerations were

made. Regarding the monogenic resistance, we chose a ***Rvi6/Vf*-resistant** cultivar, because the *Vf* locus is without doubt the most prevalent monogenic resistance source among the current commercial scab resistant apple cultivars (Gessler and Pertot, 2012). We chose **'Topaz'** because this cultivar appeared to be less sensitive to suboptimal growth conditions than 'Liberty' (respectively 35 and 79 % non-inoculatable plants and 37 and 50 % with burned leaves; Table 4.1). As a **polygenic resistant** cv. we chose **'Discovery'**, not 'Alkmene', because a lot of 'Alkmene' plants had a tendency for (temporary) growth stop of sprouted shoots. This rendered the cultivar too unreliable for further use. Regarding the **scab susceptible** cv., we chose **'Golden Delicious'** because it is the representative host cultivar susceptible to *V. inaequalis* race 1 from which our used strain 104 was originally obtained (Bénaouf and Parisi, 1998; Bus *et al*., 2009).

4.3. Optimization of the scab infection procedure

4.3.1. Experimental setup

Of each of the three cultivars ('Golden Delicious', 'Discovery' and 'Topaz') 210 plants were potted on April 1 2008. On May 15 2008, 69 plants of each of the three cultivars (10 for visual symptom evaluation, 24 for sampling for real-time PCR (see Section 4.5), 27 for sampling for protein analysis (see Chapter 5), and 8 spares) were inoculated with *V. inaequalis* race 1 strain 104. Of the remaining 141 plants per cultivar, 42 were mock-infected (10 for visual symptom evaluation, 27 for sampling for protein analysis and 5 spares).

4.3.2. Results and discussion

Despite intensive care of the apple plants, some inoculated plants showed 'burning' of their youngest leaves after the incubation period of 48 h at 95-100 % RH (comparable to Fig. 4.1b). The cause was most probably the excessive sunshine and lack of wind during this 48 h period, because of which, despite the set greenhouse temperature of 18-20 °C, the ventilation was insufficient and the temperature rose to above 25 °C (Fig. 4.2a). Because proper evaluation of leaf symptoms of scab infection would not be possible, we cut back all plants (until just above the third bud), let them grow again and inoculated them again on June 5 2008, since no sunshine was predicted the first upcoming 48 h. The weather

predictions appeared to be correct and the temperature remained within an acceptable range (Fig. 4.2b). Indeed, despite the very high relative humidity, no necrotic lesions were visible after the 48 h incubation period. Consequently, the plants were suitable for visual symptom evaluation (see Section 4.4) and sampling for real-time PCR (see Section 4.5) and protein analysis (see Chapter 5). As a control, five spare plants of each cultivar that had been inoculated the first time had not been cut back. None of them showed any scab infection related symptoms during the days and weeks after inoculation. This observation confirmed that the first scab infection attempt had failed indeed. We can conclude that in case of an excessive solar radiation, combined with a very high humidity, the temperature can become too high for a successful scab infection and 'burning' of leaves can occur because of an impaired leaf transpiration.

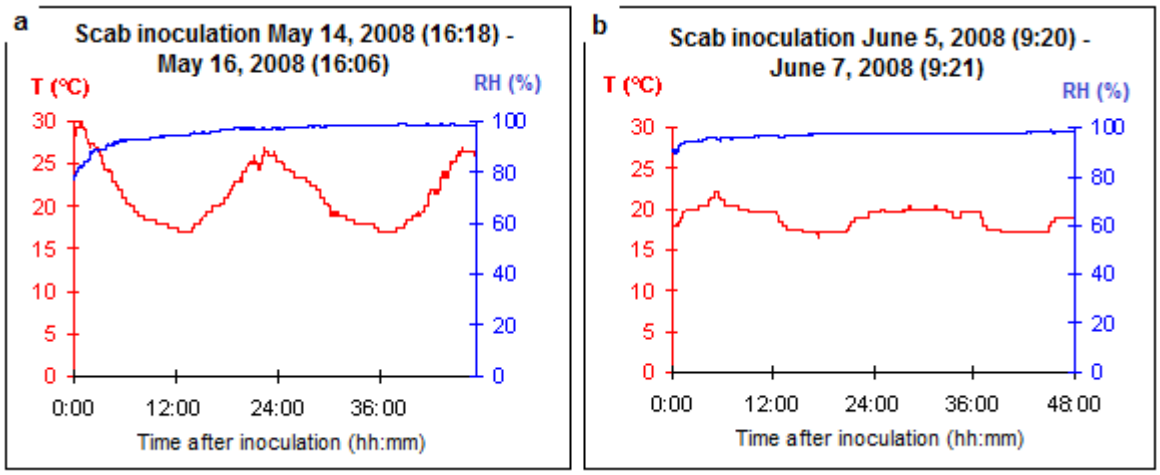

Fig. 4.2. Log-data (EasyLog, Lascar Electronics) of temperature (T) and relative humidity (RH) in the period of 48 h (at 95-100 % RH) after scab inoculation on May 15 2008 **(a)** and on June 5 2008 **(b)**.

4.4. Visual evaluation of *V. inaequalis* infection

4.4.1. Experimental setup

For each of the three cultivars ('Golden Delicious', 'Discovery' and 'Topaz'), ten inoculated plants were used for visual assessment of apple scab symptoms. At 2, 4, 6, 8, 10, 12, 14, 15, 18, 20, 22 and 25 days post-inoculation (dpi), the leaves F0, F1 and F2 were assigned to one of the five 'Chevalier classes' (Chevalier *et al.*, 1991). Additionally, sporulation as a percentage of leaf surface and chlorosis as a percentage of leaf surface were observed for the three leaves (see Section 3.4).

4.4.2. Results

The evolution of foliar disease symptoms in the scab-susceptible ('Golden Delicious'), monogenic *Rvi*6-resistant ('Topaz') and polygenic resistant ('Discovery') cultivars was studied in the time period up to 25 dpi. Results were expressed as the median TH_5-value of Chevalier classes, as described in Section 3.4. (Fig. 4.3a).

At 8 dpi, chlorotic lesions and light (0-1%) sporulation (class of Chevalier 3a) developed around the midrib of the susceptible 'Golden Delicious' F1 leaves. At 10 dpi, these symptoms developed also within leaves F0 and F2, and the degree of sporulation was increasing rapidly (class 3b). At 20 dpi, the degree of sporulation had increased up to 75 % of the leaf surface and chlorosis could no longer adequately be observed (class 4; Fig. 4.3b-c). In the *Rvi6*-resistant 'Topaz', the majority of the evaluated leaves began to display chlorotic lesions at 8-10 dpi (class of Chevalier 2; Fig. 4.3a-b), and by 12-14 dpi, necrotic lesions developed within some of these leaves (class 3a). Finally, with the polygenic resistant 'Discovery' plants, chlorotic lesions began to develop at 14 dpi on some of the inoculated leaves (Fig. 4.3a-b). However, the degree of chlorosis remained lower than with the 'Topaz' leaves during the entire period of the experiment ($p < 0.05$; Wilcoxon Mann-Whitney U test). None of the control or mock-infected control plants showed any of the above mentioned symptoms.

Next to differences in foliar disease symptoms between different cultivars, we could also observe differences in severity of the symptoms between leaves of different ages within one cultivar. As an example, leaves F1 and F2 (the two youngest, unfolded leaves on the time of inoculation) of the scab-susceptible cv. 'Golden Delicious' appeared to be more susceptible to infection than leaf F0 (the younger leaf that wasn't completely unfolded on the time of inoculation) (Fig. 4.4). Based on these results, leaves F1 and F2 were sampled for real-time PCR and protein analysis.

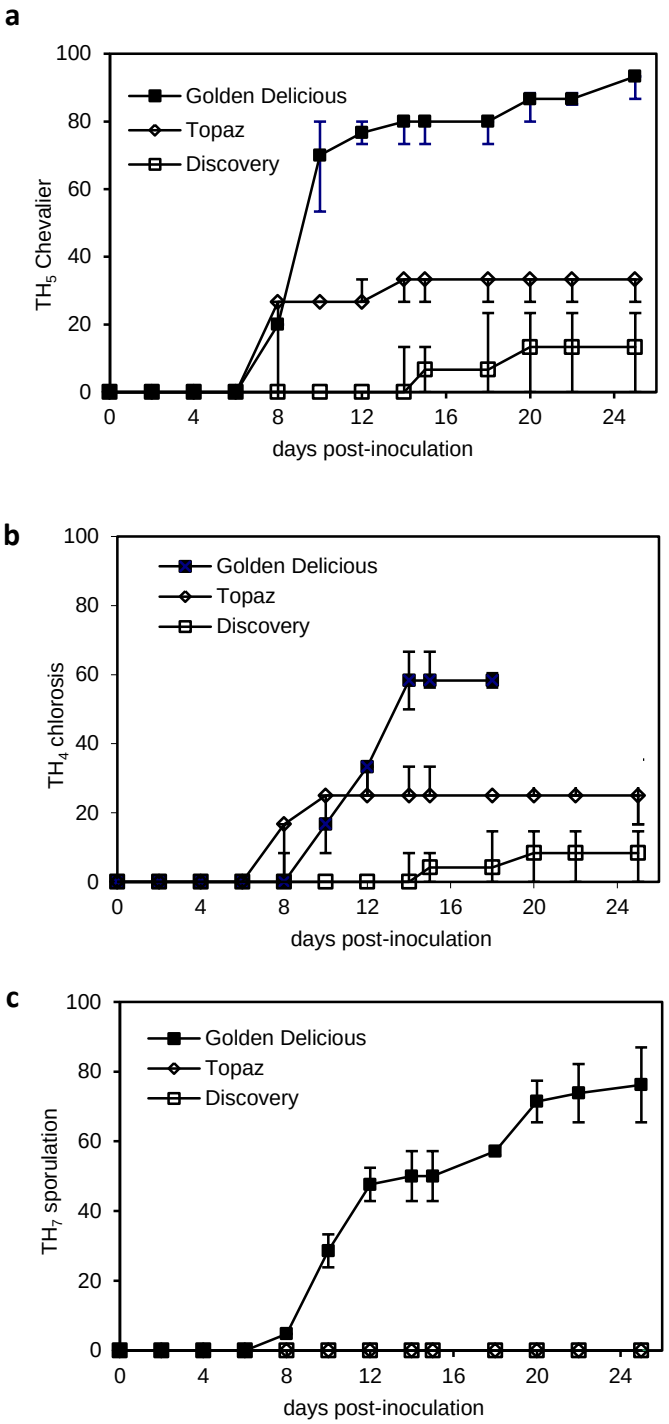

Fig. 4.3. Evolution of **(a)** the degree of *Venturia inaequalis* infection (according to the classification of Chevalier *et al*. (1991) and the degrees of chlorosis **(b)** and sporulation **(c)** of the scab-susceptible ('Golden Delicious'), monogenic *Rvi6*-resistant ('Topaz'), and polygenic resistant ('Discovery') apple leaves. Data represent medians of TH-values of ten replicate plants. Error bars indicate first and third quartiles. Because of extensive sporulation, chlorosis could not be adequately observed in 'Golden Delicious' as of 20 days post-inoculation.

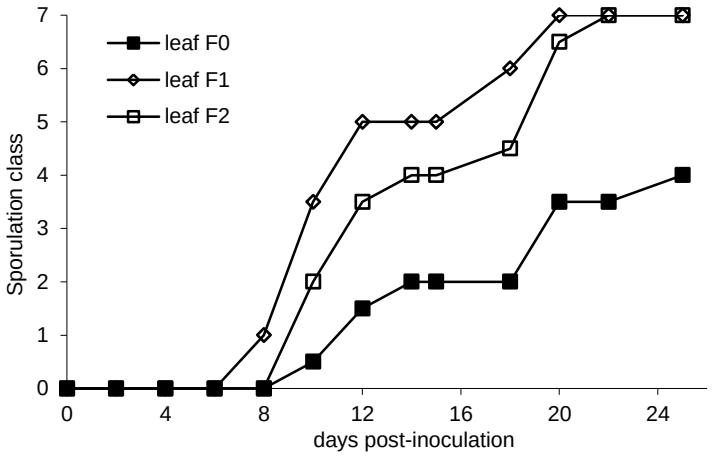

Fig. 4.4. Evolution of the degree of sporulation (according to the classification of Croxall *et al*. (1952), modified by Parisi *et al*. (1993)) of the scab-susceptible 'Golden Delicious' leaves. Data represent medians of ten replicate plants.

4.5. Real-time PCR

4.5.1. Experimental setup

4.5.1.1. Quantification of hyphal growth of *V. inaequalis*

For real-time PCR, leaves F1 and F2 of a parallel set of apple plants were harvested at 2, 3, 5, 7, 9, 13, 18 and 25 dpi. For each time point and cultivar, three biological replicates (*i.e.* three apple plants) were used. Non-inoculated control leaves were also collected. Total genomic DNA (gDNA) from (inoculated) apple leaves was extracted using the DNeasy Plant Mini Kit (Qiagen) (see Section 3.5.1). A SYBR Green I real-time PCR assay was performed using a Rotor-Gene Q instrument (Qiagen) (see Section 3.5.3). Our designed *Venturia*-specific primer pair V-5.8S-F/R was used to amplify a 123-bp fragment of the *V. inaequalis* ITS2-5.8S rDNA region (see Section 3.5.2). Quantification of *Venturia* DNA was done based on the standard curve technique, using a dilution series (10^2, 10^3, 10^4, 10^5, 10^6, and 5×10^6 fg) of gDNA from a *V. inaequalis* race 1 isolate (see Section 3.5.1). To quantify the *Venturia* DNA in an inoculated leaf sample of 10 ng apple DNA , we also carried out a *Malus*-specific quantitative PCR, using the eIF-4A primer pair and a dilution series (2, 10, and 20 ng) of gDNA prepared from non-inoculated 'Golden Delicious' leaves. All analyses were carried out in duplicate.

4.5.1.2. Sensitivity, specificity, and reproducibility

To assess the sensitivity of detection of *V. inaequalis*, real-time PCR was carried out on a dilution series of 1 fg - 10 ng gDNA prepared from the *V. inaequalis* race 1 isolate 104, and the range of linearity of the standard curve was determined. The specificity of the primer pair for *Venturia* spp. was checked using 10 ng DNA isolated from non-inoculated 'Golden Delicious', 'Topaz', or 'Discovery'. To assess the reproducibility of the real-time PCR setup, three independent real-time PCR reaction series were performed using a fresh template dilution series of *V. inaequalis* isolate 104 gDNA within each series. Real-time PCR amplification was also performed with ten different preparations of 1 ng genomic DNA of *V. inaequalis* race 1 isolates 104, 301 and EU-B05. To evaluate the effect of background host DNA and/or co-extracted leaf tissue substances on the detection efficiency of pathogen DNA, a dilution series of *V. inaequalis* gDNA in Milli-Q water was prepared, containing in addition 10 ng DNA from non-inoculated 'Golden Delicious', 'Topaz', and 'Discovery' leaves. The effect of plant DNA on amplification was determined based on a comparison of the standard curves. The influence of the amount of plant derived DNA extract on accurate quantification was tested by adding dilution series of gDNA (5, 10, and 20 ng) from non-inoculated 'Golden Delicious', 'Topaz', and 'Discovery' plants to samples containing 1 ng of *V. inaequalis* DNA.

4.5.2. Results

4.5.2.1. Validation of the selected *Venturia*-specific primer pair

Of the initial set of designed primers, one set of primers was selected after testing which amplifies a single 123 bp amplicon from *Venturia* spp. DNA (see Table 3.1 p.55). ClustalW was used to align the primer sequences to the 5.8S-ITS2 region in *Venturia* spp. and in other pathogenic ascomycetes commonly found on apple (Fig. 4.5). None of the aligned non-*Venturia* apple pathogens' 5.8S-ITS2 regions were predicted to be amplified. The basidiomycete *Gymnosporangium juniperi*-virginianae and the *Malus* x *domestica* 5.8S-ITS2 rDNA sequences were too divergent to be included in the alignment, and a BLASTn search detected no significant homology with other DNA sequences of related fungi or *Malus* x *domestica*.

```
                        5.8S                          |                ITS2
V. inaequalis (EU035460)                     TGTTCGAGCGCCATTTCTACC-CTGGAGCCCT---GCTCTGTGATGGGCC-
V. nashicola (EU035465)                      .....................-........AC---...............-
V. pirina (EU035469)                         .....................-.........C---...............-
V. asperata (AF333447)                       .....................-.........A---...............-
V. carpophila (AF065849)                     .....................-.........C---...............-
V. cerasi (AF065847)                         .....................-.........C---...............-
Alternaria mali (EF136372)                   ..........T.....G....-..CA...TT.---...TG...T.....G-
A. alternata (JF802118)                      ..........T.....G....-..CA...TT.---...TG...T.....G-
Schizothyrium pomi (JQ358786)                C.........T....A.A-..A..CA....TC---...TG..CT.....G-
Mycosphaerella graminicola (JF807056)        C.........T....A.A-..A..CC....TC---...GG..AT.....G-
M. dearnessii (JQ245448)                     ..........T......A-..A..CA....TG---...TG..AT.....G-
M. wachendorfiae (JF951143)                  ..........T......A-..A..C...T.TG---A...G..AT.....G-
M. valgourgensis (JF951152)                  ..........T......A-..A..CA....TA---...TG..AT.....G-
Helminthosporium velutinum (JN198435)        ..........T.....AC...-..CA...T..---...TG...T.....G-
H. solani (DQ865090)                         ..........T....ATC...-..CA...T..---...TG...T.....G-
H. asterinum (HM222966)                      .A........T.....AC...-..CA....TG---...TG..AT......-
Neofabraea malicorticis (AF281387)           ..........T....A.A...-..CA...T..---...TG...T.....G-
Podosphaera leucotricha(GU122230)            ..........T..GAA.AT..T..CA....TA---...TG..CT....GT-
Podospora anserina (GU327641)                ...C......T......A...-A.CA.....C-GG...T-...T....GA-
Neonectria galligena (AY677278)              ..........T......A...-..CA.....CCGG...TG...T....GA-
Phyllachora graminis (AF257111)              ..........T......C...-..CAG...-ATGC.TCTG...T...AGG-
Botrytis cinerea (AY787690)                  ..........T......A...-C.CA...TTA---...TG..AT..A.---
Botryosphaeria obtusa (AY259096)             ..........T....A.A...-..CA...T..---...TG..AT.....G-
B. dothidea (HQ871693)                       ..........T....A.A...-..CA...T..---...TG..AT.....A-
Colletotrichum gloeosporioides (FJ884081)    ..........T......A...-..CA...T..---...TG...T....G.-
C. gloeosporioides (HQ656800)                ..........T......A...-..CA...A..---...TG...T....G.-
C. gloeosporioides (HQ656791)                ..........T......A...-C.CA....TA---...TG...T....G.A
C. acutatum (HQ688676)                       ..........T......A...-..CA...A.C---...TG...T....G.-
Leptodontidium elatius (GU062242)            ..........T....A.A...-..CA...AA.---...TG...T......-
```

Fig. 4.5. Partial sequence alignment of the 5.8S-ITS2 region, showing the position of the reverse primer V-5.8S-R (reverse complement sequence; table 3.1 p.55) designed for the quantification of *Venturia* spp. by real-time PCR. To illustrate primer specificity, the sequences of *Venturia* spp. are aligned with sequences of other pathogenic ascomycetes commonly found on apple (Genbank IDs between parentheses). If the apple pathogen's 5.8S-ITS2 rDNA sequence is not known (i.e. for *Phyllachora pomigena*, *Mycosphaerella pomi*, *Helminthosporium papulosum*), the according sequences of other species from the same genus are used. The forward primer V-5.8S-F, with which primer V-5.8S-R was combined, was common for the listed fungi. Only polymorphic nucleotides are shown; (.) indicates an identical nucleotide, (-) indicates a gap in the sequence.

4.5.2.2. Sensitivity, selectivity, and reproducibility of the real-time PCR assay

A standard curve was generated for the V-5.8S-F/R primer pair using gDNA of *V. inaequalis* race 1 isolate 104 (Fig. 4.6). The correlation between Ct values and log values of the initial amounts of *V. inaequalis* DNA was nearly perfect (R^2 > 0.999), with linearity extending over a 10^5-fold range, and with a limit of detection of *circa* 100 fg gDNA. Melting curve analysis of the PCR products revealed a single dissociation peak of increased fluorescence at the melting temperature indicated in Table 3.1, demonstrating amplification specificity. There was no amplification using DNA from non-inoculated leaves of 'Golden Delicious', 'Topaz', or 'Discovery', confirming that the primers are specific for fungal DNA. To determine the

reproducibility of the assay, real-time PCR was conducted using 1 ng of each of ten different preparations of *V. inaequalis* gDNA (originating from isolates 104, 301 and EU-B05). The coefficients of variation between the Ct values of duplicate samples (technical replicates) were all < 1 %, while the mean coefficient of variation between the Ct values of ten different sample preparations (biological replicates) was +/- 2.5 %. These results demonstrate that amplifications by this real-time PCR assay are not only highly reproducible within replicates of the same sample preparation but also between different sample preparations.

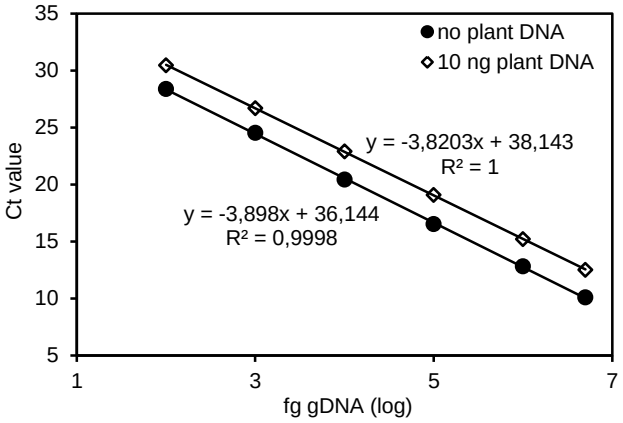

Fig. 4.6. Standard curves from real-time PCR reactions of a dilution series of *Venturia inaequalis* race 1 genomic DNA (10^2, 10^3, 10^4, 10^5, 10^6, and 5×10^6 fg) in the presence (◊) or absence (●) of 10 ng apple DNA, using primer pair V-5.8S-F/R. Data represent means of three replicate reactions (biological replicates), in case of (◊) representing addition of genomic DNA of the cultivars 'Golden Delicious', 'Topaz', and 'Discovery' respectively (error bars, representing standard errors, are too small to be displayed graphically).

4.5.2.3. Optimization of DNA extracts for real-time PCR quantification of *Venturia* spp. in apple leaves

Since the goal of this study was to quantify *Venturia* DNA in apple leaves, potential interference of the presence of plant-derived DNA on the quantification of *Venturia* DNA was investigated. Known amounts of gDNA (5, 10, and 20 ng) from non-inoculated 'Golden Delicious', 'Topaz', and 'Discovery' plants were added to samples containing 1 ng of *V. inaequalis* DNA. Fig. 4.7 shows that the inclusion of plant-derived DNA had a significant influence ($p < 0.05$) on the quantification of *V. inaequalis* DNA. However, this was a

consistent effect and no significant differences between the three cultivars could be observed. Next, a dilution series of *V. inaequalis* DNA was added to 10 ng gDNA from 'Golden Delicious', 'Topaz', or 'Discovery' to generate ratios between pathogen and plant DNA between 1:2 (reflecting a very heavy infestation) to 1:10 000 000 (reflecting early stages of infections). When a standard curve was generated for the average of three dilution series, representing the three cultivars, a nearly perfect linear correlation ($R^2 > 0.999$) was found (Fig. 4.6). The coefficients of variation between the Ct values of the three cultivars were less than 1 % at all template levels. Therefore, although plant DNA altered the absolute values of *Venturia* DNA measured, relative values were still acceptable. Therefore, to ensure consistency, DNA prepared from inoculated apple leaves was always normalized to the same amount of plant DNA i.e. 10 ng, using the *eIF-4A* primers as described (Table 3.1; Zubini *et al*., 2007).

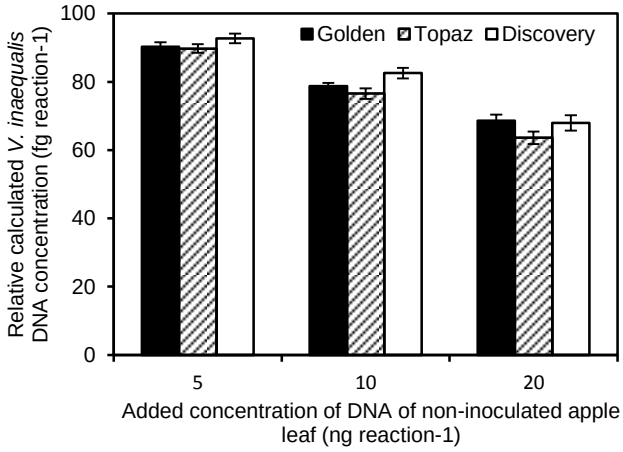

Fig. 4.7. Influence of plant-derived genomic DNA (gDNA) extract on *Venturia inaequalis* DNA quantification using real-time PCR analysis and primer pair V-5.8S-F/R. Samples containing 1 ng *V. inaequalis* gDNA were amplified in the presence of 5, 10, or 20 ng gDNA from a non-inoculated 'Golden Delicious' (black), 'Topaz' (hatched), or 'Discovery' (white) plant. Calculated gDNA concentrations are reported relative to the calculated gDNA concentrations when no plant gDNA was added. Data represent means of two replicates. Error bars indicate standard errors.

4.5.2.4. Real-time PCR quantification of hyphal growth of *V. inaequalis*

Finally, in parallel with the classical evaluation of disease symptoms, the optimized real-time PCR protocol was used to measure changes in *V. inaequalis* DNA levels in the three cultivars following artificial inoculation (Fig. 4.8).

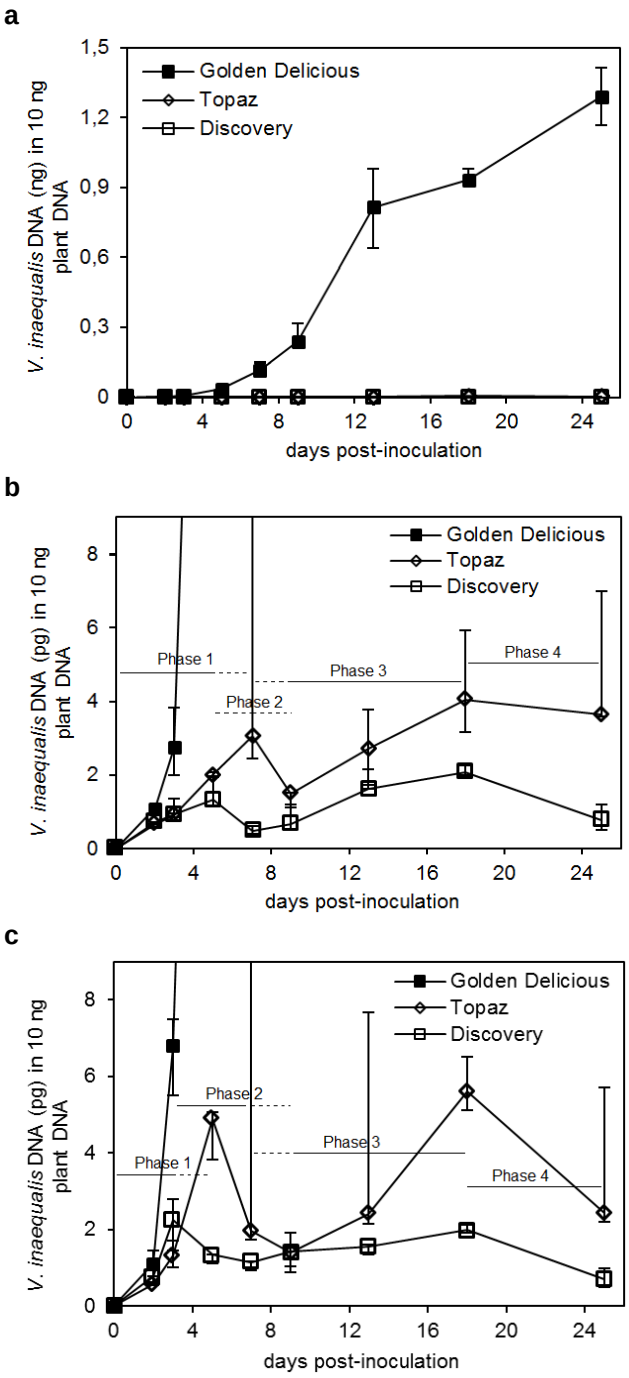

Fig. 4.8. Real-time PCR-mediated monitoring of *Venturia inaequalis* DNA quantities in total reaction volumes of 15 µl containing 10 ng apple genomic DNA extracted from the two youngest fully expanded leaves at the time of inoculation (F1 and F2), over a period of 25 days post-inoculation. Overview on the average of the two leaves **(a)**, and details of the scab-resistant cultivars 'Topaz' and 'Discovery', of the youngest F1 leaf **(b)** and the older F2 leaf **(c)**. In figures (b) and (c) the data of 'Golden Delicious' fall outside of the graph as of 5 days post-inoculation. The apparent four phases of infection of the resistant cultivars 'Topaz' and 'Discovery' are indicated in figures (b) and (c). Error bars represent the interquartile range around the median for three independent biological replicates.

In the scab-susceptible cultivar 'Golden Delicious', *V. inaequalis* DNA quantities increased gradually during the infection process, up to 1.3 ng in 10 ng plant DNA at 25 dpi (Fig. 4.8a). This evolution was very similar to the evolution in degree of sporulation (Fig. 4.3c). The Spearman rank correlation between the means of pathogen DNA content and the degree of sporulation was > 0.9 and statistically significant ($p < 0.01$). At 7 dpi, when no visual disease symptoms had yet appeared, DNA quantities had already increased to more than 100 pg per reaction. This indicates that real-time PCR allows growth to be monitored during the symptomless phase, which was confirmed for the cultivars 'Topaz' and 'Discovery' (Fig. 4.8b-c). As of 3 dpi, significantly less pathogen DNA ($p < 0.05$) was detected in these two resistant cultivars compared to the susceptible cv. 'Golden Delicious'. At 8 dpi, when the first symptoms started to appear, *V. inaequalis* DNA levels were already more than 50 times higher in 'Golden Delicious' than in 'Topaz' and 'Discovery'.

For the two resistant cultivars, real-time PCR revealed four distinct phases in the colonization of apple leaves by *V. inaequalis* (Fig. 4.8b-c). Phase 1 represents a significant increase ($p < 0.05$) in the amount of *V. inaequalis* DNA during the first days post-inoculation. Interestingly, phase 2 represents a decrease that was significant ($p < 0.05$) for leaf F1 of 'Discovery' (between 5 and 7 dpi), and for leaf F2 of 'Topaz' (between 5 and 9 dpi). Remarkably, the first relative maximum amount of *V. inaequalis* DNA that separated phase 1 and 2 was reached two days later in leaf F1 compared to leaf F2 (for both cultivars), and in 'Topaz' compared to 'Discovery' (for both leaves; Fig. 4.8b-c). Phase 3 represents a significant increase ($p < 0.05$) in *V. inaequalis* DNA levels up to 18 dpi, eventually reaching a plateau, or followed by a final decrease to 25 dpi (phase 4).

In agreement with the evolution of the degree of infection according to the classification of Chevalier (Fig. 4.3a), *V. inaequalis* DNA amounts were larger in the monogenic resistant 'Topaz' than in the polygenic resistant 'Discovery' at almost every time-point (Fig. 4.8b-c). Significant differences ($p < 0.05$) were observed at 5 dpi (leaf F2), 7 dpi (leaf F1), 18 and 25 dpi (both leaves). Significant differences existed also between individual plants of 'Topaz', at 7 dpi. The amount of *V. inaequalis* DNA detected in both leaves of one plant (> 50 pg in 10 ng plant DNA) differed significantly from the medians of those two leaves F1 and F2 (app. 3 and 2 pg, respectively).

4.6. General discussion

Visual evaluation of *V. inaequalis* infection clearly showed that the scab susceptible cv. 'Golden Delicious' was more heavily infected than the resistant cultivars 'Topaz' and 'Discovery'. However, it is uncertain if the limited development of foliar symptoms in 'Discovery' as compared to 'Topaz' means that the former is less colonized by the pathogen, thus that the defense response of 'Discovery' is more effective (Bent *et al*., 1992; Hoffman *et al*., 1999; Thomma *et al*., 1999). Moreover, the observed incubation period of one week made evaluation of early fungal development impossible, while quantification of the pathogen in this symptomless phase would give more insight into the development of the host resistance response.

Therefore, we developed the real-time PCR assay to monitor the (symptomless) growth of *V. inaequalis* in the apple leaves and to evaluate the scab resistance of the apple cultivars in a fast, objective and sensitive way.

The real-time PCR primer pair used is not exclusively specific for *V. inaequalis*, but will also amplify a fragment of the 5.8S-ITS2 region of ribosomal DNA of other *Venturia* species (Fig. 4.5). However, this is not a problem when studying the dynamics of *V. inaequalis* in artificially inoculated apple leaves, or when evaluating fungal pathogenicity and/or host resistance in a controlled greenhouse environment, when a pure *V. inaequalis* isolate is used. Moreover, none of the other *Venturia* species are known pathogens of *Malus* x *domestica*, although sexual reproduction on senescent apple leaves cannot be completely ruled out with some of them (Stehmann *et al*., 2001). Therefore, if the assay is to be used for analyzing naturally infected leaf samples from apple orchards, it is advisable to design more specific primers, to exclude cross-reaction with other *Venturia* spp. that may also be present. If necessary, an amplicon specific real-time PCR assay that makes use of a TaqMan® probe can be developed to increase the chances for species specificity. Since the sequence of the amplified amplicon of 123 bp is the same for the different *Venturia* species, the use of (high resolution) melt curve analysis to distinguish between species (Korsman *et al*., 2012) cannot be applied in our assay. For the aim of this study, development of real-time PCR primers based on a single copy gene was not considered, because the single copy nature of this target would lead to primers that are less sensitive and therefore less suitable for practical applications (Debode *et al*., 2009).

We have shown that dilution series of *Venturia* DNA can be accurately quantified over a large concentration range, in the absence or presence of host DNA, using real-time PCR and primer pair V-5.8S-ITS2-F/R. Moreover, the ITS2-based real-time PCR was very sensitive, with a detection threshold as low as 100 fg gDNA. The sensitivity of conventional PCR assays is not sufficient to detect early infection stages at low disease incidence (Schena *et al*., 2004).

Like all PCR-based detection assays, real-time PCR is affected by the presence of PCR inhibitors in DNA extracts (Wilson, 1997). However, since the inhibitory effect is dependent on the amount of plant-derived gDNA extract present, all gDNA extracts were normalized to contain 10 ng of plant gDNA. We have chosen to normalize extracts to host gDNA concentrations rather than analyzing equal amounts of host tissue, since successive gDNA extractions showed some variation in extraction efficiencies. Moreover, phenolic compounds and other secondary metabolites that could inhibit PCR reactions can be present in different amounts in healthy vs. infected and in resistant vs. susceptible apple leaves (Hrazdina, 2003). Normalizing against host gDNA using the same real-time PCR technique as with *Venturia* gDNA will most probably overcome these possible differences in PCR inhibition. The amount of 10 ng plant gDNA represented the optimal balance between PCR inhibition on the one hand and maintaining enough detection sensitivity on the other hand. For the quantification of *Venturia* DNA in heavily infected tissue of Golden Delicious leaves, the massive levels of tissue necrosis may result in aberrant PCR kinetics, disturbing the quantitative character of the technology (Brouwer *et al*., 2003). In such cases, analysis should be carried out at time points before which the tissues have become totally macerated, since obviously there is no need for PCR-based detection for tissue with clear sporulation symptoms. If PCR-based detection is still desirable in such cases, e.g. in an attempt to quantify sporulation levels, the DNA extract should be diluted to avoid the effects of inhibitors (Debode *et al*., 2009).

Finally, we have used the optimized assay to quantify *V. inaequalis* DNA levels following greenhouse inoculation of leaves of three apple cultivars with differing levels of scab resistance. Interestingly, infection of the resistant cultivars ‘Topaz’ and ‘Discovery’ by *V. inaequalis* appeared to proceed in four distinct phases. While these results still need to be confirmed in other cultivars, our current understanding of the apple – *V. inaequalis* interaction and similar results in other plant-ascomycetal pathogen studies (Stephens *et al*.,

2008) support these conclusions/results. The statistically significant initial increase in *V. inaequalis* DNA amounts in the first few days after inoculation (phase 1) probably is due to the germination of spores and an initial phase of subcuticular hyphal growth. The reduction in fungal DNA during phase 2 suggests that part of the hyphae have died off. This phenomenon was also detected during the colonization of wheat by the ascomycete *Fusarium graminearum* (Stephens *et al*., 2008). In the case of *F. graminearum*, a recent study by Josefsen *et al*. (2012) demonstrated the important role that autophagy plays in plant colonization, i.e. before phytopathogen infection is established to the extent that the pathogen can derive nutrients from the host, fungal cellular contents are degraded in cells that are no longer required, to supply nutrients to the non-assimilating fungal structures necessary for growth. Our results suggest that a similar mechanism may be occurring during the *Malus* - *Venturia* interaction. Phase 3 of *V. inaequalis* colonization of apple leaves involved a second significant increase in fungal DNA that was probably due to further fungal colonization of the subcuticular region. Eventually, the plateau or decrease in fungal DNA concentrations after 18 dpi shows that host defense mechanisms begin to gain the upper hand, and confirms the known resistance phenotypes of these two cultivars.

Since the decrease in fungal DNA levels during phase 2 was only statistically significant in part of the conditions (leaves/cultivars), we suggest that at these early stages and at low DNA amounts (10^2 and 10^3 fg), a higher number of (biological and technical) replicate reactions should be performed in order to obtain more significant results. However, the variability between plants can also have a biological significance as host defense mechanisms may develop less or more slowly in some plants. The high third quartiles with 'Topaz' at different time-points can indicate a certain loss of resistance properties within some leaves. Certainly the outlier of 'Topaz' at 7 dpi suggests a disturbed host defense (Fig. 4.8b-c).

It is well-known that disease development is also dependent on leaf maturity (Develey-Rivière and Galiana, 2007; see Section 2.3.5: Ontogenic resistance). Visual evaluation of *V. inaequalis* infection of 'Golden Delicious' leaves of different ages already confirmed this statement (Fig. 4.4). Besides, quantitative and temporal differences in rates of *V. inaequalis* colonization between leaves of different ages of 'Topaz' and 'Discovery', especially during the initial, symptomless stages (Fig. 4.8b-c), demonstrate that it is better to analyze these

leaves separately, and if necessary, to pool the real-time qPCR results, rather than bulking the leaf tissue material prior to DNA extraction. Otherwise, possible significant differences between these leaves are concealed, and even differences between time points can be suppressed.

Although in the scab-susceptible cultivar 'Golden Delicious' correlation was demonstrated between pathogen DNA content and degree of sporulation (Spearman rank correlation > 0.9; $p < 0.01$), our results show that, when comparing different cultivars, there is no general correlation between the disease symptoms visually observed and the true degree of *V. inaequalis* infection as measured by real-time PCR. This is illustrated at 9 dpi, when the amount of *Venturia* DNA detected in leaf F2 was the same for 'Topaz' and 'Discovery' (Fig. 4.8c). However, at 9 dpi, most leaves of 'Topaz' showed chlorotic lesions (class of Chevalier 2), while the leaves of 'Discovery' showed no symptoms at all (Fig. 4.3a). In addition, the leaves of most Golden Delicious plants at 8 dpi and most 'Topaz' plants at 14 dpi were classified in class 3a, while the amounts of *V. inaequalis* detected were more than 50 times higher in Golden Delicious. These differences between the extent of disease symptoms and the extent of pathogen colonization have also been shown by studies of other plant-pathogen interactions (Bent *et al*., 1992; Hoffman *et al*., 1999; Thomma *et al*., 1999). While visual symptom evaluation is still a good way of determining the fungal pathogenicity (i.e. the ability to cause disease), real-time PCR is a more appropriate method to assess its virulence (i.e. the ability to multiply within the host). Combination of both assessments can give a good idea of the extent of resistance to scab and/or tolerance (fungal growth without disease development).

The current study may also serve as a platform for future work to help understand how host resistance might affect the stages of infection. The assay will therefore be useful in the elucidation of pathogen-host relationships and is for example ideal for detecting minor changes of resistance or susceptibility in transgenic plants or mutants. Next to host factors, the sensitive real-time PCR detection technique also allows the measurement of the growth of the pathogen (or lack thereof) as a function of environmental factors such as climate and application of fungicides or plant defense enhancers (see Chapter 6).

In addition to demonstrating the utility of real-time PCR for studying (symptomless) growth of *Venturia* spp. in apple leaves, the assay also allowed discrimination between scab-

resistant and -susceptible cultivars, and to some extent even between resistant cultivars with different resistance mechanisms, during the symptomless phase already. Therefore, the application of the assay within breeding programs is promising. The outlier of 'Topaz' at 7 dpi even highlights the possibility to use real-time PCR to discriminate in an early, symptomless stage between the most resistant plants from among a sample of plants considered to be equally resistant based on the resistance genotype, and/or on visual assessment of disease severity. Thus, classical, symptom-based resistance breeding and real-time PCR could be used in a complementary fashion.

4.7. Conclusions

In conclusion, both visual evaluation of leaf symptoms and real-time PCR confirmed that 'Golden Delicious' is much more susceptible to *V. inaequalis* than 'Topaz' and 'Discovery' and that the monogenic *Rvi*6-resistant 'Topaz' is slightly more infected than the polygenic 'Discovery'. Our results demonstrate that real-time PCR is a fast and objective method to assess fungal pathogenicity and host resistance. Our developed real-time PCR protocol proved to be a sensitive and reproducible method for *in planta* quantification of *V. inaequalis* during apple leaf colonization. The assay appeared to be very effective for the quantification of *Venturia* DNA levels at early, symptomless stages of infections. Therefore, the technique cannot only be used in the study of the biology of the pathogen and the defense mechanisms of different apple cultivars, but there is a great potential for applications in breeding programs as well.

Chapter 5

Proteomic analysis of responses of apple to *V. inaequalis* infection

5.1. Introduction

Through observation of disease symptoms following *V. inaequalis* inoculation and real-time PCR quantification of hyphal growth, we were able to have an idea of the evolution of the apple – *V. inaequalis* interaction in cultivars with differences in scab susceptibility (see Chapter 4). However, to better understand the biochemical mechanisms behind the responses of apple to scab infection, we decided to use a proteomics approach. This study is one of the first to compare proteomes of leaves of apple cultivars with different susceptibilities to apple scab. The recent publication of the reference apple genome sequence (Velasco *et al.,* 2010) aided the functional identification of sequenced proteins.

5.2. Introductory experiments: evaluation of 2-DE protocols

5.2.1. Initial 2-DE methods of choice

Non-inoculated 'Golden Delicious' leaf samples were used to adapt conditions for the 2-DE analysis. Indeed, 2-DE conditions generally need be optimized for specific plant-pathogen interactions (Carpentier *et al*., 2008b). Since the 2-DE experience with the apple – *V. inaequalis* interaction was limited, optimization of 2-DE conditions was most likely to be necessary. The initial 2-DE conditions used were chosen based on earlier results from our lab (Vanhoucke, 2006).

5.2.1.1. Protein extraction and sample preparation

The two youngest fully expanded leaves on each one year old plant were harvested, pooled and stored at -80°C. Protein extraction and sample preparation were initially performed according to a variant of the extensively applied phenol extraction, methanol/ammonium acetate precipitation protocol for plant tissues (Saravanan and Rose, 2004). The leaf material was grounded in a precooled mortar in the presence of liquid nitrogen and 0.5–1.0 g of the homogenate was resuspended in 3 ml of ice-cold extraction buffer (50 mM Tris-HCl pH 8.3, 5 mM EDTA, 100 mM KCl, 50 mM DTT, 0.7 M sucrose, 5 % w/v PVPP, 1 mM PMSF) and vortexed for 30 s. The sample was incubated for 30 min at 4 °C. After centrifugation (10 min, 4000 *g*, 4 °C), the pellet was reextracted with 3 ml of extraction buffer and vortexed (30 s), incubated (30 min, 4 °C) and centrifuged (10 min, 4000 *g*, 4 °C) again. Both supernatants were combined, 5 ml of water saturated phenol was added and the sample was vortexed for 30 s. After 60 min at 4 °C and centrifugation for 10 min at 4000 *g* and 4 °C, the phenolic phase was collected. Three ml of water saturated phenol was added to the aqueous phase (and interphase) and this mixture was vortexed again for 30 s and incubated for 60 min at 4°C. After centrifugation (15 min, 4000 *g*, 4 °C), the phenolic phase was added to the first phenolic phase. This total volume was precipitated overnight with five volumes 100 mM ammonium acetate in methanol at -20 °C. This precipitation step was needed to increase the purity and the protein content of the extract (Santoni *et al*., 1999). After precipitation, the sample was centrifuged at 17 000 *g* for 60 min at 4 °C, the supernatant was removed and the pellet was rinsed twice in ice-cold acetone/0.2% DTT. Between the two rinsing steps, the sample was incubated for 60 min at -20 °C and centrifuged again (30 min, 17 000 *g*, 4°C). After one last incubation (15 min at -20°C) and centrifugation step (30 min, 17 000 *g*, 4°C), the pellet was air-dried, resuspended in 200 µl lysis buffer (7 M urea, 2 M thiourea, 4 % CHAPS, 0.2 % carrier ampholytes (Bio-Lyte 4-7, Ampholyte, Bio-Rad, UK), 2 mM DTT) and vortexed at RT until it dissolved.

5.2.1.2. Protein quantification

Total protein concentrations of leaf extracts were determined using the Bio-Rad RC-DC protein assay following the manufacturer's guidelines (Bio-Rad). This assay is compatible with reducing agents (RC; such as DTT) and detergents (DC; such as CHAPS). A dilution series (5, 10, 20, 30 and 40 µg) of bovine-γ globuline (IGG) was used as a standard curve.

5.2.1.3. 2-DE

Each protein sample was diluted with the lysis buffer to 400 µg (CBB staining) or 100 µg (silver staining) protein per 300 µl, and was applied to a 17 cm ReadyStrip IPG strip (pH 4-7 or 3-10, Bio-Rad) via active rehydration loading (12 h at 50 V). Proteins were isoelectrically focused in a Protean IEF Cell system (Bio-Rad) at 20 °C: 20 min at 250 V, 2h at 1000 V, 2 h at 2000 V, 2 h at 4000 V, 2 h at 4000-10,000 V (linear gradient) and 60,000 Vh at 10,000 V. Prior to second dimension analysis, the individual strips were equilibrated for 10 min in 6 ml equilibration solution (6 M urea, 20 % glycerol, 2 % SDS, 50 mM Tris pH 8.8) containing 2 % w/v DTT and subsequently for 10 min in 6 ml equilibration buffer containing 2.5 % w/v iodoacetamide. The separation in the second dimension was realized on the Protean II xi Cell instrument (Bio-Rad) with lab cast 1 mm SDS polyacrylamide gels (12 % T): 1 h at 16 mA/gel and 4 h at 24 mA/gel.

As an initial evaluation of extraction and precipitation conditions, IEF was performed with 7 cm IPG strips (see methods and focusing conditions in Appendix I: “IEF with 7 cm IPG strips”).

5.2.1.4. Protein visualization

Proteins were visualized either by silver staining (Blum *et al*., 1987) or by CBB R-250 staining (Neuhoff *et al*., 1988). For silver staining, the gels were fixed overnight in a fixing solution (40 % ethanol, 10 % acetic acid), washed for 20 min in 30 % ethanol, 20 min in 20 % ethanol, and 20 min in Milli-Q water. After washing, the gels were sensitized in 0.02 % $Na_2S_2O_3$ for 1 min and incubated in silver stain (0.2 % $AgNO_3$, 0.02 % formaldehyde) for 20 min. The gels were developed in 3 % Na_2CO_3, 0.0005 % $Na_2S_2O_3$, 0.05 % formaldehyde for 3 min and blocked in 1 % glycine. For CBB R-250 staining, the gels were stained overnight in a staining solution (0.1 % w/v CBB R-250, 50 % methanol and 10 % acetic acid) and destained overnight in a destaining solution (10 % methanol and 10 % acetic acid). Stained gels were scanned at a resolution of 150 dpi using the ImageScanner I (GE Healthcare) and calibrated with Labscan 5 software (GE Healthcare).

5.2.2. Results and discussion

5.2.2.1. Protein extraction and quantification

The resulting 2-DE gels showed too much streaking, especially horizontal streaking, and not enough spots (Fig. 5.1). Moreover this protocol was not that practical in use, especially because quite a lot of leaf material was needed (0.5–1.0 g). Because young leaves were sampled in our experiments, the amount of available leaf material was limited. Therefore, and because a proper protein extraction is the most important step in a well-performed 2-DE experiment, we switched to a similar protocol for protein extraction and sample preparation, that is also based on the phenol extraction, methanol/ammonium acetate precipitation protocol for plant tissues (Carpentier *et al*., 2005; see Section 3.7.1). This protocol was optimized for small amounts of tissue (50-150 mg) and proved useful for the preparation of protein extracts from recalcitrant plant tissues (Carpentier *et al.*, 2005; Righetti *et al.*, 2008).

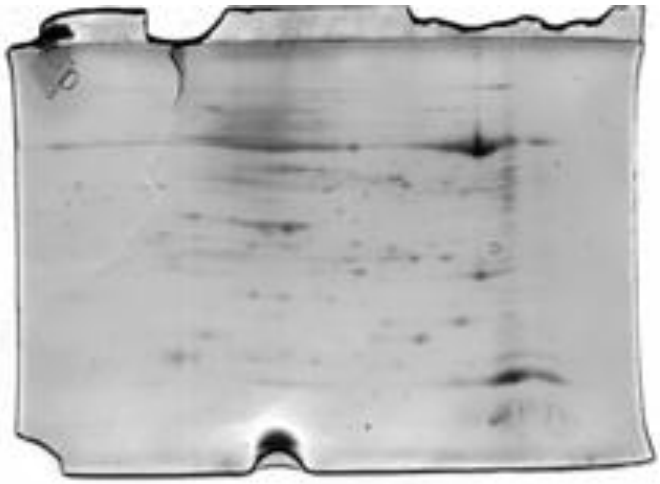

Fig. 5.1. Example of a CBB R-250 stained gel that is the result of IEF on a 7 cm ReadyStrip IPG strip (pH 4-7; Bio-Rad) with the Protean IEF Cell system (Bio-Rad), and SDS-PAGE in 1 mm SDS polyacrylamide gels (12 % T) realized on the Mini-Protean 3 instrument (Bio-Rad).

Because of increasing problems with the reproducibility of the protein quantification by means of the Bio-Rad RC-DC protein assay, total protein concentrations were determined using the 2-D Quant kit from GE Healthcare (see Section 3.7.2). With the latter, the added colorimetric reagent binds free copper ions that were added earlier to the protein sample and, as a result, it colors yellow. Therefore, the color intensity and thus the absorption of

light is inversely proportional to the protein concentration of the sample. With the RC-DC assay, on the other hand, the added colorimetric reagent is Folin's reagent, that is reduced by the with copper treated proteins and, as a result, colors blue. Therefore, the absorption of light is proportional to the protein concentration. Because the staining is mainly due to the amino acids tyrosine and tryptophan, protein-to-protein variation can arise. Because the 2-D Quant assay is independent from reaction with functional groups of amino acids, the reactivity is largely independent from the amino acid composition and, as a result, there is little protein-to-protein variation.

5.2.2.2. 2-DE and protein visualization

Because the quality of the 2-DE gels with use of this protein extraction protocol of Carpentier *et al*. (2005) was still not optimal, the protocols for 2-DE and visualization of the proteins were modified as well.

IEF: The samples were no longer applied to the IPG strips via in-gel rehydration, but via anodic cup loading. Indeed, during the rehydration loading process, the proteins are distributed randomly over the gel. Consequently, during IEF, they approach their isoelectric point from both sides with a different mobility which can lead to horizontal streaking. Cup loading should give more reliable results, especially for quantitative analyses (Görg *et al*., 2004; 2009). With most plant proteins, anodic cup loading gives better results than cathodic cup loading, because of reduced streaking caused by migration of acidic proteins (Görg *et al*., 2000; Hoving *et al*., 2002).

The IPG strips used were the Immobiline DryStrips (GE Healthcare) of 24 cm and pH 4-7. The increased length (compared to the 7 cm and 17 cm strips) improved the resolution of the protein separation and resulted in more spots. The resolving power also increased by using the narrow range pH 4-7 IPG strips compared to the broad range pH 3-10 strips. Moreover, comparison of both confirmed that most proteins of apple leaves – like most plant proteins in general – lie within the pH 4-7 region. Finally, a literature and protein database study verified that also a lot of the proteins known to be involved in plant-pathogen interactions have a theoretical pI in the range 4-7 (Konishi *et al*., 2001; Sindelarova and Sindelar, 2001; Gau *et al*., 2004; Kim *et al*., 2004; reviewed by Gonzalez-Fernandez and Jorrin-Novo, 2012; UniProtKB). Because cup loading with the Protean IEF Cell system (Bio-Rad) continuously

gave rise to burning of the IPG strips, IEF was performed on the IPGphor II system (GE Healthcare) (Fig. 5.2).

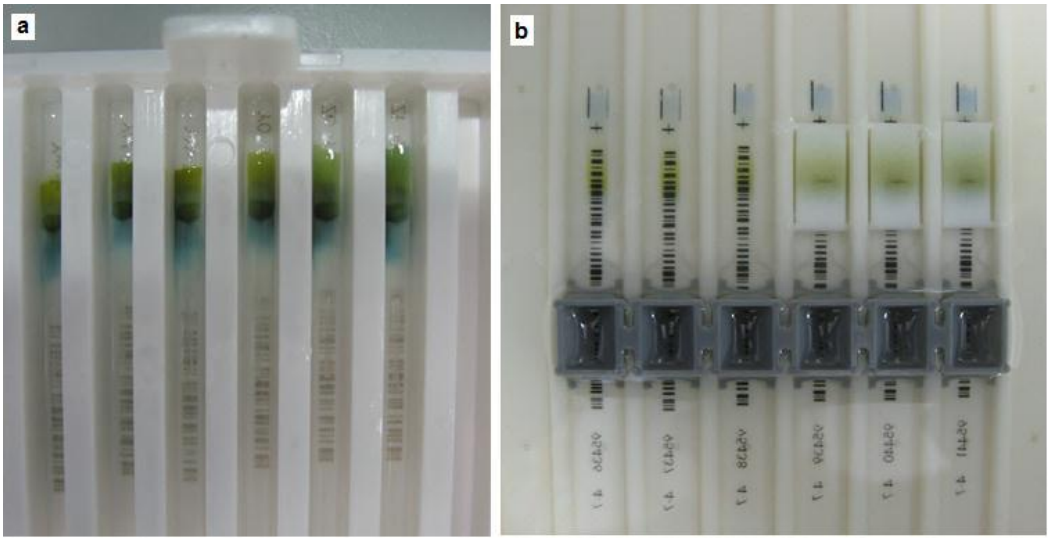

Fig. 5.2. Anodic side of six IPG strips after anodic cup loading and IEF performed on the Protean IEF Cell system of Bio-Rad (a) or on the IPGphor II system of GE Healthcare (b). The Protean IEF Cell system continuously gave rise to burning of the IPG strips (black spots). (Cups used for cup loading and paper wicks used for IEF with the IPGphor II system are also visible)

SDS-PAGE: SDS-PAGE was carried out using an Ettan DALT*six* instrument (GE Healthcare), that results in larger gels and is designed for 24 cm strips (see Section 3.7.4).

Visualization: Visualization of proteins was done by colloidal Coomassie Brilliant Blue (CBB) G-250 staining, also according to Carpentier *et al*. (2005; see Section 3.7.5). Because of the high cost of CyDye™ labeling, this fluorescent visualization technique was not yet applied in this stage.

Finally, all the optimization steps led to reproducible gels with an acceptable number of spots for this kind of 2-DE setup: 999 ± 62 (standard deviation of three replicates) (Fig. 5.3 and Appendix II).

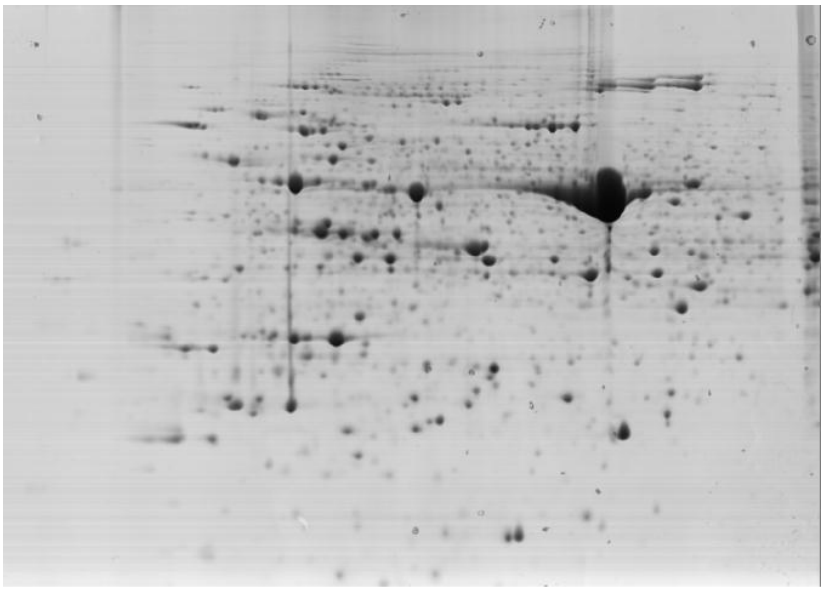

Fig. 5.3. Example of a CBB G-250 stained 2-DE gel (1067 spots) that is the result of IEF on a 24 cm ImmobilineDry Strip pH 4-7 (GE Healthcare) with the IPGphor II system (GE Healthcare), followed by SDS-PAGE in 1.5 mm lab cast gels (12.5 %) on the Ettan DALT*six* instrument (GE Healthcare). The stained gel was scanned using the ImageScanner I (GE Healthcare) and calibrated with Labscan 5 software (GE Healthcare). Image analysis was performed with the Image Master 2-D platinum software 6.0 (GE Healthcare).

5.3. Proteome analysis during infection of a resistant and a susceptible apple cultivar

5.3.1. Experimental setup

The optimized protocols for protein extraction and 2-DE analysis described in Section 5.2 were used to carry out a proteome analysis of the responses to scab infection of the apple cultivars 'Golden Delicious' (susceptible to race 1 of *V. inaequalis*) and 'Topaz' (monogenic *Rvi*6-resistant). In a first experiment, the leaf proteomes of non-inoculated (i.e. 'control') plants were analyzed ('Top-C <> Gol-C'). For each plant, leaves F1 and F2 (see Section 3.3) were harvested, pooled and stored at -80 °C. Both leaves were pooled since, for this comparison of the control conditions of both cultivars, the recently unfolded leaves F1 and F2 were sampled just before inoculation would take place (0 dpi), so the amount of leaf material was limited. Moreover, practically, pooling decreased the amount of labour-intensive 2-DE experiments by half. For proteome analysis, five replicate extractions (*cf*. five

biological replicates; each replicate represents one plant) were performed for each cultivar and the CBB G-250 staining technique was applied. The Kolmogorov-Smirnov statistical test was applied to the matched spots to test the significance of the difference between spot abundances of proteins of both cultivars (see Section 3.7).

Subsequently, two 2D-DIGE experiments were performed. In the first one, leaves F1 and F2 were sampled from control ('C'), mock-inoculated ('M') and inoculated ('I') 'Topaz' plants at 2, 3 and 5 dpi (no control leaves at 3 dpi). These time-points were chosen based on literature about similar proteomic studies of other plant-pathogen interactions (Kim *et al*., 2004; Thurston *et al*., 2005) and on earlier results from our lab (Vanhoucke, 2006). The aim of this choice was to maximize the amount of detected changes in protein abundances among the different treatments. Based on the results of this first 2D-DIGE experiment, the leaf proteome of *V. inaequalis* inoculated 'Topaz' was compared to the leaf proteome of inoculated 'Golden Delicious' plants at 5 dpi in a second 2D-DIGE experiment ('Top-I <> Gol-I'). Both cultivars were inoculated and sampled at the same time of the day.

For both 2D-DIGE experiments, three replicate protein extractions (*cf*. three biological replicates; each replicate represents one plant) were performed. A one-way analysis of variance (ANOVA) was carried out in order to detect absolute protein changes among the different treatments (see Section 3.7).

By including both control and inoculated 'Topaz' and 'Golden Delicious' plants, it was possible to verify which differences in protein accumulation between both cultivars were present after fungal infection, and which proteins were constitutively present in different concentrations in both cultivars. By including mock-inoculated 'Topaz' plants, we could identify the proteins that were differentially accumulated due to the mock-inoculation related (abiotic) stress conditions on the one hand, and the proteins of which accumulation was induced by the specific recognition of the pathogen on the other hand.

5.3.2. Results and discussion

Automatic spot detection of 10 CBB G-250 stained gels revealed 1001 ± 124 spots for 'Topaz' and 985 ± 112 spots for 'Golden Delicious'. Out of these, 923 ± 76 spots could be matched between the two cultivars. Spot detection of the CyDye^{TM} labeled gels revealed 1226 ± 74 spots for the first 2D-DIGE experiment and 1403 ± 68 spots for the second one. For a

complete overview of the protein identifications in this and next chapter, the reader is referred to Appendix III. In total, 193 spots with differences in protein abundance in one or both chapters were excised of which 169 spots (= 87.6 %) were positively identified using MALDI-TOF/TOF mass spectrometry analysis and Mascot searches of the MS/MS spectra against the *Malus* x *domestica* genome (see Section 3.7.7). Figure 5.4 shows a representative CBB G-250 stained preparative gel with the excised spots numbered and indicated.

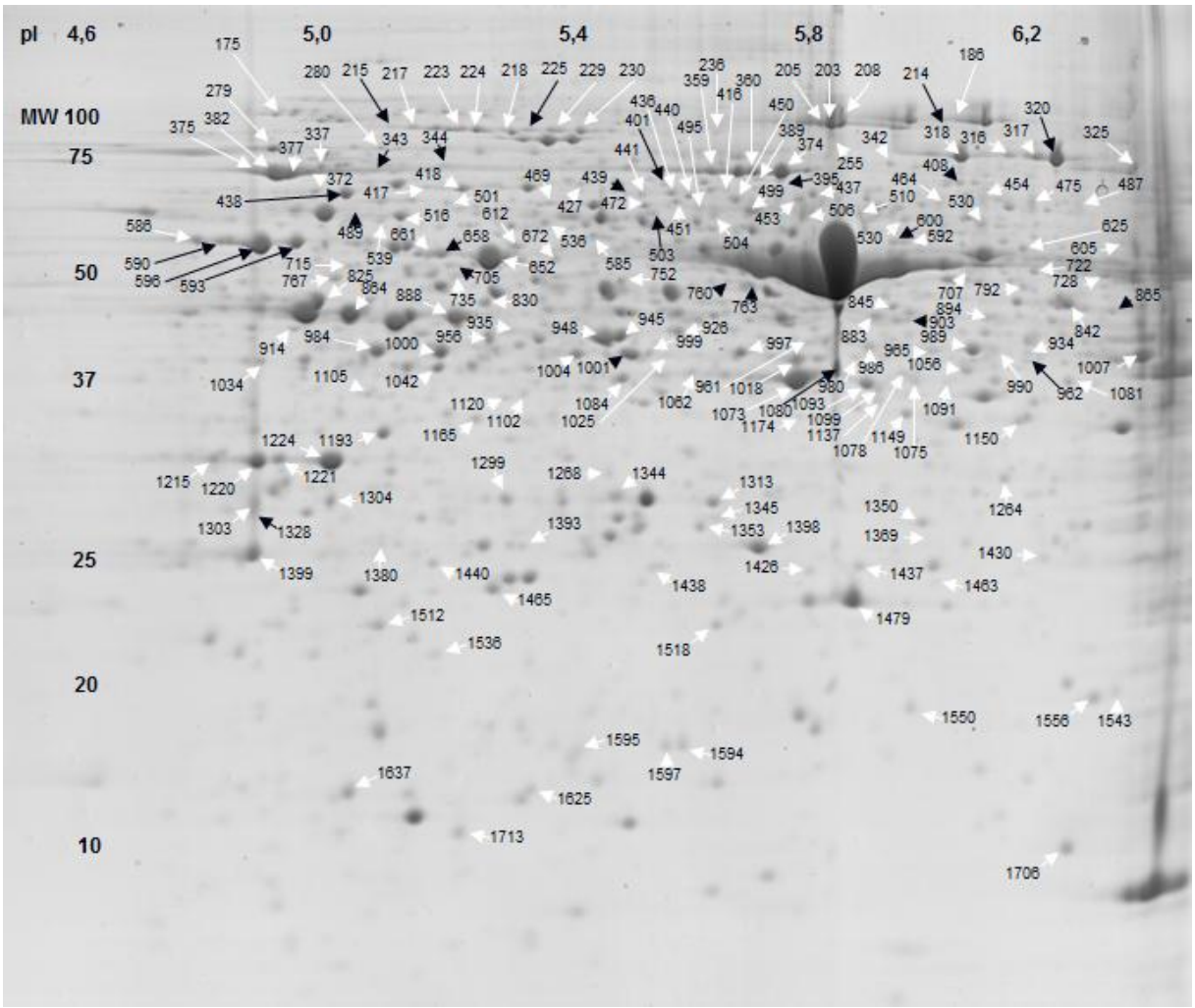

Fig. 5.4. A representative CBB G-250 stained 24 cm pI 4-7 gel of apple leaf tissue (cultivar 'Topaz' control conditions). The 193 excised spots are numbered and correspond to the spot numbers in the tables of this and next chapter and Appendix III. White arrows indicate MALDI-TOF/TOF identified spots while black arrows refer to non-identified spots.

5.3.2.1. Changes in the leaf proteome of the resistant apple cultivar 'Topaz' in response to *V. inaequalis* infection

When comparing the *V. inaequalis* inoculated and mock-inoculated conditions at 5 dpi ('I <> M'), only 4 spots were significantly differentially accumulated ($q \leq 0.05$), of which 2 were up-regulated in the scab inoculated leaf samples and 2 down-regulated. At 2 and 3 dpi, there were even no statistically significant differences between both conditions. In general, significant differences and tendencies in differential protein accumulation between the three conditions examined were most distinct at 5 dpi. At 2 and 3 dpi, the differences appeared not to be present yet, were less distinct, or at most comparable to 5 dpi, and no other trends could be observed. For further analysis and protein identification we therefore focused on the differences observed at 5 dpi.

Of the 2 up-regulated spots, only 1 (spot 1099) could be confidently matched to preparative CBB G-250 stained gel images. It was picked for identification and positively identified as an 'auxin-induced protein PCNT115-like isoform 1' (MDP0000228499). This is a pyridoxine:NADP 4-dehydrogenase that is involved in vitamin B6 metabolism. Vitamin B6 plays essential roles as a cofactor in a range of biochemical reactions. In addition, plants employ vitamin B6 as an antioxidant to protect themselves against reactive oxygen species (Havaux *et al*., 2009).

Both down-regulated spots could be matched to preparative gel spots and were identified as 'protein thylakoid formation1 (chloroplastic-like)' (spot 1350; MDP0000139684) and an uncharacterized protein (spot 1440; MDP0000178270), respectively. The thylakoid formation1 protein is involved in protein import into the chloroplast and is required for the normal organization of vesicles into mature thylakoid stacks and ultimately for leaf development (UniProtKB).

The low number of spots that were found to be significantly differentially accumulated between the *V. inaequalis* inoculated and mock-inoculated conditions was most probably due to the relatively large differences between the biological replicates (see end of this Section and Chapter 6). As a consequence, general statements concerning changes in the leaf proteome of the resistant apple cultivar 'Topaz' in response to *V. inaequalis* infection were impossible at this point.

However, because many spots seemed to show a tendency of up- or down-accumulation of infection > mock-infection > control ('I>M>C') or infection < mock-infection < control ('I<M<C') respectively, we also investigated the differences between the scab-infected and control conditions ('I <> C') in 'Topaz'. Sixty spots were significantly differentially accumulated ($q \leq 0.05$), of which 40 were up-regulated in the scab inoculated leaf samples and 20 down-regulated. Of the 40 up-regulated spots, 32 spots were positively identified, resulting in 29 individual protein identifications. Of the 20 down-regulated spots, 17 were identified, resulting in 15 individual protein identifications. The discrepancy between the number of identified spots and the number of individual protein identities indicates that some of the spots are protein isoforms or proteins carrying different post-translational modifications. The individual proteins were classified according to the Gene Ontology (GO) biological process wherein they are involved (Table 5.1 and Table 5.2).

Table 5.1. List of *V. inaequalis* inoculation up-regulated proteins in 'Topaz' (monogenic *Rvi*6-resistant cultivar) at 5 dpi.

						I>C		I>M	M>C			
Spot[a]	**Protein name[b]**	**Accession No.[c]**	**Score[d]**	**PM[e]**	**q[f]**	**I/C[g]**	**α[h]**	**I/M[g]**	**M/C[g]**	**I[i]**	**M[i]**	**C[i]**
	Cell rescue, defense and virulence											
	Defense response											
1594	major allergen Mal d 1 (PR-10)	MDP0000942516	505	6	6.3^{E}-3	8.1	0.01	3.0	2.7	a	ab	b
1595	major allergen Mal d 1 (PR-10)	MDP0000942516	556	7	3.3^{E}-4	5.9	1^{E}-3	2.3	2.6	a	ab	b
	flavonoid biosynthesis											
894	chalcone synthase	MDP0000575740	240	8	5.2^{E}-4	1.8	0.01	1.4	1.3	a	ab	b
	defense signaling mediated by R proteins											
427	enhanced disease susceptibility 1	MDP0000162236	326	14	0.035	2.0	0.05	1.3	1.5	a	ab	b
	Protein folding											
337	heat shock protein 70 (70 kDa)	MDP0000570507	515	17	0.037	1.6	0.05	1.3	1.1	a	ab	b
	Oxylipin biosynthesis											
224	linoleate 13s-lipoxygenase 2- chloroplastic	MDP0000753547	227	7	0.046	1.6	0.05	1.5	1.1	a	ab	b
	Stress response											
	Protein folding											
516	heat shock protein 60	MDP0000235765	688	23	7.1^{E}-3	1.8	1^{E}-3	1.3	1.4	a	ab	b
504	TCP (T-complex protein) domain class transcription factor	MDP0000036030	219	7	8.2^{E}-3	2.3	1^{E}-3	1.4	1.6	a	a	b
	ROS detoxification											
1713	thioredoxin h	MDP0000622392	350	5	9.4^{E}-3	2.3	0.01	1.4	1.6	a	ab	b
	Nucleotide biosynthesis											
1706	nucleoside diphosphate kinase 1 (NDPK I)	MDP0000322880	854	10	0.013	2.0	0.01	1.4	1.4	a	ab	b
530	bifunctional purine biosynthesis protein	MDP0000654452	197	9	0.021	1.6	0.01	1.4	1.1	a	ab	b
	Energy and carbohydrate metabolism											
	Glycolysis											
506	phosphofructokinase	MDP0000293776	124	6	0.015	2.5	1^{E}-3	1.6	1.5	a	ab	b

Table 5.1 - *continued*

						I>C		I>M	M>C			
Spot[a]	**Protein name[b]**	**Accession No.[c]**	**Score[d]**	**PM[e]**	**q[f]**	**I/C[g]**	**α[h]**	**I/M[g]**	**M/C[g]**	**I[i]**	**M[i]**	**C[i]**
501	pyruvate kinase	MDP0000121177	623	15	0.026	2.1	0.01	1.5	1.4	a	ab	b
499	pyruvate decarboxylase	MDP0000223243	549	11	0.034	2.1	0.01	1.4	1.4	a	ab	b
495	pyruvate decarboxylase	MDP0000223243	123	5	0.023	1.9	0.01	1.3	1.4	a	ab	b
	Glycolysis and gluconeogenesis											
450	cytosolic phosphoglucomutase	MDP0000321541	630	14	8.3^{E}-3	1.9	0.01	1.2	1.6	a	a	b
441	cytosolic phosphoglucomutase	MDP0000321541	245	8	0.037	1.5	0.05	1.2	1.2	a	ab	b
1078	fructose-bisphosphate aldolase	MDP0000151849	147	7	0.036	2.0	0.05	1.4	1.5	a	ab	b
	Tricarboxylic-acid (TCA) cycle											
1093	NAD^{+}-dependent malate dehydrogenase	MDP0000174740	577	12	0.022	1.6	0.05	1.3	1.2	a	ab	b
	TCA cycle; oxidative phosphorylation											
436	succinate dehydrogenase	MDP0000188391	324	8	6.9^{E}-3	1.9	1^{E}-3	1.2	1.7	a	a	b
	Pyruvate metabolism											
437	$NADP^{+}$-dependent malate dehydrogenase; malic enzyme	MDP0000221561	602	13	0.030	1.3	0.05	1.2	1.1	a	ab	b
1193	(putative) lactoylglutathione lyase	MDP0000319112	1030	15	0.032	1.5	0.05	1.2	1.2	a	ab	b
	Acetyl-CoA biosynthesis											
1463	dephospho-CoA-kinase	MDP0000266097	254	9	0.022	2.7	0.01	1.9	1.4	a	ab	b
715	ATP-citrate synthase	MDP0000931334	335	7	0.011	1.6	0.01	1.3	1.2	a	ab	b
	Pentose-phosphate pathway											
728	6-phosphogluconate dehydrogenase	MDP0000191398	480	13	0.011	1.5	0.01	1.2	1.3	a	ab	b
	Translation											
	aminoacyl-tRNA biosynthesis											
342	glycyl-tRNA synthetase (1, mitochondrial-like)	MDP0000226879	734	15	0.046	1.9	0.05	1.4	1.3	a	ab	b
	Cellular Organization											
	Morphogenesis											
453	Nucleosome/chromatin assembly factor	MDP0000251796	197	5	0.015	2.4	1^{E}-3	1.6	1.5	a	ab	b

Table 5.1 - *continued*

						I>C		I>M	M>C			
Spot[a]	**Protein name[b]**	**Accession No.[c]**	**Score[d]**	**PM[e]**	**q[f]**	**I/C[g]**	**α[h]**	**I/M[g]**	**M/C[g]**	**I[i]**	**M[i]**	**C[i]**
	Cellular cell wall organization											
1004	alpha-1,4-glucan-protein synthase (UDP forming)	MDP0000232047	967	18	0.038	1.7	0.01	1.1	1.5	a	ab	b
454	beta-glucosidase 24-like	MDP0000297569	350	4	0.049	2.9	0.05	1.6	1.8	a	ab	b
	Metabolism of vitamins and cofactors											
	Vitamin B6 metabolism											
1099	auxin-induced protein PCNT115-like isoform 1	MDP0000228499	1410	19	3.8^{E}-4	1.5	1^{E}-4	1.3	1.2	a	b	c
	Porphyrin and chlorophyll metabolism											
997	uroporphyrinogen (III) decarboxylase (UROD)	MDP0000364293	117	5	0.034	1.7	0.01	1.3	1.3	a	ab	b
	Unknown											
1137	EF-hand (motif containing) (calcium binding) protein	MDP0000120294	288	5	4.2^{E}-3	2.0	1^{E}-3	1.5	1.4	a	ab	b

[a] Corresponding spot number in the gel image in Fig. 5.1

[b] Proteins have been grouped according to the Gene Ontology biological process wherein they are involved

[c] MDP number of predicted apple gene (Velasco *et al*., 2010) (Gene and protein sequences can be obtained from Genome Database for Rosaceae (GDR): http://www.rosaceae.org)

[d] MOWSE score probability (protein score) for the entire protein

[e] Number of matched peptides of peptide mass fingerprinting combined with MS/MS

[f] Overall false discovery rate (FDR) corrected p-value, according to a one-way ANOVA, using the DeCyder 6.5 software

[g] The 'more abundant changes' are given as average standardized protein abundance ratios of the most abundant sample (I, I and M respectively) to the less abundant sample (C, M and C respectively), calculated with the DeCyder 6.5 software

[h] Comparison of the ^{10}log standardized protein abundances of the protein in the inoculated (I) and control (C) 'Topaz' leaves with significance levels α according to a FDR corrected one-way ANOVA, using the DeCyder 6.5 software

[i] Significance classes ($q \leq 0.05$)

Table 5.2. List of *V. inaequalis* inoculation down-regulated proteins in 'Topaz' (monogenic *Rvi*6-resistant cultivar) at 5 dpi

						I<C		I<M	M<C			
Spot[a]	Protein name[b]	Accession No.[c]	Score[d]	PM[e]	q[f]	C/I[g]	α[h]	M/I[g]	C/M[g]	I[i]	M[i]	C[i]
	Energy and carbohydrate metabolism											
	Gluconeogenesis											
1084	fructose-1,6-bisphosphatase, cytosolic	MDP0000251810	889	15	0.037	1.9	0.05	1.8	1.1	a	ab	b
	Glycolysis and gluconeogenesis; Calvin cycle											
1073	fructose-bisphosphate aldolase	MDP0000151849	828	13	0.027	1.7	0.05	1.4	1.2	a	ab	b
934	glyceraldehyde-3-phosphate dehydrogenase	MDP0000835914	826	11	0.022	2.1	0.05	1.4	1.4	a	ab	b
990	glyceraldehyde-3-phosphate dehydrogenase	MDP0000527995	593	9	0.012	2.2	1^{E}-3	1.6	1.4	a	ab	b
1007	glyceraldehyde-3-phosphate dehydrogenase	MDP0000527995	1280	13	0.019	2.9	0.01	1.6	1.8	a	ab	b
	Calvin cycle; defense response											
1000	phosphoribulokinase (putative; chloroplastic-like)	MDP0000148186	788	13	6.4^{E}-3	2.2	0.01	1.4	1.6	a	ab	b
	Photosynthesis											
1399	light-harvesting complex II protein Lhcb1	MDP0000417927	514	7	0.023	2.7	0.05	1.5	1.8	a	ab	b
1042	photosystem II stability/assembly factor HCF136, chloroplastic	MDP0000826603	1290	18	5.9^{E}-3	2.2	0.01	1.4	1.6	a	ab	b
1224	Oxygen-evolving enhancer protein 1, chloroplastic (precursor)	MDP0000248920	1090	15	0.017	2.7	0.05	1.9	1.4	a	ab	b
1215	Oxygen-evolving enhancer protein 1, chloroplastic (precursor)	MDP0000858039	743	15	0.021	2.3	0.05	1.4	1.6	a	ab	b
1220	Oxygen-evolving enhancer protein 1, chloroplastic (precursor)	MDP0000858039	1100	17	0.015	2.4	0.05	1.7	1.4	a	ab	b
1465	chlorophyll A/B binding protein	MDP0000866655	438	9	6.6^{E}-3	2.3	0.01	1.5	1.5	a	ab	b
652	chloroplast ATP synthase beta subunit	MDP0000928146	139	2	0.018	1.4	0.05	1.1	1.3	a	ab	b
	Transport facilitation											
	Plasmamembrane proton transport											
586	V-type (vacuolar) proton ATPase subunit B	MDP0000945182	545	10	0.032	1.8	0.01	1.3	1.4	a	ab	b

Table 5.2 - *continued*

						I<C		I<M	M<C			
Spot[a]	**Protein name[b]**	**Accession No.[c]**	**Score[d]**	**PM[e]**	**q[f]**	**C/I[g]**	**α[h]**	**M/I[g]**	**C/M[g]**	**I[i]**	**M[i]**	**C[i]**
	Protein import into chloroplast											
1350	protein THYLAKOID FORMATION1 (chloroplastic-like)	MDP0000139684	758	12	8.3^{E}-4	1.9	0.01	1.7	1.1	a	b	b
	Amino acid metabolism											
	degradation of glycine											
186	glycine dehydrogenase (decarboxylating)	MDP0000588069	437	12	0.023	2.6	0.05	1.7	1.5	a	ab	b
	Transcription											
	Spliceosome											
1174	arginine/serine-rich splicing factor	MDP0000387508	463	14	0.028	3.5	0.05	2.0	1.8	a	ab	b
	Regulation of protein activity											
	Protease inhibitor											
980	Serpin-ZX-like protein	MDP0000751972	131	7	0.047	1.7	0.1[j]	1.2	1.4	a	a	a
	Unknown											
1440	uncharacterized protein	MDP0000178270	480	10	0.044	1.6	0.05	1.6	1.0	a	b	b

[a] Corresponding spot number in the gel image in Fig. 5.1

[b] Proteins have been grouped according to the Gene Ontology biological process wherein they are involved

[c] MDP number of predicted apple gene (Velasco *et al*., 2010) (Gene and protein sequences can be obtained from Genome Database for Rosaceae (GDR): http://www.rosaceae.org)

[d] MOWSE score probability (protein score) for the entire protein

[e] Number of matched peptides of peptide mass fingerprinting combined with MS/MS

[f] Overall false discovery rate (FDR) corrected p-value, according to a one-way ANOVA, using the DeCyder 6.5 software

[g] The 'more abundant changes' are given as average standardized protein abundance ratios of the most abundant sample (C, M and C respectively) to the less abundant sample (I, I and M respectively), calculated with the DeCyder 6.5 software

[h] Comparison of the ^{10}log standardized protein abundances of the protein in the inoculated (I) and control (C) 'Topaz' leaves with significance levels α according to a FDR corrected one-way ANOVA, using the DeCyder 6.5 software

[i] Significance classes ($q \leq 0.05$)

[j] The difference would be statistically significant if the outlier (one of the three replicates) is left out

We were able to significantly ($q \leq 0.05$) detect differences down to average standardized abundance ratios of 1.3. Remarkably, at 5 dpi, no less than 28 of the 29 proteins that were significantly up-regulated in the infected apple leaves compared to the control leaves also showed a tendency of up-regulation in the infected leaves compared to the mock-inoculated leaves. However, although these infection-induced up-regulations showed ratios up to ~2, the differences were not statistically significant (apart from the above-mentioned 'auxin-induced protein PCNT115-like isoform 1'; Table 5.1). In the case of the Mal d 1 protein, the average standardized abundance ratio was even higher than 2 (Fig. 5.5; Table 5.1, spots 1594 and 1595). For 26 of the 29 identified proteins (e.g. Mal d 1) we can also observe a tendency of up-regulation in the mock-infected leaves compared to the control leaves (Table 5.1; Fig. 5.5). Thus in general, for these infection-induced up-regulated proteins we can observe a tendency of infection > mock-infection > control. This suggests that the mock-infection initiates a stress response and that this response is increased by fungal infection. Note that both the mock-infected and *V. inaequalis* infected plants had undergone the severe conditions of 95-100 % RH during 48 h in the dark.

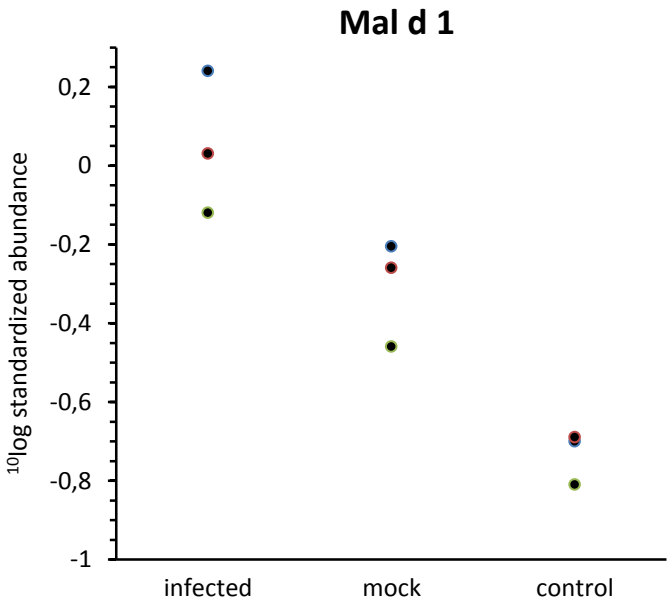

Fig. 5.5. Differential accumulation pattern at 5 dpi of spot 1595, that was identified as the 'major allergen Mal d 1', in the first 2D-DIGE experiment (Topaz). For each condition (infected, mock and control) three biological replicates (i.e. three plants) were available. The difference in accumulation was only statistically significant (ANOVA) between the conditions 'infected' and 'control' (q=2.50E-4), not between 'infected' and 'mock' (q=0.140) or between 'mock' and 'control' (q=0.0616).

With the down-regulated proteins (Table 5.2), the situation is similar to that of the up-regulated proteins. All 15 proteins that were significantly down-regulated in the infected apple leaves compared to the control leaves ('I < C'), showed also a tendency of down-regulation in the infected leaves compared to the mock-inoculated leaves, although only statistically significant in 2 cases (Table 5.2). Besides, we can also observe a tendency of down-regulation in the mock-infected leaves compared to the control leaves for 12 of the 15 proteins (Table 5.2). Thus, in general for these infection-induced down-regulated proteins we can observe an accumulation tendency of infection < mock-infection < control, equivalent to the infection > mock-infection > control tendency we saw earlier for the up-regulated proteins. This backs up our hypothesis of a mock-infection initiated stress response that is increased by fungal infection.

However, one has to keep in mind that this hypothesis is based on mainly statistically non-significant differences in protein accumulation. The amount of significant differences in protein accumulation between the infected and mock-infected condition ('I <> M') on the one hand (only four) and between the mock-infected and control condition ('M <> C') on the other hand (also only four) is remarkably low. This could be due to the rather large variations in accumulation between the three biological replicates, as is illustrated by the example of Mal d 1 (Fig. 5.5). The low amount of biological replicates (only 3) causes these variations to have quite detrimental effects on statistical significance. Our hypothesis will be further investigated in Chapter 6, where the proteomes of infected and mock-infected leaves are compared again, however this time in Aliette®-treated apple leaves, which showed less variation in protein accumulation between the biological replicates.

5.3.2.2. Up-regulation of 'Topaz' proteins known to be involved in stress responses

Of the 29 proteins that were up-regulated in the scab-infected leaf samples, 10 are known to be involved in a stress response, of which 5 are even known to play a role in a defense response to a biotic stress. These five proteins are Mal d 1, a chalcone synthase, enhanced disease susceptibility 1 (EDS1), a heat shock protein (HSP 70) and a lipoxygenase (Table 5.1).

Mal d 1 (spots 1594 and 1595), a pathogenesis-related class 10 protein (PR-10), is considered to be a major apple allergen. It has been suggested that there are at least 15 Mal d 1-related genes in the genome of the cultivated apple. Not all these *Mal d 1* members are likely to be

involved in allergenicity (Pagliarani *et al*., 2012). We identified 2 isoforms when comparing the infected and control leaves of the *Rvi*6 resistant cultivar 'Topaz'. A role of Mal d 1 in intracellular signalling in plants has been suggested and *in vitro* expression of the isoforms should help in assessing their relative roles in disease, allergic responses, senescence and nucleotide-, cytokinin- and brassinosteroid-binding (Pagliarani *et al*., 2012). The expression of a number of *Mal d 1* genes was also increased after infection in a *HcrVf2* transformed 'Gala' (Paris *et al.*, 2009). Most of the Mal d 1 gene products also accumulated in leaves of the scab-susceptible cv. 'Royal Gala' in response to challenge with *V. inaequalis* (Beuning *et al*., 2004). Therefore, its up-regulation might not necessarily be related to an effective defense response against the fungus. However, although we could confirm an up-regulation of Mal d 1 in a scab-susceptible cv. (i.e. 'Golden Delicious') upon infection (see Section 5.3.3), we established that accumulation of an isoform (spot 1595) was even higher ($q < 0.05$) in the infected monogenic resistant 'Topaz' (see Table 5.5 p.116). Moreover, when Castillejo *et al*. (2010) studied the protein accumulation responses to *Mycosphaerella pinodes* in pea, they found a different PR-10 protein (Pi49) to be more drastically up-regulated in the incompatible interaction than in the compatible interaction. PR-10 proteins, having ribonuclease activity, have been described to be induced in many plant species in response to abiotic and biotic stresses (Liu and Ekramoddoullah, 2006).

Chalcone synthases (spot 894) are a family of polyketide synthase enzymes associated with the production of chalcones, a class of organic compounds found mainly in plants as natural defense mechanisms and as biosynthetic intermediates, for example in the production of pigments. They are known to show antibacterial and antifungal activities (Jiang *et al*., 2006).

The **enhanced disease susceptibility 1 protein** (**EDS1**; spot 427) and salicylic acid, its associated non-proteinaceous signaling component that fulfills a redundant function, are important components of resistance (R) protein-mediated defense signaling against diverse pathogens in a variety of plants (Venugopal *et al*., 2009). EDS1 interacts with the 'phytoalexin deficient 4' protein (PAD4) to constitute a regulatory hub that is essential for basal resistance to invasive biotrophic and hemi-biotrophic pathogens (Wiermer *et al*., 2005). In *Arabidopsis* enhanced disease susceptibility mutants exhibit increased susceptibility to several bacterial pathogens (Rogers and Ausubel, 1997).

HSP 70 heat shock proteins (spot 337) are an important part of the cell's machinery for protein folding, and help to protect cells from stress, for example oxidative stress. This stress normally acts to damage proteins, causing partial unfolding and aggregation. By temporarily binding to hydrophobic residues exposed by stress, HSP 70 prevents these partially denatured proteins from aggregating, and allows them to refold (Morano, 2007).

Linoleate 13S-lipoxygenase (spot 224) is a common plant lipoxygenase that oxidizes linoleate and alpha-linolenate, the two most common polyunsaturated fatty acids in plants, by inserting molecular oxygen (dioxygen) at the C13 position with (S)-configuration. The enzyme produces precursors for several important compounds, including oxylipins (e.g. (+)-7-iso jasmonic acid) and the plant hormone jasmonic acid (Feussner and Wasternack, 2002). Plant oxylipins are mainly involved in the resistance to various microbial pathogens, including ascomycetes (Peng *et al*., 1994). Among other functions in the plant cell, jasmonic acid is a key regulator of direct and indirect plant defense responses (Kniskern *et al*., 2007). Several plant-pathogen interactions have been described in which lipoxygenase activity, protein, or mRNA is increased after fungal, bacterial or viral infection (Slusarenko, 1996). The accumulation of a lipoxygenase was found to be increased as well in the scab-susceptible cv. 'Elstar' after inoculation with *V. inaequalis*, and constitutively in the resistant cv. 'Remo' compared to 'Elstar' (Gau *et al.*, 2004; Paris *et al.*, 2009).

The remaining five stress response-related proteins that were up-regulated in infected 'Topaz' leaves compared to control leaves were **HSP 60, a T-complex protein (TCP) domain class transcription factor** (both are involved in protein folding), **thioredoxin h**, nucleoside diphosphate kinase 1 (NDPK I) and 'bifunctional purine biosynthesis protein' (Table 5.1). Thioredoxins are a class of small redox proteins that play a role in many important biological processes, including redox signaling. They contain a dithiol-disulfide active site and act as antioxidants by facilitating the reduction of other proteins by cysteine thiol-disulfide exchange. Their response to reactive oxygen species (ROS) reduces oxidative stress and helps to maintain cell redox homeostasis (Arnér and Holmgren, 2000). **Nucleoside diphosphate kinase 1** (**NDPK 1**; spot 1706) and **'bifunctional purine biosynthesis protein'** (spot 530) are both involved in nucleotide biosynthesis. NDPK 1 participates in the exchange of phosphate groups between the different nucleoside diphosphates. An enhanced

expression of a gene encoding for a nucleoside diphosphate kinase in rice plants exposed to bacterial pathogen infections has been reported (Cho *et al*., 2004).

Of the 15 proteins that were down-regulated in the infected 'Topaz' leaves ('I < C'), only one, the phosphoribulokinase (spot 1000), is known to be possibly involved in a defense response (Table 5.2). This enzyme mainly participates in carbon fixation.

5.3.2.3. Differential accumulation of proteins involved in the energy and carbohydrate metabolism of 'Topaz' plants

Five of the 29 **up-regulated** proteins (cytosolic phosphoglucomutase, phosphofructokinase, fructose-bisphosphate aldolase, pyruvate kinase and pyruvate decarboxylase) catalyze a reaction of the **glycolysis** (Fig. 5.6; Table 5.1). Three of the five enzymes catalyze a reaction in only the direction of glycolysis and not in the opposite direction of gluconeogenesis (Fig. 5.6). The prime functions of glycolysis are to participate in the breakdown of carbohydrates to generate ATP, reductant (NADH) and carbon skeletons for anabolic pathways. The cytosolic glycolytic network furnishes plants with the metabolic options needed for development and acclimatisation to unfavourable environmental conditions (Plaxton, 1996). It has been pointed out that when a plant is submitted to a stress, the resistance mechanisms that need to be activated in order to respond to stress require an extra energy supply (Smedegaard-Petersen and Tolstrup, 1985; Umeda *et al*., 1994; Block *et al*., 2005; Moshe *et al*., 2012).

Glycolysis is not the only catabolic biochemical process of which proteins are up-regulated in the infected leaves. The up-regulated NAD^+-dependent malate dehydrogenase (spot 1093) and succinate dehydrogenase (spot 436) enzymes (Table 5.1) participate in the **tricarboxylic-acid (TCA) or citrate cycle**. The pyruvate produced by glycolysis in the cytosol enters the mitochondria and is converted into acetyl-CoA. Acetyl-CoA is fed into this TCA cycle to be oxidized for the production of energy in the form of ATP (Fig. 5.7). Interestingly, succinate dehydrogenase is an important participant in this oxidative phosphorylation as well, generating the reduced quinone QH_2. Induction of expression of the cytoplasmic, NAD^+-dependent malate dehydrogenase has also been reported in pea plant exposed to a Cd^{2+} stress (Savenstrand and Strid, 2004).

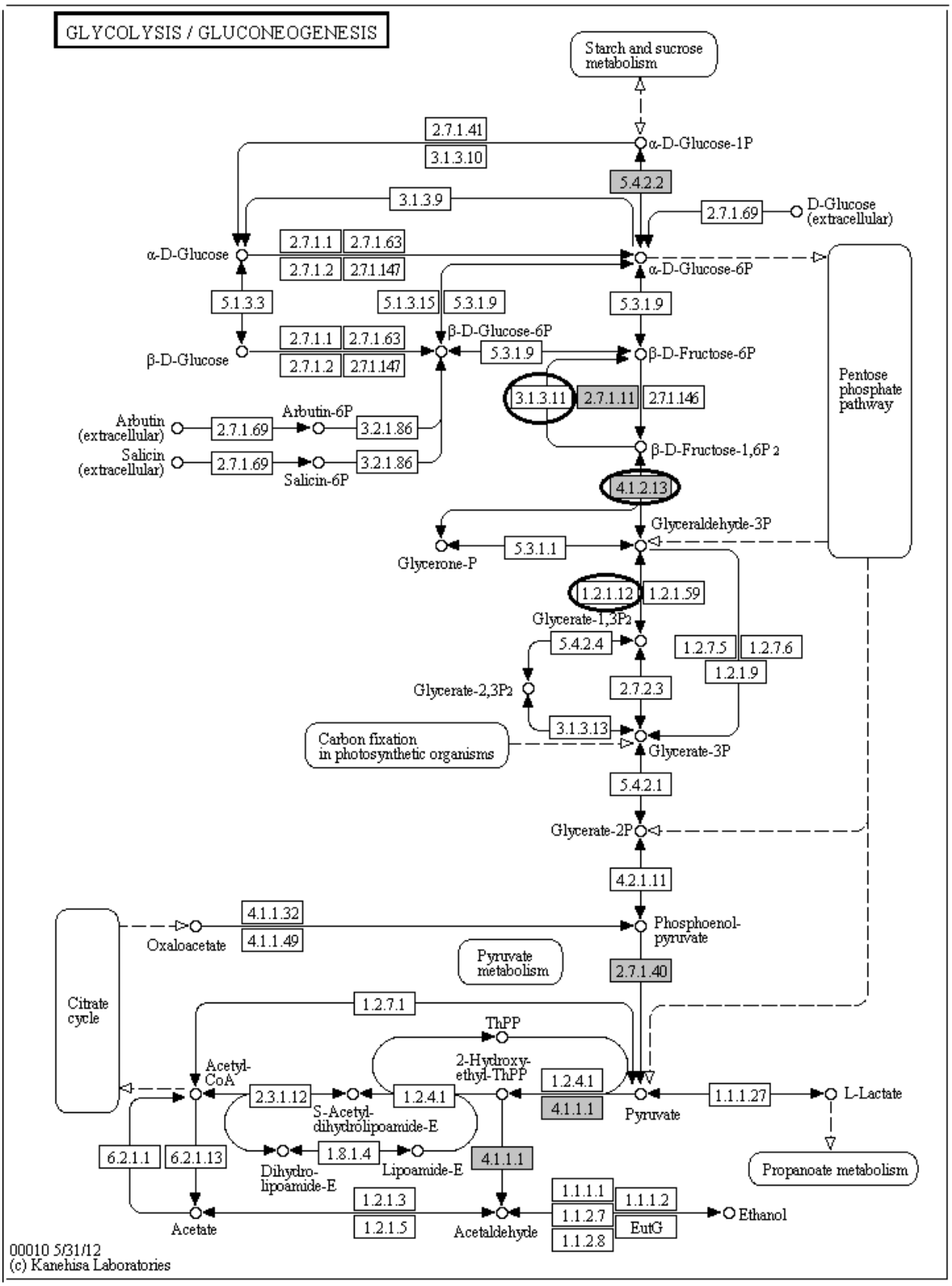

Fig. 5.6 (Legend: see next page)

Fig. 5.6 (see previous page). Five proteins involved in glycolysis (grey background) are up-regulated in the *V. inaequalis* inoculated 'Topaz' leaves compared to the control 'Topaz' leaves ('I > C'): cytosolic phosphoglucomutase (EC 5.4.2.2), phosphofructokinase (EC 2.7.1.11), fructose-bisphosphate aldolase (EC 4.1.2.13), pyruvate kinase (EC 2.7.1.40) and pyruvate decarboxylase (EC 4.1.1.1). Three down-regulated proteins (encircled) are involved in gluconeogenesis: cytosolic fructose-1,6-bisphosphatase (EC 3.1.3.11), fructose-bisphosphate aldolase (EC 4.1.2.13) and glyceraldehyde-3-phosphate dehydrogenase (EC 1.2.1.12).

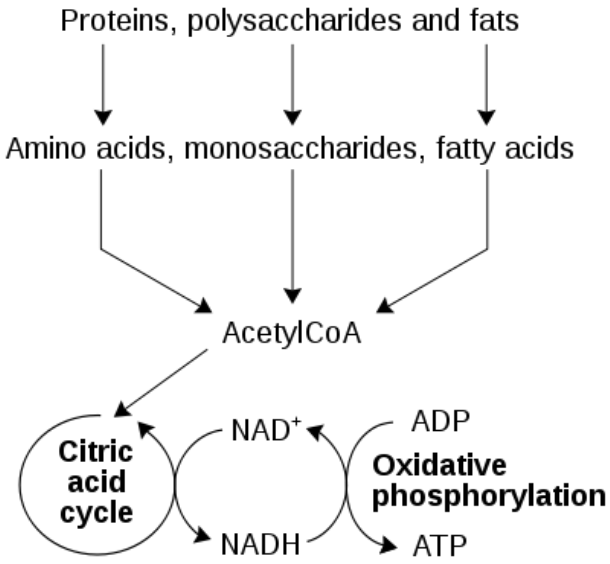

Fig. 5.7. Catabolism. In catabolism, large molecules such as polysaccharides, lipids, nucleic acids and proteins are broken down into smaller units such as monosaccharides, fatty acids, nucleotides, and amino acids, respectively. The common end product of the catabolic processes, acetyl-CoA, conveys the carbon atoms within the acetyl group to the citric acid cycle (TCA cycle). The NADH generated by the TCA cycle is fed into the oxidative phosphorylation pathway, that takes places in the mitochondria as well. The net result of these latter two, closely linked pathways is the production of energy in the form of ATP (Alberts *et al*., 1998).

Interestingly, the **$NADP^+$-dependent malate dehydrogenase or malic enzyme** (spot 437) was up-regulated in infected 'Topaz' leaves as well. This housekeeping enzyme catalyzes the oxidative decarboxylation of L-malate to produce pyruvate, CO_2 and NADPH. An increase in the level of $NADP^+$-dependent malate dehydrogenase has been suggested to be related to plant defense mechanisms through providing building blocks and also energy for the biosynthesis of defense compounds (Casati *et al*., 1999). For instance, when this enzyme was assayed in healthy and disordered infected cotyledons of marrow plants (*Cucurbita pepo* L.),

the activity within the lesion was much higher compared to the activity in the healthy tissue (Tecsi *et al*., 1996).

Dephospho-CoA-kinase (spot 1463) and **ATP-citrate synthase** (spot 715) are up-regulated as well (Table 5.1). Dephospho-CoA-kinase generates Coenzyme A (CoA) from dephospho-CoA, and ATP-citrate synthase (also known as ATP-citrate lyase) catalyzes the ATP- and CoA-dependent cleavage of citrate into oxaloacetate and acetyl-CoA (Fatland *et al*., 2002). In plants and animals, ATP-citrate synthase is used to produce cytosolic acetyl-CoA from mitochondrial produced citrate. It is the primary enzyme responsible for the synthesis of cytosolic acetyl-CoA in many tissues. Citrate is exported into the cytosol when there is an excess in mitochondrial citrate, resulting from an excess of mitochondrial acetyl-CoA entering the TCA cycle (see above). Acetyl-CoA is an important molecule in catabolism, the set of metabolic pathways that break down molecules into smaller units and release energy (Fig. 5.7).

On the other hand, three of the 15 **down-regulated** proteins (the cytosolic fructose-1,6-bisphosphatase, a fructose-bisphosphate aldolase and glyceraldehyde-3-phosphate dehydrogenase; the last with three different spots) are involved in the anabolic **gluconeogenesis** pathway (Fig. 5.6; Table 5.2). While fructose-bisphosphate aldolase and glyceraldehyde-3-phosphate dehydrogenase catalyze a reaction in a reversible way (both the direction of glycolysis and gluconeogenesis), fructose-1,6-bisphosphatase (spot 1084) only converts fructose-1,6-bisphosphate to fructose 6-phosphate in gluconeogenesis, and the reverse of the reaction is catalyzed by the up-regulated phosphofructokinase (spot 506) during glycolysis (see above; Table 5.1).

The fructose-bisphosphate aldolase and glyceraldehyde-3-phosphate dehydrogenase, together with the down-regulated phosphoribulokinase, play a role in the **Calvin cycle** (reductive pentose phosphate cycle) as well. The Calvin cycle is one of the so-called dark (light-independent) reactions used for carbon fixation in photosynthetic organisms. Interestingly, two different spots were identified as the fructose-bisphosphate aldolase (FBA) enzyme, one being up-regulated upon scab-infection (spot 1078; Table 5.1) and one being down-regulated (spot 1073; Table 5.2). Analysis of the MS/MS identified peptides confirmed that it concerns respectively a cytosolic isoform and a plastidic one. The up-regulated cytosolic FBA isoform is involved in the cytosolic glycolysis, and the down-regulated plastidic

isoform in the Calvin cycle that takes place in the stroma of chloroplasts. Up-regulation of the cytosolic FBA isoform and down-regulation of the chloroplast isoform were found previously in a resistant pea cv. upon infection with *Mycosphaerella pinodes* (Castillejo *et al*., 2010). Recently, FBA was suggested to play an important regulatory role in response to abiotic stresses in plants as well (Lu *et al*., 2012). The expression patterns of eight *Arabidopsis thaliana* FBA family genes under different stress conditions suggested that all the members showed different expression patterns in response to stresses, including ABA, NaCl, Cd, abnormal temperature and drought. The presence of protein isoforms with different accumulation patterns in response to pathogen infection have also been previously observed in *Arabidopsis* leaves (Jones *et al*., 2006) and in other plant species, e.g. mint (*Mentha arvensis*; Sinha and Chattopadhyay, 2011).

Five other down-regulated proteins, including a chloroplast ATP synthase beta subunit, are involved in the light(-dependent) reactions of **photosynthesis** (Table 5.2). Thus, together, nine of the 15 proteins that were down-regulated upon infection play a role in carbon fixation. The down-regulation at 5 dpi of a light-harvesting complex II protein (spot 1399), chlorophyll A/B binding protein (spot 1465) and other proteins involved in photosynthesis is accompanied by a decrease in chlorophyll content, that was macroscopically visible as chlorotic lesions as from 8 dpi (see Section 4.4). It was demonstrated before that the rate of photosynthesis and the capacity of the Calvin cycle are reduced in plant leaf regions invaded by (biotrophic) fungal pathogens or under biotic stress in general (Chou *et al*., 2001; Berger *et al*., 2007; Bolton, 2009). For example, interruption of the photosynthetic electron transport chain and collapse of photosynthesis was demonstrated in tobacco leaves during an incompatible interaction with *Phytophthora nicotianae* (Scharte *et al*., 2005). They propose that in photoautotrophic source leaves photosynthesis and assimilatory metabolism are switched off and processes required for defense are initiated.

5.3.2.4. Six proteins were exclusively up-regulated in the *V. inaequalis* inoculated 'Topaz' leaves

Most of the proteins discussed in last two sections show a tendency of differential accumulation between both scab-infection and mock-infection on the one hand and mock-infection and control condition on the other hand. We could identify only six proteins that

were exclusively up-regulated in the *V. inaequalis* inoculated leaves at 5 dpi (however not statistically significant) and did not show a difference in accumulation (not even a tendency) between the mock-infection and control conditions. Three of them are known to be involved in a defense response. Next to the two heat-shock proteins **HSP 60** (spot 539) **and HSP 70** (spots 337, 372 and 377), it concerned the **proteasome alpha subunit type-2-B** (spot 1393; MDP0000143951) that is known to participate in ATP/ubiquitin-dependent non-lysosomal proteolysis of poorly folded and damaged proteins in response to a (biotic) stimulus (Blast2GO). In general, proteasomes play a key role in regulated proteolysis throughout the life cycle of plants (Sullivan *et al*., 2003). They have been shown in previous studies to play an important role in programmed cell death and disease resistance in plants (Tsunezuka *et al*., 2005; Delaure *et al*., 2008).

The other three infection induced up-regulated proteins are related to protein translation: two translation elongation factors (**ef-1-gamma and ef-2**; spots 792 (MDP0000315108) and 208 (MDP0000777793), respectively) and **glycyl-tRNA synthetase** (spot 342; MDP0000226879), that is involved in aminoacyl-tRNA biosynthesis. Regulation of the translational machinery is considered to be an important component of cellular stress response (Sahi *et al*., 2006).

5.3.3. Comparison of the *Rvi*6 scab-resistant cultivar 'Topaz' with the scab race 1 susceptible cv. 'Golden Delicious'

When comparing the CBB G-250 stained gel images of the (*Rvi*6 scab-resistant) 'Topaz' and (*V. inaequalis* race 1 susceptible) 'Golden Delicious' control conditions ('Top-C <> Gol-C') at 0 dpi, 63 spots (out of 968 matching spots, i.e. 6.5 %) were significantly differentially accumulated ($p \leq 0.05$), of which 35 were up-regulated in 'Topaz' and 28 down-regulated. Of the 35 up-regulated spots, 23 were positively identified, resulting in 22 individual protein identifications (Table 5.3). Of the 28 down-regulated spots, 20 were identified, resulting in 16 protein identifications (Table 5.4).

Table 5.3. List of up-regulated proteins in 'Topaz' (monogenic *Rvi*6-resistant cultivar) compared to 'Golden Delicious' (*V. inaequalis* race 1 susceptible cultivar) before inoculation with *V. inaequalis* race 1 (control; C) and/or at five days after inoculation (I) with *V. inaequalis*

						Top-I > Gol-I		Top-C > Gol-C	
Spot[a]	**Protein name**	**Accession No.**[b]	**Score**[c]	**PM**[d]	**q**[e]	**Ratio**[f]	**α**[g]	**Ratio**[h]	**α**[i]
217	linoleate 13s-lipoxygenase 2- chloroplastic	MDP0000753547	110	6	7.7^{E}-4	2.5	1^{E}-3	1.1	ns
255	phospholipase D alpha	MDP0000300217	118	7	3.8^{E}-4	1.3	1^{E}-3	∞	0.01
280	(putative) oligopeptidase B	MDP0000208437	258	14	4.0^{E}-4	1.8	1^{E}-3	∞	0.05
316	(vitamin-b12 independent) methionine synthase	MDP0000793077	462	11	2.3^{E}-4	1.5	1^{E}-4	1.5	ns
317	(vitamin-b12 independent) methionine synthase	MDP0000793077	125	6	1.4^{E}-3	1.4	0.01	1.2	ns
360	transketolase	MDP0000142098	882	17	1.9^{E}-3	1.4	0.05	1.6	0.01
374	transketolase	MDP0000142098	1410	25	8.9^{E}-3	1.3	0.05	2.0	0.01
437	$NADP^{+}$-dependent malate dehydrogenase; malic enzyme	MDP0000221561	602	13	1.4^{E}-5	2.0	1^{E}-6	2.4	0.01
469	apple phosphoglyceromutase (apgm)	MDP0000240039	178	11	1.5^{E}-3	1.2	0.01	0.9	ns
510	2-isopropylmalate synthase	MDP0000212398	400	12	0.010	1.5	0.05	4.3	0.05
536	betaine-aldehyde dehydrogenase	MDP0000148461	548	12	1.6^{E}-3	1.5	0.01	1.9	ns
586	V-type (vacuolar) proton ATPase subunit B	MDP0000945182	545	10	6.2^{E}-3	1.1	0.05	1.2	ns
612	putative anthranilate N-benzoyltransferase protein	MDP0000267154	725	9	4.3^{E}-3	1.4	0.01	1.3	ns
625	chloroplast ATP synthase beta subunit	MDP0000928146	160	2	8.9^{E}-5	2.6	1^{E}-4	∞	0.01
672	enolase	MDP0000939989	817	15	0.010	1.2	0.05	3	0.05
722	uridine 5'-monophosphate synthase	MDP0000335264	62	1	2.4^{E}-4	1.4	0.01	1.2	0.05
825	RuBisCO activase	MDP0000944409	1010	14	0.014	1.1	ns	1.5	0.05
830	porphobilinogen synthase	MDP0000933051	612	13	8.7^{E}-4	1.5	1^{E}-3	2.0	ns
914	magnesium-chelatase subunit chlI, chloroplastic-like	MDP0000639265	505	13	3.0^{E}-4	1.4	1^{E}-4	3.9	0.01
926	phosphoglycerate kinase	MDP0000325411	1380	17	1.4^{E}-5	4.8	1^{E}-6	1.6	ns
956	protein disulfide isomerase	MDP0000201801	558	11	0.010	1.2	0.05	1.1	ns
980	Serpin-ZX-like protein	MDP0000751972	131	7	1.0^{E}-3	1.8	1^{E}-3	∞	0.05
1025	Alpha-1,4-glucan-protein synthase (UDP-forming)	MDP0000232047	83	4	6.9^{E}-4	1.3	1^{E}-3	?[j]	?[j]

1034	pyruvate dehydrogenase E1 component subunit beta	MDP0000146411	641	11	3.8^{E}-3	1.2	0.01	1.5	ns

Table 5.3 - *continued*

						Top-I > Gol-I		Top-C > Gol-C	
Spot[a]	**Protein name**	**Accession No.[b]**	**Score[c]**	**PM[d]**	**q[e]**	**Ratio[f]**	**α[g]**	**Ratio[h]**	**α[i]**
1056	quinone oxidoreductase-like protein	MDP0000269371	1190	17	4.0^{E}-4	1.6	1^{E}-3	∞	0.01
1062	esterase/lipase domain-containing protein	MDP0000130884	402	8	1.5^{E}-3	1.7	0.01	1.0	ns
1073	fructose-bisphosphate aldolase	MDP0000151849	828	13	0.022	1.2	ns	1.3	0.05
1105	fructokinase ; ribokinase	MDP0000131308	912	11	6.5^{E}-4	2.0	1^{E}-3	2.0	0.01
1262	Chalcone synthase	MDP0000575740	624	11	3.3^{E}-4	2.2	1^{E}-3	∞	0.01
1264	oxidoreductase GLYR1	MDP0000149834	529	10	4.0^{E}-5	1.9	1^{E}-5	2.7	0.01
1268	predicted dihydrofolate reductase	MDP0000514153	363	7	2.8^{E}-3	1.4	0.05	2.2	0.01
1304	uncharacterized protein	MDP0000124634	652	10	7.8^{E}-3	1.2	0.05	1.4	ns
1398	triosephosphate isomerase	MDP0000694943	794	13	3.8^{E}-4	1.3	1^{E}-3	1.2	ns
1426	proteasome subunit beta type-1	MDP0000291250	486	9	0.041	1.1	ns	4.5	0.01
1430	RuBisCO small subunit	MDP0000731480	129	6	4.0^{E}-5	1.7	1^{E}-4	∞	0.01
1437	RNA recognition motif-containing protein	MDP0000270177	315	10	9.4^{E}-4	2.8	1^{E}-3	∞	0.01
1479	oxygen-evolving enhancer protein chloroplastic-like	MDP0000361338	908	11	0.030	1.0	ns	2.5	0.05
1543	type IIF peroxiredoxin	MDP0000258515	508	9	6.1^{E}-3	1.5	0.01	?[j]	?[j]
1550	universal stress protein (USP) family protein	MDP0000415257	667	10	7.5^{E}-3	1.2	0.05	1.2	ns
1556	Uncharacterized protein	MDP0000179031	744	9	0.048	1.0	ns	5.0	0.01
1595	major allergen Mal d 1 (PR-10)	MDP0000942516	556	7	0.011	1.9	0.05	0.8	ns
1637	Mal d 1-like	MDP0000151829	515	7	6.8^{E}-3	1.9	0.05	1.0	ns

[a] Corresponding spot number in the gel image in Fig. 5.1

[b] MDP number of predicted apple gene (Velasco *et al*., 2010) (Gene and protein sequences can be obtained from GDR: http://www.rosaceae.org)

[c] MOWSE score probability (protein score) for the entire protein

[d] Number of matched peptides of peptide mass fingerprinting combined with MS/MS

[e] Overall false discovery rate (FDR) corrected p-value of the 2D-DIGE experiment, according to a one-way ANOVA, using the DeCyder 6.5 software

[f] Ratio of the average standardized abundance of the inoculated (I) 'Topaz' (Top) samples to the average standardized abundance of the inoculated 'Golden Delicious' (Gol) samples, calculated with the DeCyder 6.5 software

[g] significance level α according to a FDR corrected one-way ANOVA that compares the log standardized protein abundance of the protein in the inoculated (I) 'Topaz' leaves with the inoculated 'Golden Delicious' leaves, using the DeCyder 6.5 software; ns: not significant

[h] Ratio of the average percentage of spot volume (% vol) of the 'Topaz' control (C) samples to the average % vol of the 'Golden Delicious' control samples, calculated with the Image Master 2-D platinum software

[i] significance level α according to a Kolmogorov-Smirnov statistical test that compares the percentage of spot volume (% vol) of the protein in the control (C) 'Topaz' leaves with the control 'Golden Delicious' leaves, using the Image Master 2-D platinum software (GE Healthcare); ns: not significant

[j] too little matches

Table 5.4. List of down-regulated proteins in 'Topaz' (monogenic *Rvi*6-resistant cultivar) compared to 'Golden Delicious' (*V. inaequalis* race 1 susceptible cultivar) before inoculation with *V. inaequalis* race 1 (control; C) and/or at five days after inoculation (I) with *V. inaequalis*

						Top-I < Gol-I		Top-C < Gol-C	
Spot[a]	**Protein name**	**Accession No.[b]**	**Score[c]**	**PM[d]**	**q[e]**	**Ratio[f]**	**α^g**	**Ratio[h]**	**α^i**
175	Presequence protease 2	MDP0000146940	991	27	1.2^{E}-3	1.4	0.01	1.5	0.05
218	linoleate 13s-lipoxygenase 2- chloroplastic	MDP0000753547	193	8	4.0^{E}-5	2.2	1^{E}-5	1.0	ns
230	linoleate 13s-lipoxygenase 2- chloroplastic	MDP0000281525	177	7	9.9^{E}-4	1.7	1^{E}-3	1.1	ns
318	(vitamin-b12 independent) methionine synthase	MDP0000153762	1170	19	6.5^{E}-3	1.2	0.05	1.5	ns
325	(vitamin-b12 independent) methionine synthase	MDP0000793077	995	17	2.6^{E}-4	5.2	1^{E}-4	1.7	0.05
342	glycyl-tRNA synthetase	MDP0000226879	734	15	6.5^{E}-3	1.3	0.05	0.9	ns
389	stress-inducible protein	MDP0000191994	150	9	2.7^{E}-3	1.4	0.01	1.4	ns
416	UDP-sugar pyrophosphorylase	MDP0000156131	505	16	8.9^{E}-4	1.3	0.01	1.6	0.05
427	enhanced disease susceptibility 1	MDP0000162236	326	14	2.2^{E}-4	2.2	1^{E}-4	2.8	0.01
451	acetohydroxyacid synthase; acetolactate synthase	MDP0000621545	999	18	5.1^{E}-4	1.4	1^{E}-3	1.6	0.05
454	beta-glucosidase 24-like	MDP0000297569	350	4	2.6^{E}-4	4.8	1^{E}-4	2.6	0.01
464	beta-glucosidase 24-like	MDP0000297569	280	5	3.5^{E}-4	2.5	1^{E}-3	3.2	0.01
475	beta-glucosidase 24-like	MDP0000297569	375	5	1.5^{E}-4	4.6	1^{E}-3	2.5	0.05
487	beta-glucosidase 24-like	MDP0000297569	372	4	2.2^{E}-4	4.8	1^{E}-3	1.5	ns
539	heat shock protein 60	MDP0000185591	789	18	3.3^{E}-3	1.5	0.01	1.8	0.01
585	myo-inositol-1-phosphate synthase	MDP0000698835	490	8	4.0^{E}-4	2.0	1^{E}-3	1.6	0.01
592	putative anthranilate N-benzoyltransferase protein	MDP0000314927	297	11	1.9^{E}-3	1.3	1^{E}-3	1.7	0.01
707	6-phosphogluconate dehydrogenase	MDP0000191398	501	12	3.0^{E}-3	1.4	0.01	1.4	ns
715	ATP-citrate synthase	MDP0000931334	335	7	5.5^{E}-3	1.4	0.01	1.2	ns
842	monodehydroascorbate reductase	MDP0000261821	1360	17	3.1^{E}-3	1.3	0.01	0.9	ns
875	glutamate-1-semialdehyde-2,1-aminomutase	MDP0000149467	122	3	3.2^{E}-3	1.3	0.05	1.4	ns
961	3-dehydroquinate synthase	MDP0000273495	859	14	7.5^{E}-3	1.3	0.05	1.0	ns
965	Serpin-ZX-like protein	MDP0000751972	1510	22	2.1^{E}-5	5.2	1^{E}-5	2.2	0.01

997	uroporphyrinogen decarboxylase (UROD)	MDP0000364293	117	5	5.6^{E}-4	1.2	0.05	1.4	0.05

Table 5.4 - *continued*

						Top-I < Gol-I		Top-C < Gol-C	
Spot[a]	**Protein name**	**Accession No.[b]**	**Score[c]**	**PM[d]**	**q[e]**	**Ratio[f]**	**α^{g}**	**Ratio[h]**	**α^{i}**
999	uroporphyrinogen decarboxylase (UROD)	MDP0000269628	478	8	2.2^{E}-3	1.3	0.01	1.5	0.01
1078	fructose-bisphosphate aldolase	MDP0000151849	147	7	8.7^{E}-4	1.7	1^{E}-3	1.6	0.05
1102	fructokinase; ribokinase	MDP0000131308	1340	19	3.0^{E}-3	1.9	0.01	2.3	0.01
1120	enoyl-[acyl-carrier-protein] reductase	MDP0000207724	372	9	8.2^{E}-3	1.2	0.05	1.3	0.05
1344	light-harvesting complex II protein Lhcb1	MDP0000417927	464	7	6.9^{E}-3	1.2	0.05	0.6	ns
1345	ascorbate peroxidase	MDP0000241173	509	10	7.2^{E}-3	1.2	ns	3.6	0.01
1350	protein THYLAKOID FORMATION1, chloroplastic-like	MDP0000139684	758	12	0.012	1.3	0.05	1.0	ns
1369	triosephosphate isomerase	MDP0000152242	781	12	2.4^{E}-4	3.7	1^{E}-4	2.3	0.01
1438	RNA recognition motif-containing protein	MDP0000270177	472	13	1.2^{E}-4	2.0	1^{E}-4	1.5	ns
1512	light-harvesting complex I protein Lhca1	MDP0000222941	252	4	2.4^{E}-3	1.2	0.05	0.9	ns

[a] Corresponding spot number in the gel image in Fig. 5.1

[b] MDP number of predicted apple gene (Velasco *et al*., 2010) (Gene and protein sequences can be obtained from Genome Database for Rosaceae (GDR): http://www.rosaceae.org)

[c] MOWSE score probability (protein score) for the entire protein

[d] Number of matched peptides of peptide mass fingerprinting combined with MS/MS

[e] Overall false discovery rate (FDR) corrected p-value of the 2D-DIGE experiment, according to a one-way ANOVA, using the DeCyder 6.5 software

[f] Ratio of the average standardized abundance of the inoculated (I) 'Golden Delicious' (Gol) samples to the average standardized abundance of the inoculated 'Topaz' (Top) samples, calculated with the DeCyder 6.5 software

[g] significance level α according to a FDR corrected one-way ANOVA that compares the log standardized protein abundance of the protein in the inoculated (I) 'Topaz' leaves with the inoculated 'Golden Delicious' leaves, using the DeCyder 6.5 software; ns: not significant

[h] Ratio of the average percentage of spot volume (% vol) of the 'Golden Delicious' control (C) samples to the average % vol of the 'Topaz' control samples, calculated with the Image Master 2-D platinum software

[i] significance level α according to a Kolmogorov-Smirnov statistical test that compares the percentage of spot volume (% vol) of the protein in the control (C) 'Topaz' leaves with the control 'Golden Delicious' leaves, using the Image Master 2-D platinum software (GE Healthcare); ns: not significant

When comparing the 2D-DIGE protein profiles of both cultivars at 5 dpi ('Top-I <> Gol-I'), 166 spots (out of 1440 matching spots, i.e. 11.5 %) were significantly differentially accumulated ($q \leq 0.05$), of which 80 were up-regulated in 'Topaz' and 86 down-regulated. Of the 80 up-regulated spots, 40 were positively identified, resulting in 35 individual protein identifications (Table 5.3). Of the 86 down-regulated spots, 34 were identified, resulting in 29 protein identifications (Table 5.4). Because of more incorrect matches between the 2-DE gel images of two different cultivars, less spots could be confidently matched to the preparative gels. Consequently, the discrepancy between the number of differentially accumulated spots and the number of identified spots is higher as compared to matching of gels of the same cultivar (see Section 5.3.1).

Most proteins that were significantly differentially accumulated in both cultivars in the control conditions (0 dpi) were also differentially accumulated at 5 dpi (Tables 5.3 and 5.4). There is even only one protein that is exclusively significantly down-regulated in the control conditions in 'Topaz' compared to 'Golden Delicious', namely the ascorbate peroxidase (APX; spot 1345), a peroxide detoxifying enzyme. Moreover, a different spot (isoform) of the same enzyme (spot 1313) shows a tendency of being constitutively up-regulated in 'Topaz' compared to 'Golden Delicious' (ratio = 1.4; however not statistically significant: $p = 0.15$). Also for the fructokinase or ribokinase we observed up-regulation of one isoform (spot 1105) in 'Topaz' compared to 'Golden Delicious' and down-regulation of another isoform (spot 1102). For the Serpin-ZX-like protein (spots 980 and 965) we even observed different isoforms in the control conditions of both cultivars, and the quinone oxidoreductase-like protein (spot 1056) seemed to be unique to 'Topaz'. This genotype specific accumulation is a complex matter and can be the consequence of multiple mechanisms: different gene loci, multiple alleles, different subunit interaction, different splice forms, or different post-translational modifications. When comparing the protein profiles of both cultivars, we have to take into account that, due to the technical limitations of the 2-DE technique (e.g., the limited pI range of the detected proteins), it is possible that we did not detect all existing isoforms of a protein. Therefore, we should be careful when interpreting these data. Besides, many of the differences between both genomes/proteomes are probably not related to the differences in scab susceptibility of both cultivars. Therefore, we focused our attention to the differences in protein accumulation that were exclusively induced by scab

inoculation. Hereby we ignored the proteins of which different isoforms were differentially accumulated at 5 dpi between ‘Topaz’ and ‘Golden Delicious’ in opposite ways (both up- and downregulated; 8 in total). This way we come to a list of 5 different proteins that are exclusively up-regulated in ‘Topaz’ compared to ‘Golden Delicious’ at 5 dpi (Table 5.5) and 7 proteins that are less accumulated in ‘Topaz’ at 5 dpi (Table 5.6).

Table 5.5. List of proteins that are significantly and exclusively up-regulated in 'Topaz' compared to 'Golden Delicious' five days after inoculation.

						Top-I > Gol-I		Top-C > Gol-C	
Spot[a]	**Protein name[b]**	**Accession No.[c]**	**Score[d]**	**PM[e]**	**q[f]**	**Ratio[g]**	**α[h]**	**Ratio[i]**	**α[j]**
	Cell rescue, defense and virulence								
	Defense response								
1637	Mal d 1-like	MDP0000151829	515	7	6.8^{E}-3	1.9	0.05	1.0	ns
1595	major allergen Mal d 1 (PR-10)	MDP0000942516	556	7	0.011	1.9	0.05	0.8	ns
	Stress response								
	Protein folding								
956	protein disulfide isomerase	MDP0000201801	558	11	0.010	1.2	0.05	1.1	ns
	Energy and carbohydrate metabolism								
	Glycolysis and gluconeogenesis								
469	apple phosphoglyceromutase (apgm)	MDP0000240039	178	11	1.5^{E}-3	1.2	0.01	0.9	ns
926	phosphoglycerate kinase	MDP0000325411	1380	17	1.4^{E}-5	4.8	1^{E}-6	1.6	ns
	Unknown								
1062	esterase/lipase domain-containing protein	MDP0000130884	402	8	1.5^{E}-3	1.7	0.01	1.0	ns

[a] Corresponding spot number in the gel image in Fig. 5.1

[b] Proteins have been grouped according to the Gene Ontology biological process wherein they are involved

[c] MDP number of predicted apple gene (Velasco *et al*., 2010) (Gene and protein sequences can be obtained from GDR: http://www.rosaceae.org

[d] MOWSE score probability (protein score) for the entire protein

[e] Number of matched peptides of peptide mass fingerprinting combined with MS/MS

[f] Overall false discovery rate (FDR) corrected p-value of the 2D-DIGE experiment, according to a one-way ANOVA, using the DeCyder 6.5 software

[g] Ratio of the average standardized abundance of the inoculated 'Topaz' samples (Top-I) to the average standardized abundance of the inoculated 'Golden Delicious' samples (Gol-I), calculated with the DeCyder 6.5 software

[h] significance level α according to a false discovery rate (FDR) corrected one-way ANOVA, using the DeCyder 6.5 software

[i] Ratio of the average percentage of spot volume (% vol) of the 'Topaz' control samples (Top-C) to the average % vol of the 'Golden Delicious' control samples (Gol-C), calculated with the Image Master 2-D platinum software

[j] significance level α according to a Kolmogorov-Smirnov statistical test that compares the percentage of spot volume (% vol) of the protein in the control (C) 'Topaz' leaves with the control 'Golden Delicious' leaves, using the Image Master 2-D platinum software (GE Healthcare); ns: not significant

Table 5.6. List of proteins that are significantly and exclusively down-regulated in 'Topaz' compared to 'Golden Delicious' five days after inoculation.

						Top-I < Gol-I		Top-C < Gol-C	
Spot[a]	**Protein name[b]**	**Accession No.[c]**	**Score[d]**	**PM[e]**	**q[f]**	**Ratio[g]**	**α[h]**	**Ratio[i]**	**α[j]**
	Cell rescue, defense and virulence								
	Stress response								
	ROS detoxification								
842	monodehydroascorbate reductase	MDP0000261821	1360	17	3.1^{E}-3	1.3	0.01	0.9	ns
	Energy and carbohydrate metabolism								
	Photosynthesis								
1512	light-harvesting complex I protein Lhca1	MDP0000222941	252	4	2.4^{E}-3	1.2	0.05	0.9	ns
1344	light-harvesting complex II protein Lhcb1	MDP0000417927	464	7	6.9^{E}-3	1.2	0.05	0.6	ns
	Acetyl-CoA biosynthesis								
715	ATP-citrate synthase	MDP0000931334	335	7	5.5^{E}-3	1.4	0.01	1.2	ns
	Amino acid metabolism								
	aromatic amino acid family biosynthesis								
961	3-dehydroquinate synthase; quinate dehydrogenase	MDP0000273495	859	14	7.5^{E}-3	1.3	0.05	1.0	ns
	Translation								
	aminoacyl-tRNA biosynthesis								
342	glycyl-tRNA synthetase (1, mitochondrial-like)	MDP0000226879	734	15	6.5^{E}-3	1.3	0.05	0.9	ns
	Transport facilitation								
	Protein import into chloroplast								
1350	protein THYLAKOID FORMATION1, chloroplastic-like	MDP0000139684	758	12	0.012	1.3	0.05	1.0	ns

[a] Corresponding spot number in the gel image in Fig. 5.1

[b] Proteins have been grouped according to the Gene Ontology biological process wherein they are involved

[c] MDP number of predicted apple gene (Velasco *et al*., 2010) (Gene and protein sequences can be obtained from Genome Database for Rosaceae (GDR): http://www.rosaceae.org)

[d] MOWSE score probability (protein score) for the entire protein

[e] Number of matched peptides of peptide mass fingerprinting combined with MS/MS

[f] Overall false discovery rate (FDR) corrected p-value of the 2D-DIGE experiment, according to a one-way ANOVA, using the DeCyder 6.5 software

[g] Ratio of the average standardized abundance of the inoculated 'Golden Delicious' samples (Gol-I) to the average standardized abundance of the inoculated 'Topaz' samples (Top-I), calculated with the DeCyder 6.5 software

[h] significance level α according to a false discovery rate (FDR) corrected one-way ANOVA, using the DeCyder 6.5 software

[i] Ratio of the average percentage of spot volume (% vol) of the 'Golden Delicious' control samples (Gol-C) to the average % vol of the 'Topaz' control samples (Top-C), calculated with the Image Master 2-D platinum software

[j] significance level α according to a Kolmogorov-Smirnov statistical test that compares the percentage of spot volume (% vol) of the protein in the control (C) 'Topaz' leaves with the control 'Golden Delicious' leaves, using the Image Master 2-D platinum software (GE Healthcare); ns: not significant

5.3.3.1. Higher levels of proteins known to be involved in stress responses

Of the 5 proteins that were exclusively up-regulated in the scab-infected 'Topaz' leaves, 2 are known to be involved in a stress response (Table 5.5). Mal d 1 (spots 1637 and 1595) was already mentioned as being induced by *V. inaequalis* inoculation in 'Topaz' (see Section 5.3.1.1). Protein disulfide isomerase (PDI; spot 956) is an enzyme in the endoplasmic reticulum that catalyzes the formation and breakage of disulfide bonds between cysteine residues within proteins as they fold. This allows proteins to quickly find the correct arrangement of disulfide bonds in their fully folded state, and therefore the enzyme acts to catalyze protein folding (Gruber *et al*., 2006). In plants, there is evidence of clear linkage of up-regulated accumulation with stress responses (Fodoroff, 2006).

5.3.3.2. Down-regulation of ROS scavenging mechanisms

Of the 7 proteins that were exclusively less accumulated in 'Topaz' leaves compared to 'Golden Delicious' at 5 dpi, there is only one, monodehydroascorbate reductase (MDAR; spot 842), of which participation in a stress response is known, i.e. in a response to hydrogen peroxide (Table 5.6). In plants, MDAR is an enzymatic component of the ascorbate-glutathione cycle that is one of the major antioxidant systems of plant cells for the protection against the damages produced by reactive oxygen species such as superoxide (O_2^-) and hydrogen peroxide (Fig. 5.8; Leterrier *et al*., 2005). Superoxide is rapidly dismutated by superoxide dismutase (SOD) into H_2O_2. Ascorbic acid (AsA) reacts with H_2O_2 in the presence of ascorbate peroxidase (APX) to form monodehydroascorbate (MDA). Ascorbate can be regenerated from MDA directly by the action of the NADPH-dependent monodehydroascorbate reductase, or by the spontaneous disproportionation of MDA into ascorbate and dehydroascorbate (DHA). AsA is regenerated from DHA in a reaction catalyzed by dehydroascorbate reductase (DHAR), where reduced glutathione (GSH) is oxidized into GSSG. GSH is regenerated in the presence of NADPH by glutathione reductase (GR) (Fig. 5.8; Davletova *et al*., 2005; Leterrier *et al*., 2005). It is known that in a monogenic resistant cultivar (like 'Topaz'), R protein mediated signaling downregulates ROS scavenging mechanisms, like the glutathione-ascorbate cycle, upon pathogen attack (Apel and Hirt, 2004). Together with activation of superoxide producing oxidases, this increases intracellular levels of reactive oxygen species like hydrogen peroxide, which activate defense related genes. Overall, ROS amounts can increase to critical levels for the plant itself and induce

programmed cell death (PCD, e.g. pin-points) (Fig. 5.9; Lamb and Dixon, 1997; Apel and Hirt, 2004).

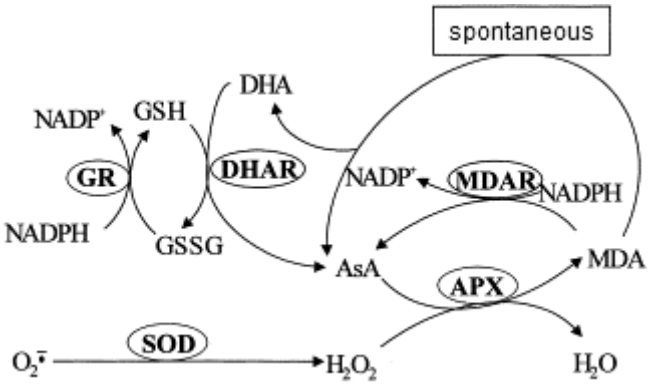

Fig. 5.8. Scheme of the ascorbate–glutathione cycle (adapted from Ito *et al.*, 1999). SOD: superoxide dismutase, APX: ascorbate peroxidase, MDAR: monodehydroascorbate reductase, DHAR: dehydroascorbate reductase, GR: glutathione reductase, AsA: reduced ascorbic acid, MDA: monodehydroascorbate, DHA: dehydroascorbate, GSH: reduced glutathione, and GSSG: oxidised glutathione. MDAR was exclusively down-regulated in 'Topaz' leaves compared to 'Golden Delicious' at 5 dpi (and not in the control conditions).

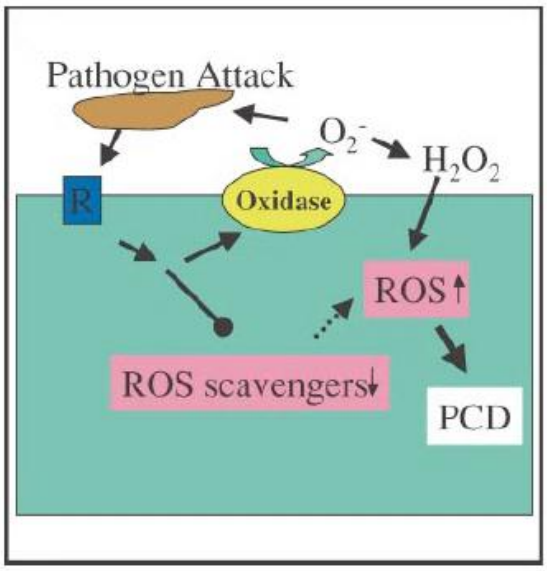

Fig. 5.9. Increase of intracellular ROS levels upon pathogen attack (Apel and Hirt, 2004). Upon pathogen attack, receptor-induced signaling activates plasma membrane or apoplast-localized oxidases that produce superoxide radicals (O_2^-) that are highly toxic and can help to kill the invading pathogen. On the other hand, O_2^- is rapidly dismutated by superoxide dismutase into hydrogen peroxide, which, in contrast to superoxide, can readily cross the plasma membrane. Intracellular ROS levels increase due not only to extracellular production of ROS but also by downregulation of ROS scavenging mechanisms. Overall, ROS amounts can increase to critical levels and induce programmed cell death (PCD).

5.3.3.3. Differential accumulation of proteins involved in the energy and carbohydrate metabolism

The apple phosphoglyceromutase (APGM; spot 469; EC 5.4.2.1) is also known to be involved in a stress response (Blast2GO). Together with phosphoglycerate kinase (spot 926; EC 2.7.2.3), that was also found to be accumulated more in infected 'Topaz' leaves compared to 'Golden Delicious', it participates in glycolysis (see Fig. 5.6). In step 8 of glycolysis the enzyme catalyzes the internal transfer of a phosphate group from C-3 to C-2 which results in the conversion of 3-phosphoglycerate (3PG) to 2-phosphoglycerate (2PG) through a 2,3-bisphosphoglycerate intermediate.

None of the 5 proteins that were exclusively up-regulated in infected 'Topaz' leaves compared to 'Golden Delicious' were involved in photosynthesis (Table 5.5). On the other hand, none of the 7 proteins that were down-regulated in 'Topaz' were involved in glycolysis, while the down-regulated chlorophyll a/b binding light-harvesting complex I protein Lhca1 (spot 1512) and light-harvesting complex II protein Lhcb1 (spot 1344) both participate in photosynthesis (Table 5.6).

5.4. Concluding remarks

When investigating the *Rvi*6-resistant cultivar 'Topaz' at 5 dpi, we could verify that by far the most infection-induced, up-regulated proteins showed a tendency of accumulation of infection > mock-infection > control, although in most cases not statistically significant (Table 5.1). The mock-infection related stress conditions seemed to cause an up-regulation of proteins mainly known to be involved in stress responses and/or in catabolism. This up-regulation seemed to be even higher in the *V. inaequalis* inoculated leaves. The fact that most of these differences in accumulation were not statistically significant was most probably due to the rather large variations in accumulation between the three biological replicates used, as was illustrated by the example of Mal d 1 (Fig. 5.5). This hypothesis will be further investigated in Chapter 6, where the proteomes of infected and mock-infected leaves are compared again, however then in Aliette®-treated apple leaves, which showed less variation in accumulation between the biological replicates.

It is not really surprising that the same (categories of) proteins showed a tendency to differentially accumulate upon both scab-infection and mock-infection. Many studies have shown that the cellular responses to a wide range of environmental challenges, including both biotic and abiotic stresses, are rather similar (Bowler and Fluhr, 2000). This might explain why plants resistant to one stress are sometimes cross-tolerant to others. The cross-talk between stress signaling pathways is thought to optimize the defense reaction by enhancing the appropriate response, while suppressing suboptimal reactions (Koorneef and Pieterse, 2008). The similarities among the plant stress responses can be striking. For example, cDNA-AFLP differential display has revealed that the majority of genes induced by the race-specific Cf9–Avr9 interaction in tobacco are also induced by wounding (Romeis *et al.*, 1999). Furthermore, the observed differences in the level and timing of the changes in accumulation might suggest that plant acclimation to different stresses is controlled by sophisticated quantitative rather than qualitative effects (Bowler and Fluhr, 2000). In that respect, the importance of the R-Avr interaction regarding the biotic stress response, as was also established in our research, is remarkable. However, the fact that susceptible plants, e.g. 'Golden Delicious', possess the possibility to effectively resist the pathogen, e.g. during ontogenic resistance, can be viewed in this context as well.

The up-regulated stress response related proteins in 'Topaz' at 5 dpi were a pathogenesis-related protein (Mal d 1), a ROS detoxification enzyme (thioredoxin), a protein involved in defense signaling mediated by R proteins (EDS1), a protein that participates in the synthesis of phenolic compounds with antifungal action (chalcone synthase), proteins that play a role in protein folding (HSP 60, HSP 70 and TCP domain class transcription factor), proteins involved in cell wall metabolism (linoleate 13S-lipoxygenase and alpha-1,4-glucan-protein synthase) and proteins that participate in nucleotide biosynthesis (nucleoside diphosphate kinase 1 and 'bifunctional purine biosynthesis protein'). The up-regulated proteins in catabolism mainly participate in the glycolysis and TCA pathways. The free energy released in these processes is used to form the high-energy compounds ATP (glycolysis), $FADH_2$ (glycolysis) and NADH (glycolysis and TCA pathway). Both of these latter molecules are recycled to their oxidized states (NAD^+ and FAD, respectively) via the electron transport chain, which generates additional ATP by oxidative phosphorylation. Many metabolic processes use ATP as an energy source. As mentioned before, energy demand and

respiration rates have been known to increase during resistance responses, since the resistance mechanisms that need to be activated in order to respond to stress require an extra energy supply (Smedegaard-Petersen and Tolstrup, 1985; Umeda *et al*., 1994; Scheideler *et al*., 2002; Block *et al*., 2005; Scharte *et al*., 2005; Moshe *et al*., 2012). The up-regulation of molecular chaperones such as the heat chock proteins HSP 60 and HSP 70 aids to alleviate the stress caused by infection (Santoro, 2000).

The hypothesis that all the infection induced down-regulated proteins showed an infection < mock-infection < control accumulation trend is in agreement with our hypothesis that the mock-infection related stress response is increased upon application of an extra, biotic stress. The down-regulated proteins were mainly involved in central anabolic processes, i.e. in carbon fixation (both light-dependent reactions of photosynthesis and light-independent reactions of the Calvin cycle) and in gluconeogenesis. Scharte *et al*. (2005) proposed that in photoautotrophic source leaves, like the unfolded leaves sampled in our experiments, upon pathogen attack, photosynthesis and assimilatory metabolism are switched off and processes required for defense are initiated. The down-regulation of photosynthesis and the simultaneous increased demand for assimilates very often leads to a transition of source tissue into sink tissue during plant-pathogen interactions (Berger *et al*., 2007).

In summary, the abundancy of several proteins involved in the energy and carbohydrate metabolism of the 'Topaz' leaves was altered upon infection, compared to control leaves, possibly in order to maintain homeostasis (Table 5.7). The big share of differentially accumulated proteins involved in energy/metabolism or stress/defense response is in agreement with previous proteomics studies of plant-fungus interactions (Castillejo *et al*., 2010; Sinha and Chattopadhyay, 2011; Sghaier-Hammami *et al*., 2012).

Table. 5.7. Main global cellular responses in young leaves of the monogenic *Rvi6*-resistant cultivar 'Topaz' at 5 days post-inoculation with *Venturia inaequalis* conidia, compared to control leaves.

Up-regulated	**Down-regulated**

• defense/stress response
• **Catabolism:**
  ○ glycolysis
  ○ TCA pathway (citric acid cycle)
	• **Anabolism:**
	  ○ gluconeogenesis
	  ○ <u>carbon fixation:</u>
	  ▪ Calvin cycle
	  ▪ photosynthesis

One of the advantages of gel-based proteomics is the fact that post-translational modifications and isoforms can be detected. However, one has to be aware of the fact that up-regulation of a protein (isoform) could be compensated for by down-regulation of another isoform that is possibly not detected during 2-DE. For example a post-translational modification affecting the iso-electric point of a protein could cause one of the isoforms to fall out of the pI range (i.e. pI 4-7) of the gel. Nevertheless, interestingly, two isoforms of a protein (fructose-bisphosphate aldolase; spots 1078 and 1073), a cytosolic one that is involved in glycolysis and a plastidic one that is involved in the Calvin cycle, were found to be up-regulated and down-regulated respectively.

When investigating the proteins that were exclusively differentially accumulated in the *Rvi*6-resistant 'Topaz' compared to the scab-susceptible 'Golden Delicious' at 5 dpi, we could identify the same (categories of) proteins as when the infected 'Topaz' leaves were compared to the control (or mock-infected) leaves. Most of the proteins that were up-regulated in 'Topaz' compared to 'Golden Delicious' are known to be involved in a stress response and/or in the glycolysis pathway. On the other hand, two of the 7 down-regulated proteins are involved in photosynthesis, while none are involved in the glycolysis or TCA pathway. It has been pointed out in other plant-pathogen interactions that enzymes involved in energy producing pathways such as glycolysis and TCA cycle are more abundant in infected resistant than susceptible plants (Moshe *et al*., 2012). Furthermore, a comparison of the interaction of *Arabidopsis* with a virulent and an avirulent strain of *Pseudomonas syringae* showed that the major difference in the changes in photosynthesis was the speed of the effects. A decrease in photosynthesis was detectable earlier with the avirulent strain than with the virulent strain (Tao *et al*., 2003). Together, these differences in the level and timing of the changes in accumulation between compatible and incompatible interactions suggest that, similar to the effect on secondary metabolism, the differences between both interactions in the effect on primary metabolism are rather quantitative than qualitative.

Classical defense-related proteins, including pathogenesis-related proteins, are also known to be up-regulated more in R-gene-mediated incompatible interactions than in compatible interactions (Bozkurt *et al*., 2010). Our proteomic analyses did however not reveal the sharp increases in accumulation of well-known PR proteins in resistant plants, such as chitinases and β-1,3-glucanase, that are able to attack the fungus by hydrolyzing its cell wall. This is

remarkable considering that the induction of these enzymes – often even with molecular weights and isoelectric points within our investigated ranges – has been well documented in several plant tissues as a response to a range of biotic and abiotic stresses (Linthorst, 1991; Sindelarova and Sindelar, 2001; Kim *et al*., 2004). However, we are not the first ones to find that such PR proteins are possibly not induced in leaves of infected resistant plants (Gorovits and Czosnek, 2007; Garcia-Neria and Rivera-Bustamante, 2011).

It is difficult to conclude from these data which proteins lay the foundation of the scab-resistance of 'Topaz' (see also our 'General Conclusions' in Chapter 7). We are inclined to think that proteins differentially accumulated at earlier time-points after infection could lie at the basis of the established stress response or altered energy metabolism. However, we could not identify any proteins that were differentially accumulated at 2 or 3 dpi and not at 5 dpi.

In the next chapter, the effect of the systemic fungicide fosetyl-Al (Aliette®) on the resistance response of 'Topaz' will be studied. Also we hope to confirm our results and hypotheses made in this chapter and detect more statistically significant differences in protein accumulation in scab-infected and mock-infected 'Topaz' leaves.

Chapter 6

Effect of preventative treatment with fosetyl-Al on responses of apple to *V. inaequalis* infection

6.1. Introduction: Fosetyl-Al, an alternative, systemic fungicide

During the past few decades, fungicides against *V. inaequalis* with new modes of action had to be developed on a regular basis because of changes to the EU legislation and because resistance to site-specific fungicides continued to develop (see Section 2.1.2). However, no contact multi-site fungicides with new modes of action have been developed recently (Chapman *et al*., 2011). The use of preventative, multi-site fungicides and elicitors that stimulate plant defense could be a way out of the impasse. Xylem mobile systemics applied to leaves are able to translocate through the cuticle and move throughout the leaf where deposited. When deposited on stems, they can move upwards into leaves. Phloem mobile systemics can move to other parts of the plant. New leaf growth is even protected for a short period. Some of these chemicals apparently act by stimulating the natural defense response in the plant.

The best understood systemically induced plant defense mechanism is 'systemic acquired resistance' (SAR; Kessmann *et al*., 1994). SAR is characterized by broad-spectrum disease resistance that is activated systemically in induced plants following localized inoculations with necrogenic pathogens which can be viruses, bacteria or fungi. Chemicals have been discovered that are able at very low rates to activate SAR type resistance in many plant species, such as cucumber, tobacco, rice and other crops, in the greenhouse as well as under field conditions (Kessmann *et al*., 1994). These resistance inducing chemicals that are able to induce broad disease resistance offer an additional option for the producer to complement genetic disease resistance and the use of curative fungicides. Their use can reduce the total

dosage and number of treatments needed for pathogen control. If integrated properly in plant health management programs, these fungicides that act through stimulation of plant defense responses and that show systemic properties can prolong the useful life of both the resistance genes and the curative fungicides presently used (Kessmann *et al*., 1994; Oostendorp *et al*., 2001).

Aliette®, a product of Bayer CropScience, is such a preventative fungicide with systemic properties. Its active ingredient, fosetyl-Al (fosetyl-aluminium), has already been found to deliver a bi-directional protection (both upwards when applied to the roots and downwards when applied to the leaves) against Oomycete-type of fungi such as *Phytophthora* and *Pythium* by stopping the growth of mycelia and reducing the production of spores (Smillie *et al*., 1989; Bayer CropScience, 2012). Aliette® also has a bacteriostatic effect on *Pseudomonas* spp, *Xanthomonas* spp, and *Erwinia amylovora*. As such it is commonly used to control fire blight in apple and pear orchards (Larue and Gaulliard, 1993). The direct mode of action of fosetyl-Al affects multiple targets in phosphate transport, phosphate use and regulatory functions within the fungus (Stehmann and Grant, 2000).

Fosetyl-Al does not only have this direct but also an indirect mode of action. It has been shown to have a strong stimulating effect on the natural defense mechanisms of the plant (Guest, 1984 and 1986; Bayer CropScience, 2012). This is because upon application fosetyl-Al dissociates to ethyl phosphonate and $Al(OH)_3$, and after uptake by the plant, ethyl phosphonate is not only translocated both through the xylem vessels (acropetal systemicity) and through the phloem system driving to both acropetal and basipetal systemicity, but is also slowly converted to phosphorous acid and EtOH (Fig. 6.1). Both ethyl phosphonate and phosphorous acid are known to contribute to the signals leading to the stimulation and/or enhancement of plant defense systems, such as the induction of phytoalexins, compounds derived from cinnamic acid, or pathogenesis-related proteins (Guest *et al*., 1988; Saindrenan *et al*., 1988).

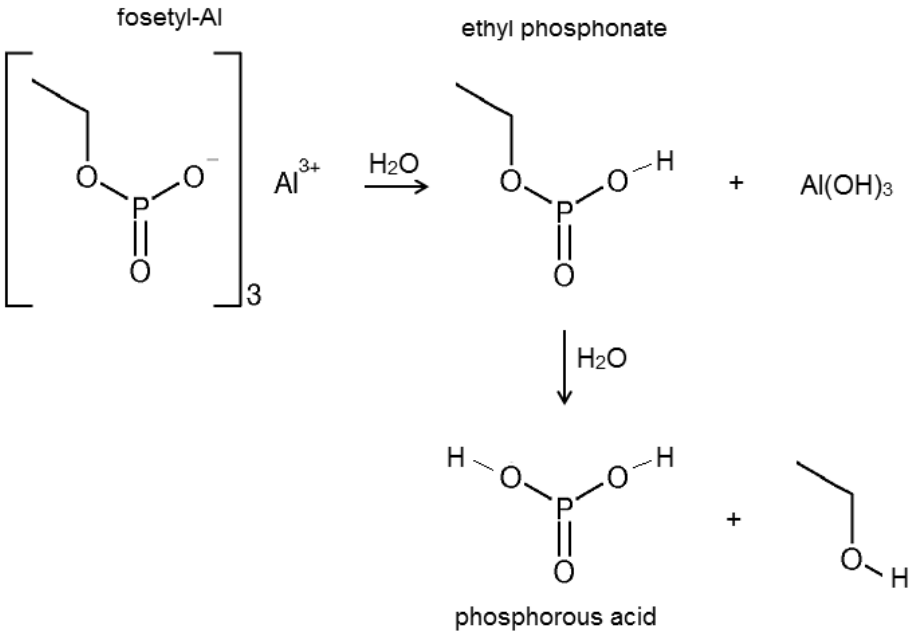

Fig. 6.1. Fosetyl-Al: dissociation to defense stimulating signals. Upon application fosetyl-Al dissociates to ethyl phosphonate and $Al(OH)_3$, and after uptake by the plant, ethyl phosphonate is slowly converted to phosphorous acid and EtOH. Both ethyl phosphonate and phosphorous acid are known to contribute to the signals leading to the stimulation and/or enhancement of plant defense systems.

Some phosphonates (or 'phosphites'), e.g. potassium phosphonate, are known to not only show a direct defense response inducing effect (in the absence of a pathogen), but a 'priming' effect as well (Eshraghi *et al*., 2011). Primed plants display either faster, stronger, or both activation of the various cellular defense responses that are induced following attack by either pathogens or insects or in response to abiotic stress (Conrath *et al*., 2006). The benefit of priming in contrast to direct defense elicitation is substantial ressource saving in the plant. Fosetyl-aluminium could also act rather by priming for pathogen resistance than by straight defense gene induction (Latorse *et al*., 2010). In conclusion, fosetyl-aluminium (or ethyl phosphonate) is a potent primer of plant defense responses supported by a limited direct effect on fungal metabolism.

In this chapter, we wanted to investigate the effect of Aliette® on susceptibility to infection by *V. inaequalis* in the *Rvi*6-resistant cultivar 'Topaz' and the susceptible cv. 'Golden Delicious', as measured by visual evaluation of leaf symptoms and by real-time quantitative PCR. At the same time, we wanted to examine at the proteome level how Aliette® influences the responses of 'Topaz' that were described in the previous chapter.

6.2. Experimental setup

Of each cultivar 'Topaz' and 'Golden Delicious' 75 one year old grafted trees were randomly divided over a greenhouse compartment. Irrigation, temperature and relative humidity were automatically controlled (see Section 3.1). Actively growing apple plants with 6-10 healthy, fully expanded leaves were sprayed with either an aqueous Aliette® suspension (2.5 g/L and 80 % fosetyl-Al; 40 plants of each cv.) or demineralized water (35 plants each) eleven and four days prior to inoculation. The Aliette® granulate was received from Dr. Marie-Pascale Latorse (Bayer CropScience). The dose rate of Aliette® used is based on the registered dose rate against *Pseudomonas* and *Erwinia*. Moreover, for this dose rate good level (50-85 % Abbott) of *V. inaequalis* control was determined in field trials (Ir. Luk De Maeyer, Bayer CropScience - personal communication). At the time of inoculation, 25 Aliette®-treated and 25 non-treated plants of each cv. were sprayed with an aqueous conidial suspension (2×10^5 spores ml^{-1}) of *V. inaequalis* race 1 strain 104 to runoff (see Section 3.3) and 10 Aliette®-treated and 5 non-treated plants of each cv. were mock-infected. The 5 remaining plants of each treatment (Aliette® application or not) and each cv. were control plants. For both cultivars, 10 Aliette®-treated and 10 non--treated *V. inaequalis* inoculated plants were used for visual assessment of apple scab symptoms. At 5, 7, 8, 10, 14, 17, 21 and 25 dpi (and for 'Golden Delicious' also at 12 dpi), the degree of infection as according to the classification of Chevalier and the degrees of sporulation and chlorosis, both as a percentage of leaf surface, were determined for leaves F0, F1, F2 and F3 (see Section 3.4). At 18 dpi, leaves F1 and F2 (and for 'Golden Delicious' also leaf F3) were harvested for DNA extraction for real-time PCR for *V. inaequalis* quantification (see Section 3.5). For 'Topaz', six biological replicates (*i.e.* six apple plants) were used for each treatment (Aliette® or not). For 'Golden Delicious', only four replicate plants for each treatment were available for DNA extraction. The time-point, 18 dpi, was chosen in order to increase the chances to find statistically significant differences in *V. inaequalis* DNA levels between Aliette® treated and non-treated plants.

Next, an analysis of the changes in accumulated proteins upon treatment with fosetyl-Al was performed. Leaf samples were taken at 5 dpi from Aliette®-treated mock-inoculated ('Al-M'), Aliette®-treated *V. inaequalis* inoculated ('Al-I') and non-Aliette®-treated inoculated ('I') 'Topaz' plants. This way, we could determine the effect of Aliette® on the response of 'Topaz' upon scab infection (comparison 'Al-I <> I'), but we could also study the differential

protein accumulation upon *V. inaequalis* inoculation in the Aliette®-treated trees ('Al-I <> Al-M'-) and compare this with the differential protein accumulation upon *V. inaequalis* inoculation in the non-treated trees ('I <> M' and 'I <> C' of former experiment; see Chapter 5). The time-point of 5 dpi was chosen based on the results from Chapter 5. For each plant, leaves F1 and F2 were harvested, pooled and stored at -80 °C. For proteome analysis, three replicate extractions (*cf*. three biological replicates or three plants) were performed for each condition. CyDye™ labeling was applied for protein visualization (see Section 3.7.3). An FDR corrected one-way ANOVA was carried out in order to assess for absolute protein changes among the different treatments (see Section 3.7).

6.3. Results and discussion

6.3.1. Effect of Aliette® on foliar disease symptoms

The evolution of foliar disease symptoms in the scab-susceptible apple cultivar 'Golden Delicious' and the monogenic *Rvi*6-resistant cultivar 'Topaz', with or without treatment with Aliette® 11 and 4 days prior to inoculation, was studied in the time period up to 25 dpi. Results were expressed as the median TH-value of Chevalier, chlorosis and sporulation classes, as described in section 3.4 (Fig. 6.2).

At 10 dpi, chlorotic lesions and light (0-1%) sporulation (class of Chevalier 3a) developed around the midrib of most non-Aliette®-treated, susceptible 'Golden Delicious' leaves. At 12 dpi, the degree of sporulation was increasing rapidly (class 3b). At 21 dpi, the degree of chlorosis was decreasing in most leaves (Fig. 6.2b) and the degree of sporulation had increased up to 75 % of the leaf surface (class 4; Fig. 6.2c). In the Aliette®-treated 'Golden Delicious' leaves, the emergence of sporulation was on average 1 to 2 days later (Fig. 6.2c). This was even more obvious when only leaf F1 was considered (Fig. 6.3). Thus, Aliette® seemed to postpone disease development to some extent.

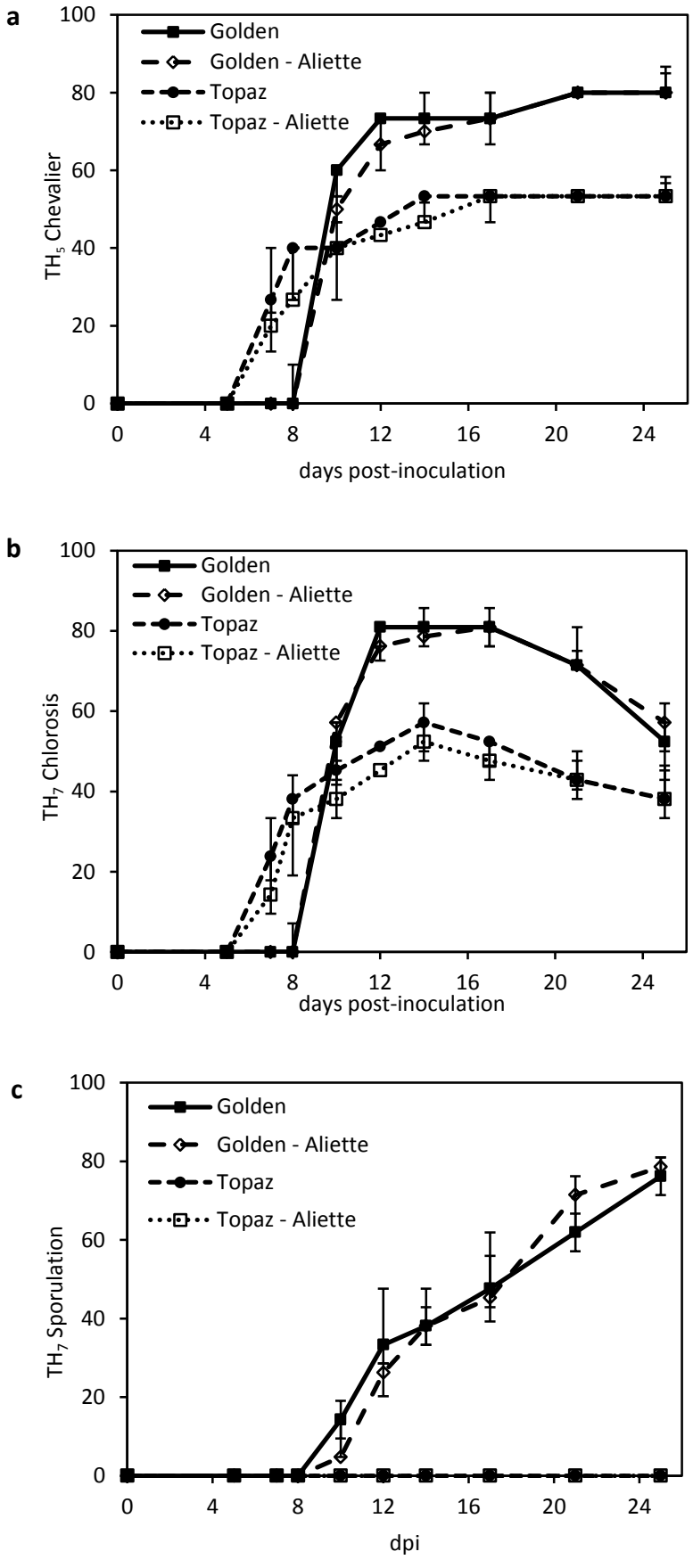

Fig. 6.2 (Legend: see next page)

Fig. 6.2 (see previous page). Evolution of foliar disease symptoms in the scab-susceptible apple cultivar 'Golden Delicious' and the monogenic *Rvi*6-resistant cultivar 'Topaz' after inoculation with *Venturia inaequalis* race 1 strain 104, with or without treatment with Aliette® 11 and 4 days prior to inoculation. **(a)** Evolution of the degree of *V. inaequalis* infection, according to the classification of Chevalier (Chevalier *et al*., 1991). **(b-c)** Evolution of the degree of chlorosis and sporulation respectively, according to the classification of Croxall *et al*. (1952), modified by Parisi *et al*. (1993). Data represent medians of TH-values of ten replicate plants (with leaves F0, F1, F2 and F3 evaluated per plant). Error bars indicate first and third quartiles.

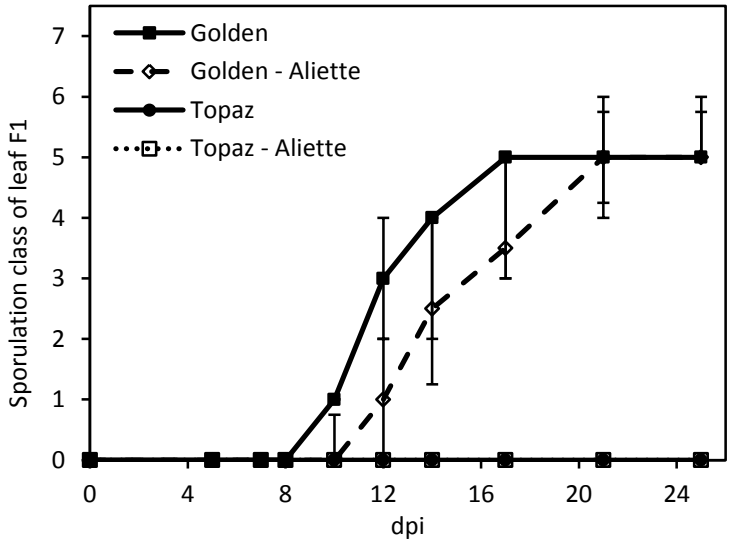

Fig. 6.3. Evolution of the degree of sporulation in Aliette®-treated and non-treated 'Golden Delicious' and 'Topaz' leaves F1 after inoculation with *Venturia inaequalis* race 1 strain 104, according to the classification of Croxall *et al*. (1952), modified by Parisi *et al*. (1993). Data represent medians of sporulation classes of ten replicate plants. Error bars indicate first and third quartiles.

In the *Rvi6*-resistant 'Topaz', the majority of the evaluated leaves began to display chlorotic lesions at 7 dpi already (class of Chevalier 2), and by 14 dpi, necrotic lesions developed within most of these leaves (class 3a). In the Aliette®-treated 'Topaz' leaves, chlorosis appeared somewhat later (1 to 2 days) and levels remained slightly lower (however statistically not significant) than in the non-treated leaves (Fig. 6.2b). Necrosis occurred 1-2 days later as well (Fig. 6.2a).

None of the control or mock-infected control plants showed any of the above mentioned symptoms of chlorosis, necrosis or sporulation, whether they had been treated with Aliette® or not.

In Section 2.3.5 we discussed the reduction in fungal infection with increasing age of host tissue (ontogenic resistance). In order to have an idea on the differences in susceptibility of apple leaves of different ages towards scab, we compared the foliar symptoms of leaves F0, F1, F2 and F3 of the non-Aliette®-treated plants separately (Fig. 6.4).

Evaluation of the foliar symptoms of 'Golden Delicious' suggested that leaf F0 was the least infected (Fig. 6.4). The fact that leaf F0 was not yet fully expanded on the time of inoculation, and therefore not fully accessible to the fungal spores, could explain this observation. Leaf F1 was expected to be the most susceptible based on literature and previous results (see Fig. 4.4 in Section 4.4.2). According to the observed chlorotic symptoms between 8 and 12 dpi, leaves F1 and F2 of 'Golden Delicious' did seem to be the most susceptible leaves (Fig. 6.4b). However, based on the classification of Chevalier (Fig. 6.4a) and sporulation symptoms (Fig. 6.4c), leaves F2 and F3 appeared to be slightly more susceptible than leaf F1.

Of the *Rvi*6-resistant 'Topaz' on the other hand, leaves F1 and F0 seemed to be the most susceptible based on the classification of Chevalier (Fig. 6.5a). In the majority of the 'Topaz' plants, only in those two leaves necrotic lesions developed as of 14 dpi. However, based on the development of chlorotic lesions, one would conclude that leaves F1 and F2, not F0, are the most susceptible leaves (Fig. 6.5b).

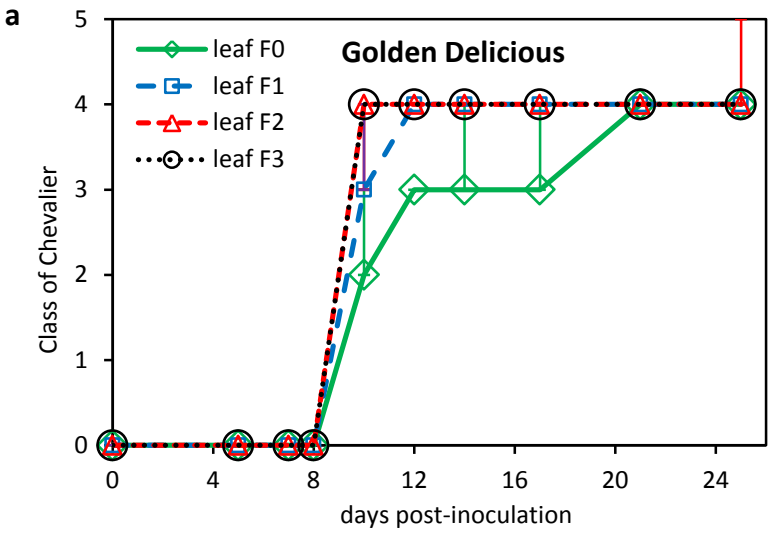
a
Golden Delicious
leaf F0
leaf F1
leaf F2
leaf F3
Class of Chevalier
days post-inoculation

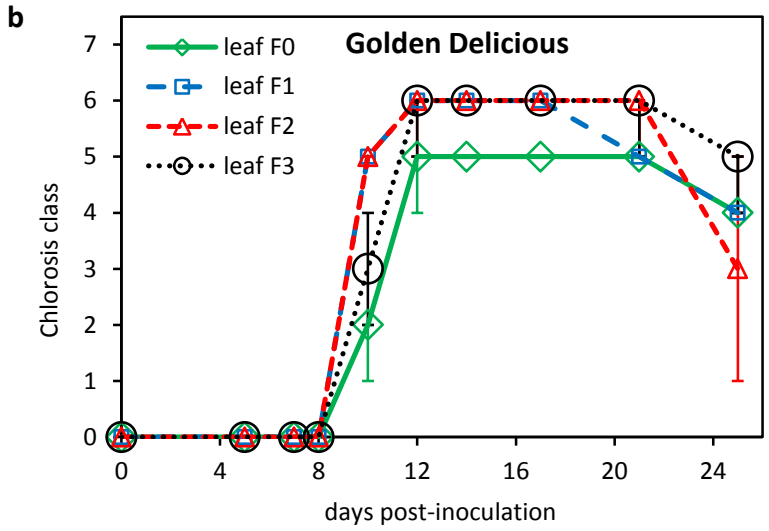
b
Golden Delicious
leaf F0
leaf F1
leaf F2
leaf F3
Chlorosis class
days post-inoculation

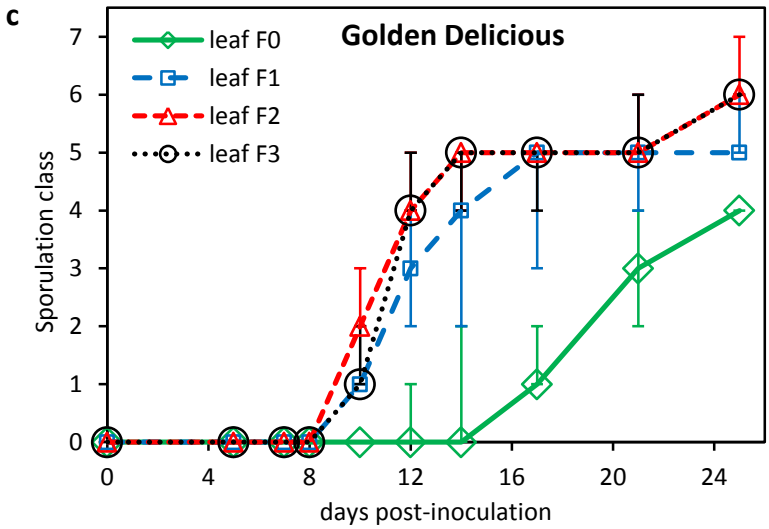
c
Golden Delicious
leaf F0
leaf F1
leaf F2
leaf F3
Sporulation class
days post-inoculation

Fig. 6.4 (see previous page). Evolution of disease symptoms of non-Aliette®-treated 'Golden Delicious' leaves F0, F1, F2 and F3 after inoculation with *Venturia inaequalis* race 1 strain 104. **(a)** Evolution of the degree of *V. inaequalis* infection, according to the classification of Chevalier (Chevalier *et al*., 1991). **(b-c)** Evolution of the degree of chlorosis and sporulation respectively, according to the classification of Croxall *et al*. (1952), modified by Parisi *et al*. (1993). Data represent medians of ten replicate plants. Error bars indicate first and third quartiles.

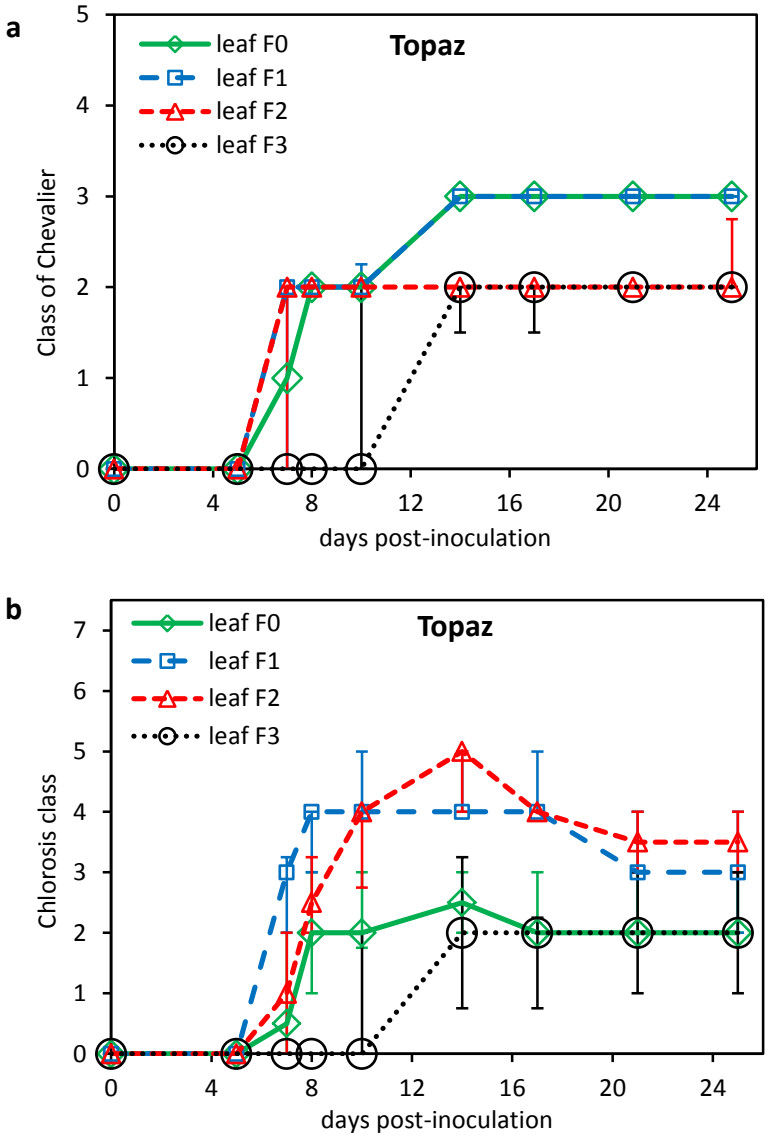

Fig. 6.5. Evolution of disease symptoms of non-Aliette®-treated leaves F0, F1, F2 and F3 of the monogenic *Rvi*6-resistant cultivar 'Topaz' after inoculation with *Venturia inaequalis* race 1 strain 104. **(a)** Evolution of the degree of *V. inaequalis* infection, according to the classification of Chevalier (Chevalier *et al*., 1991). **(b)** Evolution of the degree of chlorosis, according to the classification of Croxall *et al*. (1952), modified by Parisi *et al*. (1993). Data represent medians of ten replicate plants. Error bars indicate first and third quartiles.

For both cultivars, leaf F4 and older leaves were clearly less susceptible due to ontogenic resistance (data not shown). However, it is difficult to conclude from the extent of foliar disease symptoms which leaves are the most susceptible.

Besides, the observed phenotypic differences between the Aliette®-treated leaves and non-treated leaves were smaller than expected and not statistically significant. Real-time PCR analysis of the growth of *V. inaequalis* in the apple leaves was performed to evaluate the effect of Aliette® in a more objective way. The sensitive real-time PCR technique could be more suited for identifying significant differences in infection degree than evaluation of foliar disease symptoms.

6.3.2. Preventative treatment with Aliette® reduces hyphal growth of *V. inaequalis* in apple leaves

For real-time PCR, Aliette®-treated and non-treated *V. inaequalis* inoculated leaves F1 and F2 of both cultivars were harvested at 18 dpi (see Sections 6.2 and 3.5). For 'Golden Delicious' also leaf F3 was investigated because, unexpectedly, evaluation of foliar disease symptoms had suggested that it was one of the most susceptible leaves (see Fig. 6.4).

Real-time PCR analysis of Aliette®-treated and non-treated inoculated 'Topaz' leaves demonstrated that Aliette® reduces the *V. inaequalis* DNA levels, and thus the hyphal growth, by one half to two thirds on average (Fig. 6.6a). We could also notice that leaf F2 was not less infected than leaf F1. This was in contrast with the observed degree of infection according to the classification of Chevalier (see Fig. 6.5a). Because unlike most F1 leaves of 'Topaz', the majority of the F2 leaves did not develop necrotic lesions, they remained in class 2. There is a discrepancy between the phenotypic disease rating score and the real-time PCR data. The appearance of necrotic lesions doesn't correlate with a higher degree of infection. The difference between the Aliette®-treated and non-treated 'Topaz' leaves was statistically significant ($p < 0.05$; Wilcoxon Mann-Whitney U test) if the data of both leaves F1 and F2 of each plant were pooled.

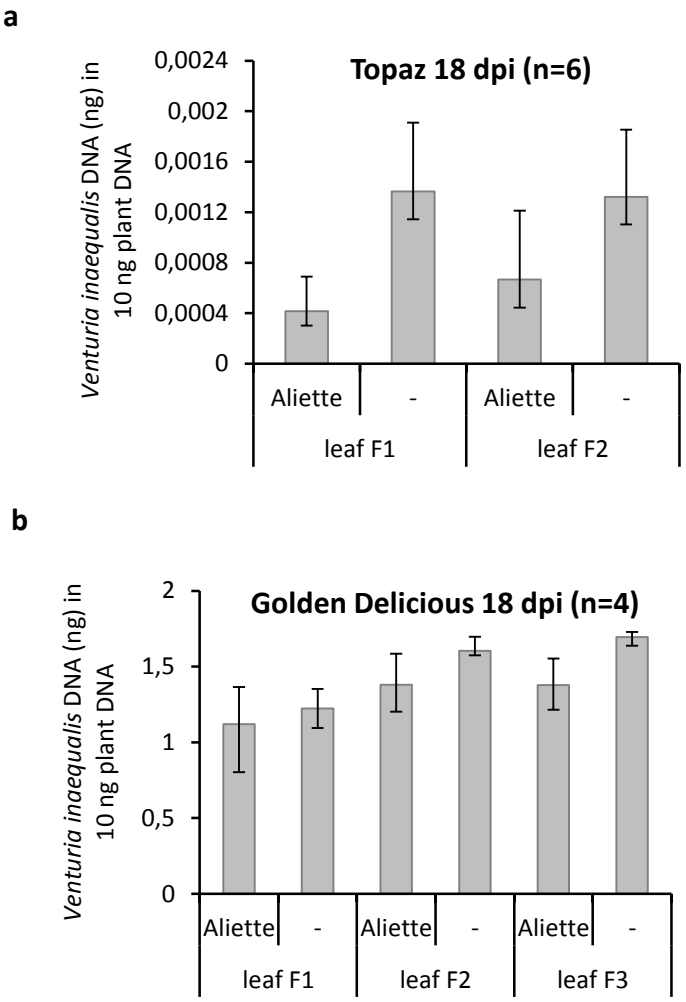

Fig. 6.6. Real-time PCR analysis of *Venturia inaequalis* DNA quantities at 18 days post-inoculation in total reaction volumes of 15 µl containing 10 ng apple genomic DNA of 'Topaz' **(a)** or 'Golden Delicious' **(b)**. The DNA was extracted from the two (a) or three (b) youngest fully expanded leaves at the time of inoculation. Data represent medians of six (a) or four (b) independent biological replicates. Error bars indicate first and third quartiles.

For the scab-susceptible cultivar 'Golden Delicious', the differences in degree of infection between the Aliette®-treated and non-treated leaves were smaller whatever the leaf position, but for all three leaves the extent of pathogen colonization was still 10-20% lower in the Aliette®-treated leaves than in the non-treated plants (Fig. 6.6b). Note that the degree of infection of 'Golden Delicious' leaves is around three orders of magnitude higher than that of 'Topaz' leaves (Fig. 6.6, Y-axis). The real-time PCR data of 'Golden Delicious' did confirm the observed degree of sporulation of the different leaves (Fig. 6.4c), in the sense that leaves F2 and F3 were slightly more infected than leaf F1. Consequently, if we pooled the data of only leaves F2 and F3, the difference between the Aliette®-treated and non-

treated plants did appear to be statistically significant ($p < 0.05$). This finding confirms that one should analyze the fungal growth in the most susceptible leaves when evaluating the influence of a substance like Aliette® on the resistance of the host. Furthermore, it shows that it is good practice not to pool the leaves prior to real-time PCR analysis in order not to lose any significant information.

6.3.3. Proteomics analysis of Aliette®-treated 'Topaz' leaves

6.3.3.1. Similar alterations in the proteomes of Aliette®-treated and non-treated leaves upon infection

First, we compared the 2D-DIGE protein profiles of the Aliette®-treated *V. inaequalis* inoculated and Aliette®-treated mock-inoculated 'Topaz' leaves F1 and F2 at 5 dpi ('Al-I <> Al-M'; see Section 6.2). This way we wanted to verify our conclusions of previous chapter regarding the scab infection induced stress response. Additionally, we also wished to investigate if there were any proteins that were differentially exclusively accumulated upon infection in the Aliette®-treated plants.

By means of an FDR corrected one-way ANOVA (see Section 3.7.6) we detected 71 spots with significantly different accumulation levels ($q \leq 0.05$), of which 29 were up-regulated in the *V. inaequalis*-inoculated Aliette®-treated leaves and 42 down-regulated. Clearly, more proteins are significantly differentially accumulated upon infection than in the non-Aliette®-treated 'Topaz' leaves of Chapter 5 (only 4: 2 up-regulated and 2 down-regulated). We were able to significantly ($q \leq 0.05$) detect differences down to a ratio of 1.1 (Tables 6.1 and 6.2). This proves the high reproducibility and the high quality of the gels. All ratios lay between 1.1 and 1.5 and were mostly comparable with the average standardized abundance ratios of the proteins in the inoculated (I) leaves to the mock-inoculated (M) leaves of Chapter 5. However, the *q*-values (FDR corrected *p*-values) were much higher in the non-Aliette®-treated leaves (Tables 5.1 and 5.2 p.94-98). Accordingly, the differences in abundance of the same proteins in the inoculated and control (C) leaves were only statistically significant ($q \leq 0.05$) down to a ratio of 1.5, and there were even non-significant differences up to ratios of more than 2 (Tables 5.1 and 5.2). Because of the higher quality of the gels in the Aliette® experiment, the differences in protein abundance between the 3 biological replicates were smaller for most spots and conditions than in the non-Aliette® experiment, which resulted in smaller *q*-values and more significant differences in accumulation.

Table 6.1. List of *V. inaequalis* inoculation up-regulated proteins in Aliette®-treated leaves ('Al-I > Al-M') and Aliette®-treatment induced up-regulated proteins in *V. inaequalis* inoculated leaves ('Al-I > I') of 'Topaz' (monogenic *Rvi*6-resistant cultivar) at 5 dpi.

						Al-I > Al-M		Al-I > I	
Spot[a]	**Protein name[b]**	**Accession No.[c]**	**Score[d]**	**PM[e]**	**q[f]**	**Ratio[g]**	**α[h]**	**Ratio[g]**	**α[h]**
	Cell rescue, defense and virulence								
	Defense response								
	Ubiquitin-dependent proteolysis								
1393	proteasome subunit alpha type-2-B	MDP0000143951	230	5	0.020	1.1	ns	1.2	0.05
	Oxylipin biosynthesis								
218	linoleate 13s-lipoxygenase 2- chloroplastic	MDP0000753547	193	8	3.4^{E}-5	1.3	0.01	1.3	0.01
224	linoleate 13s-lipoxygenase 2- chloroplastic	MDP0000753547	227	7	1.6^{E}-3			1.3	0.05
229	linoleate 13s-lipoxygenase 2- chloroplastic	MDP0000753547	82	7	6.1^{E}-3	1.5	0.01	1.5	0.05
230	linoleate 13s-lipoxygenase 2- chloroplastic	MDP0000281525	177	7	9.9^{E}-4	1.5	0.01	1.6	0.01
	Stress response								
	Ubiquitin-dependent proteolysis								
1150	26S proteasome non-ATPase regulatory subunit 14	MDP0000138737	616	12	0.011	1.3	0.05	1.1	ns
1518	proteasome subunit beta type	MDP0000137279	848	15	7.5^{E}-3	1.2	0.05	1.1	ns
	Translational elongation								
205	elongation factor ef-2	MDP0000777793	450	17	0.010	1.1	ns	1.3	0.01
208	elongation factor ef-2	MDP0000777793	515	17	6.1^{E}-4	1.1	0.01	1.1	0.01
792	elongation factor 1-gamma	MDP0000315108	283	7	0.017	1.2	0.05	1.2	0.05
	Energy and carbohydrate metabolism								
	Glycolysis and gluconeogenesis								
472	apple phosphoglyceromutase (apgm)	MDP0000240039	497	16	0.020	1.3	0.05	1.1	ns
506	phosphofructokinase	MDP0000293776	124	6	5.9^{E}-3	1.4	0.05	1.1	ns
989	phosphoglycerate kinase	MDP0000784808	1490	20	0.011	1.3	0.05	1.1	ns
499	pyruvate decarboxylase	MDP0000223243	549	11	0.016	1.4	0.05	1.1	ns
1081	fructose-bisphosphate aldolase	MDP0000273688	554	10	0.016	1.2	ns	1.3	0.05

Table 6.1 - *continued*

Spot[a]	Protein name[b]	Accession No.[c]	Score[d]	PM[e]	q[f]	Al-I > Al-M		Al-I > I	
						Ratio[g]	α[h]	Ratio[g]	α[h]
1091	fructose-bisphosphate aldolase	MDP0000151849	206	8	0.014	1.0	ns	1.2	0.05
	TCA cycle; oxidative phosphorylation								
436	succinate dehydrogenase	MDP0000188391	324	8	6.5^{E}-3	1.3	0.01	1.0	ns
	Pentose-phosphate pathway								
728	6-phosphogluconate dehydrogenase	MDP0000191398	480	13	0.030	1.1	ns	1.2	0.05
	Calvin cycle								
1430	RuBisCO small subunit	MDP0000731480	129	6	4.0^{E}-5	1.1	ns	1.2	0.05
	Photosynthesis								
1344	light-harvesting complex II protein Lhcb1	MDP0000417927	464	7	6.9^{E}-3	1.0	ns	1.2	0.05
	Translation								
	aminoacyl-tRNA biosynthesis								
605	prolyl-tRNA synthetase	MDP0000291077	164	13	5.2^{E}-3	1.1	0.05	1.2	0.01
	Transcription								
	Posttranscriptional control								
767	rna-binding post-transcriptional regulator csx1-like	MDP0000614064	944	10	0.023	1.2	0.05	1.1	ns
	Protein fate								
	Protein folding								
504	TCP (T-complex protein) domain class transcription factor alpha-like subunit	MDP0000036030	219	7	0.026	1.3	0.05	1.1	ns
550	TCP domain class transcription factor eta-like subunit	MDP0000534977	551	15	7.4^{E}-3	1.1	ns	1.3	0.05
	Nucleotide/nucleoside metabolism								
	Pyrimidine ribonucleotide biosynthesis								
722	uridine 5'-monophosphate synthase	MDP0000335264	62	1	2.4^{E}-4	1.1	0.05	1.2	0.01
	Lipid metabolism								
	Phospholipid catabolism								

Table 6.1 - *continued*

Spot[a]	Protein name[b]	Accession No.[c]	Score[d]	PM[e]	q[f]	Al-I > Al-M		Al-I > I	
						Ratio[g]	α[h]	Ratio[g]	α[h]
255	phospholipase D alpha	MDP0000300217	118	7	3.8^{E}-4	1.2	0.05	1.1	0.05
	Metabolism of vitamins and cofactors								
	Vitamin B6 metabolism								
1099	auxin-induced protein PCNT115-like isoform 1	MDP0000228499	1410	19	0.014	1.2	0.05	1.1	ns
	Porphyrin and chlorophyll metabolism								
997	uroporphyrinogen decarboxylase (UROD)	MDP0000364293	117	5	5.6^{E}-4	1.3	0.01	1.0	ns
	Cellular Organization								
	Morphogenesis								
453	Nucleosome/chromatin assembly factor group	MDP0000251796	197	5	0.019	1.2	0.05	1.1	ns
	Unknown								
1137	EF-hand (motif containing) (calcium binding) protein	MDP0000120294	288	5	0.014	1.2	0.05	1.2	ns

[a] Corresponding spot number in the gel image in Fig. 5.1

[b] Proteins have been grouped according to the Gene Ontology biological process wherein they are involved

[c] MDP number of predicted apple gene (Velasco *et al*., 2010) (Gene and protein sequences can be obtained from Genome Database for Rosaceae (GDR): http://www.rosaceae.org)

[d] MOWSE score probability (protein score) for the entire protein

[e] Number of matched peptides of peptide mass fingerprinting combined with MS/MS

[f] Overall false discovery rate (FDR) corrected p-value, according to a one-way ANOVA, using the DeCyder 6.5 software

[g] Ratio of the average standardized protein abundance in the Aliette®-treated *Venturia inaequalis* inoculated 'Topaz' leaves (Al-I) to the average standardized protein abundance in the Aliette®-treated mock-inoculated (Al-M) and non-treated V. inaequalis inoculated (I) 'Topaz' leaves respectively, calculated with the DeCyder 6.5 software

[h] Comparison of the ^{10}log standardized protein abundances in the Aliette®-treated *Venturia inaequalis* inoculated (Al-I) and Aliette®-treated mock-inoculated (Al-M) or non-treated *V. inaequalis* inoculated (I) 'Topaz' leaves respectively, with significance levels α according to a false discovery rate (FDR) corrected one-way ANOVA, using the DeCyder 6.5 software; ns: not significant

Table 6.2. List of *V. inaequalis* inoculation down-regulated proteins in Aliette®-treated leaves ('Al-I < Al-M') and Aliette®-treatment induced down-regulated proteins in *V. inaequalis* inoculated leaves ('Al-I < I') of 'Topaz' (monogenic *Rvi*6-resistant cultivar) at 5 dpi.

						Al-I < Al-M		Al-I < I	
Spot[a]	**Protein name**[b]	**Accession No.**[c]	**Score**[d]	**PM**[e]	**q**[f]	**Ratio**[g]	**α**[h]	**Ratio**[g]	**α**[h]
	Energy and carbohydrate metabolism								
	Gluconeogenesis								
1084	fructose-1,6-bisphosphatase, cytosolic	MDP0000251810	889	15	0.017	1.4	0.05	1.1	ns
	Glycolysis and gluconeogenesis; Calvin cycle								
934	glyceraldehyde-3-phosphate dehydrogenase	MDP0000835914	826	11	0.011	1.5	0.05	1.4	0.5
990	glyceraldehyde-3-phosphate dehydrogenase	MDP0000527995	593	9	0.022	1.3	ns[i]	1.4	0.5
1007	glyceraldehyde-3-phosphate dehydrogenase	MDP0000527995	1280	13	0.016	1.4	0.05	1.1	ns
1380	triosephosphate isomerase	MDP0000193489	288	6	0.019	1.2	0.05	1.2	ns
948	phosphoglycerate kinase	MDP0000325411	1250	16	6.3^{E}-3	1.4	0.05	1.1	ns
	Calvin cycle; defense response								
984	phosphoribulokinase (putative; chloroplastic-like)	MDP0000148186	735	16	0.021	1.4	0.05	1.1	ns
1000	phosphoribulokinase (putative; chloroplastic-like)	MDP0000148186	788	13	0.021	1.3	0.05	1.2	ns
	Calvin cycle								
825	RuBisCO activase	MDP0000944409	1010	14	0.014	1.5	0.05	1.1	ns
945	RuBisCO activase	MDP0000944409	716	11	0.023	1.5	0.05	1.1	ns
935	RuBisCO activase	MDP0000944409	430	9	0.019	1.6	0.05	1.5	ns
359	transketolase	MDP0000142098	492	11	0.022	1.2	0.05	1.0	ns
	Photosynthesis								
1303	light-harvesting complex II protein Lhcb1	MDP0000417927	427	6	7.9^{E}-3	1.2	ns	1.4	0.05
1399	light-harvesting complex II protein Lhcb1	MDP0000417927	514	7	4.2^{E}-3	1.3	0.05	1.4	0.01
1512	light-harvesting complex I protein Lhca1	MDP0000222941	252	4	2.4^{E}-3	1.1	ns	1.2	0.05
1042	photosystem II stability/assembly factor HCF136	MDP0000826603	1290	18	0.022	1.2	0.05	1.1	ns
1221	Oxygen-evolving enhancer protein 1, chloroplastic	MDP0000248920	834	14	5.6^{E}-3	1.4	0.01	1.3	0.05

Table 6.2 - *continued*

Spot[a]	Protein name[b]	Accession No.[c]	Score[d]	PM[e]	q[f]	Al-I < Al-M		Al-I < I	
						Ratio[g]	α[h]	Ratio[g]	α[h]
1465	chlorophyll A/B binding protein	MDP0000866655	438	9	0.014	1.3	0.05	1.3	ns
417	ATP-dependent zinc metalloprotease FtsH, chloroplastic	MDP0000289110	73	7	6.8^{E}-3	1.2	0.05	1.2	0.01
418	ATP-dependent zinc metalloprotease FtsH, chloroplastic	MDP0000289110	570	16	0.012	1.3	0.05	1.3	0.05
652	chloroplast ATP synthase beta subunit	MDP0000928146	139	2	0.014	1.4	0.05	1.3	0.05
1536	chloroplast ATP synthase delta subunit	MDP0000750535	912	12	0.020	1.3	0.05	1.2	ns
	Transport facilitation								
	Plasmamembrane proton transport								
586	V-type (vacuolar) proton ATPase subunit B	MDP0000945182	545	10	6.2^{E}-3	1.2	0.05	1.2	0.05
	Translation								
	Translational elongation								
279	elongation factor G (EF-G)	MDP0000138993	909	23	0.022	1.2	0.05	1.2	ns
888	elongation factor Tu (EF-Tu)	MDP0000184653	1070	11	0.017	1.2	0.05	1.2	ns
	Transcription								
	Spliceosome								
1174	arginine/serine-rich splicing factor	MDP0000387508	463	14	0.025	1.5	0.05	1.4	ns
	Cellular organization								
	Organization of the cytoskeleton								
864	actin	MDP0000183660	123	4	7.3^{E}-3	1.4	0.05	1.2	ns
	Amino acid metabolism								
	degradation of glycine								
186	glycine dehydrogenase (decarboxylating)	MDP0000588069	437	12	0.023	1.4	0.05	1.3	ns
	Regulation of protein activity								
	Protease inhibitor								
980	Serpin-ZX-like protein	MDP0000751972	131	7	1.0^{E}-3	1.3	ns[i]	1.3	0.05
	Cellular Organization								

Table 6.2 - *continued*

Spot[a]	Protein name[b]	Accession No.[c]	Score[d]	PM[e]	q[f]	Al-I < Al-M		Al-I < I	
						Ratio[g]	α[h]	Ratio[g]	α[h]
	Cellular cell wall organization								
1025	Alpha-1,4-glucan-protein synthase (UDP-forming)	MDP0000232047	83	4	6.9^{E}-4	1.0	ns	1.2	0.01
	Unknown								
1165	(putative) RNA binding protein	MDP0000264307	849	16	0.012	1.4	0.05	1.2	ns
1299	(predicted protein) cbbY	MDP0000152304	83	5	6.9^{E}-3	1.3	0.05	1.1	ns
1440	uncharacterized protein	MDP0000178270	480	10	0.028	1.1	ns	1.2	0.05

[a] Corresponding spot number in the gel image in Fig. 5.1

[b] Proteins have been grouped according to the Gene Ontology biological process wherein they are involved

[c] MDP number of predicted apple gene (Velasco *et al*., 2010) (Gene and protein sequences can be obtained from Genome Database for Rosaceae (GDR): http://www.rosaceae.org)

[d] MOWSE score probability (protein score) for the entire protein

[e] Number of matched peptides of peptide mass fingerprinting combined with MS/MS

[f] Overall false discovery rate (FDR) corrected p-value, according to a one-way ANOVA, using the DeCyder 6.5 software

[g] Ratio of the average standardized protein abundance in the Aliette®-treated mock-inoculated (Al-M) or non-treated *Venturia inaequalis* inoculated (I) 'Topaz' leaves to the average standardized protein abundance in the Aliette®-treated *V. inaequalis* inoculated 'Topaz' leaves (Al-I), calculated with the DeCyder 6.5 software

[h] Comparison of the ^{10}log standardized protein abundances in the Aliette®-treated *V. inaequalis* inoculated (Al-I) and Aliette®-treated mock-inoculated (Al-M) or non-treated *V. inaequalis* inoculated (I) 'Topaz' leaves, with significance levels α according to a false discovery rate (FDR) corrected one-way ANOVA, using the DeCyder 6.5 software; ns: not significant

[i] The difference would be statistically significant if the outlier (one of the three replicates) is left out

Up-regulated proteins upon infection ('Al-I > Al-M')

Of the 29 up-regulated spots, 22 were positively identified by MALDI-TOF/TOF according to the methods elaborated in Section 3.7.7, resulting in 19 individual protein identifications (Table 6.1).

According to their GOs, six of these 19 up-regulated proteins are involved in 'stress response' (Blast2GO). The infection-induced up-regulation of a linoleate 13S-lipoxygenase (spots 218, 229 and 230) was also observed in the non-Aliette®-treated 'Topaz' leaves ('I > C') in the previous Chapter (see Sections 5.3.2.1 and 5.3.2.2 and Table 5.1), although it was another isoform (spot 224). Also the translation elongation factors ef-1-gamma (spot 792) and ef-2 (spot 208) were two of the six proteins that were exclusively up-regulated in the non-Aliette®-treated *V. inaequalis* inoculated leaves compared to the mock-inoculated leaves (although differences were not statistically significant) and did not show a difference in accumulation (not even a tendency) between the mock-infection and control conditions (see Section 5.3.2.4). Both translation elongation factors were significantly up-regulated in the scab-inoculated Aliette®-treated 'Topaz' leaves ('Al-I > Al-M'; Table 6.1). The third up-regulated protein related to protein translation was this time not the glycyl-tRNA synthetase ('I > C'), but the prolyl-tRNA synthetase (spot 605), that also participates in aminoacyl-tRNA biosynthesis. Two other stress response related up-regulated proteins were the '26S proteasome non-ATPase regulatory subunit 14' (spot 1150) and a 'proteasome subunit beta type' (spot 1518). Both proteasome subunits are involved in ubiquitin-dependent proteolysis, that is suggested to play an important role in resistance (R)-gene-mediated plant disease resistance in general (Devoto *et al*. 2003; Lopez *et al*. 2005) and in the regulation of the *Rvi6*-mediated resistance to *V. inaequalis* in particular (Paris *et al.*, 2009). Another proteasome subunit was one of the 6 proteins that were exclusively up-regulated in the non-Aliette®-treated 'Topaz' leaves upon inoculation with *V. inaequalis* (see Section 5.3.2.4).

The sixth stress response related protein that was found to be up-regulated in the inoculated Aliette®-treated leaves ('Al-I > Al-M'), was the apple phosphoglyceromutase (APGM; spot 472; EC 5.4.2.1). Together with the other up-regulated enzymes phosphofructokinase (spot 506; EC 2.7.1.11), phosphoglycerate kinase (spot 989; EC 2.7.2.3) and pyruvate decarboxylase (spot 499; EC 4.1.1.1), APGM participates in glycolysis (see Fig. 5.6 p. 104). Phosphofructokinase and pyruvate decarboxylase were also found to be up-regulated upon

infection in the non-Aliette®-treated 'Topaz' leaves ('I > C'), just like the succinate dehydrogenase (that participates in the TCA cycle and in oxidative phosphorylation; spot 436), the TCP domain class transcription factor (that is involved in protein folding; spot 504), the auxin-induced protein PCNT115-like isoform 1 (involved in vitamin B6 metabolism; spot 1099), uroporphyrinogen decarboxylase (UROD; involved in porphyrin metabolism; spot 997), 'nucleosome/chromatin assembly factor group' (involved in cellular morphogenesis; spot 453) and the 'EF-hand (motif containing) (calcium binding) protein' (spot 1137; biological process unknown) (see Section 5.3.2, Table 5.1 and Fig. 5.4; Table 6.1). In total, 9 of the 19 up-regulated proteins upon infection in the Aliette®-treated 'Topaz' leaves ('Al-I' > 'Al-M') were the same as in the non-Aliette®-treated leaves ('I' > 'C') (Fig. 6.7). In the Aliette®-treated leaves, enzymes involved in nucleotide biosynthesis seemed to be up-regulated as well upon infection, since the uridine 5'-monophosphate synthase (spot 722) was found to be accumulated more in the scab-infected leaves than in the mock-infected leaves (Table 6.1).

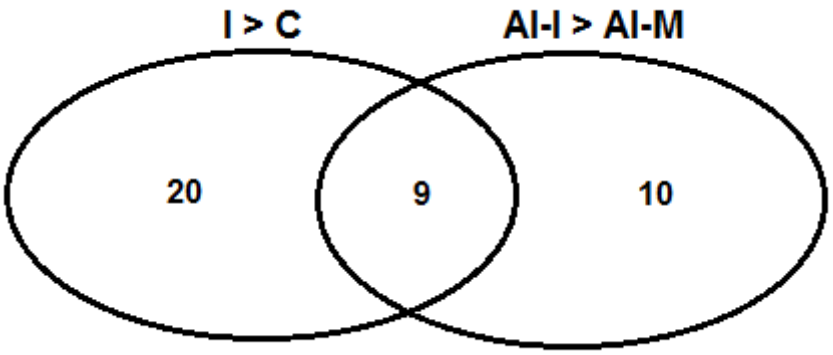

Fig. 6.7. Venn diagram illustrating the number of individual identified proteins that are up-regulated both in Aliette®-treated infected (Al-I) and non-treated infected (I) 'Topaz' leaves (intersection), compared to mock control (Al-M) and control (C) respectively.

In summary, the same kind of proteins were found to be up-regulated upon infection both in the Aliette®-treated 'Topaz' leaves ('Al-I > Al-M; this Section) and in the Aliette®-non-treated leaves ('I > C'; Section 5.3.1). Next to proteins known to be involved in stress responses, these were mainly enzymes involved in catabolism. Besides glycolysis and the TCA cycle, these catabolic processes also included ubiquitin-dependent proteolysis (proteasome subunits) and lipid catabolism (lipoxygenase and phospholipase D). Enzymes involved in the anabolic nucleotide biosynthesis, on the other hand, seemed to be up-regulated as well.

Down-regulated proteins upon infection ('Al-I < Al-M')

Of the 42 infection-induced down-regulated spots in the Aliette®-treated leaves, 32 were identified, resulting in 23 individual protein identifications (Table 6.2).

Of these 23 down-regulated proteins, 13 are involved in carbon fixation, of which 7 participate in the light-dependent reactions of photosynthesis and 6 in the so-called dark reactions of the Calvin cycle. Among these 7 photosynthetic proteins were two chloroplast ATP synthase subunits: not only the beta subunit (spot 652; *cf.* 'I < C' in Table 5.2) but also the delta subunit (spot 1536). Four of the 5 other photosynthetic proteins and a third ATP synthase subunit, a 'V-type (vacuolar) proton ATPase beta subunit' (spot 586), were also found to be down-regulated upon infection in non-Aliette®-treated leaves ('I < C' in Table 5.2; Table 6.2). In total, 11 of the 23 down-regulated proteins upon infection in the Aliette®-treated 'Topaz' leaves ('Al-I < Al-M') were the same as in the non-Aliette®-treated leaves (I < C') (Fig. 6.8).

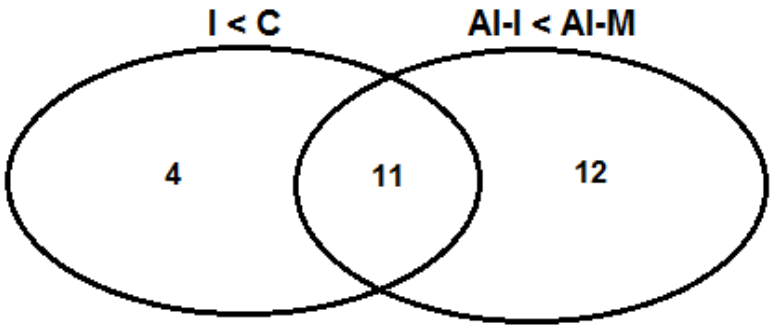

Fig. 6.8. Venn diagram illustrating the number of individual identified proteins that are down-regulated both in Aliette®-treated infected (Al-I) and non-treated infected (I) 'Topaz' leaves (intersection), compared to mock control (Al-M) and control (C) respectively.

Two of the 6 enzymes involved in the Calvin cycle were also found to be significantly down-regulated upon infection in non-Aliette®-treated leaves (Table 6.2). It concerned the phosphoribulokinase (spots 984 and 1000) and glyceraldehyde-3-phosphate dehydrogenase, the last one again with three different spots/isoforms (spots 934, 990 and 1007). The other 4 down-regulated enzymes of the Calvin cycle were the RuBisCO activase (with the three spots 825, 935 and 945), transketolase (spot 359), triosephosphate isomerase (spot 1380) and phosphoglycerate kinase (spot 948). The glyceraldehyde-3-phosphate dehydrogenase, the triosephosphate isomerase and the phosphoglycerate kinase can also play a role in

gluconeogenesis, just like the down-regulated cytosolic fructose-1,6-bisphosphatase (spot 1084). Fructose-1,6-bisphosphatase (EC 3.1.3.11) can only catalyze the reaction in the direction of gluconeogenesis, not in the direction of glycolysis (see also Section 5.3.2.3 and Fig. 5.6 p.104).

Interestingly, just like with the fructose-bisphosphate aldolase in the non-Aliette®-treated leaves (see Section 5.3.2.3), the phosphoglycerate kinase (PGK) was found to be both up-regulated (spot 989; see above) and down-regulated (spot 948) in the Aliette®-treated 'Topaz' leaves upon infection (Tables 6.1 and 6.2). Again, the two isoforms are a cytosolic one and a plastidic one, involved in glycolysis and Calvin cycle, respectively. These differentially localized PGK isoforms have been biochemically characterized and demonstrated to show differences in expression profiles in *Helianthus annuus* (sunflower) (Troncoso-Ponce *et al*., 2012). Just like fructose-bisphosphate aldolase, phosphoglycerate kinase was recently found to be regulated by abiotic stresses such as nutritional, salt and heat stress in plants (e.g. tomato leaves) and other organisms (Zhou *et al*., 2011a and b; Calcedo *et al*., 2012).

Similarly, it is remarkable that the down-regulated triosephosphate isomerase (spot 1380) is especially known to play an important role in glycolysis and is in that respect essential for efficient energy production. Its deficiency has been shown to be the most severe disorder of glycolysis (Mande *et al*., 1994), and in rice roots exposed to salt-stress, triosephosphate isomerase has been reported to be up-regulated, not down-regulated (Yan *et al*., 2005). However, Blast2GO analysis showed that spot 1380 was the plastidic isoform involved in the Calvin cycle, and not a cytosolic one involved in glycolysis.

Finally, as with the up-regulated proteins upon infection, there were also two down-regulated translation elongation factors in the Aliette® treated leaves, although other ones: elongation factor G (ef-G; spot 279) and elongation factor Tu (ef-Tu; spot 888) (Table 6.2). Down-regulation of ef-Tu in response to fungal attack has been reported previously in *Mentha* leaves (Sinha and Chattopadhyay, 2011). Combined, these changes in accumulation of translation elongation factors indicate the alteration in the proteome upon infection. The arginine/serine-rich splicing factor (spot 1174), that plays a role in nuclear mRNA splicing, was found to be down-regulated both in the Aliette®-treated and non-treated 'Topaz' leaves upon infection (Tables 5.2 and 6.2). This could also be part of the explanation for the

different isoforms observed in the lists of up- and down-regulated proteins. In general, transcriptional re-programming is known to be a key step in a plant's response to pathogen recognition (Zhang and Wang, 2005).

In summary, as with the up-regulated proteins upon infection, proteins with similar functions were found to be down-regulated upon infection in the Aliette®-treated 'Topaz' leaves ('Al-I < Al-M'; this section) as in the non-treated leaves ('I < C'; see Section 5.3.2.3) (Fig. 6.8). Most of the down-regulated enzymes are involved in the anabolic carbon fixation (both photosynthesis and Calvin cycle) and gluconeogenesis pathways, and some proteins participate in translation or transcription.

The differences in protein accumulation upon infection of the Aliette®-treated 'Topaz' leaves ('Al-I <> Al-M') discussed in this section were all statistically significant. They confirm our hypotheses regarding infection-induced up- and down-regulated pathways of previous chapter that was based on a comparison of the inoculation and control conditions ('I <> C'). The reproducibility and the quality of the 2-DE gels was better in the 2D-DIGE experiment of current chapter. There was less variation in accumulation between the three biological replicates in the different conditions, which lead to a higher amount of proteins that were significantly differentially accumulated.

6.3.3.2. Aliette® stimulates apple response to scab infection

In a next stage, the 2D-DIGE protein profiles of the Aliette®-treated *V. inaequalis* inoculated 'Topaz' leaves and the non-treated inoculated leaves were compared at 5 dpi ('Al-I <> I'; see Section 6.2). This way, we wished to investigate how Aliette® causes the observed reduction in degree of infection (see Sections 6.3.1 and 6.3.2). We wanted to determine at protein level how fosetyl-Al influences the response of 'Topaz' to *V. inaequalis* infection.

We detected 59 spots with significantly different accumulation levels ($q \leq 0.05$), of which 34 were up-regulated in the Aliette®-treated inoculated leaves and 25 down-regulated. Given the high reproducibility and the high quality of the gels, differences in standardized protein abundance down to a ratio of 1.1 could be detected (Tables 6.1 and 6.2).

Aliette®-treatment induced up-regulated proteins in V. inaequalis *inoculated 'Topaz' leaves ('Al-I > I')*

Of the 34 up-regulated spots, 17 were positively identified, resulting in 12 individual protein identifications (Table 6.3). Most of the other 17 spots were too low-abundant for positive MS/MS identification.

Of these 12 identified proteins , 4 are known to be involved in stress responses (Table 6.1). The proteasome subunit alpha type-2-B (spot 1393), that participates in ubiquitin-dependent proteolysis, had already been found to be up-regulated as part of the defense response against bacteria (Blast2GO). The enzyme can also function as a translation initiation factor. The translation elongation factors ef-1-gamma (spot 792) and ef-2 (spots 205 and 208) were also found to be up-regulated in Aliette®-treated 'Topaz' leaves upon infection ('Al-I > Al-M'; see Section 6.3.3.1 and Table 6.1). A fourth protein related to translation that was up-regulated upon infection in Aliette®-treated leaves ('Al-I > Al-M'), the prolyl-tRNA synthetase (spot 605), was also accumulated more compared to the non-treated infected leaves ('Al-I > I'). This applies also for the uridine 5'-monophosphate synthase (involved in nucleotide biosynthesis; spot 722) and the TCP domain class transcription factor (involved in protein folding), although for the latter it was an eta-like subunit of the t-complex protein 1 (spot 550) this time instead of the alpha-like subunit (spot 504). The two enzymes involved in lipid catabolism, the lipoxygenase (spots 218, 224, 229 and 230) and the phospholipase D (alpha subunit; spot 255), were found to be more abundant in the Aliette®-treated infected 'Topaz' leaves ('Al-I > I') as well. The biological role of lipoxygenases and their involvement in resistance to microbial pathogens was already discussed in Section 5.3.2.2. Expression of different lipoxygenase isoforms was also induced in wheat upon treatment with elicitors such as chitin oligosaccharides, chitosan, methyl jasmonate, and a glycopeptide elicitor prepared from germ tubes of the rust fungus *Puccinia graminis* (Bohland *et al*., 1997).

Once more, lipid catabolism and ubiquitin-dependent proteolysis were not the only catabolic processes of which proteins were up-regulated. The fructose-bisphosphate aldolase (spot 1078) and the 6-phosphogluconate dehydrogenase (spot 728) were already found to be up-regulated in the non-Aliette®-treated 'Topaz' leaves upon infection ('I > C'; see Table 5.1 p.94-96) and appeared to be accumulated even more in the Aliette®-treated inoculated leaves ('Al-I > I'; Table 6.1). The fructose-bisphosphate aldolase (EC 4.1.2.13) participates in

glycolysis (see Fig. 5.6 p. 104), but can also play a role in the pentose phosphate pathway. The role of the 6-phosphogluconate dehydrogenase (spot 728) in the latter NADPH generating pathway was already described in section 5.3.2.3.

In summary, Aliette® seemed to increase the accumulation of proteins that were already found to be up-regulated upon *V. inaequalis* infection of 'Topaz' leaves (Fig. 6.9). These proteins are mainly involved in stress responses and/or catabolic processes. Only 2 proteins were not found to be up-regulated upon infection in Aliette®-treated or non-treated leaves (Fig. 6.9: 'Al-I > I' exclusively). Remarkably, these 2 proteins, the RuBisCO small subunit (spot 1430) and the light-harvesting complex II protein Lhcb1 (spot 1344), are involved in carbon fixation. However, two other isoforms of Lhcb1 (spots 1303 and 1399) were down-regulated (see Table 6.2).

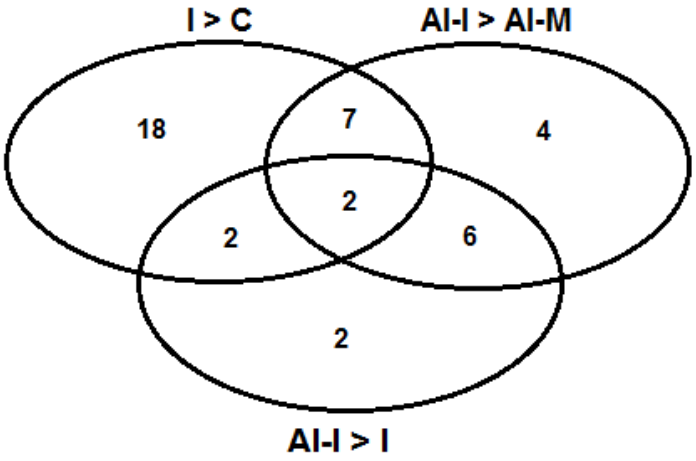

Fig. 6.9. Venn diagram illustrating the numbers of identified proteins that are up-regulated in Aliette®-treated 'Topaz' leaves upon infection (Al-I > Al-M) and/or in non-treated leaves upon infection (I > C) and/or in infected leaves induced by Aliette®-treatment (Al-I > I).

Aliette®-treatment induced down-regulated proteins in V. inaequalis *inoculated Topaz leaves ('Al-I < I')*

Of the 25 down-regulated spots, 13 were identified, resulting in 10 individual protein identifications (Table 6.2).

Lhcb1 was not the only down-regulated protein ('Al-I < I') involved in photosynthesis (*cf*. *supra*). In total, 6 of the 10 down-regulated proteins participate in carbon fixation, of which 5 in photosynthesis and 1 in the Calvin cycle (Table 6.2). Four of the 5 proteins involved in photosynthesis were also found to be down-regulated upon infection in the Aliette®-treated

leaves ('Al-I < Al-M'; see Section 6.3.3.1) and three of them also in the non-Aliette®-treated leaves ('I < C'; see Section 5.3.2.3 and Table 5.2). Both Lhca1 and Lhcb1 were also found to accumulate less in 'Topaz' leaves compared to 'Golden Delicious' exclusively after infection ('Top-I < Gol-I'; see Table 5.6 and Section 5.3.2.3). The glyceraldehyde-3-phosphate dehydrogenase (spots 934 and 990; EC 1.2.1.12) cannot only participate in the Calvin cycle, but also in gluconeogenesis (and glycolysis; see Fig. 5.6 p.104). Several isoforms (spots 934, 990 and 1007) were already found to be down-regulated upon infection in both Aliette®-treated ('Al-I < 'Al-M') and non-treated ('I < C') 'Topaz' leaves. Also the 'V-type (vacuolar) proton ATPase beta subunit' (spot 586), the Serpin-ZX-like protein (spot 980) and the uncharacterized protein of spot 1440 were already found to be down-regulated upon infection in Aliette®-treated and/or non-treated 'Topaz' leaves. In summary, this statement applies for 8 of the 10 proteins that were down-regulated in the Aliette®-treated inoculated 'Topaz' leaves compared to the non-treated inoculated leaves (Fig. 6.10). Thus, Aliette® treatment seemed to additionally reduce the accumulation of proteins that were already found to be down-regulated upon *V. inaequalis* infection of 'Topaz' leaves, i.e. mainly proteins involved in carbon fixation.

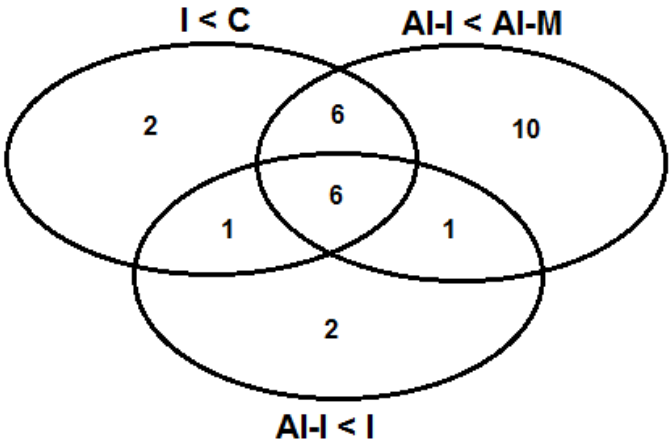

Fig. 6.10. Venn diagram illustrating the numbers of identified proteins that are down-regulated in Aliette®-treated 'Topaz' leaves upon infection (Al-I < Al-M) and/or in non-treated leaves upon infection (I < C) and/or in infected leaves induced by Aliette®-treatment (Al-I < I).

6.4. Concluding remarks

When the systemic fungicide Aliette® was applied prior to inoculation with a conidial solution of the ascomycete *V. inaequalis*, we could observe a small but not significant reduction in foliar disease symptoms (see Section 6.3.1) and in hyphal growth as measured by real-time PCR (see Section 6.3.2) at 18 dpi. The effect of Aliette® was more significant using the real-time PCR technique as compared to the phenotypic disease rating score.

The reason why the observed effect of Aliette® was quite small could be a suboptimal timing of application of the fungicide. It was originally generally accepted that one should apply the systemic fungicide at least three days prior to inoculation (De Maeyer – personal communication). Indeed, the active ingredient fosetyl-Al needs time to dissociate into ethyl phosphonate and $Al(OH)_3$ and only after take-up by the plant, ethyl phosphonate will become converted to phosphorous acid and EtOH. Both ethyl phosphonate and phosphorous acid are known to contribute to the signals leading to the stimulation and/or enhancement of plant defense systems (Guest *et al*., 1988; Saindrenan *et al*., 1988). Therefore, we applied Aliette® 11 and 4 days prior to inoculation. However, recent experiments on apple done by De Maeyer and Dr. Marie-Pascale Latorse from Bayer CropScience demonstrated that a later application of Aliette®, just before inoculation, increased its effect (De Maeyer - personal communication). Moreover, the original application guidelines were formulated for field experiments where the temperature is usually lower than in our greenhouse experiments. The higher temperature could speed up the dissociation of fosetyl-Al into its active components.

Nevertheless, by means of real-time PCR we could already observe an Aliette®-induced reduction in degree of infection, that was notably more distinct in the monogenic *Rvi*6-resistant cultivar ‘Topaz’ (reduction of *circa* 60 %) than in the scab-susceptible cv. ‘Golden Delicious’ (*circa* 15 %) (Fig. 6.6). This suggests that it is better to combine the use of (monogenic) resistance sources with the application of systemic fungicides such as Aliette® to obtain a stronger and possibly more durable resistance. However, we should note that the observed limited effect of Aliette® application on infection of the ‘Golden Delicious’ plants at 18 dpi (Fig. 6.6b) could (partly) be due to a saturation effect, since at 18 dpi the ‘Golden Delicious’ plants show already extensive sporulation symptoms (Fig. 6.2c). We should verify this hypothesis in future studies by studying the effect of Aliette® on hyphal

growth at earlier time-points after inoculation (e.g. 5 dpi) and/or lower the infection pressure by decreasing the spore concentration of the conidial suspension (that was now set on the standard 2 x 10^5 spores ml^{-1}).

When we analyzed the 2-DE protein profiles of Aliette®-treated 'Topaz' leaves, we could verify that Aliette® acts by additionally stimulating a response upon scab infection similar to the one that was already observed in the non-treated 'Topaz' leaves of Chapter 5 (i.e. same/similar proteins involved). First, comparison of the Aliette®-treated *V. inaequalis* inoculated 'Topaz' leaves with the Aliette®-treated mock-inoculated leaves ('Al-I <> Al-M') confirmed our hypotheses of the previous chapter regarding the scab infection induced stress response. So treatment with fosetyl-Al doesn't seem to alter the nature of the response. The majority of proteins that was up-regulated was still known to be involved in stress responses and/or catabolic processes such as glycolysis, TCA cycle, ubiquitin-dependent proteolysis and lipid catabolism. On the other hand, infection induced down-regulated proteins were still mainly involved in the light-dependent (photosynthesis) and light-independent (Calvin cycle) reactions of carbon fixation. However, Aliette® treatment did seem to stimulate the intensity of this response, since treated scab-inoculated 'Topaz' leaves showed an increase and reduction of accumulation of proteins ('Al-I <> I') that were already found to be up- and down-regulated respectively upon infection in non-treated leaves ('I <> C'). In summary, the energy and carbohydrate metabolism of young apple leaves was altered upon mock-infection in the monogenic resistant cv. 'Topaz', even more upon *V. inaequalis* infection (see Chapter 5), and preventative treatment with the systemic elicitor Aliette® (fosetyl-Al) additionally stimulated the response of this cultivar to infection.

In order to determine whether the effect of fosetyl-Al is a direct defense inducing effect (already in absence of *V. inaequalis*) or a 'priming' effect, we should additionally compare Aliette®-treated and non-treated mock-inoculated plants ('Al-M <> M') and Aliette®-treated and non-treated control plants ('Al-C <> C').

Chapter 7

General conclusions and future perspectives

This work aimed at further unraveling the response of apple (*Malus* x *domestica*) to infection by its most important pathogen, *Venturia inaequalis*. Up till now, most major commercial apple cultivars are highly susceptible to this disease. Given the general desire to limit the extensive fungicide applications, most Western breeding programs view the selection of disease-resistant cultivars as a priority (Gessler and Pertot, 2012). Monogenic resistance sources used so far have been overcome by the pathogen, and for the development of new, durable resistant cultivars, a better insight into the resistance mechanisms is needed.

Since the resistance mechanisms of action – even of the most widely applied *Rvi*6 (*Vf*) resistance – were still largely unknown, a high-throughput global analysis method was required. Using targeted approaches, focusing only on known resistance/defense genes, would have hold the risk of missing other important features that might contribute to resistance. We chose to use the two-dimensional gel electrophoresis (2-DE) method, that allows high-throughput analysis at the protein level (O'Farrell, 1975). The identification of proteins involved in the response of a scab-resistant cultivar to *V. inaequalis* inoculation should reveal possible targets for use as markers in resistance breeding and thus contribute to the development of durable resistance.

Studying the proteome holds some benefits over studying the transcriptome (e.g. by means of microarrays) (see Section 2.5.1). However, like every other technology, 2-DE also has its disadvantages. By analysing the proteome via 2-DE, we investigated only a fraction of the proteome. Every gel-based proteomics technique is limited by the pH range of the used IPG strips and the MW range of the acrylamide gels. Moreover, the method is not ideally suited to study low abundant proteins and membrane proteins (Thelen, 2007). Therefore, crucial choices must be made prior to analysis depending on the primary goal of the research. Since

a literature study verified that most of the proteins known to be involved in plant-pathogen interactions have a theoretical pI in the range of 4-7, and optimization experiments confirmed that most apple leaf proteins lie within this region, we chose to use the narrow range pH 4-7 IPG strips instead of the broad range pH 3-10 strips. By using strips of the maximum length of 24 cm, the resolution was improved even more. One could opt to use a series of overlapping 'ultrazoom' IPG strips with a very narrow range (Hoving *et al*., 2000), but that would result in a much higher cost, that must be evaluated against the expected gain in resolution and extra information that can be obtained. Indeed, the choice for the 'best' option is often not only based on scientific arguments, but also has to take the cost into account and a careful balance is required. 2-DE, and in particular the 2D-DIGE technology used in this research, is a rather expensive technique anyhow. For this reason, we also chose to visualize the proteins in the first experiments (e.g. the comparison of the control conditions of 'Topaz' and 'Golden Delicious') via colloidal Coomassie Brilliant Blue (CBB) G-250 staining instead of CyDye^{TM} labeling. If the proteins of interest are low abundant, prefractionation techniques, such as organelle isolation and prefractionation according to the pI of the proteins (Sahab *et al*., 2005), could be applied in order to increase the amount of visible spots without overloading the gels (Righetti *et al*., 2005). Since it was our aim to get a first, global view on the resistance mechanisms of apple against *V. inaequalis*, no specific sample preparation methods, prefractionation techniques or high resolution gels were used. This can probably account for the fact that some proteins or isoforms that were expected to show up, were not retrieved. An important example are membrane proteins, especially plasma membrane proteins. They are involved in the earliest steps of the plant defense, i.e. in pathogen recognition (Jha *et al*., 2009). Although we were mainly interested in the cellular response further downstream of this recognition, future studies should focus also on the membrane proteome. These proteins are challenging to work with due to their hydrophobic nature, low abundance and heterogeneity. They are under-represented in our 2-DE gels. Alternative proteomic platforms such as blue native PAGE, clear native PAGE, SDS/SDS PAGE and LC based approaches such as free flow electrophoresis and multidimensional protein identification technology should be further explored (Tan *et al*., 2008).

Our experience with the technology taught us that 2-DE has additional obstacles of more practical nature.

First, it became clear that the technique is time-consuming and labour-intensive and required optimization and some hands-on training before it could be readily applied to analyze the resistance mechanisms of apple against scab. Optimization was performed at nearly every step of the process, starting with protein extraction and sample preparation, protein quantification, choice of (pI range and length of) IPG strips, sample application on the IPG strips, isoelectric focusing protocols, staining protocols, etc. (see Section 5.2). Moreover, the fact that no step-wise quality control was possible, made this optimization process very time-consuming. Since only the end result of the complete process is visualized, it is hard to trace back the process step that is responsible for inferior quality 2D-gels. On top of this, a 'poor' 2D-gel could be the result of a combination of different suboptimal steps.

Second, the use of preparative gels to pick spots for identification adds another level of technical complexity. Since these preparative gels contain a higher protein load than the analytical 2D-DIGE gels, the protein patterns on these two types of gels sometimes show a shift. Moreover, the higher the protein load, the greater the risk of highly abundant proteins masking lower abundant proteins. Consequently, matching of identical proteins between preparative gels and analytical gels had to be performed manually. This is again very time-consuming and not every spot of interest could be confidently matched to the corresponding spot on the preparative gel. The latter problem accounts for the fact that not all the spots of interest (only *circa* 75 %) could be submitted to mass spectrometry for identification. To overcome this problem, one could post-stain analytical gels and use them as pick gels. However, the protein content of the picked spots would be lower and this would possibly lead to an even lower coverage of identified proteins.

Together, these limitations of the 2-DE and 2D-DIGE technology add to the fact that the 'complete' proteome cannot be covered in this way. In order to fill in missing data and confirm obtained results from a gel-based proteomic approach, other complementary high-throughput techniques should be applied. Studies have shown that gel-free, liquid chromatography-based proteomics methods such as LC-MS/MS are complementary to the gel-based approaches (Vanrobaeys *et al*., 2005; Thelen, 2007). In addition, there is a need to uplift this proteomics approach to a systems biology approach integrating data from

different `omics' platforms into an overall metabolic network model. Such model should allow for the integration of knowledge on the different mechanisms underlying resistance of apple against *V. inaequalis*.

Nevertheless, despite the above mentioned shortcomings and practical problems of 2-DE, biologically relevant results regarding differential protein accumulation could be obtained. With the obtained data, we were able to generate some hypotheses (see Chapters 5 and 6). Although we are aware that the actual validation of these hypotheses has not been addressed in this thesis, a lot of them are supported by studies of similar plant-pathogen interactions, such as:

- the infection-induced up-regulation of proteins known to be involved in defense/stress response, e.g. Mal d 1 (Beuning *et al*., 2004; Paris *et al.*, 2009), chalcone synthases (Jiang *et al*., 2006), EDS1 (Venugopal *et al*., 2009), HSP 60 and HSP 70 (Santoro, 2000; Morano, 2007), lipoxygenase (Slusarenko, 1996; Gau *et al.*, 2004; Paris *et al.*, 2009) and proteasomes (Tsunezuka *et al*., 2005; Delaure *et al*., 2008)
- the infection-induced up-regulation of proteins involved in catabolic pathways such as glycolysis and TCA cycle in order to provide an extra energy supply necessary for stress response (Smedegaard-Petersen and Tolstrup, 1985; Umeda *et al*., 1994; Scheideler *et al*., 2002; Block *et al*., 2005; Scharte *et al*., 2005; Moshe *et al*., 2012);
- the infection-induced down-regulation of proteins involved in the anabolic carbon fixation pathways, *i.e.* photosynthesis and Calvin cycle (Chou *et al*., 2001; Scharte *et al*., 2005; Berger *et al*., 2007; Bolton, 2009). Scharte *et al*. (2005) proposed that in photoautotrophic source leaves, like the unfolded leaves sampled in our experiments, upon pathogen attack, photosynthesis and assimilatory metabolism are switched off and processes required for defense are initiated. The down-regulation of photosynthesis was also supported by our own observations of a decrease in chlorophyll content, that was macroscopically visible as chlorotic lesions as from 8 dpi (see Section 4.4);
- the infection-induced down-regulation of ROS scavenging mechanisms in a monogenic resistant cultivar compared to a susceptible cultivar, which increases

intracellular levels of reactive oxygen species like hydrogen peroxide, which then activate defense related genes (Apel and Hirt, 2004).

- the similarity in cellular responses to different stresses, including abiotic stresses (such as mock-infection) and biotic stresses (such as fungal infection), and the hypothesis that plant acclimation to different stresses is controlled by sophisticated quantitative rather than qualitative effects (Romeis *et al*., 1999; Bowler and Fluhr, 2000; Koorneef and Pieterse, 2008)
- the hypothesis that the differences in the changes in abundancy of proteins (involved in primary metabolism as well as defense response) between compatible and incompatible interactions are rather quantitative than qualitative (Tao *et al*., 2003; Bozkurt *et al*., 2010; Moshe *et al*., 2012)

Other hypotheses can be a starting point for further research.

As an example, results demonstrated the power of 2-DE to reveal post-translational modifications and isoforms. The identification of different isoforms of fructose-bisphosphate aldolase (see Chapter 5), triosephosphate isomerase and phosphoglycerate kinase (see Chapter 6) and their relation with the cellular location and their functions in glycolysis/gluconeogenesis and Calvin cycle supported some of our hypotheses. Other interesting isoforms (e.g., of the defense response related major allergen Mal d 1) should be studied further in relation to their differences in accumulation in the different conditions/cultivars. We should verify if it concerns post-translational modifications (such as phosphorylation, glycosylation, glutathionylation,…) or different mechanisms leading to the different isoforms. For example, Western blotting and immunodetection with anti-phospho-amino acid antibodies could reveal the presence of phosphorylated amino acids. RNA-sequencing could be applied to study alternative splicing. Elucidation of the precise nature of the modifications would produce more insight into the conferred properties of the affected proteins and in regulation systems.

More generally, validation of the proteomics approach utilized through another, low throughput technique for instance would be appropriate (e.g. Western blotting and/or measurement of enzymatic activity for some of the enzymes found to be differentially regulated). It could also be interesting to further investigate the un- or less characterized differentially accumulated proteins.

Furthermore, even though this work and several other reports describe the effect of fungal infection on carbohydrate metabolism, there is still a considerable lack of knowledge regarding how these changes influence the outcome of the plant–pathogen interaction. This is mainly due to the complexity of the mutual relation between carbohydrate status and development of disease/resistance. On the one hand, the carbohydrate status affects the defense as well as general metabolism of the plant. On the other hand, sugars are not only nutrients and signals for the plant partner but also for the fungal partner. Functional approaches (e.g. transgenic or 'cisgenic' approaches or the analysis of knock-out or antisense plants) are necessary to elucidate how alterations in carbohydrate metabolism affect disease development and resistance induction (Berger *et al*., 2007).

Important proteins for resistance induction can give rise to the development of markers for resistance breeding within or in close vicinity of the genes encoding these proteins. Functional approaches can again be used to validate these candidate markers for resistance breeding (through greenhouse and field trials) by gain-of-function in scab-susceptible cultivars (e.g. by overexpressing the 'cisgenic' gene or by finding the way to stimulate protein accumulation) or by loss-of-function in resistant cultivars (e.g. by gene silencing). In order to breed for durable disease resistance, known markers for resistance (R) genes should be combined with markers for proteins that play crucial roles more downstream in the resistance response.

Related to this, a comparative proteomics study of a *HcrVf2*-transformed susceptible cultivar and its non-transformed parent could reveal interesting candidate markers as well. Since Szankowski *et al*. (2009) developed highly scab-resistant 'Elstar' and 'Gala' plants by introgression of not only *HcrVf2* but also its native promotor, and *HcrVf2* transcription levels and the resistance level were similar to those of classical *Rvi6*-resistant cultivars, the results could yield important information regarding differences of resistance response between transgenic plant and wild type, that would not be influenced by differences in genetic background.

In future work, the following aspects could be addressed as well:

Because of the time-consuming aspect of the optimization steps and the technique itself, we had to limit our proteomics research to one resistance mechanism only. We chose to

investigate the monogenic *Rvi*6/*Vf* resistance mechanism of cultivar 'Topaz', and not the polygenic resistance mechanism of cv. 'Discovery', because there is more knowledge on the genetic basis of the monogenic resistance mechanism. Furthermore, monogenic resistance sources are still the most widely used in scab resistance breeding. However, it would be interesting if future research would focus on the polygenic resistance mechanism(s). For example, one could test the hypothesis that an increased activity (expression) of the energy metabolism occurs in polygenic resistant plants to compensate for the cost of constitutive resistance, as was concluded by Curto *et al*. (2006) for the pea (*Pisum sativum*)-powdery mildew (*Erysiphe pisi*) interaction. Moreover, differences in (the extent of) the responses between both types of resistance could reveal possible targets for use as markers in resistance breeding and thus contribute to the development of durable resistance.

Proteome analysis of leaves of different ages could reveal interesting results as well. We could investigate for example if ontogenic resistance mechanisms, e.g. in the 'scab-suscetible' cv. 'Golden Delicious', are similar to the mechanisms responsible for the resistance of young leaves of monogenic resistant cultivars like 'Topaz'. This would support the hypothesis that, in general, plant acclimation to stress is controlled by sophisticated quantitative rather than qualitative effects (Bowler and Fluhr, 2000). Besides, we would be able to verify if ontogenic resistance mechanisms are the same for susceptible and resistant cultivars, and why this ontogenic resistance disappears again in even older, senescing leaves.

Our original idea was to evaluate the evolution of the protein profiles in time. However, because the first results of the comparison of the different conditions of 'Topaz' at 2 and 3 dpi did not yield extra information as compared to 5 dpi, as of then we focused on the latter time-point. However, in the first 2D-DIGE experiment there were also little statistically significant differences between the infected and mock-infected condition of 'Topaz' at 5 dpi. This could be improved by analyzing more biological replicates. Indeed, three replicates is a minimum. Additionally, the use of several technical replicates for each biological replicate would increase these chances. However, we have to keep in mind that the amount of leaf material for each biological replicate was limited, and that because of that, the use of technical replicates was generally not possible. Another way to reduce the biological variability and to improve the reproducibility of the results would be to pool the leaf material of different plants. However, interesting information, e.g. regarding outliers, would

get lost. Moreover, the possible gain in significant information by adding extra (biological or technical) replicates should always be evaluated against the extra time spent and the higher cost. An alternative or additional way to increase the chance of detecting statistically significant differences could be the application of local leaf infections, rather than the whole leaf, and investigation of the protein profiles of the infected areas only. Besides, analysis of the sound tissue of the same leaf in parallel could add interesting information as well, e.g. regarding systemic responses.

Increasing the number of statistically significant differences could render investigation of additional time-points interesting again. Especially the comparison of the evolution of the protein profiles with the observed evolution in leaf symptoms and degree of fungal infection could yield important information regarding the evolution of the response to infection. Indeed, as also applied in this work, it is important to relate the (changes in) protein profiles and the established information regarding the cellular response to the physiological observations (see Chapter 4). In this work, we developed a *Venturia* specific real-time PCR that appeared to be a suitable technique to monitor the hyphal development. Moreover, our results suggested that the assay is an objective method to assess fungal virulence and host resistance, and it appeared to be very effective for the quantification of *Venturia* DNA levels at early, symptomless stages of infections. As of 3 dpi, i.e. 5 days before the appearance of the first visual symptoms, significantly less pathogen DNA ($p < 0.05$) was detected in the two resistant cultivars 'Topaz' and 'Discovery' compared to the susceptible cv. 'Golden Delicious'. Therefore, the technique cannot only be used in the study of the biology of the pathogen and the defense mechanisms of different apple cultivars, but there is a great potential for applications in breeding programs as well. We formulated some hypotheses regarding the first increase and subsequent decrease in fungal development in the scab resistant cultivars 'Topaz' and 'Discovery' during the symptomless stage (see Section 4.6). A time series of protein profiles could possibly help to explain this remarkable evolution in degree of infection. In this context it would be very interesting – if practically possible with regard to availability of leaf sample material – to perform real-time PCR and proteomics analyses on the same leaves of the same plants.

In this thesis we demonstrated as well that application of a preventative, systemic fungicide such as Aliette® (with fosetyl-Al as the active ingredient) prior to scab infection can reduce

foliar disease symptoms and hyphal growth as measured by real-time PCR (see Sections 6.3.1 and 6.3.2). This reduction was notably more distinct in the monogenic *Rvi*6-resistant cultivar 'Topaz' than in the scab-susceptible cv. 'Golden Delicious'. Moreover, 2D-DIGE analysis of Aliette®-treated 'Topaz' leaves revealed additional up- and downregulation of the above mentioned infection-related differentially accumulated proteins compared to non-treated plants, and thus an additional stimulation of the response to infection of this monogenic resistant cultivar (see Section 6.3.3). These findings suggest that, for cultivating purposes, it seems useful to combine the use of (monogenic) resistance sources with the application of preventative, systemic fungicides such as Aliette®. However, we should note that the observed limited effect of Aliette® application on infection of the scab-susceptible 'Golden Delicious' plants could (partly) be due to a saturation effect at 18 dpi. In future studies the effect of Aliette® on hyphal growth at earlier time-points after inoculation (e.g. 5 dpi) should be studied as well.

The observed effects of fosetyl-Al on hyphal growth and differential protein accumulation could be more significant if the systemic fungicide would be applied at different (e.g. later) time-points. Our developed real-time PCR assay would be a suitable technique to evaluate and select optimal time-points of application, as well as to compare the effect of Aliette® with that of other elicitors/systemic fungicides. In order to determine whether the effect of fosetyl-Al or another elicitor is a direct defense inducing effect (already present in absence of a pathogen) or a 'priming' effect, we should additionally compare Aliette®-treated and non-treated mock-inoculated plants ('Al-M <> M') and Aliette®-treated and non-treated control plants ('Al-C <> C').

In conclusion, we can state that the use of the 2D-DIGE technology and our developed *Venturia* specific real-time PCR protocol delivered some interesting insights in the response of apple to *V. inaequalis* infection and allowed us to formulate several new working hypotheses. Further research is needed to validate these hypotheses and to determine whether interfering with the involved proteins and pathways – in combination with the application of a preventative, systemic fungicide such as fosetyl-Al – could represent a strategy for developing new resistant cultivars and for attaining durable resistance.

Reference list

Abraham, P., Giannone, R.J., Adams, R.M., Kalluri, U., Tuskan, G.A., and Hettich, R.L. 2013. Putting the pieces together: high-performance LC-MS/MS provides network-, pathway-, and protein-level perspectives in *Populus*. Molecular and Cellular Proteomics 12: 106-119.

Aderhold, R. 1899. Auf welche Weise können wir dem immer weiteren Umsichgreifen des Fusicladiums in unseren Apfelkulturen begegnen und welche Sorten haben sich bisher dem Pilz gegen über am widerstandsfähigsten gezeigt. Pomol. Monatsh. XLV: 899–890.

Alban, A., Olu, S., Bjorkesten, L., Andersson, C., Sloge, E., Lewis, S., and Currie, I. 2003. A novel experimental design for comparative two-dimensional gel analysis: two-dimensional difference gel electrophoresis incorporating a pooled internal standard. Proteomics 3: 36-44.

Alberts, B., Bray, D., Johnson, A., Lewis, J., Raff, M., Roberts, K., and Walter, P. 1998. Essential cell biology: An introduction to the molecular biology of the cell. Garland Publishing, New York, 630p.

Aldwinckle, H.S., Gustafson, H.L., and Lamb R.C. 1976. Early determination of genotypes for apple scab resistance by forced flowering of test cross progenies. Euphytica 25: 185–191.

Andersen, J.S., Svensson, B., and Roepstorff, P. 1996. Electrospray ionization and matrix assisted laser desorption/ionization mass spectrometry: powerful analytical tools in recombinant protein chemistry. Nature Biotechnology 14: 449-457.

Apel, K. and Hirt, H. 2004. Reactive oxygen species: Metabolism, Oxidative Stress, and Signal Transduction. Annual Review of Plant Biology 55: 373-399.

Arnér, E., Holmgren, A. 2000. Physiological functions of thioredoxin and thioredoxin reductase. European Journal of Biochemistry 267: 6102–6109.

Bartlett, D. W., Clough, J. M., Godwin, J. R., Hall, A. A., Hamer, M., and Parr-Dobranzki, B. 2002. The strobilurin fungicides. Pest Management Science 58: 649-662.

Bayer CropScience (2012) Product Information sheet Aliette®.
www.bayercropscience.be/Bayer/CropScience/BCS_Belgium.nsf/id/NL_ALietteWG

Becker, C.M., Burr, T. S., and Smith, C.A. 1992. Overwintering of conidia of *Venturia inaequalis* in apple buds in New York orchards. Plant Disease 76: 121-126.

Beisson, k F., Li-Beisson, Y., and Pollard, M. 2012. Solving the puzzles of cutin and suberin polymer biosynthesis. Current Opinion in Plant Biology 15: 329–337.

Belfanti, E., Silfverberg-Dilworth, E., Tartarini, S., Patocchi, A., Barbieri, M., Zhu, J., Vinatzer, B.A., Gianfranceschi, L, Gessler, C., and Sansavini, S. 2004. The *HcrVf* gene from wild apple confers scab resisance to a transgenic cultivated variety. Proceedings of the National Academy of Science of the United States of America 101: 886-890.

Bénaouf, G. and Parisi, L. 1998. Characterization of *Venturia inaequalis* pathogenicity on leaf discs of apple trees. European Journal of Plant Pathology 104: 785-93.

Bénaouf, G. and Parisi, L. 2000. Genetics of host-pathogen relationships between *Venturia inaequalis* races 6 and 7 and *Malus* species. Phytopathology 90: 236-242.

Benjamini, Y. and Hochberg, Y. 2000. On the adaptive control of the false discovery rate in multiple testing with independent statistics. Journal of Educational and Behavioral Statistics 25: 60-83.

Benson, D.A., Karsch-Mizrachi, I., Lipman, D.J., Ostell, J., and Wheeler, D.L. 2004. Genbank: update. Nucleic Acids Research 32: D23–D26.

Bent, A.F., Innes, R.W., Ecker, J.R., and Staskawicz, B.J. 1992. Disease development in ethylene-insensitive *Arabidopsis thaliana* infected with virulent and avirulent *Pseudomonas* and *Xanthomonas* pathogens. Molecular Plant-Microbe Interactions 5: 372-378.

Berger, S., Sinha, A. K., and Roitsch, T. 2007. Plant physiology meets phytopathology: Plant primary metabolism and plant-pathogen interactions. Journal of Experimental Botany 58: 4019-4026.

Billiard, S., Lopez-Villaviciencio, M., Devier, B., Hood, M. E., Fairhead, C., and Giraud, T. 2011. Having sex, yes, but with whom? Inferences from fungi on the evolution of anisogamy and mating types. Biological Reviews 86: 421–442.

Blein, J., Coutos-Thévenot, P., Marion, D., and Ponchet, M. 2002. From elicitins to lipid-transfer proteins: a new insight in cell signaling involved in plant defence mechanisms. Trends in Plant Science, 7: 293-296.

Block, M.D., Verduyn, C., Brouwer, D.D., and Cornelissen, M. 2005. Poly(ADP-ribose) polymerase in plants affects energy homeostasis, cell death and stress tolerance. The Plant Journal 41: 95-106.

Bohland, C., Balkenhohl, T., Loers, G., Feussner, I., and Grambow, H. J. 1997. Differential induction of lipoxygenase isoforms in wheat upon treatment with rust fungus elicitor, chitin oligosaccharides, chitosan, and methyl jasmonate. Plant Physiology 114: 679-685.

Bolton, M. D. 2009. Primary metabolism and plant defense: fuel for the fire. Molecular Plant-Microbe Interactions 22: 487-497.

Bomblies, K. and Weigel, D. 2007. Hybrid necrosis: autoimmunity as a potential gene-flow barrier in plant species. Nature Reviews Genetics 8: 382-393.

Borneman, J. and Hartin, R.J. 2000. PCR primers that amplify fungal rRNA genes from environmental samples. Applied and Environmental Microbiology 66: 4356-4360.

Borras-Hidalgo, O., Thomma, B.P.H.J., Collazo C., Chacon, O., Borroto, C.J., Ayra, C., Portieles, R., Lopez, Y., and Pujol, M. 2006. EIL2 transcription factor and glutathione synthetase are required for defense of tobacco against tobacco blue mold. Molecular Plant-Microbe Interactions 19: 399-406.

Bowen, J. A., Mesarich, C. H., Bus, V. G. M., Beresford, R. M., Plummer, K. M., and Templeton, M. D. 2011. *Venturia inaequalis*: the causal agent of apple scab. Molecular Plant Pathology 12: 105–122.

Bowler, C. and Fluhr, R. 2000. The role of calcium and activated oxygens as signals for controlling cross-tolerance. Trends in Plant Science 5, 241-246.

Bozkurt, T.O., McGrann, G.R.D., MacCormack, R., Boyd, L.A., Akkaya, M.S. 2010. Cellular and transcriptional responses of wheat during compatible and incompatible race-specific interactions with *Puccinia striiformis* f. sp. *tritici*. Molecular Plant Pathology 11: 625–640.

Braun, P. G. 1994. Development and decline of a population of *Venturia inaequalis* resistant to sterol-inhibiting fungicides. Norwegian Journal of Agricultural Science 17(Suppl.): 173-184.

Braun, P. G., and McRae, K. B. 1992. Composition of a population of *Venturia inaequalis* resistant to myclobutanil. Canadian Journal of Plant Pathology 14: 215-220.

Broggini, G., Galli, P., Parravicini, G., Gianfranceschi, L., Gessler, C., and Patocchi, A. 2009. *HcrVf* paralogs are present on linkage groups 1 and 6 of *Malus*. Genome, 52: 129-138.

Brouwer, M., Lievens, B., Van Hemelrijck, W., Van den Ackerveken, G., Cammue, B.P.A., and Thomma, B.P.H.J. 2003. Quantification of disease progression of several microbial pathogens on *Arabidopsis thaliana* using real-time fluorescence PCR. FEMS Microbiology Letters 228: 241-248.

Bus, V.G.M., Rikkerink, E.H.A., van de Weg, W.E., Rusholme, R.L., Gardiner, S.E., Bassett, H.C.M., Kodde, L.P., Parisi, L., Laurens, F.N.D., Meulenbroek, E.J., and Plummer, K.M. 2005a. The *Vh2* and *Vh4* scab resistance genes in two differential hosts derived from Russian apple R12740-7A map to the same linkage group of apple. Molecular Breeding 15: 103-116.

Bus, V.G.M., Laurens, N.D., van de Weg, W.E., Rusholme, R.L., Rikkerink, E.H.A., Gardiner, S.E., Bassett, H.C.M., Kodde, L.P., and Plummer, K.M. 2005b. The *Vh8* locus of a new gene-for-gene interaction between *Venturia inaequalis* and the wild apple *Malus sieversii* is closely linked to the *Vh2* locus in *Malus pumila* R12740-7A. New Phytologist 166: 1035-1049.

Bus, V., Rikkerink, E., Caffier, V., Durel, C., Plummer, K. 2011. Revision of the nomenclature of the differential host-pathogen interactions of *Venturia inaequalis* and *Malus*. Annual Review of Phytopathology 49: 391–413.

Bus, V.G.M., Rikkerink, E., Aldwinckle, H.S., Caffier, V., Durel, C.E., Gardiner, S., Gessler, C., Groenwold, R., Laurens, F., Le Cam, B., Luby, J., Meulenbroek, B., Kellerhals, M., Parisi, L., Patocchi, A., Plummer, K., Schouten, H.J., Tartarini, S., and van de Weg, W.E. 2009 A proposal for the nomenclature of *Venturia inaequalis* races. Acta Horticulturae 814: 739–746.

Calcedo, R., Ramirez-Garcia, A., Abad, A., Rementeria, A., Ponton, J., and Hernando, F.L. 2012. Phosphoglycerate kinase and fructose bisphosphate aldolase of *Candida albicans* as new antigens recognized by human salivary IgA. Revista Iberoamericana de micologia, 29: 172-174.

Calenge, F., Goerre, M., Gebhardt, C., van de Weg, W.E., Parisi, L. and Duel, C.-E. 2004. Quantitative trait loci (QTL) analysis reveals both broad-spectrum and isolate-specific QTL for scab resistance in an apple progeny challenged with eight isolates of *Venturia inaequalis.* Phytopathology 94: 370-379.

Carisse, O. and Bernier, J. 2002. Effect of environmental factors on growth, pycnidial production and spore germination of *Microsphaeropsis* isolates with biocontrol potential against apple scab. Mycological Research 106 1455–1462.

Carpentier, S., Coemans, B., Podevin, N., Laukens, K., Witters, E., Matsumura, H., Terauchi, R., Swenne., and Panis, B. 2008a. Functional genomics in a non-model crop: transcriptomics or proteomics? Physiologia Plantarum 133: 117-130.

Carpentier, S., Panis, B., Vertommen, A., Swennen, R., Seargeant, K., Renaut, J., Laukens, K., Witters, E., Samyn, B., and Devreese, B. 2008b. Proteome analysis of non-model plants: a challenging but powerful approach. Mass Spectrometry Reviews 27: 354-377.

Carpentier, S., Witters, E., Laukens, K., Deckers, P., Swennen, R. and Panis, B. 2005. Preparation of protein extracts from recalcitrant plant tissues: an evaluation of different methods for two-dimensional gel electrophoresis analysis. Proteomics 5: 2497-2507.

Casati, P., Drincovich, M. F., Edwards, G. E., and Andreo, C. S. 1999. Malate metabolism by NADP malic enzyme in plant defense. Photosynthesis Research 61: 99-105.

Chakrabarti, A., Panter, S.N., Harrison, K., Jones, J.D.G., and Jones, D.A. 2009. Regions of the Cf-9B disease resistance protein able to cause spontaneous necrosis in *Nicotiana benthamiana* lie within the region controlling pathogen recognition in tomato. Molecular Plant–Microbe Interactions 22: 1214–1226.

Chapman, K. S., Sundin, G. W., and Beckerman, J. L. 2011. Identification of resistance to multiple fungicides in field populations of *Venturia inaequalis*. Plant Disease 95: 921-926.

Chevalier, M., Lespinasse, Y., and Renaudin, S. 1991. A microscopic study of the different classes of symptoms coded by the *Vf* gene in apple for resistance to scab (*Venturia inaequalis*). Plant Pathology 40: 249–256.

Cho, S.M., Shin, S.H., Kin, K.S., Kim, Y.C., Eun, M.Y., and Cho, B.H. 2004. Enhanced expression of a gene encoding a nucleoside diphosphate kinase 1 (OsNDPK1) in rice plants upon infection with bacterial pathogens. Molecules and Cells 18: 390-395.

Chou, H.M., Bundock, N., Rolfe, S.A., and Scholes, J.D. 2000. Infection of *Arabidopsis thaliana* leaves with *Albugo candida* (white blister rust) causes a reprogramming of host metabolism. Molecular Plant Pathology 1: 99-113.

Conrath, U., Beckers, G.J.M., Flors, V., Garcia-Agustin, P., Jakab, G., *et al*. 2006. Priming: getting ready for battle. Molecular Plant-Microbe Interactions 19: 1062–1071.

Cordwell, S.J. 1999. Microbial genomes and missing enzymes: redefining biochemical pathways. Archives of Microbiology 172: 269-279.

Cova, V., Paris, R., Passerotti, S., Zini, E., Gessler, C., Pertot, I., Loi, N., Musetti, R., and Komjanc, M. 2010. Mapping and functional analysis of four apple receptor-like protein kinases related to LRPKm1 in HcrVf2-transgenic and wild-type apple plants. Tree Genetics and Genomes 6: 389–403.

Crandall, C. S. 1926. Apple breeding at the University of Illinois. Illinois Agricultural Experimental Station Bulletin 275: 341-600.

Crosby, J.A., Janick, J., Pecknold, P.C., Kprban, S.S., OConnor, P.A., Ries, S.M., Goffreda, J., and Voordeckers, A. 1992. Breeding apples for scab resistance - 1945-1990. Fruit Varieties Journal 46: 145-166.

Crouzet, J., Trombik, T., Fraisse, A.S., and Boutry, M. 2006. Organization and function of the plant pleiotropic drug resistance ABC transporter family. FEBS Letters 13: 1123–1130.

Daniel, R. and Guest, D. 2006. Defence responses induced by potassium phosphonate in *Phytophtora palmivora*-challenged *Arabidopsis thaliana*. Physiological and Molecular Plant Pathology 67: 194-201.

Davletova, S., Rizhsky, L., Liang, H. J., Zhong, S. Q., Oliver, D. J., Coutu, J., Shulaev, V., Schlauch, K., and Mittler, R. 2005. Cytosolic ascorbate peroxidase 1 is a central component of the reactive oxygen gene network of Arabidopsis. Plant Cell 17: 268-281.

Dayton, D.F. and Mowry, J.B. 1970. Prima, the first commercial scab-resistant apple variety. Fruit Varieties and Horticultural Digest 12: 7.

Degenhardt, J., Nasser Al-Masari, A., Kürkcüoglu, S., Szankowski, I., and Gau, A. E. 2005. Characterization by suppression subtractive hybridization of transcripts that are differentially expressed in leaves of apple scab-resistant and susceptible cultivars of *Malus domestica*. Molecular Genetics and Genomics 273: 326-335.

Delaure, S.L., Hemelrijck, W.V., De Bolle, M.F.C., Cammue, B.P.A., and De Coninck, B.M.A. 2008. Building up plant defenses by breaking down proteins. Plant Science 174: 375–385.

Devoto, A., Muskett, P.R., and Shirasu, K. 2003. Role of ubiquitination in the regulation of plant defence against pathogens. Current Opinion in Plant Biology 6: 307‑311.

DeYoung, B.J. and Innes, R.W. 2006. Plant NBS-LRR proteins in pathogen sensing and host defense. Nature Immunology 7: 1243-1249.

Diatchenko, L., Lukyanov, S., Lau, Y.F., and Siebert, P.D. 1999. Suppression subtractive hybridization: a versatile method for identifying differentially expressed genes. Methods in Enzymology 303: 349–380.

Diaz-Perales, A., Garcia-Cassado, G., Sanchez-Monge, R., Garcia-Selles, F., Barber, D., and Salcedo, G. 2002. cDNA cloning and heterologous expression of the major allergens from peach and apple belonging to the lipid-transfer protein family. Clinical and Experimental Allergy 32: 87-92.

Dominguez, E., Heredia-Guerrero, J.A., and Heredia, A. 2011. The biophysical design of plant cuticles: an overview. New Phytologist 189: 938–949.

Dunemann, F. and Egere, J. 2010. A major resistance gene from Russian apple 'Antonovka' conferring field immunity against apple scab is closely linked to the *Vf* locus . Tree Genetics and Genomes 6: 1614-2950.

Durel, C.E., Calenge, F., Parisi, L., van de Weg, W., E., Kodde, L., Liebhard, R.,Gessler, C., Thiermann, M., Dunemann, F, Gennari, F, Tartarini, S., and Lespinasse, Y. 2004. An overview of the position and

robustness of scab resistance QTLs and major genes by aligning of genetic maps in five apple progenies. Horticulturae 663: 135-140.

Durel, C.E., Parisi, L., Laurens, F., van de Weg, W.E., Liebhard, R., and Jourjon, M.F. 2003. Genetic dissection of partial resistance to race 6 of *Venturia inaequalis* in apple. Genome 46: 224–234.

Eberl, H.C., Mann, M., and Vermeulen, M., 2011. Quantitative proteomics for epigenetics. ChemBioChem 12: 224–234.

Edreva, A. 2005. Pathogenesis-related proteins: research progress in the last 15 years. Genetics Applied Plant Physiology 31: 105-124.

Erdin, N., Tartarini, S., Broggini, G., Gennari, F., Sansavini, S., Gessler, C., and Patocchi, A. 2006. Mapping of the apple scab-resistance gene *Vb*. Genome 49: 1238-1245.

Eshraghi, L., Anderson, J., Aryamanesh, N., Shearer, B., McComb, J., Hardy, G.E.StJ., and O'Brien, P.A. 2011. Phosphite primed defence responses and enhanced expression of defence genes in *Arabidopsis thaliana* infected with *Phytophthora cinnamomi*. Plant Pathology 60: 1086-1095.

Fatland, B.L., Ke, J., Anderson, M.D., Mentzen, W.I., Cui, L.W., Allred, C.C., Johnston, J.L., and Nikolau, B.J. 2002. Molecular Characterization of a Heteromeric ATP-Citrate Lyase That Generates Cytosolic Acetyl-Coenzyme a in Arabidopsis. Plant Physiology 130: 740.

Feussner, I. and Wasternack, C. 2002. The lipoxygenase pathway. Annual Review of Plant Biology 53: 275–297.

Flor, H.H. 1955. Inheritance of pathogenecity in *Melampsora lini*. Phytopathology 32: 653-669.

Flor, H.H. 1971. Current status of the gene-for-gene concept. Annual Review of Phytopathology 9: 275-296.

Fodoroff, N. 2006. Redox regulatory mechanisms in cellular stress responses. Annals of Botany 98: 289-300.

Fratelli, M., Demol, H., Puype, M., Casagrande, S., Eberini, I., Salmona, M., Bonetto, V., Mengozzi, M., Duffieux, F., Miclet, E., Bachi, A., Vandekerckhove, J., Gianazza, E., and Ghezzi, P. 2002. Identification by redox proteomics of glutathionylated proteins in oxidatively stressed human T lymphocytes. Proceedings of the National Academy of Science of the United States of America 99: 3505–3510.

Fridman, E. and Pichersky, E. 2005. Metabolomics, genomics, proteomics, and the identification of enzymes and their substrates and products. Current Opinion in Plant Biology 8: 242-248.

Galli, P., Broggini, G.A.L., Gessler, C., and Patocchi, A. 2010. Phenotypic characterization of the *Rvi15* (*Vr2*) apple scab resistance. *Journal of Plant Pathology* 92, 219–226.

Garcia-Neria, M.A. and Rivera-Bustamante, R.F. 2011. Characterization of Geminivirus resistance in an accession of Capsicum chinense Jacq. Molecular Plant Microbe Interactions 24: 172-182.

Gau, A., Koutb, M., Piotrowski, M., and Kloppstech, K. 2004. Accumulation of pathogenesis-related proteins in the apoplast of susceptible cultivar of apple (*Malus domestica* cv. Elstar) after infection by

Venturia inaequalis and constitutive expression of PR genes in the cultivar Remo. European Journal of Plant Pathology 110: 703-711.

Gessler, C. 1989. Genetics of the interaction *Venturia inaequalis-Malus*: the conflict between theory and reality. IOBC-WPRS-Bulletin 12: 168–190.

Gessler, C., Patocchi, A., Kellerhals, M., and Gianfranceschi, L. 1997. Molecular marker applied to apple breeding and map-based cloning of resistance genes. OILB-WPRS Bulletin 20: 105–109.

Gessler, C., Patocchi, A., Sansavini, S., Tartarini, S., and Gianfranceschi, L. 2006. *Venturia inaequalis* resistance in apple. CRC Critical Reviews in Plant Science 25: 473–503.

Gessler, C. and Pertot, I. 2012. Vf scab resistance of *Malus*. Trees 26: 95-108.

Gianfranceschi, L., Koller, B., Seglias, N., Kellerhals, M., and Gessler, C. 1996. Molecular selection in apple for resistance to scab caused by *Venturia inaequalis*. Theoretical apple genetics 93: 199-204.

Gisi, U., Sierotzki, H., Cook, A., and McCaffery, A. 2002. Mechanisms influencing the evolution of resistance to Qo inhibitor fungicides. Pest Management Science 58: 859-867.

Gonzalez-Fernandez, R. and Jorrin-Novo, J.V. 2012. Contribution of proteomics to the study of plant pathogenic fungi. Journal of Proteome Research 11: 3-16.

Görg, A., Drews, O., Lück, C.W., and Weiss, W. 2009. 2-DE with IPGs. Electrophoresis 30(S1): 122-132.

Görg, A., Obermaier, C., Boguth, G., Harder, A., Scheibe, B., Wildgruber, R., and Weiss, W. 2000. The current state of two-dimensional electrophoresis with immobilized pH gradients. Electrophoresis 21: 1037-1053.

Görg, A., Weiss, W., and Dunn M.J. 2004. Current two-dimensional electrophoresis technology for proteomics. Proteomics 4: 3665–3685.

Gorovits, R. and Czosnek, H. 2007. Biotic and abiotic stress responses in breeding tomato lines resistant and susceptible to Tomato yellow leaf curl virus. Plant Physiology and Biochemistry 46: 482-492.

Gosch, C., Halbwirth, H., Kuhn, J., Miosic, S., and Stich, K. 2009. Biosynthesis of phloridzin in apple (*Malus domestica* Borkh.). Plant Science 176: 223–231.

Gruber, C.W., Cemazar, M., Heras, B., Martin, J.L., and Craik, D.J. 2006. Protein disulfide isomerase: the structure of oxidative folding. Trends in Biochemical Sciences 31: 455–464.

Guest, D.I. 1984. Modification of defense responses in tobacco and *Capsicum* following treatment with fosetyl-Al [aluminium tris(o-ethyl phosphonate)]. Physiology of Plant Pathology 25: 125-134.

Guest, D.I. 1986. Evidence from light microscopy of living tissues that fosetyl-Al modifies the defense response in tobacco seedlings following inoculation by *Phytophthora nicotianae* var. *nicotianae*. Physiology and Molecular Plant Pathology 29: 251-261.

Guest, D.I., Saindrenan, P., Barchietto, T., and Bompeix, G. 1988. The phosphonates, anti-oomycete chemicals with a complex mode of action. Proceedings of the 5th International congress on Plant Pathology, Kyoto, 333.

Gupta, G.K. 1992. Apple scab (*Venturia inaequalis* (Che.) Wint.). In: Plant diseases of international importance. Vol III. Diseases of fruit crops. Kumar, J., Chaube, H.S., Singh, U.S., and Mukhopadhyay, A.N. (eds). Prentice Hall, Englewood Cliffs, New Jersey, 1-31.

Gygax, M., Gianfranceschi, Liebhard, R., Kellerhals, M., Gessler, C., and Patocchi, A. 2004. Molecular markers linked to apple scab resistance gene *Vbj* deriverd from *Malus baccata jackii*. Theoretical and Applied Genetics, 109: 1702-1709.

Havaux, M., Ksas, B., Szewczyk, A., Rumeau, D., Franck, F., Caffarri, S., and Triantaphylides, C. 2009. Vitamin B6 deficient plants display increased sensitivity to high light and photo-oxidative stress. BMC Plant Biology 9: 130.

Heid, C.A., Stevens, J., Livak, K.J., and Williams, P.M. 1996. Real time quantitative PCR. Genome Research 6: 986-994.

Hemmat, M., Brown, S., Aldwinckle, H., and Weeden, N. 2003. Identification and mapping of markers for resistance to apple scab from 'Antonovka' and 'Hansen baccata#2'. Acta Horticulturae 622: 153-161.

Hindorf, H., Rövekamp, I.F., and Henseler, K. 2000. Decision aids for apple scab warning services (*Venturia inaequalis*) in Germany. Bulletin OEPP/EPPO Bulletin 30, 59–64.

Hoffman, T., Schmidt, J.S., Zheng, X., and Bent, A.F. 1999. Isolation of ethylene-insensitive soybean mutants that are altered in pathogen susceptibility and gene-for-gene disease resistance. Plant Physiology 119: 935-950.

Holb, I.J. 2006. Effect of six sanitation treatments on leaf litter density, ascospore production of *Venturia inaequalis* and scab incidence in integrated and organic apple orchards. European Journal of Plant Pathology 115: 293–307.

Holb, I.J., Heijne, B., and Jeger, M.J. 2003. Summer epidemics of apple scab: Their relationship between measurements and their implications for the development of predictive models and threshold levels under different disease control regimes. Journal of Phytopathology 151: 335–343.

Holb, I.J., Heijne, B., and Jeger, M.J. 2004. Overwintering of conidia of *Venturia inaequalis* and the contribution to early epidemics of apple scab. Plant Disease 88: 751-757.

Hollywood, K., Brison, D., and Goodacre, R. 2006. Metabolomics: Current technologies and future trends. Proteomics 6: 4716-4723.

Hough, L.F., Shay, J.R., and Dayton, D.F. 1953. Apple scab resistance from *Malus floribunda* Sieb. Proceedings of the American Society for Horticultural Science 62: 341–347.

Hoving, S., Gerrits, B., Voshol, H., Muller, D., Roberts, R.C., and Van Oostrum, J. 2002. Preparative twodimensional gel electrophoresis at alkaline pH using narrow range immobilized pH gradients. Proteomics 2: 127-134.

Hoving, S., Voshol, H., and van Oostrum, J. 2000. Towards high performance two-dimensional gel electrophoresis using ultrazoom gels. Electrophoresis 21: 2617-2621.

Hrazdina, G., Borejsza-Wysocki, W., and Lester, C. 1997. Phytoalexin production in an apple cultivar resistant to *Venturia inaequalis*. Phytopathology 87: 868-876.

Hu, X., Nazar, R.N., and Robb, J., 1993. Quantification of *Verticillium* biomass in wilt disease development. Physiological and Molecular Plant Pathology 42: 23-36.

Hückelhoven, R. 2007. Cell wall–associated mechanisms of disease resistance and susceptibility. Annual Review of Phytopathology 45: 101-127.

Hurkman, W. and Tanaka, C. 2007. High-resolution two-dimensional gel electrophoresis: a cornerstone of plant proteomics. In: Plant Proteomics. Samaj, J. and Thelen, J. (eds.) Springer, Berlin, 14-28.

Ito, O., Ella, E., and Kawano, N. 1999. Physiological basis of submergence tolerance in rainfed lowland rice ecosystem. Field Crops Research 64: 75-90.

Jacobs, D.I., van der Heijden, R., and Verpoorte, R. 2000. Proteomics in plant biotechnology and secondary metabolism research. Phytochemical Analysis 11: 277-287.

Jha, G., Thakur, K., and Thakur, P. 2009. The *Venturia* apple pathosystem: pathogenicity mechanisms and plant defense responses. Journal of Biomedicine and Biotechnology 28: 1-10

Jiang, C., Schommer, C., Kim, S.-Y., Suh, D.-Y. 2006. Cloning and Characterization of Chalcone Synthase from the moss *Physcomitrella patens*. Phytochemistry 67: 2531–2540.

Jones, A.M.E., Thomas, V., Bennett, M.H., Mansfield, J., and Grant, M. 2006. Modifications to the *Arabidopsis* defense proteome occur prior to significant transcriptional change in response to inoculation with *Pseudomonas syringae*. Plant Physiology 142: 1603–1620.

Jones, A.L. and Walker, R.J. 1976. Tolerance of *Venturia inaequalis* to dodine and benzimidazole fungicides in Michigan. Plant Disease Reports 60: 40-44.

Joshi, S.G. 2010. Toward durable resistance to apple scab using cisgenes. PhD thesis, Wageningen University, the Netherlands.

Joshi, S.G., Schaart, J.G., Groenwold, R., Jacobsen, E., Schouten, H.J., and Krens, F.A. 2011. Functional analysis and expression profiling of *HcrVf*1 and *HcrVf*2 for development of scab resistant cisgenic and intragenic apples. Plant Molecular Biology 75: 579–591.

Karas, M. and Hillenkamp, F. 1988. Laser desorption ionization of proteins with molecular masses exceeding 10000 Daltons. Analytical Chemistry 60: 2299-2301.

Karp, N.A. and Lilley, K.S. 2005. Maximising sensitivity for detecting changes in protein expression: experimental design using minimal Cy-dyes. Proteomics 5: 3105-3115.

Kellerhals, M. and Furrer, B. 1994. Approaches for breeding apples with durable disease resistance. Euphytica 77: 31–35.

Kellerhals, M., Sauer, C., Hohn, E., Guggenbuhl, B., Frey, J., Liebhard, R., Gessler, C. 2006. Durable disease resistance and high fruit quality, a challenge for apple breeding. Bulletin OILB/SROP 29: 43–48.

Kessler, B.M. 2011. Challenges ahead for mass spectrometry and proteomics applications in epigenetics. Epigenomics 2: 163-167.

Kessmann, H., Staub, T., Hofmann, C., Maetzke, T., Herzog, J.,Ward, E., Uknes S., and Ryals, J. 1994. Induction of systemic acquired resistance in plants by chemicals. Annual Review of Plant Pathology 32: 439–459.

Kim, S. and Kang, K. 2008. Proteomics in plant defense response. In: Plant Proteomics. Agrawal, G. and Rakwal, R. (eds.) Wiley, Hoboken, New Jersey, 587-604.

Kim, S.T., Kim, S.G., Hwang, D.H., Kang, S.Y., Kim, H.J., Lee, B.H., Lee, J.J., and Kang, K.Y. 2004. Proteomic analysis of pathogen-responsive proteins from rice leaves induced by rice blast fungus, *Magnaporthe grisea*. Proteomics 4: 3569–3578.

Kniskern J.M., Traw, M.B., and Bergelson, J. 2007. Salicylic acid and jasmonic acid signaling defense pathways reduce natural bacterial diversity on *Arabidopsis thaliana*. Molecular Plant-Microbe Interactions 20: 1512-1522.

Kollar, A. 2005. Evidence for loss of ontogenetic resistance of apple leaves against *Venturia inaequalis.* European Journal of Plant Pathology 102: 1573-8469.

Köller, W., Parker, D.M., and Becker, C.M. 1991. Role of cutinase in the penetration of apple leaves by *Venturia inaequalis*. Phytopathology 81: 1375–1379.

Köller, W., Parker, D.M., Turechek, W.W., Avila-Adame, C., and Cronshaw, K. 2004. A two-phase resistance response of *Venturia inaequalis* populations to the QoI fungicides kresoxim-methyl and trifloxystrobin. Plant Disease 88: 537-544.

Köller, W. and Wilcox, W.F. 2001. Evidence for the predisposition of fungicide-resistant isolates of *Venturia inaequalis* to a preferential selection for resistance to other fungicides. Phytopathology 91: 776–781.

Komjanc, M., Festi, S., Rizzotti, L., Cattivelli, L., Cervone, F., De Lorenzo, G. 1999. A leucine-rich repeat receptor-like protein kinase (LRPKm1) gene is induced in *Malus* x *domestica* by *Venturia inaequalis* infection and salicylic acid treatment. Plant Molecular Biology 40: 945–957

Konishi, H., Ishiguro, K., and Komatsu, S. 2001. A proteomics approach towards understanding blast fungus infection of rice grown under different levels of nitrogen fertilization. Proteomics*:* 1162–1171.

Koorneef, A. and Pieterse, C.M.J. 2008. Cross-talk in defense signaling. Plant Physiology 146: 839–844.

Korsman, J., Meisel, B., Kloppers, F.J., Crampton, B.G., and Berger, D.K. 2012. Quantitative phenotyping of grey leaf spot disease in maize using real-time PCR. European Journal of Plant Pathology 133: 461-471.

Kruijt, M., de Kock, M.J.D., and de Wit, P. 2005. Receptor-like proteins involved in plant disease resistance. Molecular Plant Pathology 6: 85–97.

Kuck, K.H., Scheinpflug, H., and Pontzen, R. 1995. DMI fungicides. In: Modern Selective Fungicides, 2nd ed. Lyr, H. (ed.) Gustav Fischer Verlag, Jena, Germany, 205-258.

Kürkcüoglu, S., Degenhardt, J., Lensing, J., Al-Masri, A.N., and Gau, A.E. 2007. Identification of differentially expressed genes in *Malus domestica* after application of the non-pathogenic bacterium *Pseudomonas fluorescens* Bk3 to the phyllosphere. Journal of Experimental Botany 58: 733-741.

Küng, R., Chin, K.M., and Gisi, U. 1999. Sensitivity of *Venturia inaequalis* to cyprodinil. Modern fungicides and antifungal compounds 2: 313-322.

Kussmann, M., Raymond, F., and Affolter, M. 2006. OMICS-driven biomarker discovery in nutrition and health. Journal of Biotechnology 124: 758-787.

Lamar, R.T., Schoenike, B., Vanden Wymelenberg, A., Stewart, P., Dietrich, D.M., Cullen, D. 1995. Quantitation of fungal mRNAs in complex substrates by reverse transcription PCR and its application to *Phanerochaete chrysosporium*-colonized soil. Applied and Environmental Microbiology 61: 2122-2126.

Lamb, C. and Dixon, R.A. 1997. The oxidative burst in plant disease resistance. Annual Reviews of Plant Physiology and Plant Molecular Biology 48: 251-275.

Lane, C.S. 2005. Mass spectrometry-based proteomics in the life sciences. Cell Molecular and Life Sciences 62: 848-869.

Larue, P. and Gaulliard, J.M. 1993. Phosetyl-Al, a new weapon against fire blight in apple and pear orchards. Acta Horticulturae 338: 297-304.

Latorse, M.P., Mauprivez, L., Sirven, C., Gautier, P., and Beffa, R. 2010. Comparison of fosetyl-Al and another phosphonate on plant downy mildew protection and on *Arabidopsis thaliana* gene expression. Proceedings of th 6th International Workshop of grapevine downy and powdery mildew, Bordeaux, France, 4th – 9th July 2010. p 158

Lee, S.B., Taylor, J.W. 1992. Phylogeny of five fungus-like protoctistan *Phytophthora* species, inferred from the internal transcribed spacers of ribosomal DNA. Molecular Biology and Evolution 9: 636-653.

Lespinasse, Y., Pinet, C., and Parisi, L. 2002. European research for durable resistance to scab on apple: the DARE project. Acta Horticulturae 595: 17-22.

Leterrier, M., Corpas, F.J., Barroso, J.B., Sandalio, L.M., del Rio, L.A. 2005. Peroxisomal monodehydroascorbate reductase. Genomic clone characterization and functional analysis under environmental stress conditions. Plant Physiology 138: 2111–2123.

Li, B. and Xu, X. 2002. Infection and development of apple scab (*Venturia inaequalis*) on old leaves. Phytopathology 150: 687-691.

Liebhard, R., Gianfranceschi, L., Koller, B., Ryder, C. D., Tarchini, R., van de Weg, E., and Gessler, C. 2002. Development and characterization of 140 new microsatellites in apple (*Malus* × *domestica* Borkh.). Molecular Breeding 10: 217-241.

Liebhard, R., Koller, B., Patocchi, A., Kellerhals, M., Pfammatter, W., Jermini, M., and Gessler, C. 2003. Mapping quantitative field resistance against apple scab in a 'Fiesta' x 'Discovery' progeny. Phytopathology 93: 493–501.

Lievens, B., Brouwer, M., Vanachter, A.C.R.C., Cammue, B.P.A., Thomma, B.P.H.J. 2006. Real-time PCR for detection and quantification of fungal and oomycete tomato pathogens in plant and soil samples. Plant Science 171: 155-165.

Linthorst, H.J.M. 1991. Pathogenesis-related proteins of plants. *Critical Reviews in Plant Sciences* 10: 123–150.

Liska, A.J. and Shevchenko, A. 2003. Expanding the organismal scope of proteomics: cross-species protein identification by mass spectrometry and its implications. Proteomics 3: 19-28.

Liu, J.-J. and Ekramoddoullah, A.K.M. 2006. The family 10 of plant pathogenesis-related proteins: Their structure, regulation, and function in response to biotic and abiotic stresses. Physiological and Molecular Plant Pathology 68: 3-13.

van Loon, L., Rep, M., and Pieterse, C. 2006. Significance of inducible defense-related proteins in infected plants. Annual Review of Phytopathology 44: 135-162.

Lopez, C., Soto, M., Restrepo, S., Piègu, B., Cooke, R., Delseny, M., Tohme, J., and Verdier, V. 2005. Gene expression profile in response to *Xanthomonas axonopodis* pv. *manihotis* infection in cassava using a cDNA microarray. Plant Molecular Biology 57: 393‑410.

Lu, W., Tang, X., Huo, Y., Xu, R., Qi, S., Huang, J., Zheng, C., and Wu, C. 2012. Identification and characterization of fructose 1,6-bisphosphate aldolase genes in *Arabidopsis* reveal a gene family with diverse responses to abiotic stresses. Gene 503: 65–74.

MacDonald, M.J., and D'Cunha, G B. 2007. A modern view of phenylalanine ammonia lyase. Biochemistry and Cell Biology 85: 273–282.

MacHardy, W.E. 1996. Apple Scab: biology, epidemiology and management. The American Phytopathological Society Press, St. Paul, 546 p.

MacHardy, W.E., Gadoury, D.M., and Gessler, C. 2001. Parasitic and biological fitness of *Venturia inaequalis*: relationship to disease management strategies. Plant Diseases 85: 1036-1051.

Mackay, I.M., Arden, K.E., Nitsche, A., 2002. Real-time PCR in virology. Nucleic Acids Research 30, 1292-1305.

Mahe, A., Grisvard, J., Dron, M., 1992. Fungal-specific and plant-specific gene markers to follow the bean anthracnose infection process and normalize a bean chitinase mRNA induction. Molecular Plant-Microbe Interactions 5: 242-248.

Maliepaard, C., Alston, F., van Arkel, G., Brown, L., Chevreau, E., Dunemann, F., Evans, K. M., Gardiner, S., Guilford, P., van Heusden, A. W., Janse, J., Laurens, F., Lynn, J. R., Manganaris, A. G., den Nijs, A. P. M., Periam, N., Rikkerink, E., Roche, P., Ryder, C., Sansavini, S., Schmidt, H., Tartarini, S., Verhaegh, J. J., Vrielink-van Ginkel, M., and King, G. J. 1998. Aligning male and female linkage maps of apple (*Malus pumila* Mill.) using multi-allelic markers. Theoretical and Applied Genetics 97: 60-73.

Malnoy, M., Xu, M., Borejsza-Wysocka, E., Korban, S., and Aldwinckle, H. 2008. Two receptor like genes, *Vfa*1 and *Vfa*2, confer resistance to the fungal pathogen *Venturia inaequalis* inciting apple scab disease. Molecular Plant-Microbe Interactions 21: 448-458.

Mande, S.C., Mainfroid, V., Kalk, K. H., Goraj, K., Martial, J.A., and Hol, W.G.J. 1994. Crystal-structure of recombinant human triosephosphate isomerase at 2.8 angstrom resolution – triosephosphate isomerase-related human genetic-disorders and comparison with the trypanosomal enzyme. Protein Science 3: 810-821.

Mann, M. and Jensen, O.N. 2003. Proteomic analysis of post-translational modifications. Nature Biotechnology 21, 255-261.

Marouga, R., David, S., and Hawkins, E. 2005. The development of the DIGE system: 2D fluorescence difference gel analysis technology. Analytical and Bioanalytical Chemistry 382: 669-678.

Mata, J., Marguerat, S., and Bahler, J. 2005. Post-transcriptional control of gene expression: A genome-wide perspective. Trends in Biochemical Sciences 30: 506–514.

Mathesius, U., Imin, N., Chen, H.C., Djordjevic, M.A., J.J., Weinmann, Natera, S.H., Morris, A.C., Kerim, T., Paul, S., Menzel, C., Weiller, G.R., and Rolfe, B.G. 2002. Evaluation of proteome reference maps for cross-species identification of proteins by peptide mass fingerprinting. Proteomics 2: 1288-1303.

Mauch-Mani, B. and Slusarenko, A.J. 1996. Production of salicylic acid precursors is a major function of phenylalanine ammonialyase in the resistance of *Arabidopsis* to *Peronospora parasitica*. Plant Cell 8: 203–212.

Mayr, U., Michalek, S., Treutter, D., and Feucht, W. 1997. Phenolic compounds of apple and their relationship to scab resistance. Journal of Phytopathology 145: 69-75.

Miller, I., Crawford, J., and Gianazza, E. 2006. Protein stains for proteomic applications: Which, when, why? Proteomics 6: 5385-5408.

Mills, W.D. and LaPlante, A.A. 1954. Apple scab. In: Disease and insects in the orchard. Cornell Extension Bulletin 711: 20–28.

Morano, K.A. 2007. New tricks for an old dog: the evolving world of Hsp70. Annals of the New York Academy of Sciences 1113: 1–14.

Morrison, T.B., Weis, J.J., and Wittwer, C.T. 1998. Quantification of low-copy transcripts by continuous SYBR Green I monitoring during amplification. BioTechniques 24: 954-962.

Moshe, A., Pfannstiel, J., Brotman, Y., Kolot, M., Sobol, I., Czosnek, H., and Gorovits, R. 2012. Stress responses to Tomato Yellow Leaf Curl Virus (TYLCV) infection of resistant and susceptible tomato plants are different. Metabolomics S1:006. doi:10.4172/2153-0769.S1-006

Mysore, K.S. and Ryu, C.M. 2004. Nonhost resistance: how much do we know? Trends in Plant Science 9: 97-104.

Neuhoff, V., Arold, N., Taube, D., and Ehrhardt, W. 1988. Improved staining of proteins in polyacrylamide gels including isoelectric-focusing gels with clear background at nanogram sensitivity using coomassie brilliant blue G-250 and R-250. Electrophoresis 9: 255-262.

O'Farrell, P.H. 1975. High resolution two-dimensional electrophoresis of proteins. Journal of Biological Chemistry 250: 4007-4021.

Oostendorp, M., Kunz, W., Dietrich, B., and Staub, T. 2001. Induced disease resistance in plants by chemicals. European Journal of Plant Pathology 107: 19-28.

Pagliarani, G., Paris, R., Iorio, A.R., Tartarini, S., Del Duca, S., Arens, Peters, P.S., and van de Weg, E. 2012. Genomic organisation of the *Mal d 1* gene cluster on linkage group 16 in apple. Molecular Breeding 29: 759–778.

Panter, S.N., Hammond-Kosack, K.E., Harrison, K., Jones, J.D.G., and Jones, D.A. 2002. Developmental control of promoter activity is not responsible for mature onset of *Cf-9B*-mediated resistance to leaf mold in tomato. Molecular Plant–Microbe Interactions 15: 1099–1107.

Paris, R., Cova, V., Pagliarani, G., Tartarini, S., Komjanc, M., and Sansavini, S. 2009. Expression profiling in *HcrVf*2-transformed apple plants in response to *Venturia inaequalis*. Tree Genetics and Genomes 5: 81-91.

Parisi, L., Lespinasse, Y., Guillaumes, J., and Kruger, J. 1993. A new race of *Venturia inaequalis* virulent to apples with resistance due to the *Vf* gene. Phytopathology 83: 533–537.

Parisi, L. and Lespinasse, Y. 1996. Pathogenicity of *Venturia inaequalis* strains of race 6 on apple clones (*Malus* sp.). Plant Disease 80: 1179-1183.

Pascal, S., Bernard, A., Sorel, M., Pervent, M., Vile, D., Haslam, R.P., Napier, J.A., Lessire, R., Domergue, F., and Joubes, J. 2013. The Arabidopsis *cer26* mutant, like the *cer2* mutant, is specifically affected in the very long chain fatty acid elongation process. Plant Journal 73: 733-746.

Patocchi, A., Bigler, B., Koller, B., Kellerhals, M., and Gessler, C. 2004. *Vr*(2): a new apple scab resistance gene. Theoretical and Applied Genetics 109: 1087-1092.

Patocchi, A., Vinatzer, B.A., Gianfranceschi, L., Tartarini, S., Zhang, H.B., Sansavini, S., Gessler, C. 1999. Construction of a 550 kb BAC contig spanning the genomic region containing the apple scab resistance gene *Vf*. Molecular and General Genetics 262: 884–891.

Patocchi, A., Walser, M., Tartarini, S., Broggini, G., Gennari, F., Sansavini, S., and Gessler, C. 2005. Identification by genome scanning approach (GSA) of a microsatellite tightly associated with the apple scab resistance gene *Vm*. Genome 48: 630-636.

Peng, Y.L., Shirano, Y., Ohta, H., Hibino, T., Tanaka, K., and Shibata, D. 1994. A novel lipoxygenase from rice. Primary structure and specific expression upon incompatible infection with rice blast fungus. Journal of Biological Chemistry 269: 3755–3761.

Petkovsek, M.M., Stampar, F., and Veberic, R. 2009. Seasonal changes in phenolic compounds in the leaves of scab-resistant and susceptible apple cultivars. Canadian Journal of Plant Science 89: 745–753.

Petkovsek, M.M., Slatnar, A., Stampar, F., and Veberic, R. 2010. The influence of organic/integrated production on the content of phenolic compounds in apple leaves and fruits in four different varieties over a 2-year period. Journal of the Science of Food and Agriculture 90: 2366–2378.

Picinelli, A., Dapena, E., and Mangas, J.J. 1995. Polyphenolic pattern in apple tree leaves in relation to scab resistance. A preliminary study. Journal of Agricultural and Food Chemistry 43: 2273–2278.

Plaxton, W.C. 1996. The organization and regulation of plant glycolysis. Annual Review of Plant Physiology and Plant Molecular Biology 47: 185-214.

Qi, M. and Yang, Y. 2002. Quantification of *Magnaporthe grisea* during infection of rice plants using real-time polymerase chain reaction and northern blot/phosphoimaging analyses. Phytopathology 92: 870-876.

Rabilloud, T., Valette, C., and Lawrence, J.J. 1994. Sample application by in-gel rehydration improves the resolution of 2-dimensional electrophoresis with immobilized pH gradients in the first-dimension. Electrophoresis 15: 1552-1558.

Raffaele, S., Leger, A., and Roby, D. 2009. Very long chain fatty acid and lipid signaling in the response of plants to pathogens. Plant Signaling Behaviour 4: 94–99.

Ramonell, K., Zhang, B., Ewing, R., Chen, Y., Xu, D., Stacey, G., and Somerville, S. 2002. Microarray analysis of chitin elicitation in *Arabidopsis thaliana*. Molecular Plant Pathology 3: 301-311.

Righetti, P.G., Antonioli, P., Simò, C., and Citterio, A. 2008. Gel-based proteomics. In: Plant Proteomics. Agrawal, G.K. and Rakwal, R. (eds.) Wiley-Interscience, New York, 12-31.

Righetti, P.G., Castagna, A., Antonioli, P., and Boschetti, E. 2005. Prefractionation techniques in proteome analysis: the mining tools of the third millennium. Electrophoresis 26: 297-319.

Ririe, K.M., Rasmussen, R.P., and Wittwer, C.T. 1997. Product differentiation by analysis of DNA melting curves during the polymerase chain reaction. Analytical Biochemistry 245: 154–160.

Robert-Seilaniantz, A., Grant, M., and Jones, J.D. 2011. Hormone crosstalk in plant disease and defense: more than just jasmonate-salicylate antagonism. Annual Review of Phytopathology 49: 317–343.

Roe, M., and Griffin, T. 2006. Gel-free mass spectrometry-based high throughput proteomics: tools for studying biological response of proteins and proteomes. Proteomics 6: 4678-4687.

Rogers, E.E., Ausubel, F.M. 1997. *Arabidopsis* enhanced disease susceptibility mutants exhibit enhanced susceptibility to several bacterial pathogens and alterations in PR-1 gene expression. Plant Cell 9: 305–316.

Romeis, T., Piedras, P., Zhang, S., Klessig, D.F., Hirt, H., and Jones, J.D.G. 1999. Rapid Avr9- and Cf-9-dependent activation of MAP kinases in tobacco cell cultures and leaves: Convergence of resistance gene, elicitor, wound, and salicylate responses. Plant Cell 11: 273–287.

Rossi, V., Ponti, I., Marinelli, M., Giosue, S., and Bugiani, R. 2001. Environmental factors influencing the dispersal of *Venturia inaequalis* ascospore in orchards air. Journal of Fythopathology 149: 11-19.

newald, J., and Bjellqvist, B. 2000. An immobiline drystrip application method enabling high-capacity two-dimensional gel electrophoresis. Electrophoresis 21: 3649-3656.

Sahab, Z.J., Suh, Y., and Sang, Q.X. 2005. Isoelectric point-based prefractionation of proteins from crude biological samples prior to two-dimensional gel electrophoresis. Journal of Proteome Research 4: 2266-2272.

Sahi, C., Singh, A., Blumwald, E., and Grover A. 2006. Beyond osmolytes and transporters: novel plant salt-stress tolerance-related genes from transcriptional profiling data. Physiologia Plantarum 127: 1-9.

Saindrenan, P., Barchietto, T., Avclino, J., and Bompeix, G. 1988. Effects of phosphate on phytoalexin accumulation in leaves of cowpea infected with *Phytophthora cryptogea*. Physiological and Molecular Plant Pathology 32: 425-435.

Sansavini, S., Barbieri, M., Belfanti, E., Tartarini, S., Vinatzer, B., Gessler, C., Silfverberg, E., Gianfranceschi, L., Hermann, D., and Patocchi, A. 2003. ‘‘Gala’’ apple transformed for scab resistance with cloned *Vf* gene region construct. Acta Horticulturae 622: 113–118.

Sansavini, S., Tartarini, S., Gennari, F., Barbieri, M. 2002. Scab (*Venturia inaequalis*) resistance in apple: the *Vf*-gene and polygenic resistance in the breeding strategy at DCA–Bologna. Acta Horticulturae 595: 29–32.

Santoni, V., Rabilloud, T., Doumas, P., Rouquie, D., Mansion, M., Kieffer, S., Garin, J., and Rossignol, M. 1999. Towards the recovery of hydrophobic proteins on two-dimensional electrophoresis gels. Electrophoresis 20: 705-711.

Santoro, M.G. 2000. Heat shock factors and the control of the stress response. Biochemical Pharmacology 59, 55–63.

Saravanan, R. S. and Rose, J.K.C. 2004. A critical evaluation of sample extraction techniques for enhanced proteomic analysis of recalcitrant plant tissues. Proteomics 4: 2522-2532.

Savenstrand, H. and Strid, A. 2004. A *Pisum sativum* glyoxysomal malate dehydrogenase induced by cadmium exposure. DNA Sequence 15: 206-208.

Scharte, J., Schön, H., and Weis, E. 2005. Photosynthesis and carbohydrate metabolism in tobacco leaves during an incompatible interaction with *Phytophthora nicotianae*. Plant, Cell and Environment 28: 1421–1435.

Scheideler, M., Schlaich, N.L., Fellenberg, K., Beissbarth, T., Hauser, N.C., Vingron, M., Slusarenko, A.J., Hoheisel, J.D. 2002. Monitoring the switch from housekeeping to pathogen defense metabolism in *Arabidopsis thaliana* using cDNA arrays. Journal of Biological Chemistry 277: 10555-10561.

Schena, L., Nigro, F., Ippolito, A., and Gallitelli, D., 2004. Real-time quantitative PCR: a new technology to detect and study phytopathogenic and antagonistic fungi. European Journal of Plant Pathology 110: 893-908.

Schnabel, G., Schnabel, E.L., and Jones, A.L., 1999. Characterization of ribosomal DNA from *Venturia inaequalis* and its phylogenetic relationship to rDNA from other tree-fruit *Venturia* species. Phytopathology 89: 100-108.

Seglias, N. 1997. Genetische Kartierung quantitativer Merkmale beim Apfel. ETH Zürich Nr. 12204. 150p.

Seo, P.J. and Park, C.M. 2010. MYB96-mediated abscisic acid signals induce pathogen resistance response by promoting salicylic acid biosynthesis in *Arabidopsis*. The New Phytologist 186, 471–483.

Sghaier-Hammami, B., Redondo-López, I., Maldonado-Alconada, A.M., Echevarría-Zomeño, S., and Jorrín-Novo, J.V. 2012. A proteomic approach analysing the *Arabidopsis thaliana* response to virulent and avirulent *Pseudomonas syringae* strains. Acta Physiologiae Plantarum 34: 905-922.

Siegel, S.C.N.J. and Castellan, N.J.Jr. 1988. Nonparametric statistics for the behavioral sciences. McGraw-Hill Book Compagny, Singapore, 399p.

Silfverberg, E., Patocchi, A., Belfanti, S., Tartarini, S., Sansavini, S., Gessler, C. 2005. *HcrVf*2 introduced into Gala confers race specific scab resistance. Proceedings of the plant and animal Genome XIII conference, San Diego, California, 501.

Silfverberg-Dilworth, E., Besse, S., Paris, R., Belfanti, E., Tartarini, S., Sansavini, S., Patocchi, A., and Gessler, C. 2005. Identification of functional apple scab resistance gene promoters. Theoretical and Applied Genetics 110: 1119–1126.

Sindelárová, M. and Sindelar, L. 2001. Changes in composition of soluble intercellular proteins isolated from healthy and TMV-infected *Nicotiana tabacum* L. cv. Xanthi-nc. Biologia Plantarum 44: 567-572.

Sinha, R. and Chattopadhyay, S. 2011. Changes in the leaf proteome profile of *Mentha arvensis* in response to *Alternaria alternata* infection. Journal of Proteomics 74, 327-336.

Slusarenko, A.J. 1996. The role of lipoxygenase in plant resistance to infection. In: Lipoxygenase and Lipoxygenase Pathway Enzymes. Piazza, G. (ed.) AOCS Press, Champaign, Illinois, USA, 176-197.

Smedegaard-Petersen, V., Tolstrup, K. 1985. The limiting effect of disease resistance on yield. Annual Review of Phytopathology 23: 475-490.

Smillie, R., Grant, B.R., and Guest, D. 1989. The mode of action of phosphate: evidence for both direct and indirect modes of action on three *Phytophthora* spp. in plants. Disease Control and Pest Management 79: 921-926.

Soriano, J.M., Joshi, S.G., van Kaauwen, M., Noordijk, Y., Groenwold, R., Henken, B., van de Weg, W.E., and Schouten, H.J. 2009. Identification and mapping of the novel apple scab resistance gene *Vd*3. Tree Genetics & Genomes, 5: 475-482.

Steen, H. and Mann, M. 2004. The ABCs (and XYZs) of peptide sequencing. Nature Reviews Molecular and Cell Biology 5: 699-711.

Stehmann, C. and Grant, B.R. 2000. Inhibition of enzymes of the glycolytic pathway and hexose monophosphate bypass by phosphonate. Pesticide Biochemistry and Physiology 67, 13-24.

Stephens, A.E., Gardiner, D.M., White, R.G., Munn, A.L., and Manners, J.M., 2008. Phases of infection and gene expression of *Fusarium graminearum* during crown rot disease of wheat. Molecular Plant-Microbe Interactions 21: 1571-1581.

Stergiopoulos, I., and de Wit, P. 2009. Fungal effector proteins. Annual Review of Phytopathology 47: 233-263.

Sullivan, J., Shirasu, K., and Deng, X. 2003. The diverse roles of ubiquitin and the 26S proteasome in the life of plants. Nature Reviews Genetics 4: 948-958.

Szankowski, I., Waidmann, S., Degenhardt, J., Patocchi, A., Paris, R., Silfverberg-Dilworth, E., Broggini, G., and Gessler, C. 2009. Highly scab-resistant transgenic apple lines achieved by introgression of *HcrVf*2 controlled by different native promoter lengths. Tree Genetics and Genomes 5: 349–358.

Szkolnik, M. and Gilpatrick, J.D. 1969. Apparent resistance of *Venturia inaequalis* to dodine in New York apple orchards. Plant Disease Reports 53: 861-864.

Takemoto, D., Jones, D.A., and Hardham, A.R. 2003. GFP-tagging of cell components reveals the dynamics of subcellular re-organization in response to infection of *Arabidopsis* by oomycete pathogens. Plant Journal 33: 775–792.

Tan, S., Tan, H.T., and Chung, M. 2008. Membrane proteins and membrane proteomics. Proteomics 8: 3924-3932.

Tartarini, S., Sansavini, S., Vinatzer, B., Gennari, F., and Domizi, C. 2000. Efficiency of marker assisted selection (MAS) for the *Vf* scab resistance gene. Acta Horticulturae 538, 549–552.

Tecsi, L.I., Smith, A.M., Maule, A.J., and Leegood, R.C. 1996. A spatial analysis of physiological changes associated with infection of cotyledons of marrow plants with cucumber mosaic virus. Plant Physiology 111: 975-985.

Thelen, J. 2007. Introduction to proteomics: a brief historical perspective on contemporary approaches. In: Plant Proteomics. Samaj, J. and Thelen, J. (eds.) Springer, Berlin, 1-13.

Thevissen, K., Terras, F., and Broekaert, W. 1999. Permeabilization of fungal membranes by plant defensins inhibits fungal growth. Applied and Environmental Microbiology 65: 5451-5458.

Thomma, B.P.H.J., Eggermont, K., Tierens, K.F.M, and Broekaert, W.F. 1999. Requirement of functional EIN2 (ethylene insensitive 2) gene for efficient resistance of *Arabidopsis thaliana* to infection by *Botrytis cinerea*. Plant Physiology 121: 1093-1101.

Thurston, G., Regan, S., Rampitsch, C., Xing, T. 2005. Proteomic and phosphoproteomic approaches to understand plant–pathogen interactions. Physiological and Molecular Plant Pathology 66: 3–11.

Tonge, R., Shaw, J., Middleton, B., Rowlinson, R., Rayner, S., Young, J., Pognan, F., Hawkins, E., Currie, I., and Davison, M. 2001. Validation and development of fluorescence two-dimensional differential gel electrophoresis proteomics technology. Proteomics 1: 377-396.

Torres, M., Jones, J. & Dangl, J. (2006). Reactive oxygen species signaling in response to pathogens. Plant Physiology, 141: 373-378.

Towsend, G.R. and Heuberger, J.W. 1943. Methods for estimating losses caused by diseases in fungicide experiments. Plant Disease Reports 24: 340-343.

Treutter, D. 1998. Flavanols as defence barriers in apple leaves against the apple scab fungus (*Venturia inaequalis*). Acta Horticulturae 466: 79-82.

Troncoso-Ponce, M.A., Rivoal, J., Venegas-Calerón, M., Dorion, S., Sánchez, R., Cejudo, F.J., Garcés, R., and Martínez-Force, E. 2012. Molecular cloning and biochemical characterization of three phosphoglycerate kinase isoforms from developing sunflower (*Helianthus annuus* L.) seeds. Phytochemistry 79: 27-38.

Tsunezuka, H., Fujiwara, M., Kawasaki, T., and Shimamoto, K. 2005. Proteome analysis of programmed cell death and defense signaling using the rice lesion mimic mutant cdr2. Molecular Plant Microbe Interactions 18: 52-59.

Turechek, W.W. 2004. Apple diseases and their management. In: Diseases of fruits and vegetables. Diagnosis and management. Volume I. Naqvi, S.A.M.H. (ed.) Kluwer Academic Publishers, Dordrecht, 1-108.

Tyagi, S. and Kramer, F.R. 1996. Molecular beacons: probes that fluoresce upon hybridization. Nature Biotechnology 14: 303-308.

Umeda, M., Hara, C., Matsubayashi, Y., Li, H.H., Liu, Q., Tadokoro, F., Aotsuka, S., and Uchimiya, H. 1994. Expressed sequence tags from cultured-cells of rice (*Oryza sativa* L) under stressed conditions - analysis of transcripts of genes engaged in ATP-generating pathways. Plant Molecular Biology 25: 469-478.

Valencia-Sanchez, M.A., Liu, J., Hannon, G.J., and Parker, R. 2006. Control of translation and mRNA degradation by miRNAs and siRNAs. Genes and Development 20: 515–524.

Vandemark, G.J., Barker, B.M., and Gritsenko, M.A. 2002. Quantifying *Aphanomyces euteiches* in alfalfa with a fluorescent polymerase chain reaction assay. Phytopathology 92: 265-272.

Vanhoucke, L. 2006. Proteomics als instrument voor het ontrafelen van de verdedigingsmechanismen van appelbomen tegen schurft (*Venturia inaequalis*). Eindwerk voorgedragen tot het behalen van de graad van Bio-ingenieur in de Cel- en Genbiotechnologie. KU Leuven. (WMAG (043) 63 2006 155).

Vanrobaeys, F., Van Coster, R., Dhondt, G., Devreese, B., and Van Beeumen, J. 2005. Profiling of myelin proteins by 2D-gel electrophoresis and multidimensional liquid chromatography coupled to MALDI TOF-TOF mass spectrometry. Journal of Proteome Research 4: 2283–2293.

Velasco, R., Zharkikh, A., Affourtit, J., Dhingra, A., Cestaro, A., Kalyanaraman, A., Fontana, P., Bhatnagar, S.K., Troggio, M., Pruss, D., Salvi, S., Pindo, M., Baldi, P., Castelletti, S., Cavaiuolo, M., Coppola, G., Costa, F., Cova, V., Dal Ri, A., Goremykin, V., Komjanc, M., Longhi, S., Magnago, P., Malacarne, G., Malnoy, M., Micheletti, D., Moretto, M., Perazzolli, M., Si-Ammour, A., Vezzulli, S., *et al*. 2010. The genome of the domesticated apple (Malus × domestica Borkh.). Nature Genetics 42: 833-839.

Venugopal, S.C., Jeong, R.-D., Mandal, M.K., Zhu, S., Chandra-Shekara, A.C., Xia, Y., Hersh, M., Stromberg, A.J., Navarre, D., Kachroo, A. and Kachroo, P. 2009. Enhanced Disease Susceptibility 1 and Salicylic Acid Act Redundantly to Regulate Resistance Gene-Mediated Signaling. PLoS Genetics 5: e1000545. doi:10.1371/journal.pgen.1000545

Verma, L.R. and Sharma, R.C. 1999. Diseases of horticultural crops: fruits. Indus Publishing Company, New Delhi, 718p.

Vinatzer, B.A., Patocchi, A., Gianfranceschi, L., Tartarini, S., Zhang, H., Gessler, C., Sansavini, S. 2001. Apple contains receptor-like genes homologous to the *Cladosporium fulvum* resistance gene family of tomato with a cluster of genes cosegregating with *Vf* apple scab resistance. Molecular Plant-Microbe Interactions 14: 508–515.

Voinnet, O. 2008. Post-transcriptional RNA silencing in plant-microbe interactions: a touch of robustness and versatility. Current Opinion in Plant Biology 11: 464-470.

Whitcombe, D., Theaker, J., Guy, S.P., Brown, T., and Little, S. 1999. Detection of PCR products using self-probing amplicons and fluorescence. Nature Biotechnology 17: 804-807.

White, T.J., Bruns, T., Lee, S., and Taylor, J.A., 1990. Amplification and direct sequencing of fungal ribosomal RNA genes for phylogenetics. In: PCR Protocols: a Guide to Methods and Applications.

Wiermer, M., Feys, B.J., and Parker, J.E. 2005. Plant immunity: the EDS1 regulatory node. Current Opinion in Plant Biology 8: 383–389.

Innis, M.A., Gelfand, D.H., Shinsky, J.J., and White, T.J. (eds.) Academic Press, San Diego, California, USA, 315-322.

de Wit, P.J.G.M., Mehrabi, R., Burg, H.A., and Stergiopoulos, I. 2009. Fungal effector proteins: past, present and future. Molecular Plant Pathology 10: 735–747.

Wulff, B.B.H., Chakrabarti, A., and Jones, D.A. 2009. Recognitional specificity and evolution in the tomato–*Cladosporium fulvum* pathosystem. Molecular Plant–Microbe Interactions 22: 1191–1202.

Xu, M. and Korban, S.S. 2002. A cluster of four receptor-like genes resides in the *Vf* locus that confers resistance to apple scab disease. Genetics 162: 1995–2006.

Xu, X.M. and Robinson, J. 2005. Modelling the effects of wetness duration and fruit maturity on infection of apple fruits of Cox's Orange Pippin and two clones of Gala by *Venturia inaequalis*. Plant Pathology 54: 347–356.

Xu, M.L., Song, J., Cheng, Z., Jiang, J., Korban, S.S. 2001. A bacterial artificial chromosome (BAC) library of *Malus floribunda* 821 and contig construction for positional cloning of the apple scab resistance gene *Vf*. Genome 44: 1104–1113.

Yan, S.P., Tang, Z.C., Su, W., and Sun, W.N. 2005. Proteomic analysis of salt stress-responsive proteins in rice root. Proteomics 5: 235-244.

Zhang, Y. and Wang, L. 2005. The WRKY transcription factor superfamily: its origin in eukaryotes and expansion in plants. BMC Evolutionary Biology 5: 1-12.

Zhou, S.P., Sauve, R.J., Liu, Z., Reddy, S., Bhatti, S., Hucko, S.D., Yong, Y., Fish, T., and Thannhauser, T.W. 2011a. Heat-induced Proteome Changes in Tomato Leaves. Journal of the American Society for Horticultural Science 136: 219-226.

Zhou, S.P., Sauve, R.J., Liu, Z., Reddy, S., Bhatti, S., Hucko, S.D., Fish, T., and Thannhauser, T.W. 2011b. Identification of Salt-induced Changes in Leaf and Root Proteomes of the Wild Tomato, *Solanum chilense*. Journal of the American Society for Horticultural Science 136: 288-302.

Zubini, P., Baraldi, E., De Santis, A. Bertolini, P., and Mari, M. 2007. Expression of anti-oxidant enzyme genes in scald-resistant 'Belfort'and scald-susceptible 'Granny Smith' apples during cold storage. Journal of Horticultural Science & Biotechnology 82: 149–155.

Appendix I

IEF with 7 cm IPG strips: methods and focusing conditions (see Section 5.2.1.3)

Each protein sample was diluted with the lysis buffer to 100 µg (CBB staining) or 30 µg (silver staining) protein per 125 µl, and was applied to a 7 cm ReadyStrip IPG strip (pH 4-7 or 3-10, Bio-Rad) via active rehydration loading (12 h at 50 V). IEF was performed in the Protean IEF Cell system (Bio-Rad) at 20 °C: 20 min at 250 V, 2 h at 250-4000 V (linear gradient) and 10,000 Vh at 4000 V. The strips were equilibrated for 10 min in 2.5 ml equilibration solution (6 M urea, 20 % glycerol, 2 % SDS, 50 mM Tris pH 8.8) containing 2 % w/v DTT and subsequently for 10 min in 2.5 ml equilibration buffer containing 2.5 % w/v iodoacetamide. The separation in the second dimension was realized on the Mini-Protean 3 instrument (Bio-Rad) with lab cast 1 mm SDS polyacrylamide gels (12 % T): 30 min at 16 mA/gel and 2 h at 30 mA/gel.

Appendix II

Representative CBB G-250 stained gels of the 'Topaz' (left) and 'Golden Delicious' (right) control conditions

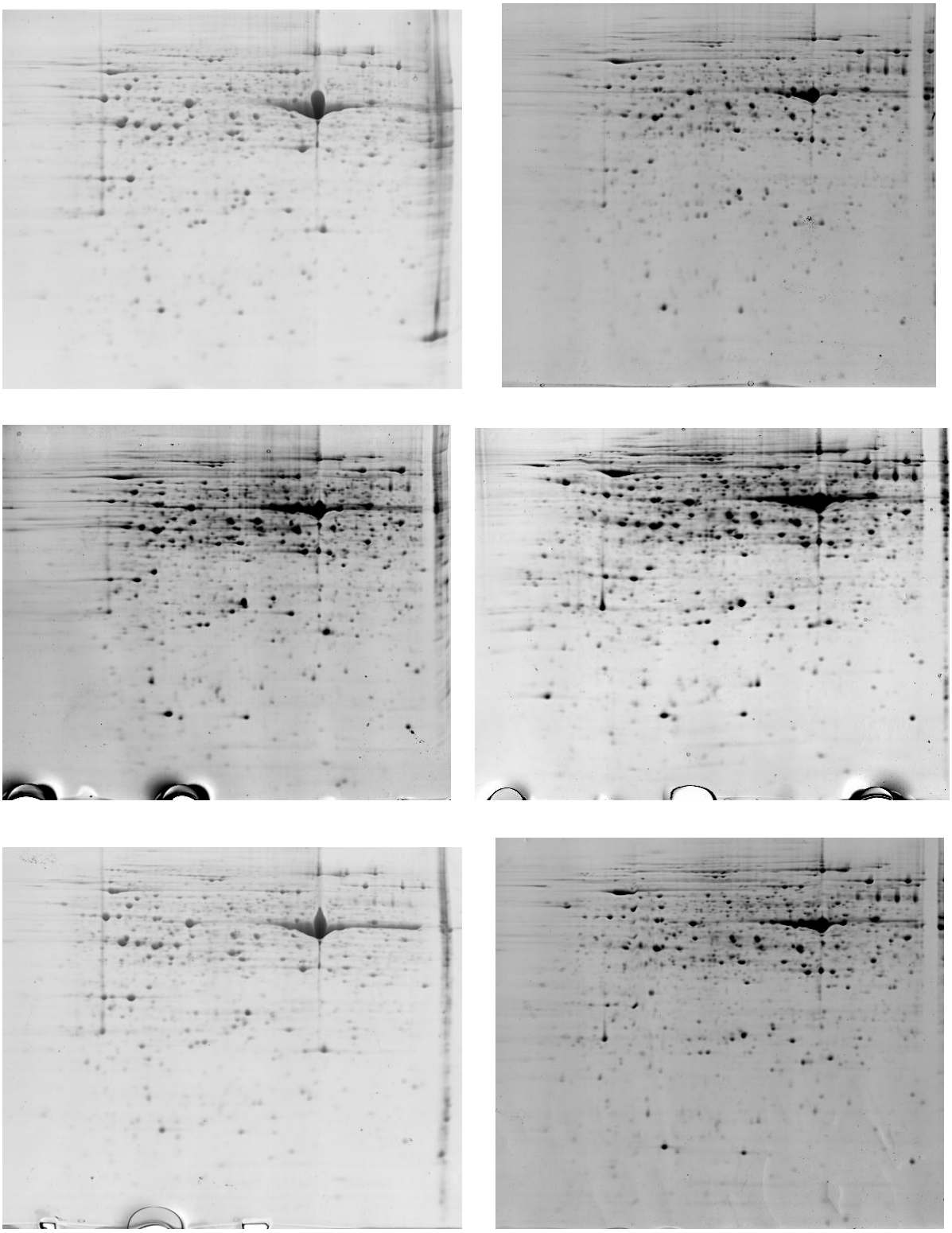

Appendix III

List of identified proteins (spots were picked from a CBB G-250 stained preparative gel of 'Topaz')

Spot[a]	Protein name	Accession No.[b]	EC[c]	Score[d]	C.I.%[e]	PM[f]	Theor.[g]		Exp.[g]	
							M_r	pI	M_r	pI
175	Presequence protease 2	MDP0000146940	-	991	100	27	147.7	6.01	120	4.93
186	glycine dehydrogenase (decarboxylating)	MDP0000588069	1.4.4.2; 1.3.1.74	437	100	12	115.0	6.69	115	6.08
203	elongation factor ef-2	MDP0000777793	-	386	100	16	95.0	5.80	95	5.84
205	elongation factor ef-2	MDP0000777793	-	450	100	17	95.0	5.80	95	5.82
208	elongation factor ef-2	MDP0000777793	-	515	100	17	95.0	5.80	95	5.86
217	linoleate 13s-lipoxygenase 2- chloroplastic	MDP0000753547	1.13.11.12	110	100	6	79.5	5.61	92	5.16
218	linoleate 13s-lipoxygenase 2- chloroplastic	MDP0000753547	1.13.11.12	193	100	8	79.5	5.61	92	5.30
223	linoleate 13s-lipoxygenase 2- chloroplastic	MDP0000753547	1.13.11.12	211	100	8	79.5	5.61	92	5.23
224	linoleate 13s-lipoxygenase 2- chloroplastic	MDP0000753547	1.13.11.12	227	100	7	79.5	5.61	92	5.25
229	linoleate 13s-lipoxygenase 2- chloroplastic	MDP0000753547	1.13.11.12	82	100	7	79.5	5.61	92	5.36
230	linoleate 13s-lipoxygenase 2- chloroplastic	MDP0000281525	1.13.11.12	177	100	7	108.9	5.93	92	5.41
255	phospholipase D alpha	MDP0000300217	3.1.4.4	118	100	7	94.5	5.83	89	5.84
279	elongation factor G (EF-G)	MDP0000138993	-	909	100	23	86.1	5.45	87	4.93
280	(putative) oligopeptidase B	MDP0000208437	3.4.21.0	258	100	14	139.7	5.48	87	5.10
316	(vitamin-b12 independent) methionine synthase	MDP0000793077	2.1.1.13; 2.1.1.14	462	100	11	84.8	6.23	85	6.17
317	(vitamin-b12 independent) methionine synthase	MDP0000793077	2.1.1.13; 2.1.1.14	125	100	6	84.8	6.23	85	6.21
318	(vitamin-b12 independent) methionine synthase	MDP0000153762	2.1.1.13; 2.1.1.14	1170	100	19	84.8	6.05	85	6.09

Spot[a]	Protein name	Accession No.[b]	EC[c]	Score[d]	C.I.%[e]	PM[f]	Theor.[g]		Exp.[g]	
							M_r	pI	M_r	pI
325	(vitamin-b12 independent) methionine synthase	MDP0000793077	2.1.1.13; 2.1.1.14	995	100	17	84.8	6.23	82	6.38
337	heat shock protein 70 (70 kDa)	MDP0000570507	1.3.1.74	515	100	17	118.1	5.94	82	5.00
342	glycyl-tRNA synthetase (1, mitochondrial-like)	MDP0000226879	6.1.1.14	734	100	15	120.3	8.70	82	5.96
359	transketolase	MDP0000142098	2.2.1.1	492	100	11	80.9	6.29	81	5.64
360	transketolase	MDP0000142098	2.2.1.1	882	100	17	80.9	6.29	81	5.70
372	heat shock protein 70 (70 kDa)	MDP0000322220	1.3.1.74	505	100	14	119.7	5.93	81	4.99
374	transketolase	MDP0000142098	2.2.1.1	1410	100	25	80.9	6.29	81	5.76
375	heat shock protein 70 (70 kDa)	MDP0000322220	1.3.1.74	828	100	16	119.7	5.93	81	4.90
377	heat shock protein 70 (70 kDa)	MDP0000322220	1.3.1.74	941	100	16	119.7	5.93	81	4.96
382	heat shock protein 70 (70 kDa)	MDP0000322220	1.3.1.74	996	100	19	119.7	5.93	81	4.93
389	stress-inducible protein	MDP0000191994	-	150	100	9	66.3	5.84	79	5.72
416	UDP-sugar pyrophosphorylase	MDP0000156131	2.7.7.9; 10; 11 and 44	505	100	16	77.6	5.92	76	5.67
417	ATP-dependent zinc metalloprotease FtsH, chloroplastic	MDP0000289110	3.6.4.3; 3.4.24.0	73	99.7	7	73.9	5.91	76	5.18
418	ATP-dependent zinc metalloprotease FtsH, chloroplastic	MDP0000289110	3.6.4.3; 3.4.24.0	570	100	16	73.9	5.91	76	5.23
427	enhanced disease susceptibility 1	MDP0000162236	-	326	100	14	69.2	5.73	73	5.41
436	succinate dehydrogenase	MDP0000188391	1.3.5.1	324	100	8	72.0	5.98	72	5.57
437	$NADP^+$-dependent malate dehydrogenase; malic enzyme	MDP0000221561	1.1.1.40	602	100	13	64.9	5.72	72	5.81
440	$NADP^+$-dependent malate dehydrogenase; malic enzyme	MDP0000221561	1.1.1.40	1100	100	21	64.9	5.72	72	5.60
441	cytosolic phosphoglucomutase	MDP0000321541	5.4.2.2	245	100	8	63.5	5.81	72	5.52
450	cytosolic phosphoglucomutase	MDP0000321541	5.4.2.2	630	100	14	63.5	5.81	71	5.68

Spot[a]	Protein name	Accession No.[b]	EC[c]	Score[d]	C.I.%[e]	PM[f]	Theor.[g]		Exp.[g]	
							M_r	pI	M_r	pI
451	acetohydroxyacid synthase; acetolactate synthase	MDP0000621545	2.2.1.6	999	100	18	71.7	6.34	71	5.58
453	Nucleosome/chromatin assembly factor group	MDP0000251796	2.3.1.48	197	100	5	58.2	6.08	69	5.79
454	beta-glucosidase 24-like	MDP0000297569	-	350	100	4	61.3	5.92	69	6.12
464	beta-glucosidase 24-like	MDP0000297569	-	280	100	5	61.3	5.92	68	6.04
469	apple phosphoglyceromutase (apgm)	MDP0000240039	5.4.2.1	178	100	11	64.4	5.40	67	5.37
472	apple phosphoglyceromutase (apgm)	MDP0000240039	5.4.2.1	497	100	16	64.4	5.40	67	5.52
475	beta-glucosidase 24-like	MDP0000297569	-	375	100	5	61.3	5.92	67	6.21
487	beta-glucosidase 24-like	MDP0000297569	-	372	100	4	61.3	5.92	67	6.30
495	pyruvate decarboxylase	MDP0000223243	4.1.1.1	123	100	5	66.0	5.99	66	5.62
499	pyruvate decarboxylase	MDP0000223243	4.1.1.1	549	100	11	66.0	5.99	66	5.70
501	pyruvate kinase	MDP0000121177	2.7.1.40	623	100	15	84.0	8.48	66	5.21
504	TCP domain class transcription factor alpha-like subunit	MDP0000036030	-	219	100	7	60.4	5.97	65	5.64
506	phosphofructokinase	MDP0000293776	2.7.1.11; 2.7.1.90	124	100	6	57.8	5.52	65	5.79
510	2-isopropylmalate synthase	MDP0000212398	2.3.3.13	400	100	12	59.3	7.28	64	5.90
516	heat shock protein 60	MDP0000235765	-	688	100	23	93.8	6.37	64	5.13
530	bifunctional purine biosynthesis protein	MDP0000654452	2.1.2.3; 3.5.4.10	197	100	9	112.7	9.00	62	6.11
536	betaine-aldehyde dehydrogenase	MDP0000148461	1.2.1.3; 1.2.1.8	548	100	12	109.5	5.91	62	5.36
539	heat shock protein 60	MDP0000185591	-	789	100	18	63.0	5.84	61	5.10
550	TCP domain class transcription factor eta-like subunit	MDP0000534977	-	551	100	15	52.0	6.09	60	6.11
585	myo-inositol-1-phosphate synthase	MDP0000698835	5.5.1.4	490	100	8	56.3	5.51	56	5.43
586	V-type (vacuolar) proton ATPase subunit B	MDP0000945182	3.6.3.0	545	100	10	54.6	4.98	56	4.80
592	putative anthranilate N-benzoyltransferase protein	MDP0000314927	2.3.1.144	297	100	11	69.4	5.93	56	5.99
605	prolyl-tRNA synthetase	MDP0000291077	6.1.1.15	164	100	13	58.5	6.47	56	6.16

Spot[a]	Protein name	Accession No.[b]	EC[c]	Score[d]	C.I.%[e]	PM[f]	Theor.[g]		Exp.[g]	
							M_r	pI	M_r	pI
612	putative anthranilate N-benzoyltransferase protein	MDP0000267154	2.3.1.144	725	100	9	172.6	7.11	56	5.32
625	chloroplast ATP synthase beta subunit	MDP0000928146	3.6.3.6	160	100	2	24.4	5.13	55	6.20
652	chloroplast ATP synthase beta subunit	MDP0000928146	3.6.3.6	139	100	2	24.4	5.13	55	5.28
661	chloroplast ATP synthase beta subunit	MDP0000928146	3.6.3.6	104	100	2	24.4	5.13	55	5.18
672	enolase	MDP0000939989	4.2.1.11	817	100	15	49.8	6.09	55	5.38
707	6-phosphogluconate dehydrogenase	MDP0000191398	1.1.1.44	501	100	12	54.1	6.24	54	6.10
715	ATP-citrate synthase	MDP0000931334	2.3.3.8; 6.2.1.5	335	100	7	26.1	4.79	54	5.05
722	uridine 5'-monophosphate synthase	MDP0000335264	4.1.1.23; 2.4.2.10	62	96.0	1	15.8	6.25	54	6.21
728	6-phosphogluconate dehydrogenase	MDP0000191398	1.1.1.44	480	100	13	54.1	6.24	54	6.13
735	26S protease regulatory subunit 6B homolog	MDP0000221873	3.6.4.3	821	100	15	50.3	5.29	54	5.22
752	argininosuccinate synthase	MDP0000196436	6.3.4.5	591	100	13	58.5	7.97	53	5.49
767	rna-binding post-transcriptional regulator csx1-like	MDP0000614064	-	944	100	10	48.3	5.26	53	5.03
792	elongation factor 1-gamma	MDP0000315108	-	283	100	7	118.4	8.97	50	6.20
825	RuBisCO activase	MDP0000944409	-	1010	100	14	52.0	6.20	47	5.00
830	porphobilinogen synthase	MDP0000933051	4.2.1.24	612	100	13	45.9	6.28	47	5.27
842	monodehydroascorbate reductase	MDP0000261821	-	1360	100	17	47.1	6.51	47	6.28
845	protein FAR1-related sequence 4-like (predicted)	MDP0000264383	1.2.1.50	1100	100	18	130.9	6.33	46	5.96
864	actin	MDP0000183660	-	123	100	4	41.9	5.31	45	5.05
875	glutamate-1-semialdehyde-2,1-aminomutase	MDP0000149467	5.4.3.8; 2.6.1.0	122	100	3	47.0	5.34	44	5.15
883	chalcone synthase	MDP0000686666	2.3.1.74	671	100	14	43.0	5.90	44	5.91
888	elongation factor Tu (EF-Tu)	MDP0000184653	2.7.7.0	1070	100	11	53.1	6.13	44	5.22
894	chalcone synthase	MDP0000575740	2.3.1.74	240	100	8	42.8	5.77	44	6.13
914	magnesium-chelatase subunit chlI, chloroplastic-like	MDP0000639265	6.6.1.1; 3.6.1.3	505	100	13	46.2	6.18	43	4.96

Spot[a]	Protein name	Accession No.[b]	EC[c]	Score[d]	C.I.%[e]	PM[f]	Theor.[g]		Exp.[g]	
							M_r	pI	M_r	pI
926	phosphoglycerate kinase	MDP0000325411	2.7.2.3	1380	100	17	50.2	7.79	43	5.59
934	glyceraldehyde-3-phosphate dehydrogenase	MDP0000835914	1.2.1.13; 1.2.1.12	826	100	11	48.5	8.00	43	6.20
935	RuBisCO activase	MDP0000944409	-	430	100	9	52.0	6.20	43	6.31
945	RuBisCO activase	MDP0000944409	-	716	100	11	52.0	6.20	43	5.49
948	phosphoglycerate kinase	MDP0000325411	2.7.2.3	1250	100	16	50.2	7.79	43	5.45
956	protein disulfide isomerase	MDP0000201801	5.3.4.1	558	100	11	40.1	5.68	43	5.28
961	3-dehydroquinate synthase	MDP0000273495	1.1.1.24; 4.2.3.4	859	100	14	49.8	8.59	42	5.80
965	Serpin-ZX-like protein	MDP0000751972	-	1510	100	22	42.4	6.34	42	6.02
980	Serpin-ZX-like protein	MDP0000751972	-	131	100	7	42.4	6.34	42	5.89
984	phosphoribulokinase (putative; chloroplastic-like)	MDP0000148186	2.7.1.19	735	100	16	45.1	6.04	42	5.10
986	polyphenol oxidase	MDP0000500159	1.10.3.1; 1.14.18.1	548	100	8	61.8	5.60	42	5.91
989	phosphoglycerate kinase	MDP0000784808	2.7.2.3	1490	100	20	42.4	6.36	42	6.10
990	glyceraldehyde-3-phosphate dehydrogenase	MDP0000527995	1.2.1.13; 1.2.1.12	593	100	9	43.3	8.10	42	6.14
997	uroporphyrinogen decarboxylase (UROD)	MDP0000364293	4.1.1.37	117	100	5	44.4	8.01	42	5.69
999	uroporphyrinogen decarboxylase (UROD)	MDP0000269628	4.1.1.37	478	100	8	42.6	8.94	42	5.53
1000	phosphoribulokinase (putative; chloroplastic-like)	MDP0000148186	2.7.1.19	788	100	13	45.1	6.04	42	5.20
1004	alpha-1,4-glucan-protein synthase (UDP forming)	MDP0000232047	2.4.1.186	967	100	18	41.6	5.66	42	5.41
1007	glyceraldehyde-3-phosphate dehydrogenase	MDP0000527995	1.2.1.13; 1.2.1.12	1280	100	13	43.3	8.10	42	6.39
1018	Alpha-1,4-glucan-protein synthase (UDP-forming)	MDP0000232047	2.4.1.186	926	100	18	41.6	5.66	41	5.78
1025	Alpha-1,4-glucan-protein synthase (UDP-forming)	MDP0000232047	2.4.1.186	83	100	4	41.6	5.66	41	5.56
1034	pyruvate dehydrogenase E1 component subunit beta	MDP0000146411	1.2.4.1	641	100	11	44.6	6.56	40	4.91
1042	photosystem II stability/assembly factor HCF136	MDP0000826603	-	1290	100	18	44.4	6.56	40	5.20

Spot[a]	Protein name	Accession No.[b]	EC[c]	Score[d]	C.I.%[e]	PM[f]	Theor.[g]		Exp.[g]	
							M_r	pI	M_r	pI
1056	quinone oxidoreductase-like protein	MDP0000269371	1.6.5.5	1190	100	17	51.4	9.34	40	6.09
1062	esterase/lipase domain-containing protein	MDP0000130884	-	402	100	8	51.2	7.71	40	5.60
1073	fructose-bisphosphate aldolase	MDP0000151849	4.1.2.13	828	100	13	77.1	4.68	39	5.78
1075	mRNA binding protein	MDP0000193729	-	934	100	12	43.9	7.16	39	6.00
1078	fructose-bisphosphate aldolase	MDP0000151849	4.1.2.13	147	100	7	77.1	4.68	39	5.97
1081	fructose-bisphosphate aldolase	MDP0000273688	4.1.2.13	554	100	10	67.3	8.59	39	6.27
1084	fructose-1,6-bisphosphatase, cytosolic	MDP0000251810	3.1.3.11; 1.3.1.74	889	100	15	37.3	5.61	39	5.48
1091	fructose-bisphosphate aldolase	MDP0000151849	4.1.2.13	206	100	8	77.1	4.68	39	6.06
1093	NAD^+-dependent malate dehydrogenase	MDP0000174740	1.1.1.37	577	100	12	50.6	6.38	39	5.91
1099	auxin-induced protein PCNT115-like isoform 1	MDP0000228499	1.1.1.65	1410	100	19	37.6	5.96	38	5.93
1102	fructokinase; ribokinase	MDP0000131308	2.7.1.15; 2.7.1.4	1340	100	19	37.0	5.60	38	5.33
1105	fructokinase ; ribokinase	MDP0000131308	2.7.1.15; 2.7.1.4	912	100	11	37.0	5.60	38	5.08
1120	enoyl-[acyl-carrier-protein] reductase	MDP0000207724	1.3.1.9	372	100	9	47.1	8.45	37	5.30
1137	EF-hand (motif containing) (calcium binding) protein	MDP0000120294	-	288	100	5	35.2	6.21	37	5.93
1149	annexin D2-like	MDP0000253809	-	1340	100	18	44.9	5.42	36	5.98
1150	26S proteasome non-ATPase regulatory subunit 14	MDP0000138737	-	616	100	12	34.9	6.31	36	6.19
1165	(putative) RNA binding protein	MDP0000264307	-	849	100	16	123.5	6.58	36	5.26
1174	arginine/serine-rich splicing factor	MDP0000387508	-	463	100	14	43.2	10.1	36	5.79
1193	(putative) lactoylglutathione lyase	MDP0000319112	4.4.1.5	1030	100	15	40.0	6.40	35	5.11
1215	Oxygen-evolving enhancer protein 1, chloroplastic	MDP0000858039	-	743	100	15	35.3	5.76	35	4.82
1220	Oxygen-evolving enhancer protein 1, chloroplastic	MDP0000858039	-	1100	100	17	35.3	5.76	35	4.90
1221	Oxygen-evolving enhancer protein 1, chloroplastic	MDP0000248920	-	834	100	14	35.3	6.09	35	4.94
1224	Oxygen-evolving enhancer protein 1, chloroplastic	MDP0000248920	-	1090	100	15	35.3	6.09	35	5.02
1262	Chalcone synthase	MDP0000575740	-	624	100	11	42.5	5.97	34	5.75

Spot[a]	Protein name	Accession No.[b]	EC[c]	Score[d]	C.I.%[e]	PM[f]	Theor.[g]		Exp.[g]	
							M_r	pI	M_r	pI
1264	oxidoreductase GLYR1	MDP0000149834	1.1.1.60; 1.1.1.44; 1.1.1.31; 1.1.1.30	529	100	10	33.9	8.36	34	6.16
1268	predicted dihydrofolate reductase	MDP0000514153	-	363	100	7	16.7	6.95	34	5.47
1299	(predicted protein) cbbY	MDP0000152304	-	83	100	5	62.9	6.62	33	5.30
1303	light-harvesting complex II protein Lhcb1	MDP0000417927	-	427	100	6	28.1	5.29	33	4.90
1304	uncharacterized protein	MDP0000124634	-	652	100	10	25.1	5.22	33	5.02
1313	ascorbate peroxidase	MDP0000241173	1.11.1.11	686	100	11	37.7	6.46	33	5.64
1344	light-harvesting complex II protein Lhcb1	MDP0000417927	-	464	100	7	28.1	5.29	33	5.48
1345	ascorbate peroxidase	MDP0000241173	1.11.1.11	509	100	10	37.7	6.46	32	5.65
1350	protein THYLAKOID FORMATION1, chloroplastic-like	MDP0000139684	-	758	100	12	36.7	8.69	32	6.00
1353	20S proteasome alpha subunit A1	MDP0000134203	3.4.25.0	638	100	9	12.9	9.52	32	5.62
1369	triosephosphate isomerase	MDP0000152242	5.3.1.1	781	100	12	27.5	6.02	30	6.01
1380	triosephosphate isomerase	MDP0000193489	5.3.1.1	288	100	6	40.0	8.81	30	5.10
1393	proteasome subunit alpha type-2-B	MDP0000143951	3.4.25.0	230	100	5	48.0	9.42	29	5.33
1398	triosephosphate isomerase	MDP0000694943	5.3.1.1	794	100	13	27.5	5.76	29	5.72
1399	light-harvesting complex II protein Lhcb1	MDP0000417927	-	514	100	7	28.1	5.29	28	4.90
1426	proteasome subunit beta type-1	MDP0000291250	-	486	100	9	37.8	7.56	28	5.80
1430	RuBisCO small subunit	MDP0000731480	4.1.1.39	129	100	6	20.3	9.04	28	6.22
1437	RNA recognition motif-containing protein	MDP0000270177	-	315	100	10	98.1	5.06	28	5.90
1438	RNA recognition motif-containing protein	MDP0000270177	-	472	100	13	98.1	5.06	28	5.55
1440	uncharacterized protein	MDP0000178270	-	480	100	10	27.8	6.49	28	5.19
1463	dephospho-CoA-kinase	MDP0000266097	2.7.1.24	254	100	9	61.1	9.48	27	6.05
1465	chlorophyll A/B binding protein	MDP0000866655	-	438	100	9	29.9	7.85	27	5.28
1479	oxygen-evolving enhancer protein chloroplastic-like	MDP0000361338	1.3.1.74	908	100	11	32.5	9.44	26	5.88
1512	light-harvesting complex I protein Lhca1	MDP0000222941	-	252	100	4	27.6	6.22	25	5.10

Spot[a]	Protein name	Accession No.[b]	EC[c]	Score[d]	C.I.%[e]	PM[f]	Theor.[g]		Exp.[g]	
							M_r	pI	M_r	pI
1518	proteasome subunit beta type	MDP0000137279	3.4.25.0	848	100	15	24.8	6.16	25	5.65
1536	chloroplast ATP synthase delta subunit	MDP0000750535	-	912	100	12	27.3	8.65	24	5.20
1543	type IIF peroxiredoxin	MDP0000258515	1.11.1.7; 1.11.1.15	508	100	9	21.6	8.77	20	6.35
1550	universal stress protein (USP) family protein	MDP0000415257	-	667	100	10	18.0	6.31	20	6.00
1556	Uncharacterized protein	MDP0000179031	-	744	100	9	18.6	6.75	20	6.32
1594	major allergen Mal d 1 (PR-10)	MDP0000942516	-	505	100	6	17.5	5.62	18	5.59
1595	major allergen Mal d 1 (PR-10)	MDP0000942516	-	556	100	7	17.5	5.62	18	5.41
1597	major allergen Mal d 1 (PR-10)	MDP0000942516	-	937	100	10	17.5	5.62	18	5.56
1625	major allergen Mal d 1 (PR-10)	MDP0000295540	-	544	100	8	17.6	5.67	17	5.34
1637	Mal d 1-like	MDP0000151829	-	515	100	7	17.5	5.23	17	5.05
1706	nucleoside diphosphate kinase 1 (NDPK I)	MDP0000322880	2.7.4.6	854	100	10	18.7	7.96	16	6.27
1713	thioredoxin h	MDP0000622392	1.8.4.0	350	100	5	14.1	5.56	16	5.23

[a] Corresponding spot number in the gel image in Fig. 5.4

[b] MDP number of predicted apple gene (Velasco *et al*., 2010) (Gene and protein sequences can be obtained from Genome Database for Rosaceae (GDR): http://www.rosaceae.org)

[c] Enzyme Commission number

[d] MOWSE score probability (protein score) for the entire protein

[e] Protein score confidence interval (%)

[f] Number of matched peptides of peptide mass fingerprinting combined with MS/MS

[g] Theoretical and experimental molecular weight (M_r) and isoelectric point (pI)

List of publications

Articles in internationally reviewed scientific journals:

Daniëls, B., De Landtsheer, A., Dreesen, R., Davey, M.W., and Keulemans, J. 2012. Real-time PCR as a promising tool to monitor growth of *Venturia* spp. in scab-susceptible and -resistant apple leaves. European Journal of Plant Pathology 134: 821-833.

Amoako-Andoh, F.O., Daniëls, B., Davey, M.W., and Keulemans, J. A systematic evaluation of sample preparation methods for the study of fruit proteomes via two-dimensional electrophoresis. Proteomics, *in revision*.

Keulemans, J., Martens, D., Buyse, E., De Landtsheer, A., Daniëls, B., Van Hemelrijck, W., and Creemers, P. 2012. Susceptibility of pear (*Pyrus communis*) cultivars for different strains of *Venturia pirina*. Proceedings IOBC/WPRS Workshop on Pome Fruit Diseases (Belgium) , *in press*.

Beert, E., Brems, H., Daniels, B., De Wever, I., Van Calenbergh, F., Schoenaers, J., Debiec-Rychter, M., Gevaert, O., De Raedt, T., Van den Bruel, A., de Ravel, T., Cichowski, K., Kluwe, L., Mautner, V., Sciot, R., and Legius, E. 2011. Atypical neurofibromas in Neurofibromatosis Type 1 are premalignant tumors. Genes, Chromosomes and Cancer 50: 1021-1032.

Meeting abstracts, presented at international conferences and symposia:

Daniëls, B., De Samblanx, S., Carpentier, S., Waelkens, E., Swennen, R., Keulemans, J., Davey, M.W. Proteome analysis of scab resistance mechanisms in apple. 28th International Horticultural Congress. Lisbon, Portugal, 22-27 August 2010.

Daniëls, B., De Landtsheer, A., Dreesen, R., Keulemans, J. Real-time PCR for detection and quantification of *Venturia inaequalis* in apple. 28th International Horticultural Congress. Lisbon, Portugal, 22-27 August 2010.

Meeting abstracts, presented at local conferences and symposia:

Daniëls, B., Keulemans, J., Davey, M.W. Proteomics: a way to unravel the battle between scab and apple. 15th PhD Symposium on Applied and Biological Sciences. Leuven, Belgium. 6 November 2009.